Iwan P. Gavrilyuk, Ivan A. Lukovsky,
Vladimir L. Makarov, Alexander N. Timokha

Evolutional Problems of the Contained Fluid

ПРАЦІ
Інституту математики НАН України

Математика та її застосування
Том 58

Засновано в 1994 році

Національна академія наук України

Інститут математики

Iwan P. Gavrilyuk, Ivan A. Lukovsky,
Vladimir L. Makarov, Alexander N. Timokha

Evolutional Problems of the Contained Fluid

Київ • 2006

УДК 532.595
Evolutional Problems of the Contained Fluid/Iwan P. Gavrilyuk, Ivan A. Lukovsky, Vladimir L. Makarov, Alexander N. Timokha – Київ: Ін-т математики НАН України, 2006. – 233 с.

This book presents three modern analytical approaches to the free boundary value problems which describe the wave motion of a fluid inside a container, the so-called sloshing. These deal with an operator theory and numerical schemes for the linear sloshing problems, the nonlinear modal methods as well as the Hamiltonian formalism in dynamics of a compressible fluid under high-frequency loading.

The book is valuable to researchers, graduate students in mechanical, civil and aeronautical engineering, nuclear engineers, physicists including nanotechnologists and pure and applied mathematicians.

Книга представляє три сучасних аналітичних підходи до краєвих задач з вільною границею, що описують хвильовий рух рідини в контейнері, так званий слошінг. Ці підходи пов'язані з операторною теорією та чисельними схемами в задачі лінійного слошінга, нелінійними модальними методами, а також Гамільтоновим формалізмом в динаміці стисливої рідини, що знаходиться під дію високочастотних навантажень.

Книга буде корисною для вчених, аспірантів та студентів старших курсів, чиєю спеціалізацією є інженерна на цивільна механіка, аеронавтика, проектування ядерних реакторів, фізика, в тому числі проблеми нанотехнології, а також чиста та прикладна математика.

Рецензенти:

член–кор. НАН України, д-р фіз.-мат. наук Ю. І. Самойленко, професор, доктор М. Германн

Затверджено до друку вченою радою Інституту математики НАН України

ISBN 966-02-2571-7
ISBN 966-02-3949-1

Contents

Foreword

This book provides a modern investigation into the free-surface wave motion of a fluid inside a container, the so-called sloshing. The container may be at rest or can be shaken or may be moved due to the hydrodynamic forces acting on the walls of the container. We all know how badly behaved cups of hot drinks can be when we try to carry two mugs with our hands, for example, through a sprung-loaded fire door, or when we rest a brimful glass on a thick-piled carpet. Sloshing theory has been stimulated by engineering problems from the automotive, aerospace and shipbuilding industries where the transport of a tank filled with a fluid has to be modelled. It is related to a complex evolutional free boundary value problem, whose history started in the 19th century. There are, of course, pure engineering, sometimes semi-empirical methods, but only the comprehensive mathematical theory of sloshing has generalised and optimised these engineering solutions. The design and tuning of ship anti-rolling devices and, most recently, the construction of earthquake-vibration absorbers for high-rise buildings in Japan can be taken as an example.

The book presented by Gavrilyuk, Lukovsky, Makarov and Timokha will be of great importance for the development of new analytical results and numerical-analytical techniques which, from my point of view, are the most interesting themes in the field of theoretical sloshing. It covers systematically all the fundamental topics and recent results for both linear and nonlinear models. Special attention is given to operator and multi-modal methods. The two main chapters deal with them. The last chapter contains a detailed analysis of the compressible potential flow and the "vibroequilibria" occurring due to high-frequency vibro-fields. Although the associated mathematical models are characterised by similar free boundary value problems, from a physical point of view, the presented material has only a small connection to the preceding chapters.

Almost all of the results in this book were obtained by joint work of the authors. They have been published in international top journals of applied mathematics and hydrodynamics. The authors were partly sponsored by the German "Deutsche Forschungsgemeinschaft" (DFG).

The introductory chapter is designed to acquaint the reader with some of the types of problems that occur in sloshing theory. Moreover, a short survey of the structure of the text is given. The linear sloshing problem is presented in Chapter 2. It is treated mathematically as a second order differential equation with an operator coefficient. Notwithstanding extensive studies of sloshing in many fields of research, there seems to be a gap between the mathematical theory and engineering practice. In an attempt to fill up this gap the authors give a unified treatment of the mathematical theory of the operator cosine function and the corresponding numerical methods. Details of the implementation are exemplified for two-dimensional sloshing in a chute with and without horizontal baffles.

Chapter 3 represents the main part of the book. It is devoted to small-dimensional systems of nonlinear ordinary differential equations, the so-called modal systems. The modal systems are "hand-made products", whose derivation is based on a variety of physical assumptions and employs both asymptotic and variational techniques. Structure and dimension of the modal systems are functions of the tank shape, the external loads and the fluid filling (depth). Bearing in mind the contribution of Lorenz to the chaos theory which deals with similar small-dimensional structures and its influence on the theory of nonlinear dynamical systems, these modal systems may give rise to new mathematical theories and techniques. In particular, it can be expected that the modal systems developed and analysed here from a more physical point of view will be thoroughly studied mathematically by experts in nonlinear analysis, bifurcation theory, numerical methods, etc.

Finally, Chapter 4 represents innovative studies on the so-called vibrocapillary equilibria. It was amazing to realise that the theory of the authors made it possible to explain the flattening of Faraday's drop for the first time. This phenomenon has been observed in 1831 and until now there was no appropriate mathematical model. The mathematical results of the this chapter can also be used in modern vibro- and nanotechnology, e.g. in the contactless precision-technique for positioning small fluid particles and droplets in space.

The book is valuable for researchers and post-graduate students in mechanical and aeronautical engineering and physicians. Due to the ex-

tensive analysis of the methods, it is especially suited to researchers with a very strong mathematical background. Mathematicians who want to deal with real world applications and numerical methods may find this book, with its amazing physical models, to be a useful resource. An interesting feature of the presentation is the use of graphs, diagrams and other aids to visualise important ideas and results.

All in all, the book about the theoretical aspects of sloshing is a wonderful text blending together the mathematical basis, good numerical-analytical techniques, and practical knowledge for solving real problems. It is destined to be a classic and will serve as an important reference for mathematicians, physicists, and theoretically inclined engineers working in sloshing theory and its applications.

Martin Hermann
Professor
Jena University, Germany

Preface

Almost since the earliest philosophers began the development of what we call "rational mechanics", curiously about how fluid behaves when contained in a vessel has been strong. Beginning with the oscillations of water in lakes and harbours occurring as the result of earthquakes, similar phenomena surround us at almost every turn, giving rise from modern technology as well as from the nature herself. Thus, geophysicists, civilian engineers and many other scientists have devoted themselves to studying these fascinating subjects. Our own experience in carrying a cup of tee or a bowl of soup may be frustrating unless we are very careful as to how we move, but may deceive us into believing that the "sloshing" of the fluid is simple. Indeed, it is not so. Depending on the type of disturbance and container shape, the free fluid surface can experience different types of motion including planar, non-planar, rotational (swirling), irregular beating, symmetric, asymmetric, quasi-periodic and even chaotic.

The idea of this monograph goes back to 1999 when the present authors have began their joint research work on the scientific project of the German Research Council (DFG) *"Combined Numerical-Analytical Methods for Solving Non-Classical Evolutional and Spectral Problems Arising in Fluid Sloshing Analysis"*. Being full of ambitions, we were then faced with a tough decision – should we focus on developing the Computational Fluid Dynamics (CFD) methods, which have been dominating in the literature on sloshing, or can go on our preliminary planed activities oriented toward analytical studies? Because of the disproportion in the literature, switching to the CFD-methods implied a tedious job, but provided a guaranteed numerical result. In contrast, the preliminary schedule of the applied mathematical project has promised an attractive work, which might not lead to immediate success in quantitative analysis of the fluid sloshing. The latter challenged us as professional mathematicians and, in spite of numerous obstacles and difficulties, we have decided to continue working on the 'mathematical sloshing'. The present book

reports some of most interesting and promising analytical-and-numerical results obtained within the framework of the applied mathematical DFG-project. The last author (A.N.Timokha) also acknowledges the sponsorships by the Alexander von Humboldt Foundation and the Centre for Ships and Ocean Structures (Centre of Excellence at Norwegian University of Science and Technology, Trondheim), whose financial supports made him possible to concentrate on preparation of this book.

Eisenach-Kiev-Leipzig-Jena-Trondheim,
July 2005

Iwan P. Gavrilyuk
Vladimir L. Makarov
Ivan A. Lukovsky
Alexander N. Timokha

1

Introduction

Since the early 1950's, because hydrodynamic forces and moments caused by a propellant form a dramatical feedback to the flight performance of jet vehicles, sloshing of the contained fluid has been of primary concern to aerospace engineering. As a consequence, new areas of research activities have emerged. Nowadays, the free boundary problems on fluid sloshing in moving and stationary containers are of great concern for civil and nuclear engineers, physicists, designers of road and ships tankers, and of course, applied mathematicians. The state-of-the-art is influenced by further studies of uncovered complex dynamic phenomena, primary of nonlinear nature. These include rotary waves (swirling), nonlinear interaction with solid/elastic structures, internal resonances, stochastic dynamics, hydrodynamic impact (slamming), g-jitter under micro-gravity field and cross-waves. The dynamics of liquefied natural gas (LNG) carriers and the hydrodynamic impact loads are problems of current interest to the designers of such systems. In populated cities, gasoline and other flammable tankers are prone rollover accidents while entering and exiting highways. Civil engineers have been studying sloshing effects on large dams, petroleum tanks and elevated water towers under ground motion. They also mount sloshing tanks on the roofs of multistory buildings as a means to mitigate building vibrations owing to earthquakes.

The two typical physical assumptions characterising the mathematical modelling of sloshing are that the fluid is assumed to be incompressible with irrotational flows and that there are no overturning waves. Applicability of the inviscid fluid model has been validated for smooth tanks (without internal structures, e.g. baffles) and non-shallow fluid depths. In addition, sloshing in macroscopic tanks situated under Earth-based conditions is characterised by large Bond numbers. This implies that the surface tensions can also be neglected (Myshkis *et al.* (1986) [132] and Billingham (2002) [28]). Reviews of experimental and theoretical studies dealing with sloshing have been given by Abramson (1966) [1], Abramson *et al.* (1974) [2], Narimanov *et al.* (1977) [135], Mikishev (1978) [122],

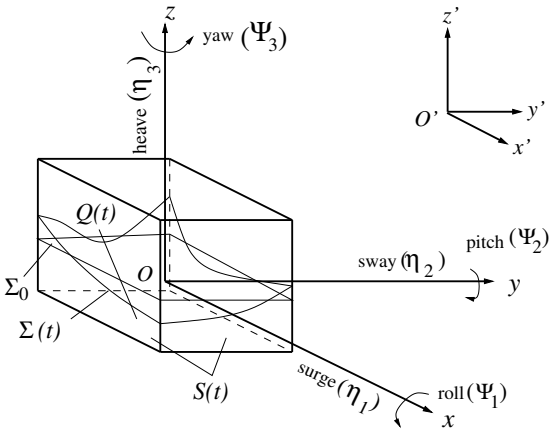

Fig. 1.1. Sketch of the fluid sloshing in a moving rectangular base tank with $\boldsymbol{v}_0 = \frac{d}{dt}(\eta_1, \eta_2, \eta_3)^T$; $\boldsymbol{\omega} = \frac{d}{dt}(\Psi_1, \Psi_2, \Psi_3)^T$. The unperturbed (hydrostatic) free surface Σ_0 is defined by the plane $z = 0$.

Mikishev & Rabinovich (1968) [124], Ibrahim *et al.* (2001,2005) [83, 82] and Faltinsen & Timokha (2000-2002) [45, 49, 50].

Derivation of the free boundary problem, which describes an inviscid fluid sloshing in a rigid tank, is outlined by Moiseev & Rumyantsev (1965) [130] and Narimanov *et al.* (1977) [135]. The problem couples the time-varying fluid domain $Q(t)$ of the constant volume V and the velocity potential $\Phi(x, y, z, t)$, which is defined inside of $Q(t)$. The domain $Q(t)$ is confined to the free boundary $\Sigma(t)$ and the wetted tank surface $S(t)$. The tank motions are described by the pair of time-dependent vectors $\boldsymbol{v}_O(t) = \dot{\boldsymbol{\eta}}(t)$ and $\boldsymbol{\omega}(t) = \dot{\boldsymbol{\Psi}}(t)$ representing instantaneous translatory and angular velocities of the mobile Cartesian coordinate system $Oxyz$ relative to an absolute coordinate system $O'x'y'z'$ (dots over $\boldsymbol{\Psi}$ and $\boldsymbol{\eta}$ denote the time-derivative) as illustrated in Figure 1.1. The problem requires either initial or (for periodic vector-functions $\boldsymbol{v}_0(t)$ and $\boldsymbol{\omega}(t)$) periodicity conditions. Physically, the initial value problem determines transient waves which are caused by combined effect of $(\boldsymbol{v}_O(t),\ \boldsymbol{\omega}(t))$ and initial perturbations of $\Sigma(t)$. The periodicity conditions imply the so-called steady-state waves.

The mathematical justification of the initial and time-periodic free boundary value problems is still an open question (even in the two-dimensional formulation). Being familiar with both former Soviet and Western literature, the present authors were not able to find rigor-

ous mathematical results for the time-periodic boundary value problem. There is only a limited set of mathematical papers that report local existence theorems for the initial boundary value problems. Almost all of these results have been documented by Shinbrot (1976) [156], Reeder & Shinbrot (1976,1979) [148, 149] and Ovsyannikov *et al.* (1985) [142]. Because of the mathematical complexity, the current studies mainly concentrate on developing the Computational Fluid Dynamics (CFD) methods. Differences and advantages of various CFD-methods have been discussed in comparative surveys by Solaas (1995) [157], Cariou and Casella (1999) [34], Gerrits (2001) [75], Ibrahim *et al.* (2001) [83], Celebi & Akyildiz (2002) [35], Sames *et al.* (2002) [153], Aliabadi *et al.* (2003) [6] and Frandsen (2004) [55].

This is a difficult mathematical problem to solve the free boundary problem on sloshing analytically. The boundary conditions at the free surface are nonlinear and the free surface varies with time in a manner not known a priory. As a result, the free surface can perform a wide spectrum of motions and demonstrate enormous set of stable and unstable dynamic regimes. Some of them are predictable by means of relatively simple engineering approaches utilising, as a rule, the concept of equivalent mechanical systems (the equivalence is taken in the sense of the same dynamic forces and moments acting on the tank wall). By properly accounting for the equivalent mechanical systems, the problem on the coupled "tank-fluid" dynamics can be reduced to small-dimensional systems of ordinary differential equations. For small-magnitude oscillations, when the free surface remains close to its hydrostatic (planar) shape Σ_0, the equivalent mechanical systems can for instance be represented by a set of mathematical pendulums or mass-spring-dashpot systems. The eigenfrequencies of these linear "pendulum" systems must coincide with the natural sloshing frequencies. Nonlinear sloshing requires to replace the systems by a compound or spherical pendulum.

Purpose of this book consists of gaining an insight into three contemporary directions of the mathematical sloshing, which are uncovered by the recent encyclopedic book by Ibrahim (2005) [82]. The first direction (represented by Chapter 2) is associated with an operator approach to the linear sloshing problems. The latter reduces the linearised evolutional boundary problem to a second-order differential operator equation. The second direction (Chapter 3) deals with weakly-nonlinear sloshing. The chapter presents some of new authors' results on the so-called nonlinear multi-modal method. The method is based on combining specific

variational and asymptotic techniques, whose fundamentals have been established by Lukovsky (1976) [113] and Miles (1976) [125]. The chapter extends the method to the tanks of complex (non-cylindrical) shape as well as documents compact modal systems, which may be adopted for description of resonant sloshing in rectangular, circular cylindrical and conical containers. Finally, Chapter 4 collects proper authors' journal publications devoted to the compressible fluid dynamics with the free surface in tanks shaking with a high frequency. This is an absolutely new area of the mathematical sloshing giving rise from modern vibrotechnology in chemical industry (the positioning of droplets), microgravity hydrodynamics and nanotechnology.

2

Evolutional operator problems in linear sloshing

2.1 Linear sloshing

This section concentrates on linear evolutional problems which describe a small-magnitude fluid sloshing in a stationary basin. The basin has cylindrical shape near the mean (hydrostatic) free surface as shown in Fig. 2.1. Details of the physical statement were discussed by John (1953) [87], Feschenko *et al.* (1969) [53], Friedmann & Shinbrot (1967) [56] and Morand & Ohayon (1995) [131].

Let $\tilde{\Omega} \in R^3$ be a closed domain (reservoir, tank, basin etc.) with an upright cylindrical endpart in the x_2-direction and $\Omega \subset \tilde{\Omega}$ be a subdomain filled by a fluid (see, Fig. 2.1). Let $\varphi(x,t)$ be the velocity potential, which is a harmonic function of the coordinates $x = (x_1, x_2, x_3)$. The velocity potential should satisfy the zero-Neumann condition, i.e. $\partial_n \varphi = \varphi_n = 0$, on the wetted tank surface Γ_1. Further, we assume that the free surface Γ is defined by the equation $x_2 = \zeta(x_1, x_3, t) + \alpha$, where α is such a constant that $x_2 = \alpha$ is the equation of the unperturbed (hydrostatic) free surface Γ_0. Using Bernoulli's integral derives the so-called dynamic condition on the free surface

$$\varphi_t + \tfrac{1}{2}(\nabla\varphi)^2 + g\zeta + g\alpha + \frac{p_0}{\rho} = const, \tag{2.1}$$

where g is the gravity acceleration, ρ is the fluid density and $p_0 = const$ is the "atmospheric" pressure. Assuming $\varphi_{x_i}, \zeta - \alpha, \zeta_{x_i},\ i = 1,2,3$ to be small, one can neglect nonlinear terms in Eq. (2.1) and trace it on Γ_0, i.e. on the plane $x_2 = \alpha$. Once doing that and substituting the final expression into the linearised kinematic condition $\zeta_t = \varphi_n$ on Γ_0, we get the following evolutional boundary problem with respect to φ:

$$\begin{aligned} &\Delta\varphi = 0 \ \text{ in } \ \Omega; \quad \varphi_n = 0 \ \text{ on } \ \Gamma_1; \quad \varphi_{tt} + g\varphi_n = f(t) \ \text{ on } \ \Gamma_0, \\ &\varphi = f_0; \quad \varphi_t = f_1 \ \text{ on } \ \Gamma_0 \ \text{ at } \ t = 0, \end{aligned} \tag{2.2}$$

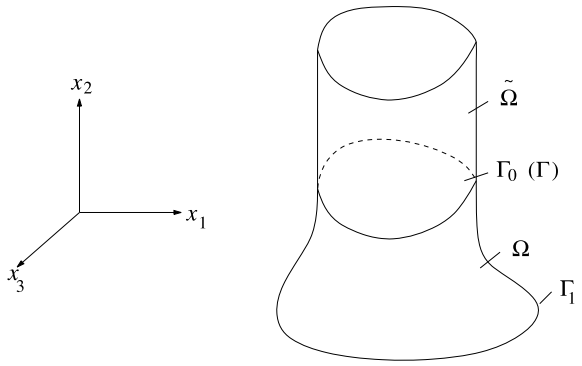

Fig. 2.1. Sketch of the tank and the adopted nomenclature.

where $f(t)$ can be cancelled ($f \equiv 0$) by the substitution $\varphi := \varphi + \tilde{\varphi}(t)$ ($\tilde{\varphi}$ is a suitable time-dependent function). The problem (2.2) contains the initial conditions introduced as follows

$$f_1(x_1, x_3) = -g(\zeta + \alpha + p_0)|_{t=0}; \quad f_0(x_1, x_3) = \varphi|_{x_2=\zeta, t=0},$$

where f_0 and f_1 are the two known functions.

By introducing the trace of the velocity potential on Γ_0 such that $u = \varphi|_{\Gamma_0}$ and considering u as a prescribed function we arrive at the Dirichlet-Neumann problem

$$\Delta\varphi = 0 \ \text{ in } \ \Omega; \quad \varphi_n|_{\Gamma_1} = 0; \quad \varphi|_{\Gamma_0} = u \tag{2.3}$$

to be solved at an instant t. The function φ depends on u uniquely and linearly so that the following linear (Poincare-Steklov) operator $\mathcal{A}$ can be defined:

$$\mathcal{A}u = g\frac{\partial\varphi}{\partial x_2}|_{\Gamma_0}, \quad u = u(x_1, x_3).$$

The condition on Γ_0 in (2.2) yields then the following Cauchy operator problem

$$\frac{\partial^2 u}{\partial t^2} + \mathcal{A}u = 0 \quad \text{on } \ \Gamma_0; \quad u(0) = u_0, \quad u'(0) = u_1, \tag{2.4}$$

where $u_0 = f_0, u_1 = f_1$.

Eq. (2.4) describes the linear sloshing. Advantages of the formulation (2.4) relative to the original boundary value problem (2.2) are (i) the

dimensionality reduction (from $\mathbb{R}^3$ to $\mathbb{R}^2$) and (ii) the possibility to apply mathematical results of the operator cosine theory. The latter will be done in the forthcoming sections.

2.2 Second order differential operator equations

The second order differential equations with an operator coefficient received a great deal of attention (see, for example, Goldstein (1984) [77] and Krein (1971) [94]) as a powerful mathematical tool to describe and study the partial differential equations. However, various representations of their solutions, e.g. semi-groups, the operator cosine (sine) functions, etc., which have been considered, are less suitable to constructing algorithmic approaches. The main goal of this section is to find explicit closed-form representations of the exact solution and their approximations, which can be easily algorithmized. More precisely, we establish a one-to-one correspondence between the continuous initial value problem and a discrete second order initial value problem with a contractive operator. Using the Laguerre and Chebyshev orthogonal polynomials, we give explicit formulae for their solutions. On the basis of these formulae we propose an algorithmic approximation possessing exponential rate of convergence, if the operator coefficient is bounded, and polynomial rate of convergence automatically depending on the smoothness of the initial data, if the operator coefficient is unbounded. One can consider our approach as a semi-discretisation of second order (in time) evolution equations which, contrary to many well known approximations (see, for example, Fujita & Suzuki (1991) [58] and Dautray & Lions (1992) [39]), automatically adapts the accuracy to the analytical properties of the exact solution.

Our approach is in some detail described by Gavrilyk & Makarov (1996,2005) [69, 72, 73], Gavrilyuk (1999) [63] and Samarskii & Makarov (2001) [152]. It is a generalisation of results by Quarteroni & Valli (1994) [147] and Tal-Ezer (1989) [161]. A similar idea was also developed by Arov *et al.* (1995) [10] for time-dependent problems of parabolic type. He considered

$$\dot{x}(t) + Ax(t) = 0, \qquad x(0) = x_0 \tag{2.5}$$

to find an algorithmic representation of the C_0-semi-groups (here, A is a bounded linear positive-defined operator in a Hilbert space H, and,

thereby, $-A$ is the infinitesimal generator of a C_0-semi-group $T(t)$). Together with (2.5), Arov *et al.* (1995) [10] introduced the discrete initial value problem

$$y_{\gamma,n+1} = T_\gamma y_{\gamma,n}, \qquad n = 0, 1, \ldots, \qquad y_0 = x_0,$$

where $T_\gamma = (\gamma I - A)(\gamma I + A)^{-1}$ is the Cayley transform of the operator A, γ is an arbitrary positive number, $\|T_\gamma\| \le q_\gamma < 1$. The solutions of the continuous and discrete initial value problems are connected by means of the formulae (one-to-one correspondence)

$$\begin{aligned} x(t) &= T(t)x_0 = \sum_{p=0}^{\infty} \varphi_p(2\gamma t) y_{\gamma,p}, \\ y_{\gamma,n} &= T_\gamma^n x_0 = (-1)^n \left[\int_0^\infty \psi_n(t) x\left(\frac{t}{2\gamma}\right) dt + x_0 \right], \end{aligned} \tag{2.6}$$

where

$$\begin{aligned} \varphi_p(2\gamma t) &= (-1)^{p+1} e^{-\gamma t} \frac{2\gamma t}{p} L_{p-1}^{(1)}(2\gamma t) = \\ &= (-1)^p e^{-\gamma t} \left[L_p^{(0)}(2\gamma t) - L_{p-1}^{(0)}(2\gamma t) \right], \\ \psi_n(t) &= -e^{-\frac{t}{2}} L_{n-1}^{(1)}(t) = e^{-\frac{t}{2}} \frac{d}{dt} L_n^{(0)}(t) \end{aligned}$$

with $L_p^{(\alpha)}(t)$ being the Laguerre polynomials (see, Szegö (1939) [160] and Suetin (1979) [159]). The corresponding formulae connecting the continuous semi-group $T(t)$ and the discrete semi-group T_γ^n are

$$\begin{aligned} T(t) &= \sum_{p=0}^{\infty} \varphi_p(2\gamma t) T_\gamma^p = e^{-\gamma t} \sum_{p=0}^{\infty} (-1)^p L_p^{(0)}(2\gamma t) T_\gamma^p (I + T_\gamma^p), \\ T_\gamma^n &= (-1)^n \left[\int_0^\infty \psi_n(t) T\left(\frac{t}{2\gamma}\right) dt + I \right]. \end{aligned}$$

As an approximation of the exact solution, one can use the truncated sum

$$x^N(t) = e^{-\gamma t} \sum_{p=0}^{N} (-1)^p L_p^{(0)}(2\gamma t)(y_{\gamma,p} + y_{\gamma,p+1}).$$

It was shown by Agmon (1962) [5] that $x^N(t)$ converges to $x(t)$ as $N \to \infty$ with a rate of geometric progression and the denominator $q_\gamma < 1$.

These results were generalised by Arov *et al.* (1995) [10], and Gavrilyuk & Makarov (1996) [68] for the case of an unbounded operator A. They showed that

$$sup_{t\in[0,\infty)}\|x(t)-x^N(t)\| \le c \begin{cases} q_\gamma^N\|x_0\|, & \text{if } A \text{ is bounded} \\ N^{-\sigma}\|A^\sigma x_0\|, & \text{if } A \text{ is self-adjoint, positive definite, } x_0 \in D(A^\sigma), \\ N^{-\sigma+\varepsilon}\|A^\sigma x_0\|, & \text{if } A \text{ is strongly positive in a Banach space, } \varepsilon \text{ is an arbitrarily small positive number, } x_0 \in D(A^\sigma). \end{cases}$$

Here and throughout the section, c denotes certain positive constants independent of N, x_0.

The idea on how to transform a second order differential equation to a discrete initial value problem and the corresponding interrelation formulae are given in the following text. We discuss a natural approximation and error estimates. An example with both temporal and spatial discretisation will be given.

2.2.1 Operator cosine function and a family of explicit representations

We consider the initial value problem

$$\ddot{x}(t) + Ax(t) = 0, \qquad x(0) = x_0, \quad \dot{x}(0) = x_0', \tag{2.7}$$

where x_0, x_0' are given elements of a Hilbert space H with the scalar product $(\cdot,\cdot)$ and the norm $\|\cdot\|$ and A is a densely defined, linear, self-adjoint, positive definite operator with the domain $D(A)$, which is the generator of the operator cosine-function $C(t)$, i.e. $(Ax,x) \ge \lambda_0\|x\|^2 \ \forall\ x \in D(A),\ A = \ddot{C}(0)$. We denote by $\rho(A)$ the resolvent set and by $\Sigma(A)$ the spectral set of the operator A. The operator sine-function $S(t)$ associated with $C(t)$ is defined by

$$S(t)f = \int_0^t C(s)f\,ds$$

. By a solution of (2.7) we mean a H-valued function $x(t)$ such that

i) $x(t)$ is continuously differentiable for $t \in [0,T]$ and the second derivative is continuous for $t \in (0,T]$;

ii) $x(t) \in D(A)$ for $t \in (0,T]$ and (2.7) is satisfied.

The operator sine- and cosine-functions are related to an initial value problem (2.7) like as the C_0-semi-groups to an initial value problem for the first order equation (2.5).

The following solution of (2.7) is given by Goldstein (1985) [77]

$$x(t) = C(t)x_0 + S(t)x_0' + \int_0^t S(t-s)f(s)ds.$$

In particular, it determines

$$x(t) = C(t)x_0 \tag{2.8}$$

as a solution of the initial value problem

$$\ddot{x}(t) + Ax(t) = 0, \qquad x(0) = x_0, \qquad \dot{x}(0) = 0. \tag{2.9}$$

We are starting from the scalar problem

$$\frac{d^2x(t)}{dt^2} + ax(t) = 0, \quad x \in (0,T]; \quad x(0) = x_0, \quad x'(0) = 0, \tag{2.10}$$

where $a > 0$ and x_0 are real numbers. The solution of (2.10) is

$$x(t) \equiv x(t;a) = \cos\sqrt{a}\, t \cdot x_0. \tag{2.11}$$

We can formally obtain a representation for $\cos\sqrt{a}\, t$ using the generating function for the Laguerre polynomials $L_n^{(\alpha)}(t)$ (Bateman & Erdeilyi (1953) [17]) as follows

$$\exp\left(-\frac{wt}{1-w}\right) = \sum_{n=0}^{\infty} L_n^{(\alpha)}(t) w^n (1-w)^{\alpha+1}, \qquad |w| < 1. \tag{2.12}$$

Set up for an arbitrary $\delta < \frac{1}{2}$

$$-\frac{w_\pm}{1-w_\pm} = \pm i\sqrt{a} + \delta, \qquad i = \sqrt{-1}. \tag{2.13}$$

Then

$$
\begin{aligned}
w_{\pm} =& \frac{\pm i\sqrt{a}+\delta}{\pm i\sqrt{a}+\delta-1} = \frac{a+\delta(\delta-1)\pm i\sqrt{a}}{a+(\delta-1)^2} = re^{\pm i\theta},\\
r^2 \equiv& r^2(a,\delta) = |w_{\pm}|^2 = (a+\delta^2)(a+(\delta-1)^2)^{-1},\\
\xi \equiv& \xi(a,\delta) = \cos\theta = (a+\delta(\delta-1))\times\\
&\times (a+\delta^2)^{-\frac{1}{2}}(a+(\delta-1)^2)^{-\frac{1}{2}},\\
\sqrt{1-\xi^2} \equiv& \sin\theta = \sqrt{a}(a+\delta^2)^{-\frac{1}{2}}(a+(\delta-1)^2)^{-\frac{1}{2}},
\end{aligned}
\tag{2.14}
$$

and we get

$$
\begin{aligned}
e^{\pm i\sqrt{a}\,t} &= e^{-\delta t}\sum_{n=0}^{\infty} L_n^{(0)}(t)\left(r^n e^{\pm in\theta} - r^{n+1}e^{\pm i(n+1)\theta}\right),\\
\cos\sqrt{a}\,t &= \frac{1}{2}\left(e^{i\sqrt{a}\,t}+e^{-i\sqrt{a}\,t}\right) =\\
&= e^{-\delta t}\sum_{n=0}^{\infty}\left[L_n^{(0)}(t) - L_{n-1}^{(0)}(t)\right] r^n\cos n\theta =\\
&= e^{-\delta t}\sum_{n=0}^{\infty} L_n^{(0)}(t)(r^n\cos\theta - r^{n+1}\cos(n+1)\theta) =\\
&= \frac{1}{2}e^{-\delta t}\sum_{n=0}^{\infty}\left[L_n^{(0)}(t) - L_{n-1}^{(0)}(t)\right](w_+^n + w_-^n),\\
\sin\sqrt{a}\,t &= \frac{1}{2i}\left(e^{i\sqrt{a}\,t}-e^{-i\sqrt{a}\,t}\right) =\\
&= -e^{-\delta t}\sum_{n=0}^{\infty}\left[L_n^{(0)}(t) - L_{n-1}^{(0)}(t)\right] r^n\sin n\theta =\\
&= \frac{1}{2i}e^{-\delta t}\sum_{n=0}^{\infty}\left[L_n^{(0)}(t) - L_{n-1}^{(0)}(t)\right](w_+^n - w_-^n).
\end{aligned}
\tag{2.15}
$$

Further, we introduce the sequences $\{u_n^{(1)}\}$ and $\{u_n^{(2)}\}$ by

$$
\begin{aligned}
u_n^{(1)} &= \frac{1}{2}(w_+^n + w_-^n) = r^n\cos n\theta = r^n T_n(\cos\theta) = r^n T_n(\xi),\\
u_n^{(2)} &= -\frac{1}{2i}(w_+^n - w_-^n) = r^n\sin n\theta = r^n\sin\theta U_{n-1}(\cos\theta) =\\
&= r^n\sqrt{1-\xi^2}U_{n-1}(\xi),
\end{aligned}
\tag{2.16}
$$

where $T_n(\xi) = \cos(n \arccos \xi)$, $U_n(\xi) = \sin((n+1)\arccos\xi)/\sqrt{1-\xi^2}$ are the Chebyshev polynomials of the first and second kind, respectively, (see, Bateman & Erdelyi (1953) [17]). Since

$$\cos(n+1)\theta - 2\cos\theta\cos n\theta + \cos(n-1)\theta = 0,$$
$$\sin(n+1)\theta - 2\cos\theta\sin n\theta + \sin(n-1)\theta = 0,$$

$\{u_n^{(1)}\}$ and $\{u_n^{(2)}\}$ admit the following recurrence formulae

$$\begin{aligned} &u_{n+1}^{(1)} - 2\xi r u_n^{(1)} + r^2 u_{n-1}^{(1)} = 0, \\ &\qquad n \geq 0, \quad u_0^{(1)} = 1, \;\; u_1^{(1)} = \xi r, \\ &u_{n+1}^{(2)} - 2\xi r u_n^{(2)} + r^2 u_{n-1}^{(2)} = 0, \\ &\qquad n \geq 0, \quad u_0^{(2)} = 0, \;\; u_1^{(2)} = r\sqrt{1-\xi^2} \equiv r\sin\theta. \end{aligned} \tag{2.17}$$

One should note that the coefficient ξr in (2.17) is given by

$$\xi r = r\cos\theta = [a + \delta(\delta-1)]\left[a + (\delta-1)^2\right]^{-1}, \tag{2.18}$$

i.e. one does not need to calculate $\sqrt{a}$ to find $\{u_n^{(1)}\}$. Finally, we can write down

$$\begin{aligned} \cos\sqrt{a}\,t &= \frac{1}{2}e^{-\delta t}\sum_{n=0}^{\infty}\left[L_n^{(0)}(t) - L_{n-1}^{(0)}(t)\right](w_+^n + w_-^n) = \\ &= e^{-\delta t}\sum_{n=0}^{\infty}\left[L_n^{(0)}(t) - L_{n-1}^{(0)}(t)\right]u_n^{(1)}, \\ \sin\sqrt{a}\,t &= \frac{1}{2i}e^{-\delta t}\sum_{n=0}^{\infty}\left[L_n^{(0)}(t) - L_{n-1}^{(0)}(t)\right](w_+^n - w_-^n) = \\ &= -e^{-\delta t}\sum_{n=0}^{\infty}\left[L_n^{(0)}(t) - L_{n-1}^{(0)}(t)\right]u_n^{(2)}. \end{aligned} \tag{2.19}$$

Returning to the abstract problem (2.9) we will show that its solution can analogously to (2.19) be represented in the form

$$\begin{aligned} x(t) \equiv x(t;A) &= (\cos\sqrt{A}\,t)x_0 = \\ &= \frac{e^{-\delta t}}{2}\sum_{n=0}^{\infty}\left[L_n^{(0)}(t) - L_{n-1}^{(0)}(t)\right](W_+^n + W_-^n)x_0 = \end{aligned}$$

$$= e^{-\delta t} \sum_{n=0}^{\infty} \left[L_n^{(0)}(t) - L_{n-1}^{(0)}(t) \right] u_n \quad (2.20)$$

and, therefore, the operator cosine-function with the generator A can be expressed as

$$C(t) \equiv \cos \sqrt{A}\, t = \frac{e^{-\delta t}}{2} \sum_{n=0}^{\infty} \left[L_n^{(0)}(t) - L_{n-1}^{(0)}(t) \right] (W_+^n + W_-^n) =$$

$$= e^{-\delta t} \sum_{n=0}^{\infty} \left[L_n^{(0)}(t) - L_{n-1}^{(0)}(t) \right] \mathcal{U}_n, \quad (2.21)$$

where

$$\begin{aligned} W_\pm =& (\pm i\sqrt{A} + \delta I)(\pm i\sqrt{A} + (\delta - 1)I)^{-1} = \\ &= \left[A + \delta(\delta - 1)I \pm i\sqrt{A} \right] \left[A + (\delta - 1)^2 I \right]^{-1}, \quad (2.22) \\ -W_\pm (I - W_\pm)^{-1} =& \pm i\sqrt{A} + \delta I, \end{aligned}$$

and the sequences of the vectors $\{u_n\}$ and the operators $\{\mathcal{U}_n\} \equiv \{\mathcal{U}_n(A)\}$ are defined by the recursion relations

$$\begin{aligned} u_{n+1} =& 2 \left[A + \delta(\delta - 1)I \right] \left[A + (\delta - 1)^2 I \right]^{-1} u_n - \\ &- \left[A + \delta^2 I \right] \left[A + (\delta - 1)^2 I \right]^{-1} u_{n-1}, \quad n \geq 1, \quad (2.23) \\ u_0 =& x_0, \quad u_1 = \left[A + \delta(\delta - 1)I \right] \left[A + (\delta - 1)^2 I \right]^{-1} x_0 \end{aligned}$$

and

$$\begin{aligned} \mathcal{U}_{n+1} =& 2 \left[A + \delta(\delta - 1)I \right] \left[A + (\delta - 1)^2 I \right]^{-1} \mathcal{U}_n - \\ &- \left[A + \delta^2 I \right] \left[A + (\delta - 1)^2 I \right]^{-1} \mathcal{U}_{n-1}, \qquad n \geq 1, \quad (2.24) \\ \mathcal{U}_0 =& I, \qquad \mathcal{U}_1 = \left[A + \delta(\delta - 1) \right] \left[A + (\delta - 1)^2 \right]^{-1}, \end{aligned}$$

respectively. Eq. (2.24) does not contain $\sqrt{A}$.

Analogously, one can define the operator sine-function with generator A by

$$S(t) \equiv \sin \sqrt{A}\, t = \frac{1}{2i} e^{\delta t} \sum_{n=0}^{\infty} \left[L_n^{(0)}(t) - L_{n-1}^{(0)}(t) \right] (W_+^n - W_-^n) =$$

$$= -e^{-\delta t} \sum_{n=0}^{\infty} \left[L_n^{(0)}(t) - L_{n-1}^{(0)}(t) \right] \mathcal{V}_n,$$

where

$$\begin{aligned} \mathcal{V}_{n+1} =& 2 \left[A + \delta(\delta - 1) I \right] \left[A + (\delta - 1)^2 I \right] \mathcal{V}_n - \\ & - \left[A + \delta^2 I \right] \left[A + (\delta - 1)^2 I \right]^{-1} \mathcal{V}_{n-1}, \quad n \geq 1, \\ \mathcal{V}_0 =& 0, \quad \mathcal{V}_1 = \sqrt{A} \left[A + (\delta - 1)^2 I \right]^{-1}. \end{aligned}$$

We can formally write down

$$\mathcal{U}_n = \mathcal{A}^n T_n(\mathcal{B}); \quad \mathcal{V}_n = \mathcal{C} \mathcal{A}^n U_{n-1}(\mathcal{B}), \tag{2.25}$$

where

$$\begin{aligned} \mathcal{A} &= \left[A + \delta^2 I \right]^{\frac{1}{2}} \left[A + (\delta - 1)^2 I \right]^{-\frac{1}{2}}, \\ \mathcal{B} &= \left[A + \delta(\delta - 1) I \right] \left[A + \delta^2 I \right]^{-\frac{1}{2}} \left[A + (\delta - 1)^2 I \right]^{-\frac{1}{2}}, \\ \mathcal{C} &= \sqrt{A} \left[A + \delta^2 I \right]^{-\frac{1}{2}} \left[A + (\delta - 1)^2 I \right]^{-\frac{1}{2}}. \end{aligned} \tag{2.26}$$

It is easy to see that

$$u_n = \mathcal{U}_n x_0 = \frac{1}{2} (W_+^n + W_-^n) x_0.$$

We introduce also the sequence of vectors

$$v_n = \mathcal{V}_n x_0 \equiv - \frac{1}{2i} (W_+^n - W_-^n) x_0$$

so that

$$\begin{aligned} (\sin \sqrt{A}\, t) x_0 = \frac{1}{2i} e^{-\delta t} \sum_{n=0}^{\infty} \left[L_n^{(0)}(t) - L_{n-1}^{(0)} \right] (W_+^n - W_-^n) x_0 = \\ = e^{-\delta t} \sum_{n=0}^{\infty} \left[L_n^{(0)}(t) - L_{n-1}^{(0)}(t) \right] u_n. \end{aligned}$$

Note, that $(\sin \sqrt{A}\ t) x_0$ can also be obtained by integration of (2.20) without the use of $\sqrt{A}$.

By formal differentiation and simple transformations of (2.20), using the relation $\frac{d}{dt}\left[L_n^{(0)}(t) - L_{n-1}^{(0)}(t)\right] = -L_{n-1}^{(0)}(t)$ (see Szegö (1939) [160] and Suetin (1979) [159]) and (2.22), we get the following series

$$\begin{aligned} x^{(1)}(t) = &- \frac{\delta}{2} e^{-\delta t} \sum_{n=0}^{\infty} \left(L_n^{(0)}(t) - L_{n-1}^{(0)}(t)\right) \left(W_+^n + W_-^n\right) x_0 - \\ &- \frac{1}{2} e^{-\delta t} \sum_{n=1}^{\infty} L_{n-1}^{(0)}(t)(W_+^n + W_-^n)x_0 = \\ =&\frac{1}{2} i\sqrt{A} e^{-\delta t} \sum_{n=0}^{\infty} \left[L_n^{(0)}(t) - L_{n-1}^{(0)}(t)\right] (W_+^n - W_-^n)x_0 = \\ =&-\sqrt{A}\sin\sqrt{A}t. \end{aligned} \tag{2.27}$$

Repeating this procedure once again we get

$$\begin{aligned} x^{(2)}(t) = &- \frac{\delta}{2} i\sqrt{A} e^{-\delta t} \sum_{n=0}^{\infty} \left[L_n^{(0)}(t) - L_{n-1}^{(0)}(t)\right] (W_+^n - W_-^n)x_0 - \\ &- \frac{1}{2} i\sqrt{A} e^{-\delta t} \sum_{n=0}^{\infty} L_{n-1}^{(0)}(t)(W_+^n - W_-^n)x_0 = \\ =&- \frac{1}{2} A e^{-\delta t} \sum_{n=0}^{\infty} \left[L_n^{(0)}(t) - L_{n-1}^{(0)}(t)\right] (W_+^n + W_-^n)x_0 = \\ =&- Ax(t). \end{aligned} \tag{2.28}$$

In order to quantify the convergence of the series (2.20), (2.27) and (2.28) in H, we need the following results:

Lemma 2.1. *Let $\delta < 0,5$ and $x_0 \in D(A^\sigma)$, $\sigma > 0$, then*

$$\begin{aligned} &\|u_n\| \le c(\sigma,\delta) n^{-\sigma} \|A^\sigma x_0\|, \quad \|Au_n\| \le c(\sigma,\delta) n^{-(\sigma-1)} \|A^\sigma x_0\|, \\ &\|v_n\| \le c(\sigma,\delta) n^{-\sigma} \|A^\sigma x_0\|, \quad \|\sqrt{A} v_n\| \le c(\sigma,\delta) n^{-(\sigma-\frac{1}{2})} \|A^\sigma x_0\|. \end{aligned}$$

If A is a bounded operator, then

$$\|u_n\| \le cq^n \|x_0\|; \quad \|v_n\| \le cq^n \|x_0\|,$$

where $q = q(\delta, A) \in (0,1)$ is a constant.

Proof. We have for an arbitrary $x_0 \in D(A^\sigma)$

$$\begin{aligned}
\|u_n\| &= \|\mathcal{U}_n x_0\| = \left\| \int_{\lambda_0}^{\infty} \lambda^{-\sigma} \chi_1^{\frac{n}{2}} T_n(\chi_2) dE_\lambda A^\sigma x_0 \right\|, \\
\|v_n\| &= \|\mathcal{V}_n x_0\| = \\
&= \left\| \int_{\lambda_0}^{\infty} \lambda^{-\sigma} \sqrt{\frac{\lambda}{(\lambda+\delta(\delta-1))^2+\lambda}}\, \chi_1^{\frac{n}{2}} U_{n-1}(\chi_2) dE_\lambda A^\sigma x_0 \right\|, \\
\|Au_n\| &= \left\| \int_{\lambda_0}^{\infty} \lambda^{-(\sigma-1)} \chi_1^{\frac{n}{2}} T_n(\chi_2) dE_\lambda A^\sigma x_0 \right\|, \\
\|\sqrt{A} v_n\| &= \left\| \int_{\lambda_0}^{\infty} \lambda^{-(\sigma-\frac{1}{2})} \sqrt{\frac{\lambda}{(\lambda+\delta(\delta-1))^2+\lambda}}\, \chi_1^{\frac{n}{2}} U_{n-1}(\chi_2) dE_\lambda A^\sigma x_0 \right\|,
\end{aligned}$$

where

$$\begin{aligned}
\chi_1 &= \frac{\lambda+\delta^2}{\lambda+(\delta-1)^2}, \\
\chi_2 &= \frac{\lambda+\delta(\delta-1)}{\sqrt{(\lambda+\delta^2)(\lambda+(\delta-1)^2)}} = \frac{\lambda+\delta(\delta-1)}{\sqrt{(\lambda+\delta(\delta-1))^2+\lambda}},
\end{aligned}$$

T_n, U_n are the Chebyshev polynomials of the first and second kind, E_λ is the spectral family associated with A. It is easy to prove that there exists a constant $c = c(\sigma, \delta)$ such that

$$|\varphi(\lambda)| \equiv |\lambda^{-\mu} \chi_1^m| \le c m^{-\mu} \ \forall\ \lambda \in [\lambda_0, \infty), \quad \mu > 0.$$

If A is a bounded operator, then $\Sigma(A) \equiv [\lambda_0, \Lambda_0]$ for a certain $\Lambda_0 < \infty$ and $\delta < 0.5$

$$|\chi_1| \le q < 1.$$

Using the inequalities

$$|T_n(\chi_2)| \le 1, \quad |U_n(\chi_2)| \le (1-\chi_2^2)^{-\frac{1}{2}} = \sqrt{\frac{(\lambda+\delta(\delta-1))^2+\lambda}{\lambda}}$$

derives the statements.
□

Furthermore, we assume that $\delta < 0.5$ and use some classical results for the Laguerre polynomials, namely, Szegö (1939) [160]:

$$t\frac{d}{dt}L_n^{(\alpha)}(t) = -tL_{n-1}^{(\alpha+1)}(t) = nL_n^{(\alpha)}(t) - (n+\alpha)L_{n-1}^{(\alpha)}(t), \tag{2.29}$$

$$L_n^{(\alpha)}(t) = \pi^{-\frac{1}{2}} e^{\frac{t}{2}} t^{-\frac{\alpha}{2}-\frac{1}{4}} n^{\frac{\alpha}{2}-\frac{1}{4}} \left[\cos(2\sqrt{nt} - \frac{\alpha\pi}{2} - \frac{\pi}{4}) + (nt)^{-\frac{1}{2}} O(1)\right],$$
$$t \in [cn^{-1}, \omega], \quad \omega < \infty, \quad \alpha > -1, \tag{2.30}$$

$$t^{\frac{\alpha}{2}+\frac{1}{4}} e^{-\frac{t}{2}} \left|L_n^{(\alpha)}(t)\right| \le cn^{\frac{\alpha}{2}-\frac{1}{4}}(1 + n^{-\frac{1}{4}} t^{\frac{5}{4}}) \ \ \forall \ \ t \ge 0, \quad \alpha + \frac{1}{2} \ge 0. \tag{2.31}$$

Useful properties of the series (2.20), (2.27), (2.28) are collected by the following auxiliary lemma:

Lemma 2.2. *Let A be a densely defined, positive definite linear operator and $x_0 \in D(A^\sigma)$, $\sigma > 0$. Then,*

1) *$\sigma > \frac{1}{4}$ implies the uniform convergence of (2.20) with respect to $t \in [0,T]$ and $x(t)$ is continuous on $[0,T]$;*

2) *$\sigma > \frac{3}{4}$ implies the uniform convergence of (2.27) with respect to $t \in [0,T]$, $x^{(1)}(t)$ is continuous on $[0,T]$ and $x^{(1)}(t) = \dot{x}(t)$;*

3) *$\sigma > \frac{5}{4}$ implies the uniform convergence of (2.28) with respect to $t \in [0,T]$, $x^{(2)}(t)$ is continuous on $[0,T]$ and $x^{(2)}(t) = \dot{x}^{(1)}(t) = \ddot{x}(t)$;*

4) *$\sigma > \frac{5}{4}$ implies $x(t) \in D(A) \ \ \forall\, t \in [0,T]$.*

Proof. It follows from (2.29) and (2.31) that

$$\left|L_n^{(0)}(t) - L_{n-1}^{(0)}(t)\right| = \frac{t}{n}\left|L_{n-1}^{(1)}(t)\right| \le$$
$$\le ct^{\frac{1}{4}} e^{\frac{t}{2}} n^{-\frac{3}{4}}(1 + n^{-\frac{1}{4}} t^{\frac{5}{4}}) = O(n^{-\frac{3}{4}}) \tag{2.32}$$

uniformly in $t \in [0,T]$. Lemma 2.1 and Eq. (2.26) imply that the series (2.20), (2.27) and (2.28) are majorized by the number series

$$c\sum_{n=1}^{\infty} n^{-(\sigma+\frac{3}{4})}, \quad c\sum_{n=1}^{\infty} n^{-(\sigma+\frac{1}{4})} \ \text{ and } \ c\sum_{n=1}^{\infty} n^{-(\sigma-\frac{1}{4})}, \tag{2.33}$$

respectively, where the first three statements of the lemma follow from.

We denote by $x^N(t)$ the truncated sum of (2.20) with $N+1$ terms. If $\sigma > \frac{5}{4}$, then

$$Ax^N(t) = e^{-\delta t} \sum_{n=0}^{N} \left(L_n^{(0)}(t) - L_{n-1}^{(0)}(t)\right) Au_n.$$

By Lemma 2.1 we get that the series

$$x_A(t) \equiv e^{-\delta t} \sum_{n=0}^{\infty} \left[L_n^{(0)}(t) - L_{n-1}^{(0)}(t) \right] Au_n = \lim_{N \to \infty} Ax^N(t)$$

converges uniformly with respect to $t \in [0, T]$ provided that $\sigma > \frac{5}{4}$. The uniform convergence of the last series as well as in Eq. (2.20) (under the assumption $\sigma > \frac{5}{4}$) and the closeness of the strongly positive operator A yield $x(t) \in D(A)$ for all $t \in [0, T]$.
□

We are now in position to show that the series (2.20) represents the solution of the problem (2.9).

Theorem 2.3. *Let the assumptions of Lemma 2.2 be satisfied and $\sigma > \frac{5}{4}$. Then, the function $x(t)$ given by (2.20) is a solution for the initial value problem (2.9).*

Proof. Since $L_n^{(0)}(0) = 1$, $L_{-1}^{(0)}(t) = 0$, one remains to show that $x(t)$ given by (2.20) satisfies the equation (2.9). The latter follows immediately from (2.20), (2.28) and Lemma 2.2.
□

Remark 2.4. The solution $x(t)$ given by (2.20) for $\sigma \in \left(\frac{1}{4}, \frac{5}{4}\right)$ is a generalised solution. The condition $x_0 \in D(A^\sigma)$ and the parameter σ characterise the regularity of x_0 and $x(t)$.

Remark 2.5. If A is a bounded operator then the series (2.20), (2.27) and (2.28) are majorized by the number series

$$c \sum_{n=1}^{\infty} n^{-\frac{3}{4}} q^n, \quad 0 < q < 1$$

provided that $x_0 \in H$. Thus, the series (2.20) represents a solution of (2.9).

2.2.2 Approximation

In this section, we study the truncated sum

$$x^N(t) = e^{-\delta t} \sum_{n=0}^{N} \left[L_n^{(0)}(t) - L_{n-1}^{(0)}(t) \right] u_n \tag{2.34}$$

as an approximate solution of the problem (2.9). The following theorem establishes the accuracy of this approximation as $N \to \infty$.

Theorem 2.6. *Let A be a densely defined, positive definite operator and $x_0 \in D(A^\sigma)$. Then*

$$\sup_{t\in[0,T]} \|x_N(t) - x(t)\| \le cN^{-(\sigma-\frac{1}{4})} \|x_0\|_{D^\sigma},$$

where $\|x_0\|_{D^\sigma} = \|A^\sigma x_0\|$.

Proof. Using Lemma 2.1 and Eq. (2.26) gives

$$\|x^N(t) - x(t)\| = \left\| e^{-\delta t} \sum_{n=N+1}^{\infty} \left[L_n^{(0)}(t) - L_{n-1}^{(0)}(t) \right] u_n \right\| \le$$

$$\le c \sum_{n=N+1}^{\infty} n^{-(\sigma+\frac{3}{4})} \|x_0\|_{D^\sigma} \le cN^{-(\sigma-\frac{1}{4})} \|x_0\|_{D^\sigma},$$

□

The domain $D(A^\theta)$ of the operator A^θ becomes a Banach space D^θ with the norm $\|x\|_{D^\theta} = \|A^\theta x\|_H$. In this space, we have, for example,

$$\|u_n\|_{D^\theta} = \left\| \int_{\lambda_0}^{\infty} \lambda^{-(\sigma-\theta)} \chi_1^{\frac{n}{2}} T_n(\chi_2) dE_\lambda A^\sigma x_0 \right\| \le cn^{-(\sigma-\theta)} \|x_0\|_{D^\sigma}$$

for $\sigma \ge \theta$. When utilising this estimate and using the scheme of the proof of Theorem 2.6, we get the following estimate:

Theorem 2.7. *Let the assumptions of Theorem 2.6 be satisfied. Then*

$$\sup_{t\in[0,T]} \left\| x^N(t) - x(t) \right\|_{D^\theta} \le cN^{-(\sigma-\theta-\frac{1}{4})} \|x_0\|_{D^\sigma}, \sigma \ge \theta.$$

Remark 2.8. If A is a bounded operator, then analogously as above we get the following estimate with an exponential decay of the error

$$\left\|x^N(t) - x(t)\right\| \leq cN^{-\frac{3}{4}}q^N\|x_0\|. \tag{2.35}$$

Remark 2.9. The operator sine-function gives rise to a solution of the following initial value problem

$$\ddot{x}(t) + Ax(t) = 0, \qquad x(0) = 0, \quad x'(0) = x_1$$

by $x(t) = -A^{-\frac{1}{2}}S(t)x_1$. Hence, the solution of (2.7) can be given by

$$x(t) = C(t)x_0 - A^{-\frac{1}{2}}S(t)x_0'. \tag{2.36}$$

Remark 2.10. Let $\tilde{x}(t)$ and $x(t)$ be solutions of the problem (2.9) related to the initial vectors $\tilde{x}_0$ and x_0. Then, proceeding as it was done above and using the estimates from Lemma 2.1 and (2.26), one gets the following stability estimate

$$\sup_{t\in[0,,T]} \|\tilde{x}(t) - x(t)\|_{D^\theta} \leq c\|\tilde{x}_0 - x_0\|_{D^\sigma}, \quad \theta \leq \sigma$$

provided that $x_0, \tilde{x}_0 \in D(A^\sigma)$, $\sigma > \frac{1}{4}$.

2.2.3 Example

Let us consider the wave equation

$$\begin{aligned} \frac{\partial^2 x}{\partial t^2} &= \frac{\partial^2 x}{\partial \xi^2}, \quad -1 < \xi < 1, \ t > 0, \quad x(t,-1) = x(t,1) = 0, \\ x(0,\xi) &= x_0(\xi), \quad \frac{\partial x(0,\xi)}{\partial t} = 0, \quad -1 < \xi < 1. \end{aligned} \tag{2.37}$$

The problem (2.37) is of the type (2.7), (2.9) with $x_0 = x_0(\xi)$, $x_0' = 0$, A acting in $H \equiv L^2(-1,1)$,

$$\begin{aligned} D(A) &= \left\{u | u \in H^2(-1,1), \ u(-1) = u(1) = 0\right\}, \\ Au &= -\frac{d^2u}{d\xi^2} \ \ \forall\, u \in D(A). \end{aligned}$$

In accordance with (2.20) we have

$$x(t,\xi) = e^{-\delta t}\sum_{p=0}^{\infty}\left(L_p^{(0)}(t) - L_{p-1}^{(0)}(t)\right)u_p(\xi), \tag{2.38}$$

where $u_{-1}(\xi) = 0$, $u_0(\xi) = x_0(\xi)$ and $u_p(\xi)$, $p \geq 1$ are the solutions of the stationary equations

$$\begin{aligned} -\frac{d^2u_1}{d\xi^2} + (\delta-1)^2u_1 &= -\frac{d^2u_0}{d\xi^2} + \delta(\delta-1)u_0, \\ u_1(-1) &= u_1(1) = 0, \\ -\frac{d^2u_{p+1}}{d\xi^2} + (\delta-1)^2u_{p+1} &= -2\frac{d^2u_p}{d\xi^2} + 2\delta(\delta-1)u_p + \\ &\quad + \frac{d^2u_{p-1}}{d\xi^2} - \delta^2u_{p-1}, \\ u_{p+1}(-1) &= u_{p+1}(1) = 0, \quad p \geq 1. \end{aligned} \tag{2.39}$$

The representations (2.38) and (2.39) define the following natural semi-discrete approximation of the problem (2.37)

$$x^N(t,\xi) = e^{-\delta t}\sum_{p=0}^{N}\left(L_p^{(0)}(t) - L_{p-1}^{(0)}(t)\right)u_p(\xi). \tag{2.40}$$

In order to get a fully discrete approximation, we discretize problems (2.39) by the Legendre collocation method. Let

$$\omega_n = \left\{\xi_i \,\middle|\, (1-\xi_i^2)\,L_n'(\xi_i) \equiv 0, \quad 0 \leq i \leq n, \quad \xi_0 = -1,\ \xi_n = 1\right\}$$

be the Gauss-Lobatto nodes, where $L_n(\xi)$ are the Legendre polynomials. We denote by I_n the interpolation operator related to ω_n, i.e.

$$I_n : C[-1,1] \to \mathbb{P}_n, \quad (I_n\varphi)(\xi_i) = u(\xi_i) \quad 0 \leq i \leq n,$$

where $\mathbb{P}_n$ is the set of polynomials of a certain degree $\leq n$. Let $\{V_n\}$ be the sequence of the $(n-1)$-dimensional subspaces of $D(A)$ defined by

$$V_n = \left\{(1-\xi^2)p_{n-2}(\xi)\,|p_{n-2}(\xi) \in \mathbb{P}_{n-2}|\right\}.$$

The operators I_n define a sequence of projection operators $\{P_n\}$, $P_n : C[-1,1] \to \mathbb{P}_n$, $D(A) \to V_n$. It is easy to see that

$$P_nAv = Av \;\forall\, v \in \mathbb{P}_n. \tag{2.41}$$

We replace equations (2.39) by the projection (collocation) equations

$$\begin{aligned}
&\hat{u}_0(\xi_j) = x_0(\xi_j),\\
&\frac{d^2\hat{u}_1(\xi_j)}{d\xi^2} + (\delta-1)^2\hat{u}_1(\xi_j) = \frac{d^2\hat{u}_0(\xi_j)}{d\xi^2} + \delta(\delta-1)\hat{u}_0(\xi_j),\\
&\frac{d^2\hat{u}_{p+1}(\xi_j)}{d\xi^2} + (\delta-1)^2\hat{u}_{p+1}(\xi_j) =\\
&= -2\,\frac{d^2\hat{u}_p(\xi_j)}{d\xi^2} + 2\delta(\delta-1)\hat{u}_p(\xi_j) +\\
&+ \frac{d^2\hat{u}_{p-1}(\xi_j)}{d\xi^2} - \delta^2\hat{u}_{p-1}(\xi_j), \quad 1 \le j \le n-1,\ p \ge 1,
\end{aligned} \tag{2.42}$$

where

$$\hat{u}_p(\xi) = (1-\xi^2)\sum_{i=0}^{n-2} a_i^{(p)}\xi^i$$

with unknown coefficients $a_i^{(p)}$, $0 \le i \le n-2$.

For each p, the equations (2.42) form a system of linear algebraic equations with respect to $a_i^{(p)}$, $0 \le i \le n-2$. The fully discrete approximate solution of (2.37) is defined by

$$x_n^N(t,\xi) = e^{-\delta t}\sum_{p=0}^{N}\left[L_p^{(0)}(t) - L_{p-1}^{(0)}(t)\right]\hat{u}_p(\xi). \tag{2.43}$$

We pose the error $z(t,\xi) = x(t,\xi) - x_n^N(t,\xi)$ as

$$z(t,\xi) = z_1(t,\xi) + z_2(t,\xi), \tag{2.44}$$

where $z_1(t,\xi) = x(t,\xi) - x^N(t,\xi)$, $\quad z_2(t,\xi) = x^N(t,\xi) - x_n^N(t,\xi)$. Owing to Theorem 2.6, we have

$$\sup_{t\in[0,T]} \|z_1(t,\cdot)\|_{L^2(-1,1)} \le cN^{-\sigma+\frac{1}{4}}\|x_0\|_{H^{2\sigma}(-1,1)} \tag{2.45}$$

under the assumption $x_0 \in D(A^\sigma) \subset H^{2\sigma}(-1,1)$.

It follows from (2.41) that

$$u_p = \mathcal{U}_p x_0, \qquad \hat{u}_p = \mathcal{U}_p P_n x_0.$$

Because $x_0 - P_n x_0 \in D(\sqrt{A})$ (see, for example, Löström (1992) [108]), one gets

$$z_2(t,\xi) = \int_{\lambda_0}^{\infty} \kappa(t,\lambda) dE_\lambda \left((A^{\frac{1}{2}}(x_0 - P_n x_0) \right),$$

$$\kappa(t,\lambda) = e^{-\delta t} \sum_{p=0}^{N} \left[L_p^{(0)}(t) - L_{p-1}^{(0)}(t) \right] \left(\frac{\lambda + \delta^2}{\lambda + (\delta - 1)^2} \right)^{\frac{p}{2}} \lambda^{-\frac{1}{2}} \times \tag{2.46}$$

$$\times T_p \left(\frac{\lambda + \delta(\delta - 1)}{\sqrt{(\lambda + \delta(\delta - 1))^2 + \lambda}} \right),$$

where E_λ is the spectral family associated with A. Proceeding as it was done in the proof of Lemma 2.1 and using (2.26), we get

$$|\kappa(t,\lambda)| \leq c \sum_{p=1}^{N} p^{-\frac{5}{4}} \leq c_1,$$

which yields (together with Eq. (2.46))

$$\sup_{t\in[0,T]} \|z_2(t,\cdot)\|_{L^2(-1,1)} \leq c \left\| A^{\frac{1}{2}}(x_0 - P_n x_0) \right\|_{L^2(-1,1)} \leq$$

$$\leq c \|x_0 - P_n x_0\|_{H^1(-1,1)}. \tag{2.47}$$

The following estimate holds for $P_n \equiv I_n$ (see Bernardi & Maday (1992)[22])

$$\|x_0 - P_n x_0\|_{H^k(-1,1)} \leq c n^{k-2\sigma} \|x_0\|_{H^{2\sigma}(-1,1)}. \tag{2.48}$$

Now, we get from (2.44), (2.45), (2.47) and (2.48)

$$\sup_{t\in[0,T]} \|x_n^N(t,\cdot) - x(t,\cdot)\|_{L^2(-1,1)} \leq c \left(N^{-\sigma+\frac{1}{4}} + n^{1-2\sigma} \right) \|x_0\|_{H^{2\sigma}(-1,1)}$$

provided that $x_0 \in D(A^\sigma)$.

Using the representation

$$z_2(t,\xi) = \int_{\lambda_0}^{\infty} \kappa_1(t,\lambda) dE_\lambda (x_0 - P_n x_0)$$

with $\kappa_1(t,\lambda) = \sqrt{\lambda}\kappa(t,\lambda)$ and the estimate

$$|\kappa_1(t,\lambda)| \leq c \sum_{p=1}^{N} p^{-\frac{3}{4}} \leq c N^{\frac{1}{4}},$$

we get (analogously to (2.2.3))

$$\sup_{t\in[0,T]} \|x_n^N(t,\cdot) - x(t,\cdot)\|_{L^2(-1,1)} \le c\left(N^{-\sigma+\frac{1}{4}} + N^{\frac{1}{4}} n^{-2\sigma}\right) \|x_0\|_{H^{2\sigma}(-1,1)}$$

provided that $x_0 \in D(A^\sigma)$.

Let us compare the asymptotic complexity of the scheme (2.43) with the conditionally stable (under the condition $\tau = ch$) explicit difference scheme of the accuracy order $O(h^2 + \tau^2)$. First, assume that the spatial grid consists of $n = 1/h$ equidistant points. To get the approximate solution at a fixed point $t = t^*$ with a given tolerance $\varepsilon \sim c(h^2 + \tau^2) \sim 2c\tau^2$, one has to do $N \sim t^*/\tau$ steps performing $cn \sim c\tau^{-1}$ arithmetical operations in each step. Hence, the complexity of the finite difference method, which we define as the number of arithmetical operations necessary for computing the approximate solution at a single fixed point, is $N_{FD} \sim t^*/\tau^2 \sim 2t^*c/\varepsilon$ (note that N_{FD} increases together with t^*). In order to balance the contribution of both discretisation parameters into the error of the scheme (2.43), we choose $N \sim n^2$. Then we have $\varepsilon \sim 2c_1 n^{-2\sigma+\frac{1}{2}}$. We must solve $\sim n^2$ systems of the linear algebraic equations (2.42) of the order n. Using the Gauss elimination, we have to carry out $\sim n^3$ operations for the first system, $\sim n^2$ operations for each of the next systems and $\sim n^4$ operations in order to calculate all the vectors $\hat{u}_p$, $p = 0, ..., N$ as well as $\sim n^2$ operations to calculate the Laguerre polynomials. Hence, the complexity of our method is $N_{CT} \sim n^4 \sim (2c_1/\varepsilon)^{\frac{4}{2\sigma-1/2}}$ (independent of t^*). We can see that for a sufficiently large σ, i.e. for the smooth initial data, we have $N_{CT} \ll N_{FD}$. Numerical experiments with smooth initial functions (for example, with $x_0(\xi) = \sin\pi\xi$ and $x_0(\xi) = \sin\pi\xi + \frac{1}{2}\sin 3\pi\xi$) confirm this conclusion.

Remark 2.11. One can get spectral discretisation without the assumption $x_0 \in D(A^\sigma)$, which admits $N \equiv N(n)$. To this end, we use a semi-discrete spectral approximation in space, for example, for the problem (2.37),

$$\ddot{x}_n(t) + A_n x_n(t) = 0, \quad x_n(0) = I_n x_0, \quad x'(0) = 0$$

with an accuracy estimate

$$\|x_n(t) - u\| \le cn^{2\sigma} \|x_0\|_{H^{2\sigma}},$$

where $x_0 \in H^{2\sigma}(-1,1)$, A_n is the collocation Gauss-Legendre approximation of the spatial operator, I_n is the related interpolation operator

by Quarteroni & Valli (1994) [147]. Further, we define the fully discrete approximation by

$$x_n^N(t) = e^{-\delta t} \sum_{p=0}^{N} \left[L_p^{(0)}(t) - L_{p-1}^{(0)}(t) \right] \hat{u}_p,$$

where $\hat{u}_p$ are the solutions of equations (2.42). Though A_n is not a self-adjoint operator, one can show that (Gavrilyuk & Makarov (1996) [68])

$$\|x_n^N - x_n\| \le cq^N \|x_0\|$$

where $q = 1 - cn^{-\mu}$, μ is a positive constant depending on δ and the spectrum of A_n. Thus,

$$\|x_n^N - x\| \le c(n^{-2\sigma} + (1 - cn^{-\mu})^N) \|x_0\|_{H^{2\sigma}}.$$

Choosing $N \sim n^{\mu+\varepsilon}$ for a positive ε, we get the method with spectral accuracy with respect to n.

Remark 2.12. Another way to overcome the demanding condition $x_0 \in D(A^\sigma)$ within the framework of the concept of adaptive algorithms consists of finding an $\tilde{x}_0 \in D(A^\sigma)$ (see, Remark following (2.36)), which approximates x_0 depending on the regularity of x_0, and, therewith, to solve the problem (2.9) with $x(0) = \tilde{x}_0$ by the presented algorithm. This makes it possible to use the following adaptive procedure for the Dirichlet boundary conditions.

Let N_0 be a fixed integer and ξ_j^α, $1 \le j \le N_0$ be the zeros of the Jacobi polynomials

$$J_{N_0}^\alpha(\xi) \equiv \frac{\Gamma(\alpha+1)}{\Gamma(2\alpha+1)} \frac{\Gamma(N_0+2\alpha+1)}{\Gamma(N_0+\alpha+1)} P_{N_0}^{(\alpha,\alpha)}(\xi),$$

which are connected with the Gegenbauer polynomials $G_n^\lambda(\xi)$ by

$$J_{N_0}^\alpha(\xi) = G_{N_0}^{(\alpha+\frac{1}{2})}(\xi).$$

We denote by $i_{N_0-1}^\alpha$ the interpolation operator related to $\{\xi_j^\alpha\}$, i.e.

$$i_{N_0-1}^\alpha \varphi \in \mathbb{P}_{N_0-1}, \quad (i_{N_0-1}^\alpha \varphi)(\xi_j^\alpha) = \varphi(\xi_j^\alpha), \ \ 1 \le j \le N_0 \ \ \forall \ \ \varphi \in C[-1,1].$$

Let $\alpha > -1$,

$$H^0_\alpha(-1,1) \equiv L^2_\alpha(-1,1) = \left\{ v \,\middle|\, \|v\|^2_{0,\alpha} = \int_{-1}^{1} v^2(\xi)\rho_\alpha(\xi)d\xi < +\infty \right\},$$

$$H^k_\alpha(-1,1) = \{v : \|v\|^2_{k,\alpha} = \sum_{l=0}^{k} \|v^{(l)}\|^2_{0,\alpha} < +\infty\}, \quad k \geq 1$$

be the Sobolev spaces associated with the measure $\rho_\alpha(\xi)d\xi = (1-\xi^2)^\alpha d\xi$, and define $H^s_\alpha(-1,1)$ for a real s by interpolation of Bernardi & Maday (1992) [22]. Henceforth, let k be equal to $\frac{m}{2}$ or $\frac{m+1}{2}$ for any integer $m \geq 1$ and assume that $-1 < \alpha < 1$. Then, for any real number $\sigma > \max\{\frac{1}{2}, \frac{1+\alpha}{2}\}$ and for any φ such that $(1-\xi^2)^k\varphi$ belongs to $H^\sigma_\alpha(-1,1)$, the following result is known (Bernardi & Maday (1992) [22], p.98)

$$\left\| (1-\xi^2)^k (\varphi - i^{\alpha+m}_{N_0-1}\varphi) \right\|_{0,\alpha} \leq c N_0^{\frac{1}{2}-\sigma} \left\| (1-\xi^2)^k \varphi \right\|_{\sigma,\alpha}. \tag{2.49}$$

Now, consider $x_0(\xi)$ from (2.37), which belongs to $H^{2\sigma}(-1,1)$, but x_0 does not belong to $D(A^\sigma)$ for $\sigma > 1$. To simplify the exposition, we assume that $\sigma = 2s$ for an integer s (the case $\sigma \in \mathbb{R}$ can be regarded analogously using results by Löström (1992) [108]). The domain of the operator A^σ consists of all $u \in H^{2\sigma}(-1,1)$ such that $u^{(2j)}(-1) = u^{(2j)}(1) = 0$, $0 \leq j \leq \sigma - 1$.

We choose $\alpha = 0$ and $k = 2\sigma - 1$, i. e. $m = 4\sigma - 2$. Then, we have

$$x_0(\xi) = (1-\xi^2)^k \varphi(\xi), \quad \varphi(\xi) = (1-\xi^2)^{-k} x_0(\xi)$$

and $(1-\xi^2)^k\varphi$ belongs to $H^{2\sigma}(-1,1) \equiv H^{2\sigma}_0(-1,1)$. Obviously, it holds

$$\tilde{x}_0(\xi) \equiv (1-\xi^2)^k i^m_{N_0-1}\varphi \in D(A^\sigma)$$

and owing to (2.49)

$$\|\tilde{x}_0 - x_0\|_{L^2(-1,1)} = \left\| (1-\xi^2)^k (\varphi - i^m_{N_0-1}\varphi) \right\|_{L^2(-1,1)} \leq$$
$$\leq c N_0^{\frac{1}{2}-2\sigma} \|x_0\|_{H^{2\sigma}(-1,1)}.$$

Due to Remark 2.10, we have

$$\sup_{t\in[0,T]} \|\tilde{x}(t) - x(t)\| \leq c N_0^{\frac{1}{2}-2\sigma} \|x_0\|_{H^{2\sigma}(-1,1)}$$

and, therefore, the results of Theorems 2.6 and 2.7 hold true for the problem (2.9) with the solution $\tilde{x}(t)$, $\tilde{x}(0) = \tilde{x}_0$.

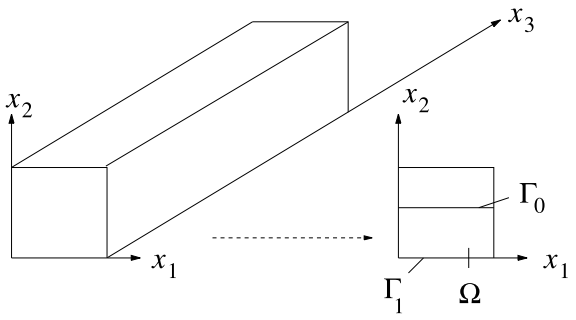

Fig. 2.2. Sketch of a chute and adopted denoting

2.3 Linear sloshing in an infinite chute

Let $\phi(x,t)$ be the velocity potential, which is a harmonic function in the region (reservoir, tank) $\tilde{\Omega} = \{x : 0 \le x_1 \le 2\pi,\ 0 \le x_2 \le \zeta + 2\pi, -\infty \le x_3 \le +\infty\}$. We assume that the free surface is defined by the equation $x_2 = \zeta(x_1, x_3, t) + 2\pi$. As described in the beginning of this chapter, when adopting the linear sloshing theory, one can neglect nonlinear terms in the boundary conditions and trace them on the unperturbed free surface, i.e. on the plane $x_2 = 2\pi$. The potential is then taken to be defined in the known domain $\Omega = \{x : 0 \le x_\alpha \le 2\pi,\ \alpha = 1, 2, -\infty \le x_3 \le +\infty\}$. We denote $\Gamma_0 = \{x : 0 \le x_1 \le 2\pi,\ -\infty \le x_3 \le +\infty,\ x_2 = 2\pi\}$, $\Gamma_1 = \Gamma \setminus \Gamma_0$, where Γ is the entire boundary of Ω (see, Fig. 2.2). For brevity, we also assume $g = 1$. In accordance with procedure from the introductory part of the chapter, we arrive at the following mathematical problem

$$\frac{d^2u}{dt^2} + \mathcal{A}u = 0 \quad \text{on} \quad \Gamma_0; \qquad u(0) = u_0, \quad u'(0) = u_1, \tag{2.50}$$

with the Poicaré-Steklov operator $\mathcal{A}u = \frac{\partial\varphi}{\partial x_2}|\Gamma_0$, where $u : \mathbb{R}_+ \to H$ is a vector-valued function and $u_0 = f_0,\ u_1 = f_1$.

If we consider an infinite (in the x_3-direction) chute as the domain $\tilde{\Omega}$, functions f_0, f_1 may be independent of x_3 and the pressure p may also be independent of t. As a result, we get the two-dimensional sloshing problem in the rectangle (see, Fig. 2.2) $\Omega \equiv \Omega_{2\pi} = \{x = (x_1, x_2) : 0 \le x_\alpha \le 2\pi,\ \alpha = 1, 2\}$ and its analogy, namely, the homogeneous one-dimensional evolution problem (2.50) on $\Gamma_0 = \{x = (x_1, 2\pi) : 0 \le x_1 \le 2\pi\}$.

In order to solve (2.50) numerically, one has to discretize both the time derivative (temporal discretisation) and the operator $\mathcal{A}$ (spatial discretisation). The finite difference methods are often used for the temporal discretisation that implies a fixed convergence rate with respect to the temporal discretisation parameter even though the exact solution is infinitely differentiable. This was done by Ashralyev & Sobolev (1994) [12], Branble *et al.* (1977) [30], Fujita & Susuki (1991) [58], Quarteroni & Valli (1994) [147] and Samarsky (1984) [151]. A broad range of applications and a convenient algorithmic "step-by-step"-structure are advantages of these discretisations.

New methods of the temporal discretisation based on the Cayley transform (CT-methods) were recently developed by Arov & Gavrilyuk (1993) [11], Arov *et al.* (1995) [10], Garipov (1967) [62] and Amosov (1990) [7] for the first order evolution equations and by Gavrilyuk & Makarov (1999) [70] for the second order equations. These methods preserve all the advantages of the finite difference methods in the case of time-independent operators and, in addition, have the remarkable property that the convergence rate with respect to a temporal parameter is either exponential (for the analytical solution) or polynomial, which depends automatically on the smoothness of the exact solution (spectral property).

Various methods of the spatial discretisation for evolution equations with a linear integral operator coefficient including the boundary element and the boundary collocation methods are presented by Amosov (1990) [7], Kress (1989) [95], Kress & Sloan (1993) [97] and Schatz *et al.* (1990) [154]. These showed that the collocation methods provide exponential convergence for the analytical initial data. Gavrilyuk *et al.* (1998) [71] used a combination of the CT-method with a trigonometric collocation method to get a fully discrete approximation for the first order evolution problem with a spatial pseudo-differential operator coefficient. This method has the spectral property with respect to both the temporal and spatial discretisation parameters.

The goal of this section is to study the problem (2.50) and to combine the CT-method by Gavrilyuk & Makarov (1999) [70] with special trigonometric collocation method to obtain a fully discrete spectral approximation (see, Gavrilyuk *et al.* (2001) [64]). By using an explicit representation of the exact solution by the CT-method, we reduce the problem (2.50) to a sequence of stationary recurrence relations of the second order. Further, a collocation procedure for the discretisation of these equations using a

trigonometric interpolation adapted for the operator $\mathcal{A}$ will be proposed. This interpolation and its estimates constitute the subject of § 2.3.2. The linear sloshing in a chute will be analysed in § 2.3.1, but sloshing in tanks with a horizontal baffle (rib) will be studied in § 2.3.3. The fully discrete approximation for the latter case will be justified in § 2.3.3.

2.3.1 Operator formulation for linear sloshing in a chute

We consider the problem (2.3) and, by using the separation of variables, derive that the solution of (2.3) can be presented as

$$\phi(x) = \frac{1}{2\pi}\int_0^{2\pi} u(\xi)d\xi + \frac{1}{\pi}\int_0^{2\pi} u(\xi)\tilde{K}(x,\xi)d\xi$$

with

$$\tilde{K}(x,\xi) = \sum_{n=1}^{\infty} \frac{1}{\cosh n\pi} \cosh\frac{nx_2}{2}\cos\frac{nx_1}{2}\cos\frac{n\xi}{2}.$$

Because the functions $F = \left\{\frac{1}{\sqrt{2\pi}}, \left\{\frac{1}{\sqrt{\pi}}\cos\frac{n\xi}{2}\right\}_{n=1}^{\infty}\right\}$ are orthonormal on $[0, 2\pi]$, denoting x_1 by x gives the following representation of the operator $\mathcal{A}$

$$(\mathcal{A}u)(x) = \frac{1}{\pi}\int_0^{2\pi} u(\xi)K(x,\xi)d\xi, \tag{2.51}$$

where

$$K(x,\xi) = \sum_{n=1}^{\infty} \frac{n}{2}\tanh n\pi \cos\frac{nx}{2}\cos\frac{n\xi}{2}. \tag{2.52}$$

Alternatively, the problem (2.50) can also read as

$$\frac{\partial^2 u(x,t)}{\partial t^2} + \frac{1}{2\pi}\int_0^{2\pi} u(\xi,t)\sum_{n=1}^{\infty} n\tanh n\pi\cos\frac{nx}{2}\cos\frac{n\xi}{2}d\xi = 0,$$

$$x \in [0,2\pi]\ \ u(x,0) = u_0(x), \quad \frac{\partial u(x,0)}{\partial t} = 0.$$

The operator $\mathcal{A}$ defined by (2.51) is self-adjoint and nonnegative definite. It is easy to show that its eigenvalues are $\lambda_k = \frac{k}{2}\tanh k\pi$ with the corresponding eigenfunctions $v_k(x) = \cos\frac{kx}{2}$, $k = 0, 1, \ldots$. Either piecewise continuous function $\varphi(x)$ defined on $[0, 2\pi]$ with $\varphi'(0) = \varphi'(2\pi) = 0$ can always be represented by the Fourier series

$$\frac{\hat\varphi_0}{2}+\sum_{k=1}^{\infty}\hat\varphi_k\cos\frac{kx}{2}\ \text{with}\ \begin{cases}\hat\varphi_0=\frac{1}{2\pi}\int_0^{2\pi}\varphi(x)dx;\\ \hat\varphi_k=\frac{1}{\pi}\int_0^{2\pi}\varphi(x)\cos\frac{kx}{2}dx,\end{cases}$$

which converges to $\varphi(x)$ at the points of continuity and to $(\varphi(x+0)+\varphi(x-0))/2$ at the points of discontinuity. Outside of the interval $[0,2\pi]$, this series converges to the even periodical extension of $\varphi(x)$.

Let us extend $u(x)$ even onto the interval $[0,4\pi]$ and then periodically onto $(-\infty,\infty)$. We denote this extension by $\tilde v(x)$. The function $v(x)=\tilde v(2x)$ has the following properties: **(a)** $v(x)$ is 2π-periodic; **(b)** $v(x)$ is even with respect to the point π, i.e. $v(x)=v(2\pi-x)$; **(c)** $u(x)=v(\frac{x}{2}),\ x\in[0,2\pi]$.

It is easy to see that the Fourier coefficients

$$\hat u_k=\frac{1}{\pi}\int_0^{2\pi}u(x)\cos\frac{kx}{2}dx,\quad \hat v_k=\frac{1}{2\pi}\int_0^{2\pi}v(x)e^{-ikx}dx,\quad k\neq 0$$

are connected by the relations $\hat u_k=4\hat v_k$,

$$\hat u_0=\frac{1}{2\pi}\int_0^{2\pi}u(x)dx=\frac{1}{2\pi}\int_0^{2\pi}v(x)dx=\hat v_0$$

and $\hat v_k=\hat v_{-k}$. If $\tilde v\in H^s[0,4\pi]$, then $v\in H^s[0,2\pi]$ and

$$\|v\|_p^2=\sum_{m=-\infty}^{\infty}(1+m^2)^p|\hat v_m|^2=2\sum_{m=1}^{\infty}(1+m^2)^p|\hat v_m|^2+|\hat v_0|^2=$$
$$=\tfrac12\sum_{m=1}^{\infty}(1+m^2)^p|\hat u_m|^2+|\hat u_0|^2$$

for the Sobolev norm of v.

Since

$$\mathcal{A}u=\frac{1}{\pi}\int_0^{2\pi}u(\xi)\sum_{n=1}^{\infty}\frac{n}{2}\tanh n\pi\cos\frac{nx}{2}\cos\frac{n\xi}{2}d\xi=$$
$$=\sum_{n=1}^{\infty}\frac{n}{2}\tanh n\pi\cdot\hat u_n\cos\frac{nx}{2},$$

we see that $\mathcal{A}:H^p\to H^{p-1}$ (for all $p\in\mathbb{R}$) is an even pseudo-differential operator of the order 1.

2.3.2 Interpolation operators and a discrete model

To discretize the operator $\mathcal{A}$ by an quadrature collocation method, we will need a suitable interpolation procedure. Because of special structure of the kernel (2.52), the use of the trigonometric interpolation polynomials by Amosov (1990) [7], Kress (1989) [95] and Kress & Sloan (1993) [97] leads to a matrix discretisation $\mathcal{A}_N$ with elements appearing as infinite series (a consequence of the fact that the corresponding trigonometric polynomials are not invariant with respect to $\mathcal{A}$). That is why, we use the following class $\hat{\mathbf{T}}_N$ of the trigonometric polynomials:

$$p(x) = \sum_{k=0}^{2N-1} \alpha_k \cos \frac{kx}{2},$$

which is not a subset of the polynomials by Amosov (1990) [7], Kress (1989) [95] and Kress & Sloan (1993) [97].

Our error analysis below (see, Theorem 2.13) shows that, contrary to the optimal order $\mathcal{O}(N^{q-p})$ for the interpolation polynomials by Amosov (1990) [7], Kress (1989) [95] and Kress & Sloan (1993) [97], the optimal convergence rate of our method in the scale of the Sobolev norms is $\mathcal{O}(N^{q-p+\frac{1}{2}})$. This is a consequence of the fact that the second sum in $\hat{R}_{N,m}$ is independent of m. The sum vanishes when the function $u(x)$ defined on $[0, 2\pi]$ is odd with respect to the middle point $x = \pi$. For this subset of functions we get the convergence order $\mathcal{O}(N^{q-p})$.

Let $\omega_N = \{x_j \equiv x_j^{(N)} = \frac{j\pi}{N},\ j = 0, 1, \cdots 2N-1\}$ be a portion of the interval $[0, 2\pi]$ and $u(x)$ be a function defined on $[0, 2\pi]$. We define the interpolation operator $\hat{P}_N$ and the interpolation polynomial $\hat{I}_N(x; u)$ by

$$\hat{P}_N : C[0, 2\pi] \to \hat{\mathbf{T}}_N, \quad u \to \hat{I}_N(x; u) : \hat{I}_N\left(x_j^{(N)}; u\right) = u\left(x_j^{(N)}\right), \quad j = 0, 1, ..., 2N-1.$$

To find an explicit representation of $I_N(x; u)$, we use the following simple relations

$$t_{kl} \equiv \sum_{j=0}^{2N-1} \cos \frac{kx_j}{2} \cos \frac{lx_j}{2} = \begin{cases} 2N, & k = l = 0, \\ N, & k = l \neq 0, \\ \dfrac{1 - (-1)^{k+l}}{2}, & k \neq 0, \end{cases}$$

$$\sum_{j=0}^{2N-1} \cos \alpha j = \mathrm{Re} \sum_{j=0}^{2N-1} e^{i\alpha j} = \mathrm{Re} \frac{1 - e^{2i\alpha N}}{1 - e^{i\alpha}},$$

$$\sum_{j=0}^{2N-1} (-1)^j \cos \alpha j = \mathrm{Re} \frac{1 - e^{2i\alpha N}}{1 + e^{i\alpha}},$$

$$\sum_{j=0}^{2N-1} (-1)^j \cos \frac{kx_j}{2} \cos \frac{\mu x_j}{2} = \frac{1 - (-1)^{k+\mu}}{2}.$$

Let us define the matrix S by

$$S = \left[\cos \frac{(i-1)(j-1)\pi}{2N} \right]_{i,j=1,\ldots,2N}. \tag{2.53}$$

Note, that S is not orthogonal matrix and, therefore, it can be inversed explicitly in the usual way. Denoting the interpolation conditions as $\hat{I}_N(x;u) = \sum_{k=0}^{2N-1} d_k \cos \frac{kx}{2}$ leads to the equations

$$\sum_{k=0}^{2N-1} d_k \cos \frac{k}{2} x_j = u_j, \quad j = 0, 1, ..., 2N-1$$

or, in the matrix form, to

$$\mathbf{d} = S^{-1}\mathbf{u} \tag{2.54}$$

with $\mathbf{d} = (d_0, ..., d_{2N-1})$, $\mathbf{u} = (u_0, ..., u_{2N-1})$. It is easy to check that $S^{-1} =$

$$= \frac{1}{N} \begin{pmatrix} 0 & 1 & 0 & \cdots & 1 \\ 1 & -1 + \cos \frac{\pi}{2N} & 1 + \cos \frac{2\pi}{2N} & \cdots & -1 + \cos \frac{2N-1}{2N}\pi \\ 0 & 1 + \cos \frac{2\pi}{2N} & -1 + \cos \frac{4\pi}{2N} & \cdots & 1 + \cos \frac{2(2N-1)}{2N}\pi \\ \cdots & \cdots & \cdots & \cdots & \cdots \\ 1 & -1 + \cos \frac{2N-1}{2N}\pi & 1 + \cos \frac{2(2N-1)}{2N}\pi & \cdots & -1 + \cos \frac{(2N-1)^2}{2N}\pi \end{pmatrix}$$

and, as consequence,

$$d_0 = \frac{1}{N}\sum_{k=1}^{N} u_{2k-1};$$

$$d_{2p} = \frac{1}{N}\sum_{k=1}^{2N-1}\left[(-1)^{k+1} + \cos\frac{2pk\pi}{2N}\right]u_k,\ p = 1,\dots,N-1,$$

$$d_{2p-1} = \frac{1}{N}u_0 + \frac{1}{N}\sum_{k=1}^{2N-1}\left[(-1)^{k} + \cos\frac{(2p-1)k\pi}{2N}\right]u_k,\quad p = 1,\dots,N,$$

Additionally, we can write the Lagrange representation of the trigonometric interpolation polynomials

$$\hat{I}_N(x;u) = \sum_{n=0}^{2N-1} \hat{l}_n^{(N)}(x)u_n \tag{2.55}$$

with the fundamental interpolation polynomials $\hat{l}_n^{(N)}(x)$ given by

$$\hat{l}_0^{(N)}(x) = \frac{1}{N}\sum_{p=1}^{N}\cos\frac{2p-1}{2}x; \qquad \hat{l}_m^{(N)}(x) = \frac{1-(-1)^m}{2N} +$$

$$+\frac{1}{N}\sum_{p=1}^{2N-1}\cos\frac{px}{2}\left[\cos\frac{pm\pi}{2N} + (-1)^{p+m-1}\right],\quad m = 1,2,...,2N-1.$$

Now, we are in the position to prove the following result:

Theorem 2.13. *For the trigonometric interpolation polynomial $\hat{I}_N$ the error estimate*

$$\|u - \hat{I}_N(\cdot;u)\|_q \le cN^{q-p+\frac{1}{2}}\|u\|_p,\quad 0 \le q \le p,\ \frac{1}{2} < p \tag{2.56}$$

holds provided that $v \in H^p$, where c is a constant depending on p and q.

Proof. We have for $m = 2sN+\mu,\ 0 \le \mu < 2N,\ s = 0,1,...$ that $\cos\frac{mx_j}{2} = (-1)^{sj}\cos\frac{\mu x_j}{2}$ and

$$I_N\left(x;\cos\frac{mx}{2}\right) = \begin{cases} \cos\frac{\mu x}{2}, & s-\text{even} \\ \cos\frac{2N-\mu}{2}x, & s-\text{odd},\ \mu \ne 0 \\ 2\sum\limits_{p=1}^{2N-1}(-1)^{p-1}\cos\frac{px}{2} - 1, & s-\text{odd},\ \mu = 0. \end{cases}$$

The interpolation error can be represented by

$$\hat{R}_N(x) = u - \hat{I}_N(x;u) = \sum_{s=0}^{\infty}\sum_{\mu=0}^{2N-1} \hat{u}_{2sN+\mu} \cos\frac{2sN+\mu}{2}x -$$
$$- \sum_{s=0}^{\infty}\sum_{\mu=0}^{2N-1} \hat{u}_{4sN+\mu} \cos\frac{\mu x}{2} -$$
$$- \sum_{s=1}^{\infty}\sum_{\mu=0}^{2N-1} \hat{u}_{2(2s-1)N+\mu} \hat{I}_N\left(x; \cos\frac{2(2s-1)N+\mu}{2}x\right) =$$
$$= \sum_{s=1}^{\infty}\sum_{\mu=0}^{2N-1} \hat{u}_{2sN+\mu} \cos\frac{2sN+\mu}{2}x - \sum_{s=1}^{\infty}\sum_{\mu=0}^{2N-1} \hat{u}_{4sN+\mu} \cos\frac{\mu x}{2} -$$
$$- \sum_{s=1}^{\infty}\sum_{\mu=0}^{2N-1} \hat{u}_{4sN-\mu} \cos\frac{\mu x}{2} - 2\sum_{s=1}^{\infty} \hat{u}_{2(2s-1)N}\left[\sum_{p=1}^{2N-1}(-1)^{p-1}\cos\frac{px}{2} - \frac{1}{2}\right].$$

For the Fourier coefficients $\hat{R}_{N,m}$ of $\hat{R}_N(x)$ we get

$$\hat{R}_{N,m} = \hat{u}_m, \quad m \geq 2N;$$
$$\hat{R}_{N,0} = -\sum_{s=1}^{\infty}\hat{u}_{4sN} + \sum_{s=1}^{\infty}\hat{u}_{2(2s-1)N} = -\sum_{s=1}^{\infty}(-1)^s\hat{u}_{2sN},$$
$$\hat{R}_{N,m} = -\sum_{s=1}^{\infty}(\hat{u}_{4sN+m} + \hat{u}_{4sN-m}) - 2(-1)^{m-1}\sum_{s=1}^{\infty}\hat{u}_{2(2s-1)N},$$
$$m = 1, \ldots, 2N-1$$

and

$$\|R_N\|_q^2 \equiv 2\sum_{m=1}^{\infty}(1+m^2)^q|\hat{R}_{N,m}|^2 + |\hat{R}_{N,0}|^2 = S_1 + S_2 + S_3,$$

where

$$S_1 = 2 \sum_{m \geq 2N} (1+m^2)^q |\hat{u}_m|^2; \qquad S_3 = \left| \sum_{s=1}^{\infty} (-1)^s \hat{u}_{2sN} \right|^2,$$

$$S_2 = 2 \sum_{m=1}^{2N-1} (1+m^2)^q \left| -\sum_{s=1}^{\infty} (\hat{u}_{4sN+m} + \hat{u}_{4sN-m}) - \right.$$

$$\left. -2(-1)^{m-1} \sum_{s=1}^{\infty} \hat{u}_{2(2s-1)N} \right|^2.$$

For $p \geq q$ we have the estimate

$$S_1 \leq (1+4N^2)^{q-p} \sum_{m \geq 2N} (1+m^2)^p |\hat{R}_{N,m}|^2 \leq cN^{2(q-p)} \|u\|_p^2.$$

By using the Cauchy inequality, we get

$$\left| \sum_{s=1}^{\infty} \hat{u}_{4sN+r} \right|^2 = \left| \sum_{s=1}^{\infty} \left[1+(4sN+r)^2\right]^{-\frac{p}{2}} \left[1+(4sN+r)^2\right]^{\frac{p}{2}} \hat{u}_{4sN+r} \right|^2 \leq$$

$$\leq \sum_{s=1}^{\infty} \left[1+(4sN+r)^2\right]^{-p} \sum_{s=1}^{\infty} \left[1+(4sN+r)^2\right]^p |\hat{u}_{4sN+r}|^2 \leq$$

$$\leq (2N)^{-2p} \sum_{s=1}^{\infty} (2s+\frac{r}{2N})^{-2p} \sum_{s=1}^{\infty} \left[1+(4sN+r)^2\right]^p |\hat{u}_{4sN+r}|^2.$$

The series

$$\sum_{s=1}^{\infty} (2s+t)^{-2p}, \quad 0 \leq t \leq 1$$

converges uniformly for $p > \frac{1}{2}$ and, therefore, is bounded by an absolute constant. Hence, we have

$$S_2 \leq 8 \sum_{m=1}^{2N-1} (1+m^2)^q \left(\left| \sum_{s=1}^{\infty} u_{4sN+m} \right|^2 + \left| \sum_{s=1}^{\infty} u_{4sN-m} \right|^2 \right) +$$

$$+ 16 \sum_{m=1}^{2N-1} (1+m^2)^q \left| \sum_{s=1}^{\infty} \hat{u}_{2(2s-1)N} \right|^2 \leq$$

$$\leq c \left\{ \sum_{m=1}^{2N-1} (1+m^2)^q (2N)^{-2p} \sum_{s=1}^{\infty} \left(\left[1+(4sN+m)^2\right]^p |\hat{u}_{4sN+m}|^2 + \right.\right.$$

$$+ [1 + (4sN - m)^2]^p |\hat{u}_{4sN-m}|^2) +$$
$$+ \sum_{m=1}^{2N-1} (1 + m^2)^q (2N)^{-2p} \sum_{s=1}^{\infty} \left[1 + (2(2s-1)N)^2\right]^p |\hat{u}_{2(2s-1)N}|^2 \Bigg\} \leq$$
$$\leq c \left\{ N^{2(q-p)} \|u\|_p^2 + N^{2(q-p)+1} \|u\|_p^2 \right\} \leq c N^{2(p-q)+1} \|u\|_p^2 .$$

Analogously, one can get the estimate

$$S_3 \leq c N^{2(q-p)} \|u\|_p^2 .$$

Combining these estimates leads to the statement of the theorem.
□

Remark 2.14. The estimate of Theorem 2.13 is optimal in the sense that there exist p, q and a function $u(x)$, for which it is attainable. Actually, let us consider a function $u(x)$ with the Fourier coefficients

$$\hat{u}_{2(2s-1)N} = \frac{1}{[2(2s-1)N]^2},\ s = 1, \ldots; \quad \hat{u}_m = 0,\ m \neq 2(2s-1)N.$$

Using the relations

$$\hat{R}_{N,m} = 2(-1)^m \sum_{s=1}^{\infty} \hat{u}_{2(2s-1)N}, \quad m = 1, ..., 2N-1,$$
$$\hat{R}_{N,0} = \sum_{s=1}^{\infty} \hat{u}_{2(2s-1)}; \quad \hat{R}_{N,m} = 0, \quad m \geq 2N,$$

we have

$$||u||_p^2 = ||u||_1^2 = \frac{1}{2} \sum_{s=1}^{\infty} \left(1 + (2(2s-1)N)^2\right) (2(2s-1)N)^{-4} =$$
$$= c_1 N^{-2} + \mathcal{O}(N^{-4}),$$

$$||\hat{R}_N(x)||_q^2 = ||\hat{R}_N(x)||_{1/2}^2 =$$
$$= \left(2 \sum_{s=1}^{\infty} \hat{u}_{2(2s-1)N}\right)^2 \left(\frac{1}{2} \sum_{m=1}^{2N-1} (1 + m^2)^{1/2} + 1\right) =$$

$$= \frac{1}{4N^4}\left(\sum_{s=1}^{\infty}(2s-1)^{-2}\right)^2\left(\frac{1}{2}\sum_{m=1}^{2N-1}(1+m^2)^{1/2}+1\right)$$
$$= 16c_1^2N^{-2}+\mathcal{O}(N^{-3})$$

for $p=1, q=\frac{1}{2}$, where

$$c_1 = \frac{1}{8}\sum_{s=1}^{\infty}(2s-1)^{-2}.$$

It is easy to find that

$$\lim_{N\to\infty}\frac{||\hat{R}_N(x)||_q^2}{||u||_p^2} = 16c_1,$$

i.e. there exist positive constants A, B such that

$$A||u||_p \le ||\hat{R}_N(x)||_q \le B||u||_p.$$

Let $\mathbf{T}_N$ be the set of trigonometric polynomials of the form

$$v(t) = \sum_{m=0}^{N} a_m \cos mt + \sum_{m=1}^{N-1} b_m \sin mt$$

and $I_N(x;u) \in \mathbf{T}_N$ be the interpolation polynomial for u related to the nodes $x_j^{(N)} = j\pi/N,\ j=0,1,...,2N-1$. Kress (1989) [95] and Kress & Sloan (1993) [97] established that

$$I_N(x;u) = \sum_{k=0}^{2N-1} u\left(x_k^{(N)}\right) l_k^{(N)}(x),$$

where

$$l_k^{(N)}(x) = \frac{1}{2N}\left\{1+2\sum_{m=1}^{N-1}\cos m\left(x-x_k^{(N)}\right)+\cos N\left(x-x_k^{(N)}\right)\right\}.$$

We denote by $P_N : C[0,2\pi] \to \mathbf{T}_N,\ u \mapsto I_N(x;u)$ the interpolation operator and will use it for functions, which are even with respect to the point $x=\pi$. In that case, $u\left(x_k^{(N)}\right) = u\left(x_{2N-k}^{(N)}\right)$, which leads to the interpolation polynomial in the following form

$$I_N(x;u) = \sum_{k=0}^{N} u\left(x_k^{(N)}\right) \tilde{l}_k^{(N)}(x) \tag{2.57}$$

with

$$\tilde{l}_k^{(N)}(x) = \frac{1}{N(1+\delta_{0,k}+\delta_{N,k})} \sum_{m=0}^{N} (2-\delta_{m,0}-\delta_{m,N}) \cos mx \cos mx_k^{(N)},$$
$$k = 0, 1, ..., N.$$

For this interpolation, the following estimate holds true (see, Kress (1989) [95] and Kress & Sloan (1993) [97])

$$\|u - I_N(\cdot;u)\|_q \le cN^{q-p}\|u\|_p, \quad 0 \le q \le p, \quad \frac{1}{2} < p\,. \tag{2.58}$$

In order to get a discretisation of the operator $\mathcal{A}$, we calculate $(\mathcal{A}\hat{I}_N)(x)$ and collocate it at the points of ω_N. This gives

$$(\mathcal{A}\hat{I}_N)(x) = \sum_{k=0}^{2N-1} d_k \frac{k}{2} \tanh k\pi \cdot \cos\frac{kx}{2};$$

setting $x = x_j^{(N)}$ and using (2.53), (2.54) lead to the matrix equation

$$\left[(\mathcal{A}\hat{I}_N)(x_j)\right]^T_{j=0,1,...,2N-1} = S\Lambda S^{-1}\mathbf{u}$$

with $\Lambda = \text{diag}\,[\frac{k}{2}\tanh k\pi]_{k=0,1,...,2N-1}$. Therefore, one gets the matrix

$$\mathcal{A}_N = S\Lambda S^{-1}$$

as a discretisation of the operator $\mathcal{A}$ on the grid ω_N. The eigenvalues of $\mathcal{A}_N$ coincide with the first $2N$ eigenvalues of $\mathcal{A}$ and are given by $\lambda_k^{(N)} \equiv \lambda_k = \frac{k-1}{2}\tanh(k-1)\pi$. Moreover, the corresponding eigenvectors are $\mathbf{u}_k = S^{-1}e_k,\ k = 1, 2, ..., 2N$, where $e_k = (\delta_{kj})_{j=1,...,2N}$.

Now, we can combine this discretisation of the spatial operator $\mathcal{A}$ and the time discretisation from Section 2.1. A solution of the problem (2.50) can be represented by (2.20) in accordance with Theorem 2.3. The approximation of this solution by the truncated sum (2.34) and its accuracy are given by Theorem 2.6. This theorem was based on the estimates $\left|L_n^{(0)}(t) - L_{n-1}^{(0)}(t)\right| = O(n^{-\frac{3}{4}})$ and the representation

$$u_n = \int_{\lambda_0}^{\infty} \lambda^{-\sigma} \chi_1^{\frac{n}{2}} T_n(\chi_2) dE_\lambda \mathcal{A}^\sigma u_0,$$

where λ_0 is the lower bound of the spectrum of $\mathcal{A}$, E_λ is the spectral family of $\mathcal{A}$ and $T_n(\chi)$ are the Chebyshev polynomials,

$$\chi_1 = \frac{\lambda + \delta^2}{\lambda + (\delta - 1)^2}, \quad \chi_2 = \frac{\lambda + \delta(\delta - 1)}{\sqrt{(\lambda + \delta(\delta - 1))^2 + \lambda}}. \tag{2.59}$$

For the operator $\mathcal{A}$ given by (2.51), $\mathcal{A} \geq 0$, $\lambda_0 = 0$ is an isolated simple eigenvalue with the corresponding eigenfunction $v_0 \equiv 1$ and the rest of the spectrum lies in the interval $[\lambda_1, \infty)$, $\lambda_1 > 0$.

Define $u_0(x) = \hat{u}_0(x) + \alpha_0$, where $\alpha_0 = \int_0^{2\pi} u_0(x)dx$ and $\hat{u}_0(x) = u_0(x) - \alpha_0 \in (\text{Ker } \mathcal{A})^\perp$, $\alpha_0 \in \text{Ker } \mathcal{A}$. Then, obviously, the solution of (2.50) can be expressed as

$$u(x,t) = u_1(x,t) + \alpha_0; \quad u_1(x,t) = \left(\cos\sqrt{\mathcal{A}}t\right) \hat{u}_0$$

and the representation (2.20) holds with

$$u_n = \int_{\lambda_1}^{\infty} \lambda^{-\sigma} \chi_1^{\frac{n}{2}} T_n(\chi_2) dE_\lambda \mathcal{A}^\sigma \hat{u}_0.$$

We call the truncated sum

$$u_{1,M}(x,t) = e^{-\delta t} \sum_{k=0}^{M} L_k^{(0)}(t)[u_k(x) - u_{k+1}(x)]$$

the semi-discrete approximation for u_1. Replacing u_0 by its interpolation polynomial $\hat{P}_N u_0$ leads to the following problem

$$\frac{\partial^2 \tilde{u}}{\partial t^2} + \mathcal{A}\tilde{u} = 0, \quad \tilde{u}(0) \equiv \tilde{u}_0 = \hat{P}_N u_0, \quad \tilde{u}'(0) = 0$$

and, analogously,

$$\tilde{u}(x,t) = \tilde{u}_1(x,t) + \tilde{\alpha}_0,$$

where

$$\tilde{\alpha}_0 = \int_0^{2\pi} \hat{P}_N u_0 dx; \;\; \tilde{u}_1(t,x) = (\cos\sqrt{\mathcal{A}}t)\hat{\tilde{u}}_0; \;\; \hat{\tilde{u}}_0(x) = \tilde{u}_0 - \tilde{\alpha}_0 \in (\text{Ker } \mathcal{A})^\perp.$$

We define the fully discrete approximation for $u_1(x,t)$ as

$$u_{1,M}^N(x,t) = e^{-\delta t} \sum_{k=0}^{M} L_k^{(0)}(t) \left[\hat{u}_k(x) - \hat{u}_{k+1}(x)\right],$$

where $\hat{u}_k(x)$ satisfy

$$(\mathcal{A} + (\delta-1)^2 I)\hat{u}_{k+1} = 2(\mathcal{A} + \delta(\delta-1)I)\hat{u}_k - (\mathcal{A} + \delta^2 I)\hat{u}_{k-1}, \quad k \geq 1,$$

$$(\mathcal{A} + (\delta-1)^2 I)\hat{u}_1 = (\mathcal{A} + \delta(\delta-1)I)\hat{u}_0, \;\; \hat{u}_0 = \hat{P}_N \tilde{\hat{u}}_0 \in (\mathrm{Ker}\mathcal{A})^{\perp}.$$

Theorem 2.15. *For the error of the fully discrete approximation, the following estimate holds true*

$$\sup_{t\in[0,T]} \left\| u(\cdot,t) - u_{1,M}^N(\cdot,t) - \tilde{\alpha}_0 \right\|_s \leq c \left(M^{s-r+\frac{1}{4}} + N^{s-r+\frac{1}{2}} \right) \|u_0\|_r.$$

Proof. Since $\hat{P}_N \mathcal{A} u = \mathcal{A} u \;\forall\; u \in \hat{\mathbf{T}}_N$, these equations are equivalent to the following collocation equations

$$\begin{aligned}
\left[(\mathcal{A} + (\delta-1)^2 I)\hat{u}_{k+1}\right]\left(x_j^N\right) &= 2\left[(\mathcal{A} + \delta(\delta-1)I)\hat{u}_k\right]\left(x_j^N\right) - \\
&\quad - \left[(\mathcal{A} + \delta^2 I)\hat{u}_{k-1}\right]\left(x_j^N\right), \\
\left[(\mathcal{A} + (\delta-1)^2 I)\hat{u}_1\right]\left(x_j^{(N)}\right) &= \left[(\mathcal{A} + \delta(\delta-1)I)\hat{u}_0\right]\left(x_j^{(N)}\right), \qquad (2.60) \\
\hat{u}_0\left(x_j^{(N)}\right) &= \tilde{u}_0\left(x_j^{(N)}\right) - \tilde{\alpha}_0, \quad k \geq 1,
\end{aligned}$$

where $x_j^{(N)} = \frac{j\pi}{N}$, $j = 0, 1, ..., 2N-1$.

The matrix form of (2.60) reads

$$(\mathcal{A}_N + (\delta-1)^2 I)\hat{\mathbf{u}}_{k+1} = 2(\mathcal{A}_N + \delta(\delta-1)I)\hat{\mathbf{u}}_k - (\mathcal{A} + \delta^2 I)\hat{\mathbf{u}}_{k-1},$$

$$(\mathcal{A}_N + (\delta-1)^2 I)\hat{\mathbf{u}}_1 = (\mathcal{A}_N + \delta(\delta-1)I)\hat{\mathbf{u}}_0, \quad \hat{\mathbf{u}}_0 = \mathbf{u}_0 - \tilde{\alpha}_0,$$

where $\hat{\mathbf{u}} = (\hat{u}_k(x_0^{(N)})), ..., \hat{u}_k(x_{2N-1}^{(N)}))^T$, $\mathbf{u}_0 = (u_0(x_0^{(N)})), ..., u_0(x_{2N-1}^{(N)}))^T$.

We have for the total error

$$\left\| u(\cdot,t) - u_{1,M}^N(\cdot,t) - \tilde{\alpha}_0 \right\| \leq \left| \int_0^{2\pi} \left(u_0(x) - \hat{P}_N u_0(x) \right) dx \right| +$$

$$+ \|u_1 - u_{1,M}\| + \left\|u_{1,M} - u_{1,M}^N\right\| \ .$$

Representing

$$\begin{aligned} u_{1,M}(t,x) &= \int_{\lambda_1}^{\infty} f^{(M)}(t,\lambda) dE_\lambda \hat{u}_0(x); \\ u_{1,M}^N(t,x) &= \int_{\lambda_1}^{\infty} f^{(M)}(t,\lambda) dE_\lambda \hat{\tilde{u}}_0(x) \end{aligned} \tag{2.61}$$

with

$$\begin{aligned} f^{(M)}(t,\lambda) &= e^{-\delta t} \sum_{k=0}^{M} L_k^{(0)}(t) \chi_1^{\frac{n}{2}} \left[T_n(\chi_2) - \chi_1^{\frac{1}{2}} T_{n+1}(\chi_2)\right] = \\ &= e^{-\delta t} \sum_{k=0}^{M} L_k^{(0)}(t) \left\{ \chi_1^{\frac{n+1}{2}} [T_n(\chi_2) - T_{n+1}(\chi_2)] + T_n(\chi_2) \chi_1^{\frac{n}{2}} \left[1 - \chi_1^{\frac{1}{2}}\right] \right\} = \\ &= e^{-\delta t} \sum_{k=0}^{M} L_k^{(0)}(t) \left\{ -2\chi_1^{\frac{n+1}{2}} \sin\left(n + \frac{1}{2}\right) \arccos \chi_2 \times \right. \\ &\qquad \left. \times \sqrt{\frac{1-\chi_2}{2}} + T_n(\chi_2) \chi_1^{\frac{n}{2}} \left[1 - \chi_1^{\frac{1}{2}}\right] \right\} \end{aligned}$$

and using the estimates

$$\left| e^{-\frac{t}{2}} L_n^{(0)}(t) \right| \le 1, \qquad |T_n(\chi_2)| \le 1,$$

$$|1 - \chi_2| = \left| \frac{\lambda}{\sqrt{(\lambda + \delta(\delta-1))^2 + \lambda} \left(\sqrt{(\lambda + \delta(\delta-1))^2 + \lambda} + \lambda + \delta(\delta-1)\right)} \right| \le$$

$$\le \lambda^{-1}, \quad \lambda \in [0, \infty),$$

$$1 - \sqrt{\chi_1} = \left[\frac{1 - 2\delta}{\lambda + (\delta-1)^2}\right] \left[\sqrt{\frac{\lambda + \delta^2}{\lambda + (\delta-1)^2}} + 1\right]^{-1} \le (1 - 2\delta)\lambda^{-1},$$

we get that there exists a positive constant c such that

$$\left| f^{(M)}(t,\lambda) \right| \le c \ \forall \ t \in [0,T], \quad \lambda \in [0, \infty)$$

and owing to Theorem 2.13

$$\|u_1(t) - u_{1,M}(t)\| \le c M^{-\sigma + \frac{1}{4}} \|\mathcal{A}^\sigma \hat{u}_0\| \ .$$

Because $\mathcal{A}$ is bounded from H^p into H^{p-1} for all p, one holds

$$\|u_1(t) - u_{1,M}(t)\|_s \le cM^{s-r+\frac{1}{4}}\|\hat{u}_0\|_r \le \\ \le cM^{s-r+\frac{1}{4}}(\|u_0\|_r + |\alpha_0|) \le cM^{s-r+\frac{1}{4}}\|u_0\|_r.$$

Accounting for (2.61), we derive the inequality

$$\left\|u_{1,M}(t) - u_{1,M}^N(t)\right\| = \left\|\int_{\lambda_1}^{\infty} f^{(M)}(t,\lambda)dE_\lambda(\hat{u}_0 - \hat{\tilde{u}}_0)\right\| \le c\|\hat{u}_0 - \hat{\tilde{u}}_0\|,$$

and, in particular,

$$\left\|u_{1,M}(t) - u_{1,M}^N(t)\right\|_s \le c\|\hat{u}_0 - \hat{\tilde{u}}_0\|_s \le \\ \le c\left(\|u_0 - \hat{P}_N u_0\|_s + |\alpha_0 - \tilde{\alpha}_0|\right). \quad (2.62)$$

Using the embedding theorem we have

$$|\alpha_0 - \tilde{\alpha}_0| \le \sqrt{2\pi}\|u_0 - \hat{P}_N u_0\|_0 \le c\|u_0 - \hat{P}_N u_0\|_s, \quad (2.63)$$

for $s \ge 0$ and, due to Theorem 2.13,

$$\|u_0 - \hat{P}_N u_0\|_s \le cN^{s-r+\frac{1}{2}}\|u_0\|_r. \quad (2.64)$$

Therefore, we deduce from (2.62), (2.63) and (2.64) that

$$\left\|u(\cdot,t) - u_{1,M}^N(\cdot,t) - \tilde{\alpha}_0\right\|_s \le c\left(M^{s-r+\frac{1}{4}} + N^{s-r+\frac{1}{2}}\right)\|u_0\|_r$$

in what follows the statement.
□

2.3.3 Sloshing in a chute with baffles, a discrete model

Let us consider an infinite chute with two identical horizontal baffles (ribs) of the width a attached to the vertical walls and located at the height $x_2 = b$ as shown in Fig. 2.3. The original sloshing problem must therefore be solved in the "non-smooth", non-Lipschitz's domain $\Omega^{(a,b)} = \{x = (x_1, x_2) : 0 \le x_1 \le 2\pi,\ 0 \le x_2 \le 4\pi\}$.

Let us also denote $\Gamma_0 = \{x = (x_1, x_2) : 0 \le x_1 \le 2\pi,\ x_2 = 4\pi\}$, $\Omega_1 = \{x = (x_1, x_2) : 0 \le x_1 \le 2\pi,\ b \le x_2 \le 4\pi\}$, $\Omega_2 = \{x = (x_1, x_2) :$

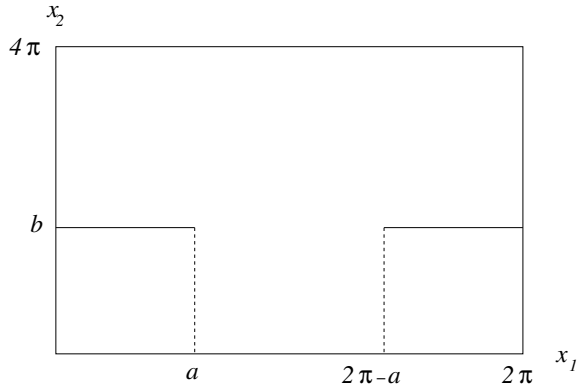

Fig. 2.3. Cross-section of a chute with baffles.

$0 \le x_1 \le 2\pi,\ 0 \le x_2 \le b\}$ and $\gamma_1, \gamma_2, \gamma$ be the line segments $\gamma_1 = \{x = (x_1, x_2) : 0 \le x_1 \le a,\ x_2 = b\}$, $\gamma_2 = \{x = (x_1, x_2) : 2\pi - a \le x_1 \le 2\pi,\ x_2 = b\}$, $\gamma = \{x = (x_1, x_2) : a \le x_1 \le 2\pi - a,\ x_2 = b\}$. We denote by $\varphi(x_1) \equiv \varphi(x)$ the unknown normal derivative of the potential on γ. Then the normal derivative of ϕ is defined on $\gamma_1 \cup \gamma_2 \cup \gamma$ and

$$\varphi_1(x_1) = \frac{\partial \phi}{\partial x_2}\Big|_{x_2=2\pi} = \begin{cases} 0, & x \in \gamma_1 \cup \gamma_2, \\ \varphi(x_1), & x \in \gamma\ . \end{cases}$$

Note, that the potential ϕ is solution of the following boundary value problem

$$\delta\phi = 0,\ x \in \Omega^{(a,b)};\ \ \phi(x) = u(x),\ x \in \Gamma_0;\ \ \frac{\partial \phi(x)}{\partial n} = 0,\ x \in \Gamma \backslash \Gamma_0 \cup \gamma_1 \cup \gamma_2. \tag{2.65}$$

The problem (2.65) is uniquely solvable, but we impose the resolvability condition for the corresponding Neumann problem as follows

$$\int_a^{2\pi - a} \varphi(\xi) d\xi = 0.$$

Without loss of generality, set up $b = 2\pi$. By separating the variables, one gets the following solutions in Ω_1 and Ω_2

$$\phi(x_1, x_2) = \frac{1}{\pi} \int_0^{2\pi} u(\xi) K_1(x_1, x_2, \xi) d\xi -$$

$$-\frac{2}{\pi}\int_a^{2\pi-a}\varphi(\xi)K_{12}(x_1,x_2,\xi)d\xi, \qquad (x_1,x_2)\in\Omega_1$$
$$\phi(x_1,x_2)=a_0+\frac{2}{\pi}\int_a^{2\pi-a}\varphi(\xi)\tilde{K}_2(x_1,x_2,\xi)d\xi, \quad (x_1,x_2)\in\Omega_2,$$

where a_0 is an arbitrary constant,

$$K_1(x_1,x_2,\xi)=\frac{1}{2}+\sum_{n=1}^{\infty}\cos\frac{nx_1}{2}\frac{\cosh n(\pi-\frac{x_2}{2})}{\cosh n\pi}\cos\frac{n\xi}{2},$$

$$K_{12}(x_1,x_2,\xi)=\sum_{n=1}^{\infty}\cos\frac{nx_1}{2}\frac{\sinh n(2\pi-\frac{x_2}{2})}{n\cosh\pi n}\cos\frac{n\xi}{2},$$

$$\tilde{K}_2(x_1,x_2,\xi)=\sum_{n=1}^{\infty}\frac{1}{n\sinh\pi n}\cos\frac{nx_1}{2}\cosh\frac{nx_2}{2}\cos\frac{n\xi}{2}.$$

This gives the following equation on γ (henceforth, we denote x_1 by x)

$$\frac{1}{\pi}\int_0^{2\pi}u(\tau)K_1(x,\tau)d\tau-\frac{2}{\pi}\int_a^{2\pi-a}\varphi(\xi)K_{22}(x,\xi)d\xi-a_0=0\,, \quad (2.66)$$

where

$$K_{11}(x,\tau)\equiv K_1(x_1,2\pi,\tau)=\frac{1}{2}+\sum_{n=1}^{\infty}\frac{1}{\cosh n\pi}\cos\frac{nx}{2}\cos\frac{n\tau}{2},$$
$$K_{22}(x,\xi)\equiv K_{12}(x_1,2\pi,\xi)+\tilde{K}_2(x_1,2\pi,\xi)= \quad (2.67)$$
$$=2\sum_{n=1}^{\infty}\frac{\coth 2\pi n}{n}\cos\frac{nx}{2}\cos\frac{n\xi}{2}.$$

Using the formula by Kanwal (1997) [89], p.205

$$-2\sum_{n=1}^{\infty}\frac{1}{n}\cos\frac{nx}{2}\cos\frac{n\xi}{2}=\ln 2\left|\cos\frac{x}{2}-\cos\frac{\xi}{2}\right|,$$

we further get

$$K_{22}(x,\xi)=-\ln 2\left|\cos\frac{x}{2}-\cos\frac{\xi}{2}\right|+2\sum_{n=1}^{\infty}\frac{e^{-2\pi n}}{n\sinh 2\pi n}\cos\frac{nx}{2}\cos\frac{n\xi}{2}.$$

Changing the variables in the second integral of (2.66) by

$$\cos\frac{\xi}{2}=\cos\frac{a}{2}\cos\tau;\quad \cos\frac{x}{2}=\cos\frac{a}{2}\cos\theta;$$
$$\varphi(\xi)=\sqrt{\frac{1-\cos^2\frac{\xi}{2}}{\cos^2\frac{a}{2}-\cos^2\frac{\xi}{2}}}\tilde{\varphi}(\xi) \tag{2.68}$$

we arrive at

$$\frac{1}{\pi}\int_0^{2\pi}u(\tau)\tilde{K}_{11}(\theta,\tau)d\tau-\frac{1}{\pi}\int_0^{2\pi}\psi(\tau)\tilde{K}_{22}(\theta,\tau)d\tau-a_0=0, \tag{2.69}$$

where

$$\tilde{K}_{11}(\theta,\tau)=\frac{1}{2}+\sum_{n=1}^{\infty}\frac{1}{\cosh n\pi}\cos\frac{n\tau}{2}T_n\left(\cos\frac{a}{2}\cos\theta\right),$$
$$\tilde{K}_{22}(\theta,\tau)=-\ln\left[2\left|\cos\frac{a}{2}\right|\,|\cos\theta-\cos\tau|\right]+$$
$$+2\sum_{n=1}^{\infty}\frac{e^{-2\pi n}}{n\sinh 2\pi n}T_n\left(\cos\frac{a}{2}\cos\theta\right)T_n\left(\cos\frac{a}{2}\cos\tau\right),$$
$$\psi(\tau)=\tilde{\varphi}\left(2\arccos\left(\cos\frac{a}{2}\cos\tau\right)\right)$$

and $T_n(\tau)$ are the Chebyshev polynomials of the first kind.

Note, that the function $\psi(\tau)$ is an even function with respect to the point $\tau=\pi$ and $\int_0^{2\pi}\psi(\tau)d\tau=0$. We denote by E_0 the space of all such functions. In what follows, we will need the integral

$$f_{m,n}\left(\cos\frac{a}{2}\right)=\int_0^{2\pi}\cos m\theta T_n\left(\cos\frac{a}{2}\cos\theta\right)d\theta,$$

which can be calculated by implementing the following formulae (see, Kress (1989) [95] p. 167)

$$\frac{ab}{\pi}\int_0^{2\pi}\frac{e^{in\tau}d\tau}{(a^2+b^2)-(a^2-b^2)\cos(t+\tau)}=\left(\frac{a-b}{a+b}\right)^n e^{-int}, \tag{2.70}$$

$$\frac{1}{2\pi}\int_0^{2\pi}\ln\left(\frac{4}{e}\sin^2\frac{t-\tau}{2}\right)d\tau=-1,\quad n=0,\ldots, \tag{2.71}$$

and generating the functions for the Chebyshev, Legendre and Jacobi polynomials

$$\frac{1-tz}{1-2tz+z^2}=\sum_{n=0}^{\infty}T_n(z)t^n, \tag{2.72}$$

$$\frac{1}{\sqrt{1-2xw+w^2}}=\sum_{n=0}^{\infty}P_n(x)w^n, \tag{2.73}$$

$$2^{\alpha+\beta}R^{-1}(1-w+R)^{-\alpha}(1+w+R)^{-\beta}=\sum_{n=0}^{\infty}P_n^{(\alpha,\beta)}(x)w^n, \tag{2.74}$$

where $R=\sqrt{1-2xw+w^2}$. Using (2.72) gives

$$\sum_{n=0}^{\infty}t^n f_{m,n}\left(\cos\frac{a}{2}\right)=\int_0^{2\pi}\cos m\theta\frac{1-t\cos\frac{a}{2}\cos\theta}{1-2t\cos\frac{a}{2}\cos\theta+t^2}d\theta=$$

$$=\frac{1-t^2}{2}\int_0^{2\pi}\frac{\cos m\theta}{1-2t\cos\frac{a}{2}\cos\theta+t^2}d\theta+\pi\delta_{m,0}.$$

Setting $a^2+b^2:=1+t^2,\ a^2-b^2:=2t\cos\frac{a}{2}$ in (2.70), we deduce

$$\sum_{n=0}^{\infty}t^n f_{m,n}\left(\cos\frac{a}{2}\right)=\frac{\pi(1-t^2)}{[1-2t^2\cos a+t^4]^{1/2}}\times$$

$$\times\left[\frac{2t\cos\frac{a}{2}}{1+t^2+[1-2t^2\cos a+t^4]^{1/2}}\right]^m+\pi\delta_{m,0}, \tag{2.75}$$

from where

$$f_{m,n}\left(\cos\frac{a}{2}\right)=\frac{1}{n!}\frac{d^n}{dt^n}\left\{\frac{\pi(1-t^2)}{\sqrt{1-2t^2\cos a+t^4}}\times\right.$$

$$\left.\times\left(\frac{2t\cos\frac{a}{2}}{1+t^2+\sqrt{1-2t^2\cos a+t^4}}\right)^m\right\}_{t=0}.$$

It is easily seen, that $f_{m,n}(\cos\frac{a}{2})=0$ for $n<m$ and $f_{m,m}(\cos\frac{a}{2})=\pi(\cos\frac{a}{2})^m,\ m\geq 1$. To get an explicit formula for the case $m=0$, we set up $x=\cos a,\ w=t^2,\alpha=0,\beta=m$ in (2.73), (2.74) and, by using (2.75), get

$$f_{0,0}(\cos\frac{a}{2}) = 2\pi, \quad f_{0,2n-1}\left(\cos\frac{a}{2}\right) = 0,$$
$$f_{0,2n}\left(\cos\frac{a}{2}\right) = \pi\left[P_n^{(0,0)}(\cos a) - P_{n-1}^{(0,0)}(\cos a)\right] = \tag{2.76}$$
$$= \pi\left(P_n(\cos a) - P_{n-1}(\cos a)\right), \quad n = 1, 2, ...,$$

and

$$f_{m,m+2k+1}(\cos\frac{a}{2}) = 0,\ m \geq 1,\ k = 0, 1, ...,$$
$$f_{m,m+2k}(\cos\frac{a}{2}) = \pi\left(\cos\frac{a}{2}\right)^m\left(P_k^{(0,m)}(\cos a) - P_{k-1}^{(0,m)}(\cos a)\right),\ k = 1, 2, ...$$

The formula (2.71) implies

$$\frac{1}{2\pi}\int_0^{2\pi} \ln 2|\cos\theta - \cos\tau| d\theta =$$
$$= \frac{1}{2\pi}\int_0^{2\pi} \ln 4\left|\sin\frac{\theta-\tau}{2}\right| d\theta + \frac{1}{2\pi}\int_0^{2\pi} \ln\left|\sin\frac{\tau-(2\pi-\theta)}{2}\right| d\theta = \tag{2.77}$$
$$= \frac{1}{2\pi}\int_0^{2\pi} \ln 4\sin^2\frac{\theta-\tau}{2} d\theta = 0.$$

Now, we are in position to determine the constant a_0. Integrating (2.69) in $\theta \in [0, 2\pi]$ and using (2.76)+(2.77) give

$$a_0 = \frac{1}{\pi}\int_0^{2\pi} u(\tau)\left[\frac{1}{2} + \sum_{n=1}^{\infty}\frac{1}{\cosh n\pi}\cos\frac{n\tau}{2}\cdot\frac{1}{2\pi}\int_0^{2\pi} T_n\left(\cos\frac{a}{2}\cos\zeta\right)\right] d\zeta -$$
$$- \frac{1}{\pi}\int_0^{2\pi}\psi(\tau)\Big\{-\ln\left|\cos\frac{a}{2}\right| +$$
$$+ 2\sum_{n=1}^{\infty}\frac{e^{-2\pi n}}{n\sinh 2\pi n} T_n\Big(\cos\frac{a}{2}\cos\tau\Big)\frac{1}{2\pi}\int_0^{2\pi} T_n\Big(\cos\frac{a}{2}\cos\zeta\Big) d\zeta\Big\} d\tau =$$
$$= \frac{1}{2\pi}\int_0^{2\pi} u(\tau)\left\{1 + \sum_{n=1}^{\infty}\frac{1}{\cosh 2\pi n}\cos n\tau\left[P_n(\cos a) - P_{n-1}(\cos a)\right]\right\} d\tau -$$
$$- \frac{1}{\pi}\int_0^{2\pi}\psi(\tau)\Big\{-\ln\left|\cos\frac{a}{2}\right| +$$
$$+ \sum_{n=1}^{\infty}\frac{e^{-4\pi n}}{2n\sinh 4\pi n} T_{2n}\Big(\cos\frac{a}{2}\cos\tau\Big)\left[P_n(\cos a) - P_{n-1}(\cos a)\right]\Big\} d\tau. \tag{2.78}$$

After substituting (2.78) into (2.69), we arrive at the following equation coupling u and ψ

$$\frac{1}{2\pi}\int_0^{2\pi} u(\xi)K_1(\theta,\xi)d\xi + \frac{1}{2\pi}\int_0^{2\pi}\psi(\xi)\ln\left(\frac{4}{e}\sin^2\frac{\theta-\xi}{2}\right)d\xi - \\ -\frac{1}{2\pi}\int_0^{2\pi}\psi(\xi)K_2(\theta,\xi)d\xi = 0,$$

where

$$K_1(\theta,\xi) = \sum_{n=1}^{\infty}\frac{1}{\cosh n\pi}\cos\frac{n\xi}{2}\left[T_n\left(\cos\frac{a}{2}\cos\theta\right) - \right.$$

$$\left. -\frac{1}{2\pi}\int_0^{2\pi} T_n\left(\cos\frac{a}{2}\cos\zeta\right)d\zeta\right] = \sum_{n=1}^{\infty}\frac{1}{\cosh n\pi}\cos\frac{n\xi}{2}T_n\left(\cos\frac{a}{2}\cos\theta\right) -$$

$$-\frac{1}{2}\sum_{n=1}^{\infty}\frac{1}{\cosh 2\pi n}\cos n\xi\left[P_n(\cos a) - P_{n-1}(\cos a)\right],$$

$$K_2(\theta,\xi) = -1 + 2\sum_{n=1}^{\infty}\frac{e^{-2\pi n}}{n\sinh 2\pi n}T_n\left(\cos\frac{a}{2}\cos\xi\right)\left[T_n\left(\cos\frac{a}{2}\cos\theta\right) - \right.$$

$$\left. -\frac{1}{2\pi}\int_0^{2\pi} T_n\left(\cos\frac{a}{2}\cos\zeta\right)d\zeta\right] =$$

$$= -1 + 2\sum_{n=1}^{\infty}\frac{e^{-2\pi n}}{n\sinh 2\pi n}T_n\left(\cos\frac{a}{2}\cos\xi\right)T_n\left(\cos\frac{a}{2}\cos\theta\right) -$$

$$-\sum_{n=1}^{\infty}\frac{e^{-4\pi n}}{2n\sinh 4\pi n}T_{2n}\left(\cos\frac{a}{2}\cos\xi\right)\left[P_n(\cos a) - P_{n-1}(\cos a)\right].$$

The kernels K_1, K_2 are 2π-periodic with respect to both variables, and infinitely differentiable.

We define the operators L, B_2 acting in the space E_0 by

$$(L_1\psi)(\theta) = \frac{1}{2\pi}\int_0^{2\pi}\psi(\xi)\ln\left(\frac{4}{e}\sin^2\frac{\theta-\xi}{2}\right)d\xi\,,$$

$$(B_2\psi)(\theta) = \frac{1}{2\pi}\int_0^{2\pi}\psi(\xi)K_2(\theta,\xi)d\xi$$

and the operator B_1 acting in a space of functions defined on $[0, 2\pi]$ by

$$(B_1u)(\theta) = \frac{1}{2\pi}\int_0^{2\pi} u(\xi)K_1(\theta,\xi)d\xi\ .$$

It is easy to see that on the class E_0, it holds

$$(B_2\psi)(\theta) = \frac{1}{\pi}\int_0^{2\pi}\psi(\xi)\left\{\sum_{n=1}^{\infty}\frac{e^{-2\pi n}}{n\sinh 2\pi n}\left[T_n\left(\cos\frac{a}{2}\cos\xi\right) - \right.\right.$$
$$\left. - \frac{1}{2\pi}\int_0^{2\pi} T_n\left(\cos\frac{a}{2}\cos\zeta\right)d\zeta\right]\left[T_n\left(\cos\frac{a}{2}\cos\theta\right) - \right.$$
$$\left.\left. -\frac{1}{2\pi}\int_0^{2\pi} T_n\left(\cos\frac{a}{2}\cos\zeta\right)d\zeta\right]\right\}d\xi,$$

i.e. the operator B_2 is symmetric, $B_2 = B_2^*$.

We define the operator $\mathcal{A}^{(a)}$ by

$$\left(\mathcal{A}^{(a)}u\right)(x) = \frac{\partial\phi(x_1,4\pi)}{\partial x_2} = (\mathcal{A}u)(x) + \left(B_1^*\psi\right)(x), \tag{2.79}$$

where $\mathcal{A}$ is given by (2.51). Thus, the operator formulation of the linear sloshing problem in $\Omega^{(a)} \equiv \Omega^{(a,2\pi)}$ can be written in the following form

$$\begin{aligned}
&\frac{\partial^2 u(x,t)}{\partial t^2} + (\mathcal{A}^{(a)}u)(x) = 0\ ,\ t \geq 0,\ x \in (0,2\pi),\\
&(B_1u)(x) + (L\psi)(x) - (B_2\psi)(x) = 0\ , x \in (a, 2\pi - a)\\
&u(x,0) = u_0(x), \quad \frac{\partial u(x,0)}{\partial t} = 0.
\end{aligned} \tag{2.80}$$

First, let us show that the case $a = 0$ reduces the formulation (2.80) to (2.50) in the rectangle $\Omega_{4\pi} = \{x = (x_1,x_2) : 0 \leq x_1 \leq 2\pi,\ 0 \leq x_2 \leq 4\pi\}$. As matter of the fact, multiplying (2.69) by $\cos j\theta$ and integrating in θ over $(0,2\pi)$ yield

$$\int_0^{2\pi} u(\xi)\frac{1}{\cosh j\pi}\cos\frac{j\xi}{2}d\xi - 4\int_0^{2\pi}\psi(\xi)\frac{\coth j2\pi}{j}\cos\frac{j\xi}{2}d\xi = 0,$$

$j = 1,\ldots;\ a_0 = 0$, i.e. the Fourier coefficients of u and ψ are coupled by

$$\hat{\psi}_j = \frac{j}{4\cosh j\pi\coth 2\pi j}\hat{u}_j, \quad j = 1,2,... \tag{2.81}$$

with

$$\hat{u}_j = \frac{1}{\pi}\int_0^{2\pi} u(\xi)\cos\frac{j\xi}{2}d\xi, \quad \hat{\psi}_j = \frac{1}{\pi}\int_0^{2\pi} \psi(\xi)\cos\frac{j\xi}{2}d\xi.$$

Using (2.81) gives

$$\left(\mathcal{A}^{(a)}u\right)(x) = \sum_{n=1}^{\infty}\frac{n}{2}\tanh n\pi\cdot\hat{u}_n\cdot\cos\frac{nx}{2} + \sum_{n=1}^{\infty}\frac{1}{\cosh\pi n}\cdot\hat{\psi}_n\cdot\cos\frac{nx}{2} = \\ = \sum_{n=1}^{\infty}\frac{n}{2}\tanh 2\pi n\cdot\hat{u}_n\cdot\cos\frac{nx}{2}.$$

This expression coincides with a formula for the operator $\mathcal{A}$ from (2.51) in the case when the baffle is absent and the height of the reservoir is 4π. It can be shown that $\mathcal{A}^{(a)}$ coincides with $\mathcal{A}$ for $a=\pi$ as well.

Let us show that the operator $\mathcal{A}^{(a)}$ is self-adjoint and non-negative definite in $L_2(0,2\pi)$. We define φ and ψ as solutions of the Laplace equation in $\Omega^{(a)}$ such that $\varphi(x,4\pi)=u(x)$, $\psi(x,4\pi)=u(x)$, $x\in[0,2\pi]$, $\frac{\partial\varphi}{\partial n}=0$, $\frac{\partial\psi}{\partial n}=0$ on the rest of the boundary and on the bank of the cut. Accounting for singularities at the edges, the following integration by parts is justified

$$0=\int_{\Omega^{(a)}}\Delta\varphi\cdot\psi ds = \int_{\Omega^{(a)}}\operatorname{grad}\varphi\cdot\operatorname{grad}\psi ds - \int_0^{2\pi}(\mathcal{A}u)(x)\psi(x)dx,$$

i.e. $\mathcal{A}^{(a)}: H^{\frac{1}{2}}(\Gamma_0)\to H^{-\frac{1}{2}}(\Gamma_0)$ is a symmetric non-negative pseudo-differential operator of the order 1.

We rewrite Eq. (2.80) in the following form

$$(L-B_2)\psi = -B_1 u,$$

where the operator L is an even pseudo-differential operator of the order -1. It defines an isomorphism from H^p onto H^{p+1} for all $p\in\mathbb{R}$. Because the kernel of B_2 is infinitely differentiable, this operator maps H^p boundedly into H^q for any pairs p,q. In view of the boundary value problem for the potential ϕ in $\Omega^{(a)}$, which is uniquely resolvable, the operator $L-B_2$ has a trivial null-space and, therefore, $L^{-1}B_2$ is compact. According to the Riesz-Fredholm theory, the operator $L-B_2: H^p\to H^{p+1}$ is an isomorphism. Thus,

$$\psi = -(L-B_2)^{-1}B_1 u$$

and the operator $\mathcal{A}^{(a)} : H^p \to H^{p-1}$ can also be represented by

$$\mathcal{A}^{(a)}u = \left[\mathcal{A} - B_1^*(L - B_2)^{-1}B_1\right]u.$$

The following theorem states the monotonicity of the eigenvalues of $\mathcal{A}^{(a)}$ versus a:

Theorem 2.16. *The eigenvalues $\lambda_n(a)$ of the operator $\mathcal{A}^{(a)}$ have the following properties*
i) $\lambda_n(a) \le \lambda_n(a')$ *for* $0 \le a' \le a \le \pi,\ n = 0, 1, ...$
ii) $\frac{n}{2}\tanh \pi n = \lambda_n(\pi) \le \lambda_n(a) \le \lambda_n(0) = \frac{n}{2}\tanh 2\pi n,\ n = 0, 1, ...$

Proof. It follows from (2.79), (2.80) that for all u, ψ coupled by (2.80)

$$\begin{aligned}\left(\mathcal{A}^{(a)}u, u\right) &= \left(\mathcal{A}^{(a)}u, u\right) - (B_1u + (L - B_2)\psi, \psi) = \\ &= (\mathcal{A}u, u) - ((L - B_2)\psi, \psi) = \\ &= \frac{1}{\pi}\int_0^{2\pi}\int_0^{2\pi} u(x)u(s)\sum_{n=1}^{\infty} n\tanh n\pi \cos\frac{nx}{2}\cos\frac{ns}{2}dsdx + \qquad (2.82)\\ &+ \frac{4}{\pi}\int_a^{2\pi-a}\int_a^{2\pi-a}\varphi(x)\varphi(s)\sum_{n=1}^{\infty}\frac{1}{\cosh n\pi}\cos\frac{nx}{2}\cos\frac{ns}{2}dxds\end{aligned}$$

and

$$\begin{aligned}&\frac{1}{\pi}\int_0^{2\pi} u(\tau)\left[\frac{1}{2} + \sum_{n=1}^{\infty}\frac{1}{\cosh n\pi}\cos\frac{nx}{2}\cos\frac{n\tau}{2}\right]d\tau - \\ &\qquad - \frac{4}{\pi}\int_a^{2\pi-a}\varphi(\xi)\sum_{n=1}^{\infty}\frac{\coth 2n\pi}{n}\cos\frac{nx}{2}\cos\frac{n\xi}{2}d\xi - a_0 = 0.\end{aligned}$$

Let H_n be a finite-dimensional subspace of $H \equiv L_2(0, 2\pi)$, i.e.

$$\lambda_n(a) = \sup_{H_n \subset H}\inf_{u \in H_n}\frac{(\mathcal{A}^{(a)}u, u)}{(u, u)}.$$

We denote by $(u_n^{(a)}, \psi_n^{(a)})$ the pair, for which

$$\inf_{u \in H_n}\frac{(\mathcal{A}^{(a)}u, u)}{(u, u)} = \frac{(\mathcal{A}^{(a)}u_n^{(a)}, u_n^{(a)})}{(u_n^{(a)}, u_n^{(a)})}.$$

Then it follows from (2.82) for $0 \le a' < a \le \pi$

$$\inf_{n\in H_n} \frac{(\mathcal{A}^{(a)}u,u)}{(u,u)} = \frac{(\mathcal{A}^{(a)}u_n^{(a)},u_n^{(a)})}{(u_n^{(a)},u_n^{(a)})} \le$$

$$\le \frac{(\mathcal{A}^{(a)}u_n^{(a')},u_n^{(a')})}{(u_n^{(a')},u_n^{(a')})} \le \frac{(\mathcal{A}^{(a')}u_n^{(a')},u_n^{(a')})}{(u_n^{(a')},u_n^{(a')})} = \inf_{u\in H_n} \frac{(\mathcal{A}^{(a')}u,u)}{(u,u)},$$

from where $\lambda_n(a) \le \lambda_n(a'), \quad 0 \le a' \le a \le \pi,\ n = 0,1,...,$ specifically,

$$\frac{n}{2}\tanh \pi n = \lambda_n(\pi) \le \lambda_n(a) \le \lambda_n(0) = \frac{n}{2}\tanh 2\pi n.$$

□

An interest is to investigate dependence of the eigenvalues as functions of vertical position of the baffles characterised by b. In this case, we get the kernels

$$K_{11}(x,\tau) = \frac{1}{2} + \sum_{n=1}^{\infty} \frac{1}{\cosh n(2\pi - \frac{b}{2})} \cos\frac{nx}{2}\cos\frac{n\tau}{2},$$

$$K_{22}(x,\xi) = \sum_{n=1}^{\infty} \frac{\cosh 2\pi n}{n \sinh\frac{nb}{2}\cosh n(2\pi - \frac{b}{2})} \cos\frac{nx}{2}\cos\frac{n\xi}{2}$$

instead of (2.67) as well as the operator

$$\left(\mathcal{A}^{(a,b)}u\right)(x) = \frac{1}{\pi}\int_0^{2\pi} u(\xi)\sum_{n=1}^{\infty}\frac{n}{2}\tanh n\left(2\pi - \frac{b}{2}\right)\cos\frac{nx}{2}\cos\frac{n\xi}{2}d\xi +$$

$$+ \frac{1}{\pi}\int_a^{2\pi-a}\varphi(\xi)\sum_{n=1}^{\infty}\frac{1}{\cosh n(2\pi - \frac{b}{2})}\cos\frac{nx}{2}\cos\frac{n\xi}{2}d\xi$$

instead of the operator $\mathcal{A}^{(a)}$. Similarly,

$$\left(\mathcal{A}^{(a,b)}u,u\right) = \frac{1}{\pi}\int_0^{2\pi}\int_0^{2\pi} u(x)u(s)\times$$

$$\times\sum_{n=1}^{\infty} n\tanh n\left(2\pi - \frac{b}{2}\right)\cos\frac{nx}{2}\cos\frac{ns}{2}dsdx + \frac{4}{\pi}\int_a^{2\pi-a}\int_a^{2\pi-a}\varphi(x)\varphi(s)\times$$

$$\times \sum_{n=1}^{\infty} \frac{\cosh 2n\pi}{2n \sinh n\frac{b}{2} \cosh n(2\pi - \frac{b}{2})} \cos\frac{nx}{2} \cos\frac{ns}{2} ds dx$$

replaces (2.82).

Theorem 2.17. *The eigenvalues $\lambda_n(a,b)$ of the operator $\mathcal{A}^{(a,b)}$ have the following properties:*
i) *for a fixed $a \in (0,\pi]$, it holds*

$$\lambda_n(a,b) \le \lambda_n(a,b'), \quad 0 \le b' \le b \le 4\pi, \quad n = 0,1,...$$

ii) $\frac{n}{2}\tanh n\left(2\pi - \frac{b}{2}\right) = \lambda_n(\pi,b) \le \lambda_n(a,b) \le \lambda_n(a,0) = \lambda_n(0) = \frac{n}{2}\tanh 2\pi n,$
iii) $n\tanh\frac{a}{2}/\coth 2\pi \le \lambda_n(a,4\pi)$.

(For a fixed b, Theorem 2.16 holds for $\lambda_n(a,b)$ as a function of a).

Proof. The first two estimates are owing to the decrease of the kernels versus b and the proof of Theorem 2.16.

In order to obtain the third estimate, when $b = 4\pi$, we need to formulate the eigenvalue problem in this special case. The integral equation (2.66) leads to

$$\frac{1}{\pi}\int_0^{2\pi} u(\tau)\left[\frac{1}{2} + \sum_{n=1}^{\infty} \cos\frac{nx}{2}\cos\frac{n\tau}{2}\right] d\tau -$$
$$-\frac{2}{\pi}\int_a^{2\pi-a} \varphi(\xi) \sum_{n=1}^{\infty} \frac{\coth 2\pi n}{n} \cos\frac{nx}{2}\cos\frac{n\xi}{2} d\xi - a_0 = 0,\ a < x < 2\pi - a$$

or, accounting for representation of $u(x)$ via the Fourier series, we have

$$u(x) = \frac{2}{\pi}\int_a^{2\pi-a} \varphi(\xi) \sum_{n=1}^{\infty} \frac{\coth 2\pi n}{n} \cos\frac{nx}{2}\cos\frac{n\xi}{2} d\xi - a_0.$$

Since

$$\left(\mathcal{A}^{(a,4\pi)}u\right)(x) = \frac{\partial\phi}{\partial x_2}\Big|_{x_2=4\pi} = \varphi(x), \quad a \le x \le 2\pi - a,$$

the eigenvalue problem $\mathcal{A}^{(a,b)}u = \lambda u$ can be written as

$$\varphi(x) = \frac{2\lambda}{\pi}\int_a^{2\pi-a}\varphi(\xi)\sum_{n=1}^{\infty}\frac{\coth 2\pi n}{n}\cos\frac{nx}{2}\cos\frac{n\xi}{2}d\xi - a_0,\ a < x < 2\pi - a.$$

Multiplying this equation by $\varphi(x)$, integrating over $[a, 2\pi - a]$ and accounting for $\int_a^{2\pi-a}\varphi(\xi)d\xi = 0$ give

$$\int_a^{2\pi-a}\varphi^2(x)dx = \frac{2\lambda}{\pi}\sum_{n=1}^{\infty}\frac{\coth 2\pi n}{n}\left[\int_a^{2\pi-a}\varphi(\xi)\cos\frac{n\xi}{2}d\xi\right]^2,$$

$$\frac{1}{\lambda_n} = \frac{\sup_{H_n^{(a)}\subset H^{(a)}}\inf_{\varphi\in H_n^{(a)}}\frac{2}{\pi}\sum_{n=1}^{\infty}\frac{\coth 2\pi n}{n}\left[\int_a^{2\pi-a}\varphi(\xi)\cos\frac{n\xi}{2}d\xi\right]^2}{\int_a^{2\pi-a}\varphi^2(x)dx} \le$$

$$\le \frac{2\coth 2\pi}{\pi}\frac{\sup_{H_n^{(a)}\subset H^{(a)}}\inf_{\varphi\in H_n^{(a)}}\sum_{n=1}^{\infty}\left[\int_a^{2\pi-a}\varphi(\xi)\cos\frac{n\xi}{2}d\xi\right]^2}{\int_a^{2\pi-a}\varphi^2(x)dx} \equiv$$

$$\equiv \frac{2\coth 2\pi}{\pi\lambda^*},$$

where $H_n^{(a)}$ is a n-dimensional subspace of $H^{(a)} \equiv L_2(a, 2\pi - a)$. The numbers λ_n^* are solutions of the problem

$$\int_a^{2\pi-a}\varphi^*(x)dx = \lambda^*\sum_{n=1}^{\infty}\frac{1}{n}\left[\int_a^{2\pi-a}\varphi^*(\xi)\cos\frac{n\xi}{2}d\xi\right]^2 =$$

$$= \lambda^*\int_0^{2\pi}\int_0^{2\pi}\varphi^*(\xi)\varphi^*(x)\sum_{n=1}^{\infty}\frac{1}{n}\cos\frac{n\xi}{2}\cos\frac{nx}{2}dxd\xi. \quad (2.83)$$

Changing variables in accordance with (2.68) leads to

$$\int_0^{2\pi}\frac{\sqrt{1-\cos^2\frac{a}{2}\cos^2\theta}}{\cos\frac{a}{2}\sin\theta}\psi^2(\theta)d\theta =$$

$$= -\lambda^*\int_0^{2\pi}\int_0^{2\pi}\psi(\theta)\psi(\tau)\ln\frac{4}{e}\sin^2\frac{\theta-\tau}{2}d\theta d\tau,$$

$$\varphi^*(\xi) = \sqrt{\frac{1-\cos^2\frac{\xi}{2}}{\cos^2\frac{a}{2}-\cos^2\frac{\xi}{2}}}\tilde{\varphi}^*(\xi);\quad \psi(\tau) = \tilde{\varphi}^*\left(2\arccos(\cos\frac{a}{2}\cos\tau)\right).$$

By using the estimate

$$\frac{\sqrt{1-\cos^2\frac{a}{2}\cos^2\theta}}{\cos\frac{a}{2}\sin\theta} \geq \tan\frac{a}{2}$$

and the minimax principle, we see that the eigenvalues of the problem (2.83) are majorized from below by eigenvalues of the problem

$$\tan\frac{a}{2}\int_0^{2\pi}[\psi^*(\theta)]^2 d\theta = -\lambda^{**}\int_0^{2\pi}\int_0^{2\pi}\psi^*(\theta)\psi^*(\tau)\ln\frac{4}{e}\sin^2\frac{\theta-\tau}{2}d\theta d\tau.$$

This problem has the solution

$$\psi_m^*(\theta) = \cos m\theta, \quad \lambda_m^{**} = \frac{m}{\pi}\tan\frac{a}{2}, \quad m = 1, 2, ...$$

i. e.

$$\lambda_m \geq \frac{\lambda_m^*\pi}{2\coth 2\pi} \geq \frac{\lambda_m^{**}\pi}{2\coth 2\pi} = \frac{m\tan\frac{a}{2}}{2\coth 2\pi}.$$

□

To establish a finite-dimensional approximation, we use the following quadrature rules based on the trigonometric interpolation (2.57) (for even with respect to the point π functions ψ) and Eq. (2.55):

$$(L\psi)(\theta) \equiv \frac{1}{2\pi}\int_0^{2\pi}\psi(\tau)\ln\left(\frac{4}{e}\sin^2\frac{\theta-\tau}{2}\right)d\tau \approx$$
$$\approx \frac{1}{2\pi}\int_0^{2\pi} I_N(\tau;\psi)\ln\left(\frac{4}{e}\sin^2\frac{\theta-\tau}{2}\right)d\tau = \sum_{k=0}^{N} R_k^{(N)}(\theta)\psi(x_k^{(N)})$$
$$\equiv (L\psi_N)(\theta),$$

$$(\mathcal{A}u)(x) \equiv \frac{1}{2\pi}\int_0^{2\pi} u(\xi)\sum_{j=1}^{\infty} j\tanh j\left(2\pi-\frac{b}{2}\right)\cos\frac{jx}{2}\cos\frac{j\xi}{2}d\xi =$$
$$= \frac{1}{2\pi}\int_0^{2\pi}\hat{I}_N(\xi;u)\sum_{j=1}^{\infty} j\tanh j\left(2\pi-\frac{b}{2}\right)\cos\frac{jx}{2}\cos\frac{j\xi}{2}d\xi \approx$$
$$\approx \sum_{p=0}^{2N-1}\hat{R}_p^{(N)}(x)u\left(x_p^{(N)}\right) \equiv (\mathcal{A}u_N)(x),$$

$$(B_1u)(x) = \frac{1}{2\pi}\int_0^{2\pi} u(\tau)K_1(x,\tau)d\tau \approx \frac{1}{2\pi}\int_0^{2\pi} \hat{I}_N(\tau;u)K_1(x,\tau)d\tau = \\ = \sum_{k=0}^{2N-1} R_{1,k}^{(N)}(x)u\left(x_k^{(N)}\right) \equiv (B_1u_N)(x),$$

$$(B_2\psi)(\theta) = \frac{1}{2\pi}\int_0^{2\pi} \psi(\tau)K_2(\theta,\tau)d\tau \approx \frac{1}{2\pi}\int_0^{2\pi} I_N(\tau;\psi)K_2(\theta,\tau)d\tau = \\ = \sum_{k=0}^{N} R_{2,k}^{(N)}(\theta)\psi_{(x_k^{(N)})} \equiv (B_2\psi_N)(\theta),$$

$$(B_1^*\psi)(\theta) = \frac{1}{2\pi}\int_0^{2\pi} \psi(\tau)K_1(\tau,\theta)d\tau \approx \frac{1}{2\pi}\int_0^{2\pi} I_N(\tau;\psi)K_1(\tau,\theta)d\tau = \\ = \sum_{k=0}^{N} R_{3,k}^{(N)}(\theta)\psi(x_k^{(N)}) \equiv (B_1^*\psi_N)(\theta),$$

where

$$u_N(\xi) = \hat{I}_N(\xi;u) \equiv \hat{P}_Nu; \quad \psi_N(\tau) = I_N(\tau;\psi) \equiv P_N\psi,$$

$$R_k^{(N)}(\theta) = \tilde{R}_k^{(N)}(\theta) + \tilde{R}_{2N-k}^{(N)}(\theta); \quad x_{2N-k}^{(N)} = \frac{(2N-k)\pi}{N} = 2\pi - x_k^{(N)},$$

$$R_k^{(N)}(\theta) = -\frac{1}{N}\left\{1 + 2\sum_{m=1}^{N-1}\frac{1}{m}\cos m\theta\cos mx_k^{(N)} + \right. \\ \left. + \frac{1}{N}\cos N\theta\cos Nx_k^{(N)}\right\}, k = 1,2,...,N-1,$$

$$R_0^{(N)}(\theta) = \tilde{R}_0^{(N)}(\theta), \quad R_N^{(N)}(\theta) = \tilde{R}_N^{(N)}(\theta),$$

$$\tilde{R}_k^{(N)}(\theta) = \frac{1}{2\pi}\int_0^{2\pi} l_k^{(N)}(\tau)\ln\left(\frac{4}{e}\sin^2\frac{\theta-\tau}{2}\right)d\tau =$$

$$= -\frac{1}{2N}\left\{1 + 2\sum_{m=1}^{N-1}\frac{1}{m}\cos m(\theta - x_k^{(N)}) + \right. \\ \left. + + \frac{1}{N}\cos N(\theta - x_k^{(N)})\right\}, k = 0,...,2N-1,$$

$$\hat{R}_p^{(N)}(x) = \frac{1}{2\pi}\int_0^{2\pi} \hat{l}_p^{(N)}(\xi)\sum_{j=1}^{\infty} j\tanh j(2\pi-\frac{b}{2})\cos\frac{jx}{2}\cos\frac{j\xi}{2}d\xi =$$

$$= \begin{cases} \frac{1}{2N}\sum_{j=1}^{N}(2j-1)\tanh(2j-1)(2\pi-\frac{b}{2})\cos\frac{2j-1}{2}x, & p=0 \\ \frac{1}{2N}\sum_{j=1}^{2N-1} j\tanh j(2\pi-\frac{b}{2})\left[\cos\frac{jp\pi}{2N}+(-1)^{j+p-1}\right]\cos\frac{jx}{2}, p=1,\ldots,2N-1, \end{cases}$$

$$R_{1,k}^{(N)}(x) = \frac{1}{2\pi}\int_0^{2\pi}\hat{l}_k^{(N)}(\tau)K_1(x,\tau)d\tau =$$

$$= \begin{cases} \frac{1}{2N}\sum_{p=1}^{N}\frac{1}{\cosh(2p-1)(2\pi-\frac{b}{2})}T_{2p-1}(\cos\frac{a}{2}\cos\theta), \quad k=0, \\ \frac{1}{2N}\sum_{p=1}^{2N-1}\left[\cos\frac{pk\pi}{2N}+(-1)^{p+k-1}\right]\frac{1}{\cosh p(2\pi-\frac{b}{2})}T_p(\cos\frac{a}{2}\cos\theta)- \\ -\frac{1}{4N}\sum_{p=1}^{N-1}\left[\cos\frac{pk\pi}{N}+(-1)^{k-1}\right]\frac{1}{\cosh 2p(2\pi-\frac{b}{2})}\times \\ \times\left[P_p(\cos a)-P_{p-1}(\cos a)\right], \quad k=1,\ldots,2N-1, \end{cases}$$

$$R_{2,k}^{(N)}(\theta) = \frac{1}{N(1+\delta_{0,k}+\delta_{N,k})}\sum_{m=1}^{N}(2-\delta_{m,N})\cos mx_k^{(N)}\left(\cos\frac{a}{2}\right)^m\times$$

$$\times\left\{\frac{\cosh 2m\pi-\sinh 2m\pi-\sinh m(b-2\pi)}{2m\sinh\frac{mb}{2}\cosh m(2\pi-\frac{b}{2})}T_m(\cos\frac{a}{2}\cos\theta)-\right.$$

$$[P_m(\cos a)-P_{m-1}(\cos a)]\frac{\cosh 4m\pi-\sinh 4m\pi-\sinh 2m(b-2\pi)}{8m\sinh mb\cosh 2m(2\pi-\frac{b}{2})}\times$$

$$\left[P_m^{(0,m)}(\cos a)-P_{m-1}^{(0,m)}(\cos a)\right]+$$

$$+\sum_{j=m+1}^{\infty}\frac{\cosh 4j\pi-\sinh 4j\pi-\sinh 2j(b-2\pi)}{4j\sinh jb\cosh 2j(2\pi-\frac{b}{2})}\times$$

$$\times\left[T_{2j}(\cos\frac{a}{2}\cos\theta)-\frac{P_j(\cos a)}{2}+\frac{P_{j-1}(\cos a)}{2}\right]\times$$

$$\left.\times\left[P_j^{0,m}(\cos a)-P_{j-1}^{0,m}(\cos a)\right]\right\}+$$

$$+\left\{\frac{-1+\sum_{j=1}^{\infty}\frac{\cosh 4j\pi-\sinh 4j\pi-\sinh 2j(b-2\pi)}{4j\sinh jb\cosh 2j(2\pi-\frac{b}{2})}}{N(1+\delta_{0,k}+\delta_{N,k})}\times\right.$$

$$\left.\times\left[T_{2j}(\cos\frac{a}{2}\cos\theta)-\frac{P_j(\cos a)}{2}+\frac{P_{j-1}(\cos a)}{2}\right][P_j(\cos a)-P_{j-1}(\cos a)]\right\},$$

$$R_{3,k}^{(N)}(\theta)=\frac{1}{2N(1+\delta_{0,k}+\delta_{N,k})}\sum_{m=1}^{N}(2-\delta_{m,N})\cos mx_k^{(N)}\left(\cos\frac{a}{2}\right)^m\times$$

$$\times\left[\frac{\cos\frac{m\theta}{2}}{\cosh m(2\pi-\frac{b}{2})}+\sum_{j=m+1}^{\infty}\frac{\cos j\theta}{\cosh 2j(2\pi-\frac{b}{2})}\times\right.$$

$$\left.\times\left(P_j^{(0,m)}(\cos a)-P_{j-1}^{(0,m)}(\cos a)\right)\right],\ x_k^{(N)}=\frac{k\pi}{N},\ k=0,1,...,2N-1.$$

Using these numerical quadratures, we define the following discrete approximation $\mathcal{A}_N^{(a,b)}$ for the operator $\mathcal{A}^{(a,b)}$:

$$\left(\mathcal{A}_N^{(a,b)}u_N\right)\left(x_j^{(N)}\right)\equiv\sum_{k=0}^{2N-1}\hat{R}_k^{(N)}\left(x_j^{(N)}\right)u_N\left(x_k^{(N)}\right)+$$

$$+\sum_{k=0}^{N}R_{3,k}^{(N)}\left(x_j^{(N)}\right)\psi_N\left(x_k^{(N)}\right),\quad j=0,1,...,2N-1,\quad (2.84a)$$

$$\sum_{k=0}^{N}\left[R_k^{(N)}\left(x_i^{(N)}\right)-R_{2,k}^{(N)}\left(x_i^{(N)}\right)\right]\psi_N\left(x_k^{(N)}\right)-$$

$$-\sum_{k=0}^{2N-1}R_{1,k}^{(N)}\left(x_i^{(N)}\right)u_N\left(x_k^{(N)}\right),\quad i=0,..,N.\quad (2.84b)$$

In view of the inclusions $\mathcal{A}u_N\in\hat{\mathbf{T}}_N$, $B_1\psi_N\in\mathbf{T}_N$, $L\psi_N\in\mathbf{T}_N$ for $u_N\in\mathbf{T}_N$, $\psi_N\in\mathbf{T}_N$, we can rewrite (2.84) in the following form

$$\left(\mathcal{A}_N^{(a,b)}u_N\right)\left(x_j^{(N)}\right)\equiv\left(\mathcal{A}u_N+B_1^*\psi_N\right)\left(x_j^{(N)}\right),\quad j=0,1,...,2N-1,$$

$$\left[(L-B_2)\,\psi_N\right]\left(x_i^{(N)}\right)=-(B_1u_N)\left(x_i^{(N)}\right),\quad i=0,1,...,N,$$

or in the following operator form

$$\mathcal{A}_N^{(a,b)} u_N \equiv \mathcal{A} u_N + \hat{P}_N B_1^* \psi_N, \quad (L - P_N B_2 P_N)\,\psi_N = -B_1 \hat{P}_N u_N,$$

from where $\mathcal{A}_N^{(a,b)} = \mathcal{A} - \hat{P}_N B_1^* (L - P_N B_2 P_N)^{-1} B_1 \hat{P}_N$ on $\hat{\mathbf{T}}_N$.

It is easy to see that $\mathcal{A}_N^{(a,b)}$ is a symmetric operator. Since $\mathcal{A}, L, B_2$ are non-negative definite, we get from the line

$$\left(\mathcal{A}_N^{(a,b)} u_N, u_N\right) = (\mathcal{A} u_N, u_N) + \left(\hat{P}_N B_1^* \psi_N, u_N\right) + (P_N B_2 P_N \psi_N, \psi_N) -$$
$$- (L\psi_N, \psi_N) - (B_1 P_N^* u_N, \psi_N) = (\mathcal{A} u_N, u_N) - (L\psi_N, \psi_N) +$$
$$+ (B_2 P_N \psi_N, P_N \psi_N)$$

that the operator $\mathcal{A}_N^{(a,b)}$ is also non-negative definite. The dependence of $\left(\mathcal{A}_N^{(a,b)} u_N, u_N\right)$ on b is only due to the kernels, therefore, we can analogously as above prove the following result:

Theorem 2.18. *The eigenvalues $\lambda_n^{(N)}(a,b)$ of the operator $\mathcal{A}_N^{(a,b)}$ have the properties:*
i) *for a fixed $a \in (0,\pi]$, it holds*

$$\lambda_n^{(N)}(a,b) \le \lambda_n^{(N)}(a,b') \text{ if } 0 \le b' \le b \le 4\pi, \quad n = 0,1,...,2N-1$$

ii) $0 \le \lambda_n^{(N)}(a,b) \le \lambda_N^{(N)}(a,0) = \frac{n}{2}\tanh 2\pi n, \quad n = 0,1,...,2N-1.$

Let us consider the operators

$$\mathcal{B} = B_1^*(L - B_2)^{-1} B_1 \quad \text{and} \quad \mathcal{B}_N = \hat{P}_N B_1^* (L - P_N B_2 P_N)^{-1} B_1 \hat{P}_N$$

and show that $\|(B - B_N)v\|_q \le c N^{q-p} \|v\|_p$.

Since B_1, B_1^*, B_2 are integral operators with infinitely-differentiable kernels, they are bounded from H^p into H^q for an arbitrary pair p, q. The operator L is an even pseudo-differential operator of the order $\beta = -1$. Because $\ker(L - B_2) = \emptyset$ in H^p $\forall p \in \mathbb{R}$, the operator $L^{-1}B_2 : H^p \to H^p$ is compact. By using the Rietz-Fredholm theory, the operator $L - B_2 : H^p \to H^{p+1}$ is an isomorphism. Analogously, the operator $L - P_N B_2 P_N : H^p \to H^{p+1}$ is also an isomorphism. Hence, the operator $\mathcal{B}$ is bounded from H^p into H^q for any $p, q \in \mathbb{R}$.

In the following, the original theorem 2.3 by Kress & Sloan (1993) [97] for the operator $\mathcal{A}^{(a,b)} + \varepsilon I \equiv \mathcal{A} + \varepsilon I - \mathcal{B}$ with a positive ε will be implemented. To do that, we need to estimate $\|\mathcal{B}v - \mathcal{B}_N v\|_{q-\beta}$, where β

is the order of the pseudo-differential operator $\mathcal{A}$ and, in our case, $\beta = 1$. We have

$$\begin{aligned}\|\mathcal{B}v - \mathcal{B}_N v\|_{q-1} \le & \left\|(I-\hat{P}_N)B_1^*(L-B_2)^{-1}B_1 v\right\|_{q-1} + \\ & + \left\|\hat{P}_N B_1^*\left[(L-B_2)^{-1} - (L-P_N B_2 P_N)^{-1}\right] B_1 v\right\|_{q-1} + \\ & + \left\|\hat{P}_N B_1^*(L-P_N B_2 P_N)^{-1} B_1 (I-\hat{P}_N) v\right\|_{q-1} \equiv J_1 + J_2 + J_3.\end{aligned}$$

Using the estimates (2.56), (2.58), one gets

$$\begin{aligned}J_1 \equiv & \left\|(I-\hat{P}_N)B_1^*(L-B_2)^{-1}B_1 v\right\|_{q-1} \le \\ & \le cN^{q-p+\frac{1}{2}}\left\|B_1^*(L-B_2)^{-1}B_1 v\right\|_p \le cN^{q-p+\frac{1}{2}}\|v\|_{p-2},\end{aligned}$$

$$\begin{aligned}J_2 & \le c\left\|(L-B_2)^{-1}(B_2 - P_N B_2 P_N)(L-P_N B_2 P_N)^{-1}B_1 v\right\|_{q-1} \le \\ & \le c\left\|(B_2 - P_N B_2 P_N)(L-P_N B_2 P_N)^{-1}B_1 v\right\|_{q-2} \le \\ & \le c\Big[\left\|(I-P_N)B_2(L-P_N B_2 P_N)^{-1}B_1 v\right\|_{q-2} + \\ & + \left\|P_N B_2(I-P_N)(L-P_N B_2 P_N)^{-1}B_1 v\right\|_{q-2}\Big] \le \\ & \le cN^{q-p}\left\|B_2(L-P_N B_2 P_N)^{-1}B_1 v\right\|_{p-2} + \\ & + cN^{q-p}\left\|(L-P_N B_2 P_N)^{-1}B_1 v\right\|_{p-2} \le cN^{q-p}\|v\|_{p-3}, \\ J_3 & \le cN^{q-p+\frac{1}{2}}\|v\|_{p-2}.\end{aligned}$$

Therefore, we have

$$\|\mathcal{B}v - \mathcal{B}_N v\|_{q-1} \le cN^{q-p+\frac{1}{2}}\|v\|_{p-2}. \tag{2.85}$$

The operator $\mathcal{A} + \varepsilon I$, $\varepsilon > 0$ is an even pseudo-differential operator of the order $\beta = 1$ from H^p into H^{p-1}, B maps boundedly H^p into H^q for any p, q. Hence, we can deduce that all the assumptions of Theorem 2.3 by Kress & Sloan (1993) [97] are fulfilled for the operator $\mathcal{A}^{(a,b)} + \varepsilon I = \mathcal{A} + \varepsilon I - \mathcal{B}$ with $\beta = 1$, $\alpha = 2$ and we derived the following result on the approximation of the solution of the equation

$$\left(\mathcal{A}^{(a,b)} + \varepsilon I\right) u = f$$

by the solution of the projection equation

$$\left[(\mathcal{A}^{(a,b)}+\varepsilon I)u_N\right]\left(x_j^{(N)}\right)=f\left(x_j^{(N)}\right), \quad j=0,...,2N-1,\ u_N\in\hat{\mathbf{T}}_N: \tag{2.86}$$

Theorem 2.19. *For sufficiently large N and for each $u\in H^p$ with $f=(\mathcal{A}^{(a,b)}+\varepsilon I-\mathcal{B})u\in C[0,2\pi]$, there exists an unique solution $u_N\in\hat{\mathbf{T}}_N$ of (2.86) and we have the asymptotic error estimate*

$$\|u-u_N\|_q\le cN^{q-p+\frac{1}{2}}\|u\|_p,\quad 2\le q\le p,\ \frac{5}{2}<p.$$

Table 2.1. Numerical example 1.

		Init.function u_{01}		Init.function u_{02}	
t	$N=M$	$x=0$	$x=\pi$	$x=0$	$x=\frac{\pi}{4}$
0.0	32	1.99935470	0.667135941	0.999984739	0.707095979
	64	2.00000645	0.666559303	1.00000004	0.707106779
	128	1.99999997	0.666684459	0.999999989	0.707106767
0.4	32	1.84602194	0.684517612	0.921055934	0.651284961
	64	1.84625296	0.684398403	0.921061753	0.651288992
	128	1.84625472	0.684364133	0.921061384	0.651288681
0.8	32	1.45377950	0.736305259	0.696714448	0.492651612
	64	1.45352783	0.736473071	0.696709841	0.492648153
	128	1.45352783	0.736485387	0.696708112	0.492646979
1.2	32	0.984628650	0.820270975	0.362357462	0.256225428
	64	0.984886538	0.819979388	0.362363433	0.256229676
	128	0.984885574	0.819970732	0.362360429	0.256227522
1.6	32	0.604350837	0.929137928	-0.029197610	-0.020645888
	64	0.604368983	0.929258949	-0.029191373	-0.020641384
	128	0.604365633	0.929290539	-0.0291955889	-0.020644423
2.0	32	0.401562094	1.055552539	-0.416132328	-0.294250044
	64	0.401175985	1.05599311	-0.416137522	-0.294253594
	128	0.401175858	1.05593659	-0.416142381	-0.294257120

Now, let us consider the linear sloshing problem for a tank with baffles

$$\frac{\partial^2u(x,t)}{\partial t^2}+\left(\mathcal{A}^{(a,b)}u\right)(x,t)=0,\quad u(x,0)=u_0(x),\ \frac{\partial u(x,0)}{\partial t}=0. \tag{2.87}$$

Analogously to § 2.3.3, we define a fully discrete model for (2.87) as follows

$$
\begin{aligned}
&u(x,t) \approx u_M^N(x,t) = u_{1,M}^N(x,t) + \tilde{\alpha}_0; \quad \tilde{\alpha}_0 = \int_0^{2\pi} \hat{P}_N u_0 \, dx, \\
&u_{1,M}^N(x,t) = e^{-\delta t} \sum_{k=0}^{M} L_k^{(0)}(t) \left[\hat{u}_k(x) - \hat{u}_{k+1}(x)\right],
\end{aligned}
\tag{2.88}
$$

$$
\begin{aligned}
&\left[\mathcal{A}_N^{(a,b)} + (\delta-1)^2 I\right] \hat{u}_{k+1} = \\
&\quad = 2\left[\mathcal{A}_N^{(a,b)} + \delta(\delta-1) I\right] \hat{u}_k - \left[\mathcal{A}_N^{(a,b)} + \delta^2 I\right] \hat{u}_{k-1}, \\
&\left[\mathcal{A}_N^{(a,b)} + (\delta-1)^2 I\right] \hat{u}_1 = \left[\mathcal{A}_N^{(a,b)} + \delta(\delta-1) I\right] \hat{u}_0; \\
&k = 1, ..., \quad \hat{u}_0 = \hat{P}_N \hat{\tilde{u}}_0.
\end{aligned}
\tag{2.89}
$$

For the error $z_k^N = \hat{u}_k - u_k$, we have the equations

$$
\begin{aligned}
&\left[\mathcal{A}_N^{(a,b)} + (\delta-1)^2 I\right] z_{k+1} = \\
&= 2\left[\mathcal{A}_N^{(a,b)} + \delta(\delta-1) I\right] z_k - \left[\mathcal{A}_N^{(a,b)} + \delta^2 I\right] z_{k-1} + \Psi_k, \quad k = 1, ..., \\
&\left[\mathcal{A}_N^{(a,b)} + (\delta-1)^2 I\right] z_1 = \left[\mathcal{A}_N^{(a,b)} + \delta(\delta-1)\right] z_0 + \Psi_0; \quad z_0 = \hat{P}_N \hat{\tilde{u}}_0 - \hat{\tilde{u}}_0,
\end{aligned}
$$

where

$$
\begin{aligned}
\Psi_k &= \left(\mathcal{A}^{(a,b)} - \mathcal{A}_N^{(a,b)}\right)(u_{k+1} - 2u_k + u_{k-1}) = \\
&= -(\mathcal{B} - \mathcal{B}_N)(u_{k+1} - 2u_k + u_{k-1}), \quad k = 1, 2, ... \\
\Psi_0 &= \left(\mathcal{A}^{(a,b)} - \mathcal{A}_N^{(a,b)}\right)(u_1 - u_0) = -(\mathcal{B} - \mathcal{B}_N)(u_1 - u_0),
\end{aligned}
$$

in view of $\hat{u}_k \in \hat{\mathbf{T}}_n$.

The solution to (2.89) is

$$
z_k = \int_{\lambda_1}^{\infty} \chi_1^{\frac{k}{2}} T_k(\chi_2) dE_\lambda z_0 + \int_{\lambda_1}^{\infty} \sum_{j=0}^{k-1} \chi_1^{\frac{k-1-j}{2}} T_{k-1-j}(\chi_2) dE_\lambda \Psi_j,
$$

where χ_1, χ_2 are given by (2.59) and E_λ is the spectral family of $\mathcal{A}_N^{a,b)}$. Now, we obtain the estimate

Table 2.2. Numerical example 2.

		Init.function u_{01}		Init.function u_{02}	
t	$N=M$	$x=0$	$x=\pi$	$x=0$	$x=\frac{\pi}{4}$
0.0	32	1.99973741	0.665822571	0.999998413	0.707112122
	64	1.99998758	0.666772062	0.999871225	0.707050394
	128	1.99999950	0.666670902	0.999992879	0.707123463
0.4	32	1.92617202	0.667551049	0.984525031	0.696184567
	64	1.92453411	0.667946195	0.972940151	0.694437271
	128	1.92452998	0.667979826	0.972897148	0.694421946
0.8	32	1.73454538	0.671862594	0.938595726	0.663704146
	64	1.72761319	0.672072730	0.893652081	0.658601141
	128	1.72761549	0.672056915	0.893671869	0.658592867
1.2	32	1.49316318	0.677594719	0.863633023	0.610685201
	64	1.47796014	0.679210401	0.768119107	0.605395965
	128	1.47795799	0.679226274	0.768098848	0.605423247
1.6	32	1.26913832	0.686991619	0.761946428	0.538784993
	64	1.24173157	0.689794784	0.604610604	0.541510470
	128	1.24173645	0.689759249	0.604658022	0.541486437
2.0	32	1.09617648	0.700770528	0.636684139	0.450215771
	64	1.05292316	0.703513532	0.413966893	0.47038831
	128	1.05291576	0.703571717	0.413888784	0.470375459

$$\|z_k\|_q \le q_N^k \|z_o\|_q + \sum_{j=0}^{k-1} q_N^{k-1-j} \|\Psi_j\|_q, \tag{2.90}$$

with

$$q_N = \sqrt{1 - \frac{1-2\delta}{\frac{2N-1}{2}\tanh 2\pi(2N-1) + (\delta-1)^2}}.$$

Using the estimate (2.85), we get

$$\begin{aligned} &\|\Psi_j\|_q \le cN^{q-p+\frac{1}{2}} \|u_{j+1} - 2u_j + u_{j-1}\|_{p-1}, \quad j = 1, 2, ..., \\ &\|\Psi_0\|_q \le cN^{q-p+\frac{1}{2}} \|u_1 - u_0\|_{p-1}. \end{aligned} \tag{2.91}$$

Substituting (2.91) into (2.90) we have

$$\|z_k\|_q \le cN^{q-p+\frac{1}{2}} \Big\{ q_N^k \|\hat{\tilde{u}}\|_p + q_N^{k-1} \|u_1 - u_0\|_{p-1} +$$

$$+\sum_{j=1}^{k-1} q_N^{k-1-j}\|u_{j+1}-2u_j+u_{j-1}\|_{p-1}\Big\}.$$

In the following, we use the estimate

$$\|u_j\|_{p-1} \le cj^{-1}\left\|\mathcal{A}_N^{(a,b)}\hat{\tilde{u}}_0\|_{p-1} \le cj^{-1}\|\hat{\tilde{u}}_0\right\|_p$$

and get

$$\|z_k\|_q \le cN^{q-p+\frac{1}{2}}\left\{q_N^k+\sum_{j=0}^{k-1}\frac{q_N^{k-1-j}}{j+1}\right\}\|\hat{\tilde{u}}_0\|_p \le cN^{q-p+\frac{1}{2}}\sum_{j=0}^{k}\frac{q_N^{k-j}}{j+1}\|\hat{\tilde{u}}_0\|_p\,.$$

For the error

$$u_{1,M}(x,t)-u_{1,M}^N(x,t)=e^{-\delta t}\sum_{k=0}^{M}L_k^{(0)}(t)[z_{k+1}-z_k],$$

one can obtain the estimate

$$\sup_{t\in[0,T]}\|u_{1,M}(\cdot,t)-u_{1,M}^N(\cdot,t)\|_q \le cN^{q-p+\frac{1}{2}}\sum_{k=0}^{M}\sum_{j=0}^{k}\frac{q_N^{k-j}}{j+1}\|\hat{\tilde{u}}_0\|_p =$$

$$= cN^{q-p+\frac{1}{2}}\sum_{j=0}^{M}\sum_{k=j}^{M}\frac{q_N^{k-j}}{j+1}\hat{\tilde{u}}_0\|_p = cN^{q-p+\frac{1}{2}}\sum_{j=0}^{M}\frac{1}{j+1}\frac{q_N^{M-j+1}-1}{q_N-1}\|\hat{\tilde{u}}_0\|_p \le$$

$$\le cN^{q-p+\frac{1}{2}}\ln M\frac{1}{1-q_N}\|\hat{\tilde{u}}_0\|_p \le cN^{q-p+\frac{3}{2}}\ln M\|\hat{\tilde{u}}_0\|_p.$$

When performing other estimates similarly to those of Theorem 2.15, we arrive at the following statement:

Theorem 2.20. *For the error of the fully discrete approximation (2.88), the following estimate holds true*

$$\sup_{t\in[0,T]}\|u(\cdot,t)-u_{1,M}^N(\cdot,t)-\tilde{\alpha}_0\|_q \le c\left(M^{q-p+\frac{1}{4}}+N^{q-p+\frac{3}{2}}\ln M\right)\|u_0\|_p.$$

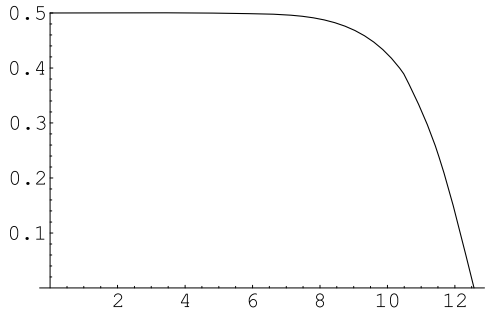

Fig. 2.4. The eigenvalue $\lambda_1^{(128)}\left(\frac{\pi}{2}, b\right)$ as function of b.

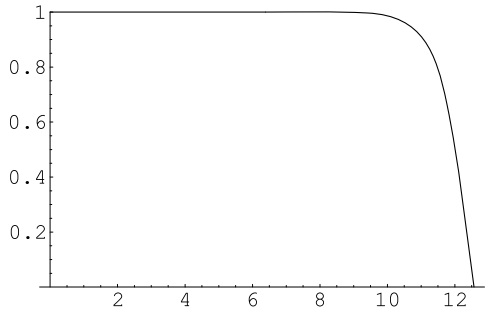

Fig. 2.5. The eigenvalue $\lambda_2^{(128)}\left(\frac{\pi}{2}, b\right)$ as function of b.

2.3.4 Numerical examples

Let us consider the problem (2.87) with the initial functions (Ryshik & Gradstein (1963) [150])

$$u_{01}(x) = \sum_{k=1}^{\infty} \frac{\cos kx}{2^k} = \frac{2(2 - \cos x)}{5 - 4\cos x}, \quad x \in [0, 2\pi]$$

and

$$u_{02}(x) = \cos x, \quad x \in [0, 2\pi]$$

Using our numerical method for the case $\sigma = 0, a = \frac{\pi}{2}, b = 2\pi$, we present numerical results in Table 2.1. These show that the doubling of M provides the doubling of the significant digits. This indicates the exponential convergence, which we expected from our error analysis. Further,

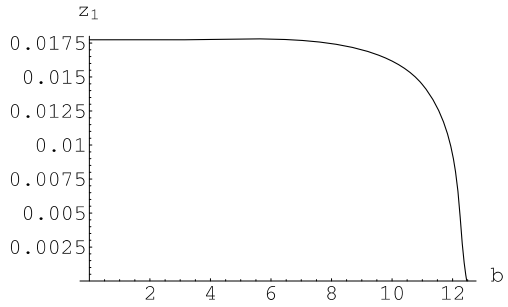

Fig. 2.6. $z_1\,(b) = |u\,(\pi, 0.4) - u_{01}\,(\pi)\,|$ versus b.

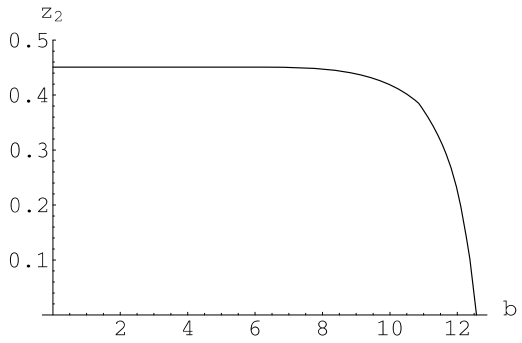

Fig. 2.7. $z_2\,(b) = |u\,(\frac{\pi}{4}, 1.2) - u_{02}\,(\frac{\pi}{4})\,|$ versus b.

Table 2.2 presents numerical results for the case $\sigma = 0, a = \frac{\pi}{2}, b = 4\pi - \frac{\pi}{16}$, i.e. when the baffles are situated near the fluid surface. One can also observe the exponential convergence as well as the decay of the potential downward from the free surface.

Figs. 2.4 and 2.5 present dependence of the first two eigenvalues $\lambda_1^{(N)}\,(a,b)$ $\lambda_2^{(N)}\,(a,b)$ of the discrete operator $\mathcal{A}_N^{(a,b)}$ (for $b = 2\pi$) on the baffle length a. These demonstrate the monotonic decaying of both eigenvalues, which is predictable from the physics of sloshing. Finally, Figs. 2.6 and 2.7 show the difference of the surface potential from the initial surface potential versus b.

3

Nonlinear modal theory

3.1 Modal equations

3.1.1 Free boundary problem

Let an incompressible perfect fluid occupy partly a rigid tank (cavity) Q of a moving solid body as shown in Fig. 3.1. Motion of the body is described in an absolute Cartesian coordinate system $O'x'y'z'$ by the given pair of time-dependent vectors $\boldsymbol{v}_O(t)$ and $\boldsymbol{\omega}(t)$ implying instantaneous translatory and angular velocities, respectively. The inner fluid flows are described in a non-inertial Cartesian coordinate system $Oxyz$ rigidly framed with the body. Since any absolute position vector $\boldsymbol{r}'(t) = (x', y', z')$ can be decomposed into the sum of $\boldsymbol{r}'_O(t) = \mathbf{O'O}$ and the relative position vector $\boldsymbol{r} = (x, y, z)$ (see, Fig. 3.1), the gravity potential is a function of (x, y, z) and t, namely, $U(x, y, z, t) = -\boldsymbol{g} \cdot \boldsymbol{r}'$, $\boldsymbol{r}' = \boldsymbol{r}'_O + \boldsymbol{r}$, where $\boldsymbol{g}$ is the gravity acceleration.

Henceforth, we assume irrotational flows and introduce the velocity potential $\Phi(x, y, z, t)$, which describes the absolute velocity as function of (x, y, z, t), i.e.

$$\boldsymbol{v}_a = \nabla\, \Phi.$$

Derivations of the corresponding free boundary problem, which couples $\Phi(x, y, z, t)$ and the free surface motions, are for instance given in the books by Moiseev & Rumyantsev (1968) [130], Narimanov *et al.* (1977) [135] and Lukovsky (1990) [114]. The problem takes the following form

$$\Delta\Phi = 0 \quad \text{in } Q(t), \tag{3.1a}$$

$$\frac{\partial\Phi}{\partial\nu} = \boldsymbol{v}_0 \cdot \boldsymbol{\nu} + \boldsymbol{\omega} \cdot [\boldsymbol{r} \times \boldsymbol{\nu}] \quad \text{on } S(t), \tag{3.1b}$$

$$\frac{\partial\Phi}{\partial\nu} = \boldsymbol{v}_0 \cdot \boldsymbol{\nu} + \boldsymbol{\omega} \cdot [\boldsymbol{r} \times \boldsymbol{\nu}] - \frac{\xi_t}{|\nabla\xi|} \quad \text{on } \Sigma(t), \tag{3.1c}$$

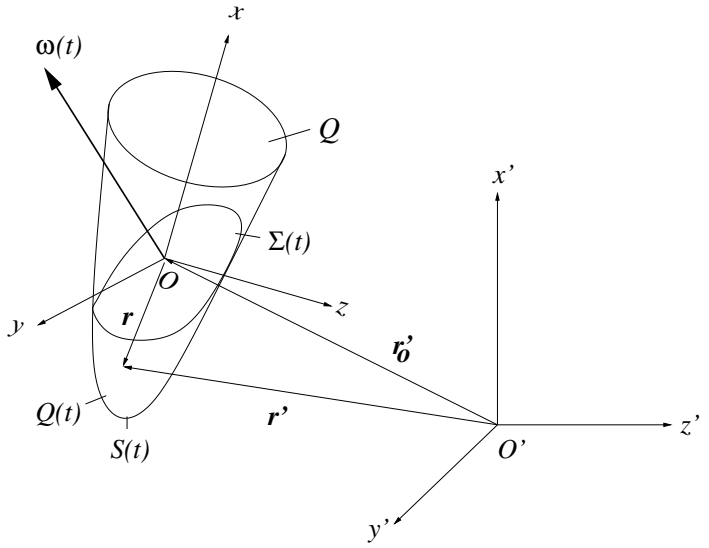

Fig. 3.1. Sketch of a moving tank and adopted nomenclature.

$$\frac{\partial \Phi}{\partial t} + \tfrac{1}{2}(\nabla \Phi)^2 - \nabla \Phi \cdot (\boldsymbol{v}_0 + \boldsymbol{\omega} \times \boldsymbol{r}) + U = 0 \quad \text{on } \Sigma(t), \tag{3.1d}$$

$$\int_{Q(t)} dQ = \text{const}, \tag{3.1e}$$

where $S(t)$ is the wetted walls/bottom, $\boldsymbol{\nu}$ is the outer normal to $\partial Q(t) = S(t) \cup \Sigma(t)$ and $\xi(x, y, z, t) = 0$ determines the free surface $\Sigma(t)$.

The last integral condition (3.1e) expresses the fluid mass (volume) conservation and appears as the resolvability condition of the Neumann boundary value problem (3.1a)–(3.1c)

$$\frac{d}{dt}\int_{Q(t)} dQ = -\int_{\Sigma(t)} \frac{\xi_t}{|\nabla \xi|}\, dS + \underbrace{\int_{S(t)+\Sigma(t)} (\boldsymbol{v}_0 \cdot \boldsymbol{\nu} + \boldsymbol{\omega} \cdot [\boldsymbol{r} \times \boldsymbol{\nu}])\, dS}_{=0} = \int_{S(t)+\Sigma(t)} \frac{\partial \Phi}{\partial \nu}\, dS = 0 \tag{3.2}$$

(see, detailed discussion of this point by Lukovsky & Timokha (1995) [117] and Faltinsen & Timokha (2002) [51]). Eq. (3.1c) is often called the

kinematic boundary condition. Eq. (3.1d), the so-called dynamic boundary condition, is obtained by using Bernoulli's integral for the pressure written in the moving coordinate system $Oxyz$ (see, Kochin *et al.* (1964) [93]). Physically, Eq. (3.1d) states that the pressure on the free surface is equal to an "atmospheric" constant p_0. The hydrodynamic pressure p in $Q(t)$ can be computed via the Bernoulli integral as follows

$$\frac{\partial \Phi}{\partial t} + \tfrac{1}{2}(\nabla \Phi)^2 - \nabla \Phi \cdot (\boldsymbol{v}_0 + \boldsymbol{\omega} \times \boldsymbol{r}) + U + \frac{p - p_0}{\rho} = 0 \quad \text{in} \quad Q(t), \quad (3.3)$$

where $\partial \Phi / \partial t$ is calculated in the moving coordinate system, i.e. for a point rigidly connected with the system $Oxyz$.

The evolutional free boundary problem (3.1) should be completed by either initial or periodicity conditions. The initial (Cauchy) conditions must define the initial shape of the free surface, $\Sigma(t_0)$, and the initial normal velocity of $\Sigma(t)$:

$$\xi(x, y, z, t_0) = \xi_0(x, y, z), \quad \frac{\partial \Phi}{\partial \nu}\Big|_{\Sigma(t_0)} = \phi_0(x, y, z), \quad (3.4)$$

where ξ_0 and ϕ_0 are given functions.

An appropriate periodicity condition, which is associated with steady-state wave regimes, may read as follows

$$\begin{aligned} &\xi(x, y, z, t + T) = \xi(x, y, z, t), \\ &\nabla \Phi(x, y, z, t + T) = \nabla \Phi(x, y, z, t) \quad \text{in} \quad Q(t + T) = Q(t). \end{aligned} \quad (3.5)$$

Here, the latter condition is mathematically justified by the first condition, which can be interpreted as the identity of instantaneous fluid shapes at t and $t+T$, namely, the first condition postulates that $Q(t+T) \equiv Q(t)$.

3.1.2 Modal system by Miles-Lukovsky

Perhaps, Narimanov (1957) [134] has been first, who proposed an algorithm for reduction of the free boundary problem (3.1) to an infinite-dimensional system of nonlinear ordinary differential equations, the so-called **modal system**. The modal system couples generalised coordinates and impulses, which are associated with the time-dependent coefficients in Fourier expansions of the free surface and the velocity potential, respectively. Later on, in 1976, Miles [125] and Lukovsky [113] have independently proposed a variational procedure for deriving the modal

system. This variational procedure was recently modernised by Faltinsen *et al.* (2000) [45]. Following Lukovsky (1990) [114] and Faltinsen *et al.* (2000) [45], we should consider the boundary value problem (3.1), in which the unknowns are Φ and ξ, and, in the parallel way, the following Bateman–Luke variational principle, in which the pressure is treated as the Lagrangian.

PRESSURE-INTEGRAL LAGRANGIAN (BATEMAN-LUKE) VARIATIONAL PRINCIPLE. *The boundary value problem (3.1) can be described by examining the necessary conditions for the extrema of the functional*

$$W = \int_{t_1}^{t_2} L dt, \tag{3.6}$$

where the Lagrangian L is the pressure-integral

$$L = \int_{Q(t)} (p - p_0) dQ = \\ = -\rho \int_{Q(t)} \left[\frac{\partial \Phi}{\partial t} + \tfrac{1}{2} (\nabla \Phi)^2 - \nabla \Phi \cdot (\boldsymbol{v}_0 + \boldsymbol{\omega} \times \boldsymbol{r}) + U \right] dQ \tag{3.7}$$

and the test functions satisfy

$$\delta \Phi(x, y, z, t_i) = 0; \qquad \delta \xi(x, y, z, t_i) = 0, \quad i = 1, 2. \tag{3.8}$$

The idea of using the pressure integral as the Lagrangian in hydrodynamic problems was first proposed by Hargneaves (1908) [79]. The canonical formulation of the principle was given by Bateman (1944) [15], Luke (1967) [111] (for gravity surface waves in infinite basins) and Lukovsky (1990) [114] (sloshing in mobile tanks). The latter author gave the proof of the formulation (3.6)–(3.8).

The original derivations of a nonlinear modal system following from the Bateman-Luke principle, which were given by Lukovsky (1990) [114] and Faltinsen *et al.* (2000) [45], are restricted to the tank shapes Q having vertical walls in a neighbourhood of the free surface (see, Fig. 3.2). Under assumption that no overturning occurs, one can express ξ as

$$\xi(x, y, z, t) = z - f(x, y, y)$$

and, therefore, the normal velocity component on $\Sigma(t)$ in the body-fixed system is

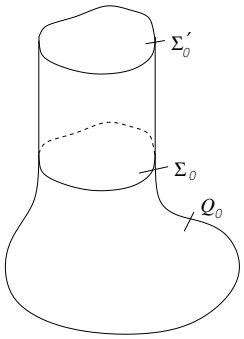

Fig. 3.2. Sketch of admissible shapes, for which the Miles-Lukovsky system can be derived. Σ_0 is the unperturbed (hydrostatic) free surface.

$$-\frac{\xi_t}{|\nabla\xi|} = \frac{f_t}{\sqrt{1+f_x^2+f_y^2}}.$$

.

Further, in accordance with Lukovsky (1990) [114], the velocity potential is expressed as

$$\Phi(x,y,z,t) = \boldsymbol{v}_0 \cdot \boldsymbol{r} + \boldsymbol{\omega} \cdot \boldsymbol{\Omega} + \varphi. \tag{3.9}$$

Here, the vector–function $\boldsymbol{\Omega}(x,y,z,t) = (\Omega_1, \Omega_2, \Omega_3)$ (Stokes-Joukowski potential) is the solution of the following Neumann boundary value problem

$$\begin{aligned} &\Delta\boldsymbol{\Omega} = 0 \quad \text{in} \quad Q(t); \quad \frac{\partial\Omega_1}{\partial\nu}|_{S(t)+\Sigma(t)} = y\nu_3 - z\nu_2, \\ &\frac{\partial\Omega_2}{\partial\nu}|_{S(t)+\Sigma(t)} = z\nu_1 - x\nu_3; \frac{\partial\Omega_3}{\partial\nu}|_{S(t)+\Sigma(t)} = x\nu_2 - y\nu_1, \end{aligned} \tag{3.10}$$

where ν_1, ν_2, ν_3 are projections of the outer normal $\boldsymbol{\nu}$ onto the $Oxyz$-axes and the function $\varphi(x,y,z,t)$ is a solution of the Neumann boundary value problem

$$\Delta\varphi = 0 \ \text{ in } Q(t); \quad \frac{\partial\varphi}{\partial\nu}|_{S(t)} = 0; \quad \frac{\partial\varphi}{\partial\nu}|_{\Sigma(t)} = \frac{f_t}{\sqrt{1+f_x^2+f_y^2}}. \tag{3.11}$$

Owing to (3.2), the Neumann boundary value problems for $\boldsymbol{\Omega}$ and φ are to within a constant uniquely resolvable. The solution depends

parametrically on t. Besides, by using (3.9) and the boundary problems for $\boldsymbol{\Omega}$ and φ it follows that $\boldsymbol{\Phi}$ satisfies the Laplace equation and the Neumann boundary conditions of (3.1). The dynamic condition (pressure balance) on $\Sigma(t)$ gives the final equation connecting $f, \boldsymbol{\Omega}$ and φ.

Let the function $f(x, y, t)$ be expressed as

$$f(x, y, t) = \sum_{i=1}^{\infty} \beta_i(t) f_i(x, y), \tag{3.12}$$

where $f_i(x, y)$ is a complete (to within a constant) system of functions satisfying the condition of volume conservation $\int_{\Sigma_0} f_i(x, y) dx dy = 0$ and $\beta_i(t)$ are defined as the generalised coordinates. Henceforth, Σ_0 is the unperturbed (hydrostatic) free surface.

Further,

$$\varphi(x, y, z, t) = \sum_{n=1}^{\infty} R_n(t)\, \varphi_n(x, y, z), \tag{3.13}$$

where the complete system of functions $\{\varphi_n(x, y, z)\}$ satisfies the Laplace equation in the whole domain Q and $R_n(t)$ are interpreted as the generalised impulses. Since the system $\{\varphi_n(x, y, z)\}$ is complete on any single-connected surface drawn inside the tank domain, it is also complete on Σ_0. The Stokes-Joukowski potentials are assumed to be known functions of β_i.

Remark 3.1. The representation (3.13) needs a set of harmonic functions $\{\varphi_n\}$, which are complete in the whole Q or, at least, in all the admissible instantaneous fluid domains $Q(t)$. Because Q has cylindrical shape in vicinity of the mean free surface Σ_0, such a family of harmonic functions $\{\varphi_n(x, y, z)\}$ can under certain limitations coincide with solutions of the following spectral boundary problem with spectral parameter $\varkappa_n$:

$$\Delta\varphi_n = 0 \ \text{ in } Q_0; \quad \frac{\partial \varphi_n}{\partial \nu} = 0 \ \text{ on } S; \quad \frac{\partial \varphi_n}{\partial \nu} = \varkappa_n \varphi_n \ \text{ on } \Sigma_0,$$
$$\int_{\Sigma_0} \varphi_n dS = 0. \tag{3.14}$$

This is the same as the eigenvalue problem for the natural linear sloshing. Its solutions can be found analytically only for a limited class of tank shapes. Examples are a vertical circular cylinder or a rectangular three-dimensional tank. A numerical method should be used to find φ_n for more

general shapes as it was demonstrated by Solaas & Faltinsen (1997) [158] for the two-dimensional sloshing. A different approach is to use a patching procedure. Solution in cylindrical portion of Q (see, Fig. 3.2) can then be expressed as

$$\varphi_n(x,y,z) = \sum_k (b_{nk}\exp(-\lambda_k z) + a_{nk}\exp(\lambda_k z))\phi_k(x,y) \qquad (3.15)$$

with unknown coefficients b_{nk} and a_{nk}. Here, $\varkappa_k$ and ϕ_k are solutions of the following two-dimensional spectral boundary problem

$$\Delta_2\phi_k(x,y) + \lambda_k^2\phi_k = 0 \text{ in } \Sigma_0;\ \frac{\partial\phi_k}{\partial n} = 0 \text{ on } \partial\Sigma_0;\ \int_{\Sigma_0}\phi_k dS = 0, \quad (3.16)$$

where $\partial\Sigma_0$ is the intersection line between Σ_0 and S. When the auxiliary problem (3.16) is formulated in circular (ring-shaped) or rectangular cross-sections Σ_0, $\{\phi_k\}$ are expressed by Bessel functions and/or sinusoidal functions. Otherwise, a numerical procedure is required. Solution in the remaining non-cylindrical part can be found by a numerical method; it should be matched with (3.15) on a transmission surface.

Remark 3.2. What are mathematical limitations in using the eigenfunctions of (3.14) as a harmonic basis in (3.13)? First, the eigenfunctions must be smoothly expandable over the mean fluid surface Σ_0 up to an artificial boundary Σ_0' implying an upper bond of the admissible wave elevations (see, Fig. 3.2). The patching procedure, which is described in Remark 3.1, provides this expansion. Second, more demanding limitation consists of the completeness of $\{\varphi_n\}$ for any admissible shapes of $Q(t)$. Timokha (2002) [163] showed that the eigenfunctions constitute a complete set of harmonic functions in Q_0, but not in Q_0' (the latter is formed by the artificial Σ_0'). This fact is true even for simple cylindrical Qs, in which (3.14) has an analytical solution. In view of this difficulty, the most authors interpret $\{\varphi_n\}$ of (3.14) as an "asymptotic" harmonic basis, namely, assume that $\Sigma(t)$ is to some extent asymptotically close to its unperturbed state Σ_0. Implicitly, this assumption implies that only asymptotic solutions of the Miles-Lukovsky system are mathematically correct, if (3.14) is used.

By substituting (3.9) into (3.7) the Lagrangian L takes the following form

$$L = -\rho \int\limits_{Q(t)} \Big[\dot{\boldsymbol{v}}_0 \cdot \boldsymbol{r} + \frac{\partial}{\partial t}(\boldsymbol{\omega} \cdot \boldsymbol{\Omega}) + \tfrac{1}{2}\nabla(\boldsymbol{\omega} \cdot \boldsymbol{\Omega}) \cdot \nabla(\boldsymbol{\omega} \cdot \boldsymbol{\Omega}) - \\ - \boldsymbol{\omega} \cdot (\boldsymbol{r} \times \nabla(\boldsymbol{\omega} \cdot \boldsymbol{\Omega})) - \tfrac{1}{2} v_0^2 - \boldsymbol{\omega} \cdot (\boldsymbol{r} \times \boldsymbol{v}_0) - \\ - \boldsymbol{\omega} \cdot (\boldsymbol{r} \times \nabla\varphi) + \nabla(\boldsymbol{\omega} \cdot \boldsymbol{\Omega}) \cdot \nabla\varphi \Big] dQ + L_r, \quad (3.17)$$

where

$$L_r = -\rho \int_{Q(t)} \left[\frac{\partial \varphi}{\partial t} + \frac{1}{2}(\nabla\varphi)^2 + U \right] dQ. \quad (3.18)$$

The two last integrand terms in square brackets of (3.17) cancel each other from Green's formula, i.e.

$$\int_{Q(t)} \nabla(\boldsymbol{\omega} \cdot \boldsymbol{\Omega}) \cdot \nabla\varphi - (\boldsymbol{\omega} \times \boldsymbol{r}) \cdot \nabla\varphi dQ = \\ = \int_{S(t)+\Sigma(t)} \left(\frac{\partial(\boldsymbol{\omega} \cdot \boldsymbol{\Omega})}{\partial \nu} - (\boldsymbol{\omega} \times \boldsymbol{r}) \cdot \boldsymbol{\nu} \right) \varphi dS = 0.$$

We also introduce the quadratic symmetric inertia tensor $\boldsymbol{J}^1(t)$ with components J^1_{ij} defined by the equality

$$-\rho \int_{Q(t)} \left(\tfrac{1}{2}\nabla(\boldsymbol{\omega} \cdot \boldsymbol{\Omega}) \cdot \nabla(\boldsymbol{\omega} \cdot \boldsymbol{\Omega}) - \boldsymbol{\omega} \cdot (\boldsymbol{r} \times \nabla(\boldsymbol{\omega} \cdot \boldsymbol{\Omega})) \right) dQ = \\ = -\tfrac{1}{2}\omega_1^2 J^1_{11} - \tfrac{1}{2}\omega_2^2 J^1_{22} - \tfrac{1}{2}\omega_3^2 J^1_{33} - \omega_1\omega_2 J^1_{12} - \omega_1\omega_3 J^1_{13} - \omega_2\omega_3 J^1_{23}.$$

The components J^1_{ij} can be calculated as follows

$$J^1_{11} = \rho \int\limits_{Q(t)} \left(y\frac{\partial \Omega_1}{\partial z} - z\frac{\partial \Omega_1}{\partial y} \right) dQ = \rho \int\limits_{S(t)+\Sigma(t)} \Omega_1 \frac{\partial \Omega_1}{\partial \nu} dS,$$

$$J^1_{22} = \rho \int\limits_{Q(t)} \left(z\frac{\partial \Omega_2}{\partial x} - x\frac{\partial \Omega_2}{\partial z} \right) dQ = \rho \int\limits_{S(t)+\Sigma(t)} \Omega_2 \frac{\partial \Omega_2}{\partial \nu} dS,$$

$$J^1_{33} = \rho \int\limits_{Q(t)} \left(x\frac{\partial \Omega_3}{\partial y} - y\frac{\partial \Omega_3}{\partial x} \right) dQ = \rho \int\limits_{S(t)+\Sigma(t)} \Omega_3 \frac{\partial \Omega_3}{\partial \nu} dS,$$

$$J^1_{12} = J^1_{21} = \rho \int\limits_{Q(t)} \left(z\frac{\partial \Omega_1}{\partial x} - x\frac{\partial \Omega_1}{\partial z} \right) dQ = \rho \int\limits_{Q(t)} \left(y\frac{\partial \Omega_2}{\partial z} - z\frac{\partial \Omega_2}{\partial y} \right) dQ =$$

$$= \rho \int\limits_{S(t)+\Sigma(t)} \Omega_1 \frac{\partial \Omega_2}{\partial \nu} dS = \rho \int\limits_{S(t)+\Sigma(t)} \Omega_2 \frac{\partial \Omega_1}{\partial \nu} dS,$$

$$J^1_{13} = J^1_{31} = \rho \int\limits_{Q(t)} \left(x \frac{\partial \Omega_1}{\partial y} - y \frac{\partial \Omega_1}{\partial x} \right) dQ = \rho \int\limits_{Q(t)} \left(y \frac{\partial \Omega_3}{\partial z} - z \frac{\partial \Omega_3}{\partial y} \right) dQ =$$

$$= \rho \int\limits_{S(t)+\Sigma(t)} \Omega_1 \frac{\partial \Omega_3}{\partial \nu} dS = \rho \int\limits_{S(t)+\Sigma(t)} \Omega_3 \frac{\partial \Omega_1}{\partial \nu} dS,$$

$$J^1_{23} = J^1_{32} = \rho \int\limits_{Q(t)} \left(x \frac{\partial \Omega_2}{\partial y} - y \frac{\partial \Omega_2}{\partial x} \right) dQ = \rho \int\limits_{Q(t)} \left(z \frac{\partial \Omega_3}{\partial x} - x \frac{\partial \Omega_3}{\partial z} \right) dQ =$$

$$= \rho \int\limits_{S(t)+\Sigma(t)} \Omega_2 \frac{\partial \Omega_3}{\partial \nu} dS = \rho \int\limits_{S(t)+\Sigma(t)} \Omega_3 \frac{\partial \Omega_2}{\partial \nu} dS.$$

The Lagrangian L (3.17) can be rewritten as

$$\begin{aligned} L = -[&\dot v_{01} l_1 + \dot v_{02} l_2 + \dot v_{03} l_3 + \dot\omega_1 l_{1\omega} + \dot\omega_2 l_{2\omega} + \dot\omega_3 l_{3\omega} + \omega_1 l_{1\omega t} + \omega_2 l_{2\omega t} + \\ &+ \omega_3 l_{3\omega t} - \tfrac{1}{2}(\omega_1^2 J^1_{11} + \omega_2^2 J^1_{22} + \omega_3^2 J^1_{33}) - \omega_1\omega_2 J^1_{12} - \omega_1\omega_3 J^1_{13} - \\ &- \omega_2\omega_3 J^1_{23} - \tfrac{1}{2} m_1 (v_{01}^2 + v_{02}^2 + v_{03}^2) + (\omega_2 v_{03} - \omega_3 v_{02}) l_1 + \\ &+ (\omega_3 v_{01} - \omega_1 v_{03}) l_2 + (\omega_1 v_{02} - \omega_2 v_{01}) l_3] + L_r, \end{aligned} \tag{3.19}$$

where

$$\begin{aligned} &m_1 = \rho \int_{Q(t)} dQ;\ l_{k\omega} = \rho \int_{Q(t)} \Omega_k dQ;\ l_{k\omega t} = \rho \int_{Q(t)} \frac{\partial \Omega_k}{\partial t} dQ, \\ &l_1 = \rho \int_{Q(t)} x dQ;\ l_2 = \rho \int_{Q(t)} y dQ;\ l_3 = \rho \int_{Q(t)} z dQ. \end{aligned} \tag{3.20}$$

The vectors $\boldsymbol{l} = \{l_k\}, \boldsymbol{l}_\omega = \{l_{k\omega}\}, \boldsymbol{l}_{\omega t} = \{l_{k\omega t}\}$ depend only on $\beta_i(t)$ and $\dot\beta_i(t)$.

It follows from (3.13) that

$$\begin{aligned} L_r &= -\rho \int_{Q(t)} \left[\sum_{n=1} \dot R_n \varphi_n + \tfrac{1}{2} \sum_{n,\ k} R_n R_k (\nabla\varphi_n, \nabla\varphi_k) + U \right] dQ = \\ &= -\left[\sum_n A_n \dot R_n + \tfrac{1}{2} \sum_{n,\ k} A_{nk} R_n R_k - g_1 l_1 - g_2 l_2 - g_3 l_3 - m_1 \boldsymbol{g} \cdot \boldsymbol{r}_0' \right], \end{aligned} \tag{3.21}$$

where

$$A_n = \rho \int_{Q(t)} \varphi_n dQ,$$
$$A_{nk} = A_{kn} = \rho \int_{Q(t)} (\nabla\varphi_n, \nabla\varphi_k) dQ = \rho \int_{\Sigma(t)+S(t)} \varphi_n \frac{\partial \varphi_k}{\partial \nu} dS \tag{3.22}$$

are functions of $\beta_i(t)$.

The Lagrangian L is originally a function of two independent variables $f(x,y,z,t)$ and $\Phi(x,y,z,t)$. The independent variables become the time–varying functions $\beta_i(t), i \geq 1$ and $R_n(t), n \geq 1$ after substituting (3.9), (3.12) and (3.13) into the Lagrangian. The variations of the functional (3.6) by $\beta_i(t)$ and $R_n(t)$ for given $\boldsymbol{v}_0(t)$ and $\boldsymbol{\omega}(t)$ are

$$\delta W = \int_{t_1}^{t_2} \left[\sum_n A_n \delta \dot{R}_n + \sum_{n,\ k} A_{nk} R_k \delta R_n + \sum_i \left(\sum_n \dot{R}_n \frac{\partial A_n}{\partial \beta_i} + \right.\right.$$
$$+ \omega_1 \frac{\partial l_{1\omega t}}{\partial \beta_i} + \omega_2 \frac{\partial l_{2\omega t}}{\partial \beta_i} + \omega_3 \frac{\partial l_{3\omega t}}{\partial \beta_i} + \tfrac{1}{2} \sum_{n,\ k} R_n R_k \frac{\partial A_{nk}}{\partial \beta_i} + \dot{\omega}_1 \frac{\partial l_{1\omega}}{\partial \beta_i} + \dot{\omega}_2 \frac{\partial l_{2\omega}}{\partial \beta_i} +$$
$$\dot{\omega}_3 \frac{\partial l_{3\omega}}{\partial \beta_i} + (\dot{v}_{01} - g_1 + \omega_2 v_{03} - \omega_3 v_{02}) \frac{\partial l_1}{\partial \beta_i} + (\dot{v}_{02} - g_2 + \omega_3 v_{01} - \omega_1 v_{03}) \frac{\partial l_2}{\partial \beta_i} +$$
$$+ (\dot{v}_{03} - g_3 + \omega_1 v_{02} - \omega_2 v_{01}) \frac{\partial l_3}{\partial \beta_i} - \tfrac{1}{2}\omega_1^2 \frac{\partial J_{11}^1}{\partial \beta_i} - \tfrac{1}{2}\omega_2^2 \frac{\partial J_{22}^1}{\partial \beta_i} -$$
$$\left. - \tfrac{1}{2}\omega_3^2 \frac{\partial J_{33}^1}{\partial \beta_i} - \omega_1\omega_2 \frac{\partial J_{12}^1}{\partial \beta_i} - \omega_1\omega_3 \frac{\partial J_{13}^1}{\partial \beta_i} - \omega_2\omega_3 \frac{\partial J_{23}^1}{\partial \beta_i} \right) \delta\beta_i +$$
$$\left. + \left(\omega_1 \frac{\partial l_{1\omega t}}{\partial \dot{\beta}_i} + \omega_2 \frac{\partial l_{2\omega t}}{\partial \dot{\beta}_i} + \omega_3 \frac{\partial l_{3\omega t}}{\partial \dot{\beta}_i} \right) \delta\dot{\beta}_i \right] dt = 0. \tag{3.23}$$

The following infinite system of nonlinear differential equations with respect to the modal functions $R_n(t)$ and $\beta_i(t)$ has been called **the Miles-Lukovsky modal system**. It is obtained by integrating by parts in (3.23) and using the condition (3.8) for the test functions:

$$\frac{d}{dt} A_n - \sum_k R_k A_{nk} = 0, \quad n = 1, 2, \ldots; \tag{3.24}$$

$$\sum_n \dot{R}_n \frac{\partial A_n}{\partial \beta_i} + \tfrac{1}{2} \sum_n \sum_k \frac{\partial A_{nk}}{\partial \beta_i} R_n R_k + \dot{\omega}_1 \frac{\partial l_{1\omega}}{\partial \beta_i} + \dot{\omega}_2 \frac{\partial l_{2\omega}}{\partial \beta_i} + \dot{\omega}_3 \frac{\partial l_{3\omega}}{\partial \beta_i} +$$

$$+\omega_1\frac{\partial l_{1\omega t}}{\partial\beta_i}+\omega_2\frac{\partial l_{2\omega t}}{\partial\beta_i}++\omega_3\frac{\partial l_{3\omega t}}{\partial\beta_i}-\frac{d}{dt}\left(\omega_1\frac{\partial l_{1\omega t}}{\partial\dot\beta_i}+\omega_2\frac{\partial l_{2\omega t}}{\partial\dot\beta_i}+\omega_3\frac{\partial l_{3\omega t}}{\partial\dot\beta_i}\right)+$$
$$+(\dot v_{01}-g_1+\omega_2 v_{03}-\omega_3 v_{02})\frac{\partial l_1}{\partial\beta_i}+(\dot v_{02}-g_2+\omega_3 v_{01}-\omega_1 v_{03})\frac{\partial l_2}{\partial\beta_i}+$$
$$+(\dot v_{03}-g_3+\omega_1 v_{02}-\omega_2 v_{01})\frac{\partial l_3}{\partial\beta_i}-\tfrac{1}{2}\omega_1^2\frac{\partial J^1_{11}}{\partial\beta_i}-\tfrac{1}{2}\omega_2^2\frac{\partial J^1_{22}}{\partial\beta_i}-\tfrac{1}{2}\omega_3^2\frac{\partial J^1_{33}}{\partial\beta_i}-$$
$$-\omega_1\omega_2\frac{\partial J^1_{12}}{\partial\beta_i}-\omega_1\omega_3\frac{\partial J^1_{13}}{\partial\beta_i}-\omega_2\omega_3\frac{\partial J^1_{23}}{\partial\beta_i}=0. \quad (3.25)$$

The values $\partial l_k/\partial\beta_i$ are given by

$$\frac{\partial l_3}{\partial\beta_i}=\rho\int_{\Sigma_0} f_i^2 dS\beta_i=\lambda_{i3}\beta_i,$$
$$\frac{\partial l_2}{\partial\beta_i}=\rho\int_{\Sigma_0} y f_i dS=\lambda_{i2};\ \ \frac{\partial l_1}{\partial\beta_i}=\rho\int_{\Sigma_0} x f_i dS=\lambda_{i1}. \quad (3.26)$$

Concluding remarks

Miles [125] and Lukovsky [113] showed that the Bateman-Luke variational principle makes it possible to derive an infinite-dimensional system of nonlinear ordinary differential equations (modal system (3.24) + (3.25)) describing the nonlinear sloshing of an incompressible perfect fluid with irrotational flow. The infinite-dimensional system is fully equivalent to the original free boundary problem (3.1) for arbitrary rigid body motions; it does not include assumptions about the smallness of surface wave amplitudes and can be used for modelling different 'fluid–structure' problems including the problem on coupling the 'ship–fluid cargo' motions. Its limitations are that the admissible instantaneous free surface shapes should allow for the normal form $z = f(x, y, t)$ and the contact lines must belong to an upright cylindrical portion of the tank. This means that plunging breakers cannot be described.

The system (3.24) + (3.25) couples nonlinearly the generalised coordinates $\beta_i(t)$ and impulses $R_n(t)$, which appear as the Fourier coefficients in expansions of the free surface and the velocity potential, respectively. The Fourier functional sets, for both surface $\{f_i\}$ and domain $\{\varphi_n\}$ modes, do not generally need to be the linear sloshing modes (natural modes) in the variational procedure, but these must have analytical structure. Nevertheless, practical choice for cylindrical tanks consists of utilising the natural sloshing modes (eigenfunctions of (3.14)). As a consequence,

in view of Remark 3.2, to guarantee the completeness of $\{\varphi_n\}$, an asymptotic technique should be suggested.

Assuming asymptotic relationships between $\beta_i(t)$ truncates the modal system to a finite-dimensional form. Such an asymptotic truncation may be based on the so-called Moiseyev asymptotics (see, Moiseev (1958) [129], Ockendon & Ockendon [139], Ockendon *et al.* (1996) [141], Faltinsen (1974) [43], Miles (1984) [126, 127], Lukovsky (1990) [114], Faltinsen *et al.* (2000) [45]), whose applicability has been justified in the case of finite fluid depths. Asymptotic relationships of "shallow sloshing" were reported by Chester (1968) [36] Chester & Bones (1968) [37], Ockendon & Ockendon (1973,2001) [139, 140] and Faltinsen & Timokha (2002) [51].

Perko-like modal systems (see, the original paper by Perko (1969) [145]), in which truncation of the modal system is not associated with asymptotic relationships, are rare exceptions in the literature. Recent simulations by the Perko-like systems are reported by La Rocca *et al.* (2000,2002) [99, 100] and Shankar & Kidambi (2002) [155].

In the forthcoming analysis, the system of ordinary differential equations (3.24) will be considered as a linear system of algebraic equations with respect to R_k, i.e.

$$\sum_k A_{nk}(\beta_i)R_k = \frac{d}{dt}A_n(\beta_i), \quad n = 1, \ldots .$$

By using an asymptotic technique we can then find R_n as a function of β_i and $\dot{\beta}_i$. After substituting R_n into (3.25), one gets a system of the second-order nonlinear differential equations with respect to β_i.

3.1.3 The Miles-Lukovsky system for non-cylindrical tanks

The Miles-Lukovsky technique is based on the Fourier representation of the free surface (3.12) in the $Oxyz$-coordinate system rigidly fixed with a moving tank. The technique is applicable only if the tank walls are vertical in vicinity of the mean (hydrostatic) free surface. Otherwise, $\{f_i(y,z)\}$[1] have time-dependent domains of definition.

The present section is devoted to the case of strongly non-vertical walls. The study is based on a spatial transformation technique proposed by Lukovsky (1975) [112] and developed by Lukovsky & Timokha (2002)

[1] Following the original publications, sloshing in non-cylindrical tank will be considered under assumption that Ox is the vertical axis.

[120]. This assumes that the original tank cavity can be transformed to an artificial cylindrical domain (in curvilinear coordinates (x_1, x_2, x_3)), where the free surface allows for the normal parametrisation

$$\xi^*(x_1, x_2, x_3, t) = x_1 - f^*(x_2, x_3, t) = 0 \tag{3.27}$$

and

$$f^*(x_2, x_3, t) = \text{const} + \beta_0(t) + \sum_{i=1}^{\infty} \beta_i(t) f_i^*(x_2, x_3). \tag{3.28}$$

Strategy. Let us consider an open artificial cylindrical domain $Q^* = (0, d) \times D$ in the $Ox_1x_2x_3$-coordinate system and let Q be the interior of a rigid tank in the $Oxyz$-system. We define smooth transformations that map Q to Q^* and back as follows

$$\begin{gathered} x_1 = x, \quad x_2 = x_2(x, y, z), \quad x_3 = x_3(x, y, z); \\ x = x_1, \quad y = y(x_1, x_2, x_3), \quad z = z(x_1, x_2, x_3). \end{gathered} \tag{3.29}$$

Here, (3.29) does not change the maximum height d, the Oyz-plane has to be tangent to $S = \partial Q$ and $x > 0$ for $(x, y, z) \in Q$ and the Ox_2x_3-plane should be superposed with the bottom of Q^* (Fig. 3.3). The transformations (3.29) are also obligated to have the positive Jacobian

$$J^*(x_1, x_2, x_3) = \frac{D(x, y, z)}{D(x_1, x_2, x_3)}; \quad (J(x, y, z) = 1/J^*) \tag{3.30}$$

inside of Q^* and, except a limited set of isolated points, on the boundary $S^* = \partial Q^*$. Such a single point with $J^* = 0$ invertible appears for conical, parabolic etc. domains, because (3.29) maps the bottom of Q^* to the origin O (the situation is schematically depicted in Fig. 3.3). These singular points are assumed to be bound away from the mean free surface $\Sigma_0 : \ x = h$.

Linear natural modes. If $\boldsymbol{v} = \boldsymbol{\omega} = \mathbf{0}$, the free boundary problem (3.1) can be linearised relative to the trivial solution $\xi = x + \text{const}$, $\Phi = \text{const}$, which determines a hydrostatic fluid shape Q_0 (Fig. 3.3). The linearisation implies the smallness of $\nabla\Phi$ and ∇f $(\Sigma(t) : \ x = f(y, z, t))$, and, apparently, becomes mathematically justified only in a curvilinear coordinate system. The procedure includes transformation (3.29) (admitting (3.27)-(3.28)), considers (3.1) in the (x_1x_2, x_3)-coordinates, assumes $|\Phi^*| \sim |f^* - h| \sim |\nabla^*\Phi| \sim |\nabla^* f^*| = O(\varepsilon) \ll 1$ and, finally, neglects the $o(\epsilon)$-term. After linearising (3.1), we set up $\Phi^* = i\sqrt{g\varkappa}\varphi^*(x_1, x_2, x_3)$

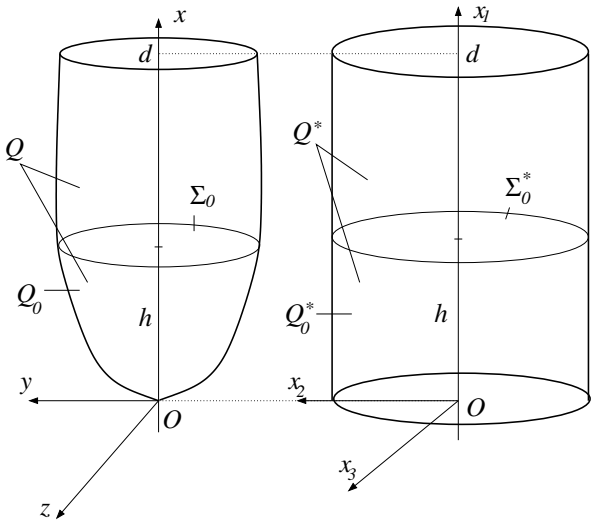

Fig. 3.3. Sketch of an admissible transformation.

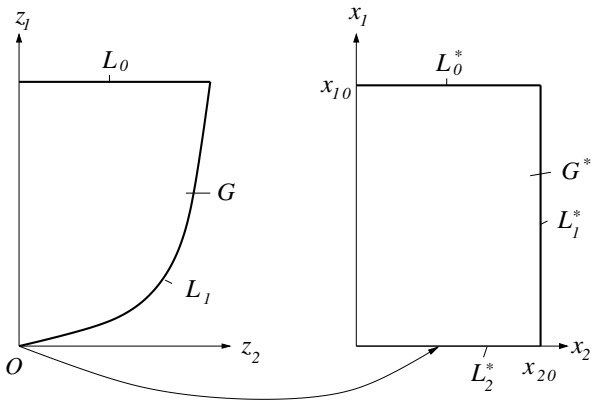

Fig. 3.4. Transformations of the meridional cross-section.

$\exp(i\sqrt{g\varkappa}t)$; $f^* = \exp(i\sqrt{g\varkappa}t)F(x_1, x_2)$ and obtain the following spectral boundary problem in $Q_0^* = (0, h) \times D$ with spectral parameter $\varkappa$ on Σ_0^* : $x_1 = h$

$$\Delta^*\varphi^* = 0 \ \text{ in } \ Q_0^*; \ \ \frac{\partial\varphi^*}{\partial\nu^*} = 0 \ \text{ on } \ S_0^*; \ \ \varkappa\varphi^* = \frac{\partial\varphi^*}{\partial\nu^*} \ \text{ on } \ \Sigma_0^*, \qquad \int_{\Sigma_0^*} \frac{\partial\varphi^*}{\partial\nu^*} J^* dx_2 dx_3 = 0, \tag{3.31}$$

where Q_0^* is the transformed mean fluid domain, S_0^* and Σ_0^* are the transformed mean wetted walls and surface, respectively, and

$$\Delta^*\varphi^* = \Delta\varphi = g^{ij}\left(\frac{\partial^2\varphi^*}{\partial x_i \partial x_j} - \Gamma_{ij}^k \frac{\partial\varphi^*}{\partial x_k}\right); \quad \frac{\partial\varphi^*}{\partial\nu^*} = \nabla\varphi\cdot\boldsymbol{\nu} = g^{ij}\frac{\partial\varphi^*}{\partial x_j}\nu_i,$$

where $\nu_i(x_1, x_2, x_3), i = 1, 2, 3$ imply projections on the covariant unit vectors in the (x_1, x_2, x_3)- coordinates and Γ_{kl}^l are the Christoffel symbols

$$\Gamma_{ij}^k = \frac{1}{2} g^{\alpha k}\left(\frac{\partial g_{i\alpha}}{\partial x_j} + \frac{\partial g_{i\alpha}}{\partial x_i} - \frac{\partial g_{ij}}{\partial x_k}\right), \quad i, j, k = 1, 2, 3$$

based on the metric tensor

$$g_{ij} = \frac{\partial\boldsymbol{r}}{\partial x_i}\frac{\partial\boldsymbol{r}}{\partial x_j}, \quad i, j = 1, 2, 3, \tag{3.32}$$

which keep invariant the metrics

$$dS^2 = (dx)^2 + (dy)^2 + (dz)^2 = g^{ij}(x_1, x_2, x_3) dx_i dx_j; \ \ dQ = J^* dQ^*. \tag{3.33}$$

The following theorems establish that the spectral problem (3.31) is equivalent to the well-known spectral problem (3.14) in the xyz-coordinates (appropriate theory may be found in Feschenko *et al.* (1969) [53]), but for non-cylindrical domains Q_0:

$$\Delta\varphi = 0 \ \text{ in } Q_0; \qquad \frac{\partial\varphi}{\partial\nu} = 0 \ \text{ on } S_0; \ \ \frac{\partial\varphi}{\partial\nu} = \varkappa\varphi \ \text{ on } \Sigma_0; \ \ \int\limits_{\Sigma_0} \frac{\partial\varphi}{\partial\nu}\, dydz = 0. \tag{3.34}$$

Theorem 3.3. *Let functions $\psi, \varphi \in C^2(Q_0)$ be square integrable together with their first derivatives and $\psi^*, \varphi^* \in C^2(Q_0^*)$ be the tensor images of these functions defined by (3.29). The closure of $\{\varphi^*\}$ in the metrics $||\varphi^*||^2 = \langle\varphi^*, \varphi^*\rangle_*$ defined by the scalar product*

$$\langle\varphi,\psi\rangle = \int\limits_{Q_0}((\nabla\varphi,\nabla\psi)+\varphi\psi)dQ = \\ = \int\limits_{Q_0^*}((\nabla^*\varphi^*,\nabla^*\psi^*)+\varphi^*\psi^*)J^*dQ^* = \langle\varphi^*,\psi^*\rangle_* \quad (3.35)$$

constitutes the Hilbert space $W^1_{J^*,2}(Q_0^*) = \{\varphi^* : ||\varphi^*||^2_* < \infty\}$, *which is isometrically equivalent to the Sobolev space* $W_2^1(Q_0)$ *and*

$$(\varphi,\psi) = \int_{\Sigma_0}(\varphi\psi)dydz = \int_{\Sigma_0^*}(\varphi^*\psi^*)J^*dx_2dx_3 = (\varphi^*,\psi^*)_*, \\ [\varphi,\psi] = \int_{Q_0}(\nabla\varphi,\nabla\psi)dQ = \int_{Q_0^*}(\nabla^*\varphi^*,\nabla^*\psi^*)J^*dQ^* = [\varphi^*,\psi^*]_*. \quad (3.36)$$

Besides, the following Green identity

$$\int_{Q^*}(\varphi^*\Delta^*\psi^* + \nabla^*\varphi^*\nabla^*\psi^*)dQ^* = \int_{\partial Q^*\setminus G}\varphi^*\frac{\partial\psi^*}{\partial\nu^*}d\sigma, \quad (3.37)$$

holds for the smooth functions $\varphi^*, \psi^* \in W^1_{J^*,2}(Q_0^*)$ *(*$G = \{(x_1,x_2,x_3) : J^* = 0\}$*).*

Proof. The two metric spaces $W_2^1(Q_0)$ and $W^1_{J^*,2}(Q_0^*)$ are isometrically equivalent as closures in the equivalent metrics. The formulas (3.35) and (3.36) hold true for smooth functions, therefore, the metric spaces have equivalent scalar products, i.e. (3.35).

The following derivation line proves Green's identity (3.37)

$$\int_{Q_0^*}(\varphi^*\Delta^*\psi^* + \nabla^*\varphi^*\nabla^*\psi^*)J^*dQ^* = \int_{Q_0}(\varphi\Delta\psi + \nabla\varphi\nabla\psi)dQ = \\ = \int_{\partial Q_0}\varphi\frac{\partial\psi}{\partial\nu}d\sigma = \int_{\partial Q_0\setminus(J^*=0)}\varphi\frac{\partial\psi}{\partial\nu}d\sigma = \\ = \int_{\partial Q_0^*\setminus\{(x_1,x_2,x_3):J^*=0\}}\varphi^*\frac{\partial\psi^*}{\partial\nu^*}d\sigma.$$

□

Theorem 3.4. *The spectral boundary problems (3.31) and (3.34) are equivalent on an admissible pre-compact sets* $D_{T^*} = \{\varphi^* \in W^1_{J^*,2}(Q_0^*) : \frac{\partial\varphi^*}{\partial\nu^*} \in L_2(\Sigma_0^*);\ \int_{\Sigma_0^*}\varphi^*J^*dx_2dx_3 = 0\}$ *and* $D_T = \{\varphi \in W_1^2(Q_0) : \frac{\partial\varphi}{\partial\nu} \in L_2(\Sigma_0); \int_{\Sigma_0}\varphi dydz = 0\}$, *respectively.*

Proof. Let us consider the operator T^* defined by the Dirichlet-Neumann problem

$$\Delta^*\varphi^* = 0 \text{ in } Q_0^*; \quad \varphi^* = u^* \text{ on } \Sigma_0^*; \quad \frac{\partial\varphi^*}{\partial\nu} = 0 \text{ on } \ S_0^*$$

so that $T^*u^* = \frac{\partial\varphi^*}{\partial\nu}|_{\Sigma_0^*}, \varphi^* \in D_{T^*}$.

The spectral problem (3.31) has the following operator statement

$$T^*u^* = \varkappa u^*, \quad u^* \in \bar{L}_2(\Sigma_0^*) = \{\varphi^*|_{\Sigma_0^*} : \varphi^* \in D_{T^*}\}$$

and, due to (3.37), the variational problem

$$[\varphi^*, \eta^*]_* - \varkappa(\varphi^*, \eta^*)_* = 0, \quad \eta^* \in D_{T^*} \tag{3.38}$$

is equivalent to $[\varphi, \eta] - \varkappa(\varphi, \eta) = 0, \ \eta \in D_T$.
□

Linear natural modes for axial-symmetric tanks. If Q_0 is of an axial-symmetric shape, admissible transformations of Q_0 to Q_0^* can be combined with separation of spatial variables. This leads to an infinite series of two-dimensional spectral problems in a rectangular domain. Reduction to these two-dimensional problems includes two steps. The first step implies the substitution

$$x = z_1, \quad y = z_2 \cos z_3, \quad z = z_2 \sin z_3 \tag{3.39}$$

together with expression for φ:

$$\varphi_m(z_1, z_2, z_3) = \psi_m(z_1, z_2)\begin{matrix}\cos\\ \sin\end{matrix}(mz_3), \quad m = 0, 1, 2, \dots \ . \tag{3.40}$$

Inserting (3.39)-(3.40) into (3.34) leads to the following family of spectral problems in the meridional plane Oz_2z_1:

$$\begin{aligned}
&\frac{\partial}{\partial z_2}(z_2\frac{\partial\psi_m}{\partial z_1}) + \frac{\partial}{\partial z_2}(z_2\frac{\partial\psi_m}{\partial z_2}) - \frac{m^2}{z_2}\psi_m = 0 \text{ in } G,\\
&\frac{\partial\psi_m}{\partial\nu} = 0 \text{ on } L_1; \quad |\psi_m(z_1, 0)| < \infty, \quad m = 0, 1, 2, \dots,\\
&\frac{\partial\psi_m}{\partial z_2} = \varkappa\psi_m \ \text{ on } \ L_0; \quad \int_{L_0} \psi_0 z_2 dz_2 = 0,
\end{aligned} \tag{3.41}$$

where L_0 and L_1 are the boundaries of G (see, Fig. 3.4); $\boldsymbol{\nu}$ is the outer normal to L_1 (theory of (3.41) is given in [115]).

The second step assumes

$$z_1 = x_1, \quad z_2 = \zeta(x_1, x_2), \quad (z_3 = x_3), \tag{3.42}$$

which maps G to G^* as shown in Fig. 3.4 ($L_0 \to L_0^*, L_1 \to L_1^*$). In the $Ox_1x_2x_3$-coordinate system, the spectral problems (3.41) take the form

$$\begin{gathered}
p\frac{\partial^2\psi_m}{\partial x_1^2} + 2q\frac{\partial^2\psi_m}{\partial x_1\partial x_2} + s\frac{\partial^2\psi_m}{\partial x_2^2} + \left(\frac{\partial p}{\partial x_1} + \frac{\partial q}{\partial x_2}\right)\frac{\partial\psi_m}{\partial x_1} + \\
+ \left(\frac{\partial s}{\partial x_2} + \frac{\partial q}{\partial x_1}\right)\frac{\partial\psi_m}{\partial x_2} - cm^2\psi_m = 0 \ \text{ in } \ G^*, \\
p\frac{\partial\psi_m}{\partial x_1} + q\frac{\partial\psi_m}{\partial x_2} = \varkappa p\psi_m \ \text{ on } \ L_0^*; \quad s\frac{\partial\psi_m}{\partial x_2} + q\frac{\partial\psi_m}{\partial x_1} = 0 \ \text{ on } \ L_1^*, \\
\int_0^{x_{20}} \psi_0\zeta\frac{\partial\zeta}{\partial x_2}dx_2 = 0 \quad m = 0, 1, 2, \ldots,
\end{gathered} \tag{3.43}$$

where

$$\begin{aligned}
&p(x_1, x_2) = \zeta\frac{\partial\zeta}{\partial x_2}; \ q(x_1, x_2) = pa; \quad s(x_1, x_2) = p(a^2 + b^2), \\
&a(x_1, x_2) = \frac{\partial x_2}{\partial\zeta}; \quad b(x_1, x_2) = \frac{\partial x_1}{\partial\zeta}; \quad c(x_1, x_2) = \frac{1}{\zeta}\frac{\partial\zeta}{\partial x_2}.
\end{aligned} \tag{3.44}$$

As follows from Theorems 3.3 and 3.4, the problem (3.43) does not need any boundary conditions on the artificial bottom L_2^* and along $x_2 = 0$. However, ψ_m should be bounded at $x_1 = 0$ and $x_2 = 0$, simultaneously.

The modal system. We employ the Bateman-Luke variational formulation (3.6)–(3.8). Lukovsky & Timokha (2002) [120] have mathematically established that the Lagrangian (3.7) is invariant relative to transformations (3.29), namely,

$$L \equiv L^* = -\rho\int\limits_{Q^*(t)} \left[\frac{\partial\Phi^*}{\partial t} + \frac{1}{2}(\nabla^*\Phi^*)^2 - \nabla^*\Phi^*\cdot(\boldsymbol{v}_0 + \boldsymbol{\omega}\times\boldsymbol{r})^* + U^*\right]J^*dQ^*, \tag{3.45}$$

where $Q^*(t)$ is the transformed domain,

$$\begin{aligned}
&U^* = U(x(x_1, x_2, x_3), y(x_1, x_2, x_3), z(x_1, x_2, x_3), t), \\
&\Phi^* = \Phi(x(x_1, x_2, x_3), y(x_1, x_2, x_3), z(x_1, x_2, x_3), t), \\
&\nabla\Phi = \nabla^*\Phi^* = \left(g^{1,j}\frac{\partial\Phi^*}{\partial x_j}, g^{2,j}\frac{\partial\Phi^*}{\partial x_j}, g^{3,j}\frac{\partial\Phi^*}{\partial x_j}\right)
\end{aligned}$$

(stars in $(\boldsymbol{v}_0 + \boldsymbol{\omega} \times \boldsymbol{r})^*$ denote projections on the unit vectors of a curvilinear coordinate system).

By adopting derivations from § 3.1.2 with the modal solutions

$$f^* = x_{10} + \beta_0(t) + \sum_{i=1}^{\infty} \beta_i(t) f_i^*(x_2, x_3), \tag{3.46a}$$

$$\Phi^* = \boldsymbol{v}_0 \cdot \boldsymbol{r} + \sum_{n=1}^{\infty} Z_n(t) \varphi_n(x_1, x_2, x_3), \tag{3.46b}$$

where $x_{10} = h$, $\{f_i^*(x_2, x_3)\}$, $\{\varphi_n(x_1, x_2, x_3)\}$ are the basic systems of functions on Σ_0^* and in Q_0^*, respectively, and, for brevity, $\boldsymbol{\omega} = \mathbf{0}$, we get the following infinite-dimensional nonlinear modal system

$$\frac{d}{dt} A_n - \sum_k A_{nk} Z_k = 0, \quad n = 1, 2, \ldots \ , \tag{3.47a}$$

$$\sum_n \dot{Z}_n \frac{\partial A_n}{\partial \beta_i} + \frac{1}{2} \sum_{nk} \frac{\partial A_{nk}}{\partial \beta_i} Z_n Z_k + (\dot{v}_{01} - g_1) \frac{\partial l_1}{\partial \beta_i} + (\dot{v}_{02} - g_2) \frac{\partial l_2}{\partial \beta_i} + (\dot{v}_{03} - g_3) \frac{\partial l_3}{\partial \beta_i} = 0, \ i = 1, 2, \ldots . \tag{3.47b}$$

This system couples the generalised coordinates $Z_n(t), \beta_i(t)$ and $A_n(\beta_i)$, $A_{nk}(\beta_i)$, $l_k(\beta_i)$ defined by the integrals

$$\begin{aligned} A_n &= \rho \int_D \left(\int_0^{f^*} \varphi_n J^* dx_1 \right) dx_2 dx_3, \\ A_{nk} &= \rho \int_D \left(\int_0^{f^*} (\nabla^* \varphi_n^*, \nabla^* \varphi_k^*) J^* dx_1 \right) dx_2 dx_3, \end{aligned} \tag{3.48}$$

$$\begin{aligned} \frac{\partial l_1}{\partial \beta_i} &= \rho \int_{\Sigma_0^*} F_i [x_1 J^*(x_1, x_2, x_3)]_{x_1 = f^*} dx_2 dx_3, \\ \frac{\partial l_2}{\partial \beta_i} &= \rho \int_{\Sigma_0^*} F_i [y(x_1, x_2, x_3) J^*(x_1, x_2, x_3)]_{x_1 = f^*} dx_2 dx_3, \\ \frac{\partial l_3}{\partial \beta_i} &= \rho \int_{\Sigma_0^*} F_i [z(x_1, x_2, x_3) J^*(x_1, x_2, x_3)]_{x_1 = f^*} dx_2 dx_3 \end{aligned} \tag{3.49}$$

(the upper limit f^* in the integrals (3.48) depends on $\beta_i(t)$ owing to (3.46a)).

3.2 Two-dimensional sloshing in a rectangular tank

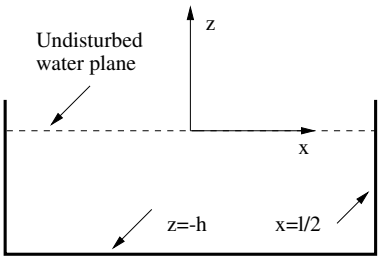

Fig. 3.5. Coordinate system.

We consider a mobile rectangular rigid tank filled partly by an inviscid incompressible fluid. The mean fluid depth is h and l is the tank breadth (see, Fig. 3.5). The flow is two-dimensional in the (x,z)-plane. Then

$$\boldsymbol{v}_0 = (v_{0x}, 0, v_{0z}); \quad \boldsymbol{\omega} = (0, \omega(t), 0),$$
$$\boldsymbol{r} = (x, 0, z), \quad \boldsymbol{\Omega}(x, 0, z) = (0, \Omega(x, z, t), 0) \tag{3.50}$$

and $\Omega(x,z,t)$ is the solution of the following boundary value problem

$$\Delta\Omega = 0 \quad \text{in} \quad Q(t); \qquad \frac{\partial\Omega}{\partial\nu}|_{S(t)+\Sigma(t)} = z\nu_1 - x\nu_3. \tag{3.51}$$

Owing to (3.9), the velocity potential $\Phi(x,0,z,t)$ takes the form

$$\Phi(x,0,z,t) = v_{0x}x + v_{0z}z + \omega(t)\,\Omega(x,z,t) + \sum_{n=1}^{\infty} R_n(t)\,\varphi_n(x,z), \tag{3.52}$$

where $\{\varphi_n(x,z)\}$ is a complete system of two-dimensional harmonic functions. Further, the origin lies on the mean free surface at the centerplane of the tank and $z = f(x,t)$ determines the perturbed free surface $\Sigma(t)$.

The fluid domain is

$$Q(t) = \{(x,z) : -h < z < f(x,t); -l/2 < x < l/2\} \tag{3.53}$$

and $f(x,t)$ is expressed by (3.12). The complete (to within a constant) orthogonal system of functions $\{f_i(x)\}$ should satisfy the volume conservation condition

$$\int_{-l/2}^{l/2} f_i(x)dx = 0. \tag{3.54}$$

The general infinite–dimensional modal system (3.24) + (3.25) has in two dimensions the following form

$$\frac{d}{dt}A_n - \sum_k R_k A_{nk} = 0, \;\; n = 1, 2, \ldots; \tag{3.55}$$

$$\sum_n \dot{R}_n \frac{\partial A_n}{\partial \beta_i} + \tfrac{1}{2}\sum_n \sum_k \frac{\partial A_{nk}}{\partial \beta_i} R_n R_k + \dot{\omega}\frac{\partial l_{2\omega}}{\partial \beta_i} + \omega \frac{\partial l_{2\omega t}}{\partial \beta_i} -$$
$$- \frac{d}{dt}\left(\omega \frac{\partial l_{2\omega t}}{\partial \dot{\beta}_i}\right) + (\dot{v}_{01} - g_1 + \omega v_{03})\frac{\partial l_1}{\partial \beta_i} + (\dot{v}_{03} - g_3 - \omega v_{01})\frac{\partial l_3}{\partial \beta_i} -$$
$$- \tfrac{1}{2}\omega^2 \frac{\partial J^1_{22}}{\partial \beta_i} = 0. \tag{3.56}$$

3.2.1 Asymptotic modal system

As shown by Faltinsen *et al.* (2000) [45], the modal system (3.55) + (3.56) can be approximated to surface waves with one primary dominating mode corresponding to the first natural mode. This approximation holds true when the small-magnitude body motions are horizontal and/or rotational and quasi-periodic with average frequency close to the first resonance frequency. It is also necessary that the fluid depth is not shallow and the fluid does not hit the tank ceiling (see, physical arguments presented by Faltinsen (1974) [43], Mikishev (1978) [122] and, recently, by Faltinsen & Timokha (2001,2002) [49, 51]). The smallness of the rigid body motions is assumed relative to the tank breadth and water depth.

Derivation of the finite-dimensional asymptotic analogue of the system (3.55) + (3.56) requires an asymptotic relation between the dominating mode amplitude and the excitation amplitude. It is assumed, as in the theory by Faltinsen (1974) [43] that

$$O\left(\frac{\beta_1^3}{l^3}\right) = O\left(\frac{H}{l}\right) = O\left(\frac{\psi_0}{2\pi}\right) \sim \epsilon, \tag{3.57}$$

where $\epsilon \ll 1$. Here, H is translatory (surge) motion magnitude and ψ_0 is angular (pitch) magnitude. Further, we deduce (see rigorous mathematical details by Hermann & Timokha (2005) [81]) that $\beta_2/l = O(\epsilon^{2/3}), \beta_3/l = O(\epsilon)$ and $\beta_i/l \le O(\epsilon), \;\; i \ge 4$.

The modes $f_i(x)$ in (3.12) as well as $\varphi_i(x,z)$ in (3.13) must be chosen as the solutions of the spectral problem (3.14), i.e.

$$\begin{aligned} &\Delta\varphi_i = 0 \quad (-l/2 < x < l/2, -h < z < 0), \\ &\frac{\partial\varphi_i}{\partial x}|_{x=-l/2, x=l/2} = 0; \quad \frac{\partial\varphi_i}{\partial z}|_{z=-h} = 0; \quad \frac{\partial\varphi_i}{\partial z} = \lambda_i\varphi_i \quad (z=0). \end{aligned} \tag{3.58}$$

This implies

$$\lambda_i = \frac{\pi i}{l}\tanh(\frac{i\pi}{l}h); \quad f_i(x) = \cos(\frac{\pi i}{l}(x+l/2)),$$
$$\varphi_i(x,z) = f_i(x)\frac{\cosh(\frac{\pi i}{l}(z+h))}{\cosh(\frac{\pi i}{l}h)}. \tag{3.59}$$

Eqs. (3.12) + (3.13) take the following form

$$\begin{aligned} f(x,t) &= \sum_{i=1}^{\infty}\beta_i(t)f_i(x), \\ \varphi(x,z,t) &= \sum_{i=1}^{\infty}R_i(t)f_i(x)\frac{\cosh(\frac{i\pi}{l}(z+h))}{\cosh(\frac{i\pi}{l}h)}. \end{aligned} \tag{3.60}$$

By accounting for the asymptotic relationship (3.57), the smallness of H relative to l and keeping only terms up to ϵ in the modal system (3.55), (3.56) we get

$$\frac{d}{dt}A_n - \sum_k R_k A_{nk} = 0, \quad n = 1,2,\ldots; \tag{3.61}$$

$$\sum_n \dot{R}_n\frac{\partial A_n}{\partial\beta_i} + \tfrac{1}{2}\sum_{n,\ k}\frac{\partial A_{nk}}{\partial\beta_i}R_nR_k + \dot{\omega}\frac{\partial l_{2\omega}}{\partial\beta_i} + \omega\frac{\partial l_{2\omega t}}{\partial\beta_i} -$$
$$- \frac{d}{dt}\left(\omega\frac{\partial l_{2\omega t}}{\partial\dot{\beta}_i}\right) + (\dot{v}_{01} - g_1)\lambda_{i1} + (\dot{v}_{03} - g_3)\beta_i\lambda_{i3} = 0. \tag{3.62}$$

Asymptotic expansions of the integrals $A_i, A_{nk}, l_{2}\omega, l_{2\omega t}$ have to be used in (3.61) and (3.62). Here $A_i, A_{nk}, l_{2\omega}, l_{2\omega t}$ are defined by (3.22) and (3.20) as integrals over the instantaneous fluid volume position. The integrals are divided into integrals over the fluid volume Q_0, and over the

remaining part Q_δ. Q_δ is determined by β_i. Further, the integrand of the integrals over Q_δ can be expanded in Taylor series by $\beta_i \sim l\ \epsilon$. Keeping terms up to ϵ gives

$$\begin{aligned}
A_1 &= \frac{\rho l}{2}(\beta_1 + E_1(\beta_1\beta_2 + \beta_2\beta_3) + E_0(\beta_1^3 + 2\beta_1\beta_2^2 + \beta_1^2\beta_3)),\\
A_2 &= \frac{\rho l}{2}(\beta_2 + E_2(\beta_1^2 + 2\beta_1\beta_3) + 8E_0\beta_1^2\beta_2),\\
A_3 &= \frac{\rho l}{2}(\beta_3 + 3E_3\beta_1\beta_2 + 3E_0\beta_1^3);
\end{aligned} \tag{3.63}$$

$$\begin{aligned}
A_{11} &= \rho l(E_1 + 8E_1E_0\beta_1^2 - (2E_0 - E_1^2)\beta_2),\\
A_{12} &= A_{21} = \rho l((4E_0 + 2E_1E_2)\beta_1 + (-4E_0 + 2E_1^2)\beta_3),\\
A_{13} &= A_{31} = 3l\rho(2E_0 + E_1E_3)(\beta_2 + 2E_4\beta_1^2),\\
A_{22} &= \rho l(2E_2);\quad A_{23} = A_{32} = 3l\rho(4E_0 + 2E_2E_3)\beta_1;\\
A_{33} &= \rho l(3E_3),
\end{aligned} \tag{3.64}$$

where

$$E_0 = \frac{1}{8}\left(\frac{\pi}{l}\right)^2,\quad E_i = \frac{\pi}{2l}\tanh(\frac{\pi i}{l}h),\quad i \geq 1. \tag{3.65}$$

Further, we express R_n as

$$R_n = \sum_i \gamma_i\dot{\beta}_i + \sum_{ij}\gamma_{ij}\dot{\beta}_j\beta_i + \sum_{ijk}\gamma_{ijk}\dot{\beta}_i\beta_j\beta_k + ...$$

and substitute it into (3.61). Explicit values of $\gamma_i, \gamma_{ij}, \gamma_{ijk}$ are found by gathering similar terms. The result is

$$\begin{aligned}
R_1 =& \frac{\dot{\beta}_1}{2E_1} + \frac{E_0}{E_1^2}\dot{\beta}_1\beta_2 - \frac{E_0}{E_1E_2}\dot{\beta}_2\beta_1 + \frac{E_0}{E_1}\left(-\frac{1}{2} + \frac{4E_0}{E_1E_2}\right)\beta_1^2\dot{\beta}_1,\\
R_3 =& \frac{\dot{\beta}_3}{6E_3} - \frac{E_0}{E_1E_3}\dot{\beta}_1\beta_2 - \frac{E_0}{E_2E_3}\dot{\beta}_2\beta_1 +\\
&+ \dot{\beta}_1\beta_1^2\left(\frac{3E_2}{2E_3} - \frac{2E_0E_4}{E_1E_3} - E_4 + \frac{4E_0^2}{E_1E_2E_3} + \frac{2E_0E_2}{E_1E_3}\right),\\
R_2 =& \frac{1}{4E_2}\left(\dot{\beta}_2 - \frac{4E_0}{E_1}\beta_1\dot{\beta}_1\right);\quad R_i = \frac{\dot{\beta}_i}{2iE_i},\quad i \geq 4
\end{aligned} \tag{3.66}$$

and

$$
\begin{aligned}
\dot{R}_1 =& \frac{\ddot{\beta}_1}{2E_1} + \frac{E_0}{E_1^2}\ddot{\beta}_1\beta_2 - \frac{E_0}{E_1E_2}\ddot{\beta}_2\beta_1 + \dot{\beta}_1\dot{\beta}_2\left(\frac{E_0}{E_1^2} - \frac{E_0}{E_1E_2}\right) + \\
&+ \frac{E_0}{E_1}\left(-\frac{1}{2} + \frac{4E_0}{E_1E_2}\right)\beta_1^2\ddot{\beta}_1 + 2\frac{E_0}{E_1}\left(-\frac{1}{2} + \frac{4E_0}{E_1E_2}\right)\dot{\beta}_1^2\beta_1, \\
\dot{R}_3 =& \frac{\dot{\beta}_3}{6E_3} - \frac{E_0}{E_1E_3}\ddot{\beta}_1\beta_2 - \frac{E_0}{E_2E_3}\ddot{\beta}_2\beta_1 - \\
&- \left(\frac{E_0}{E_1E_3} + \frac{E_0}{E_2E_3}\right)\dot{\beta}_1\dot{\beta}_2 + (\ddot{\beta}_1\beta_1^2 + 2\dot{\beta}_1^2\beta_1)\times \\
&\times \left(\frac{3E_2}{2E_3} - \frac{2E_0E_4}{E_1E_3} - E_4 + \frac{4E_0^2}{E_1E_2E_3} + \frac{2E_0E_2}{E_1E_3}\right), \\
\dot{R}_2 =& \frac{1}{4E_2}(\ddot{\beta}_2 - \frac{4E_0}{E_1}(\beta_1\ddot{\beta}_1 + \dot{\beta}_1^2)); \quad \dot{R}_i = \frac{\ddot{\beta}_1}{2iE_i}, \quad i \geq 4.
\end{aligned}
\tag{3.67}
$$

By calculating λ_{ij} we get

$$
\begin{aligned}
\lambda_{i1} &= \rho\int_{-l/2}^{l/2} x\cos(\frac{i\pi}{l}(x + l/2))dx = \rho\left(\frac{l}{i\pi}\right)^2((-1)^i - 1), \\
\lambda_{i3} &= \rho\int_{-l/2}^{l/2} \cos^2(\frac{i\pi}{l}(x + l/2))dx = \frac{\rho l}{2}.
\end{aligned}
\tag{3.68}
$$

$l_{2\omega}$ and $l_{2\omega t}$ (see, (3.20)) depend on $\Omega(x, z, t)$ which is the solution of the boundary value problem (3.51). $\Omega(x, z, t)$ depends parametrically on $\beta_i(t)$ due to the free surface $\Sigma(t)$. Since $\partial l_{2\omega}/\partial\beta_i$ and $\partial l_{2\omega t}/\partial\beta_i$ are multiplied by terms of $O(\epsilon)$ in (3.62), it is sufficient to include only linear terms by β_i in the integrals $l_{2\omega}$ and $l_{2\omega t}$. The problem (3.51) takes the following form

$$
\begin{aligned}
&\Delta\Omega = 0 \text{ in } Q(t); \quad \frac{\partial\Omega}{\partial z} = -x \ (z = -h); \quad \frac{\partial\Omega}{\partial x} = z \ (x = \frac{l}{2}, -\frac{l}{2}), \\
&\frac{\partial\Omega}{\partial\nu} = -x\frac{1}{\sqrt{1 + (f_x)^2}} - z\frac{f_x}{\sqrt{1 + (f_x)^2}} \quad (z = f(x, t)).
\end{aligned}
\tag{3.69}
$$

The solution can be found by a Joukowski–type substitution with additional terms for fluctuations of the free surface. This gives

$$
\Omega = xz - 2\sum_{i=1}^{\infty} a_i f_i \frac{\sinh(\frac{\pi}{l}i(z + h/2))}{\cosh(\frac{\pi}{2l}ih)} +
$$

$$+\sum_{i=1}^{\infty}\chi_i(t)f_i\frac{\cosh(\frac{\pi}{l}i(z+h))}{\cosh(\frac{\pi}{l}ih)}. \quad (3.70)$$

The coefficients a_i are found from the condition $\chi_i(t)\equiv 0,\ i\geq 1$, if and only if, $\beta_i\equiv 0,\ i\geq 1$. Substitution of (3.70) into (3.69) gives

$$\sum_{i=1}^{N}a_i f_i\frac{i\pi}{l}=x \quad \text{or} \quad a_i=\frac{2l^2}{(i\pi)^3}[(-1)^i-1]. \quad (3.71)$$

The functions $\chi_i(t)$ follow from (3.69) after substitution of (3.70) and (3.71) and performing the Taylor series technique for the free surface $\Sigma(t)$ (with respect to β_i). The linear terms of $l_{2\omega}$ and $l_{2\omega t}$ do not depend on $\chi_i(t)$. To show this we set up (3.70) in the corresponding integrals

$$l_{2\omega}=-2\rho\sum_{i=1}^{\infty}a_i\tanh(\frac{i\pi}{2l}h)\beta_i\int_{-l/2}^{l/2}f_i^2dx+$$
$$+\rho\sum_{i=1}^{\infty}\chi_i(t)\frac{l}{i\pi}\tanh(\frac{i\pi}{l}h)\int_{-l/2}^{l/2}f_i dx; \quad (3.72)$$

$$l_{2\omega t}=\rho\sum_{j=1}^{\infty}\dot{\chi}(t)\frac{l}{i\pi}\tanh(\frac{i\pi}{l}h)\int_{-l/2}^{l/2}f_i dx. \quad (3.73)$$

It follows from the volume conservation condition (3.54) that

$$l_{2\omega t}=0;\ \ l_{2\omega}=-2\rho\sum_{i=1}^{\infty}\beta_i\left(\frac{l}{i\pi}\right)^3[(-1)^i-1]\tanh\left(\frac{i\pi}{2l}h\right). \quad (3.74)$$

The derivatives with respect to β_i give

$$\frac{\partial l_{2\omega t}}{\partial\beta_i}=0,\ \ \frac{\partial l_{2\omega}}{\partial\beta_i}=-2\rho\left(\frac{l}{i\pi}\right)^3[(-1)^i-1]\tanh\left(\frac{i\pi}{2l}h\right),\quad i\geq 1. \quad (3.75)$$

Finally, by defining the angular position of the mobile coordinate system $Oxyz$ with respect to $O'x'y'z'$ as $\psi(t)$ we obtain correctly to $O(\epsilon)$ that

$$g_3=-g;\ \ g_1=g\psi(t). \quad (3.76)$$

The terms in (3.62) $\ddot{\psi}\frac{\partial l_{2\omega}}{\partial\beta_i}+(-g_3)\beta_i\lambda_{3i}+(-g_1)\lambda_{1i}$ caused by the forced pitch excitation can be rewritten as

$$-\rho\left(\frac{l}{i\pi}\right)^2[(-1)^i-1]\left(\frac{2l}{i\pi}\tanh(\frac{i\pi}{2l}h)\ddot{\psi}(t)+g\psi(t)\right)+g\beta_i. \qquad (3.77)$$

When substituting the above formula in (3.62), we get the following system of ordinary differential equations describing oscillations of a fluid in a rectangular tank performing arbitrary small-magnitude motions (keeping terms up to $O(\epsilon)$ in the nonlinear equations):

$$\begin{aligned}
&(\ddot{\beta}_1+\sigma_1^2\beta_1)+d_1(\ddot{\beta}_1\beta_2+\dot{\beta}_1\dot{\beta}_2)+d_2(\ddot{\beta}_1\beta_1^2+\dot{\beta}_1^2\beta_1)+d_3\ddot{\beta}_2\beta_1+\\
&\quad+P_1(\dot{v}_{0x}-S_1\dot{\omega}-g\psi)+Q_1\dot{v}_{0z}\beta_1=0,\\
&(\ddot{\beta}_2+\sigma_2^2\beta_2)+d_4\ddot{\beta}_1\beta_1+d_5\dot{\beta}_1^2+Q_2\dot{v}_{0z}\beta_2=0, \qquad (3.78)\\
&(\ddot{\beta}_3+\sigma_3^2\beta_3)+d_6\ddot{\beta}_1\beta_2+d_7\ddot{\beta}_1\beta_1^2+d_8\ddot{\beta}_2\beta_1+d_9\dot{\beta}_1\dot{\beta}_2+d_{10}\dot{\beta}_1^2\beta_1+\\
&\quad+P_3(\dot{v}_{0x}-S_3\dot{\omega}-g\psi)+Q_3\dot{v}_{0z}\beta_3=0.
\end{aligned}$$

The linear equations describing higher modes read as

$$\ddot{\beta}_i+\sigma_i^2\beta_i+P_i(\dot{v}_{0x}-S_i\dot{\omega}-g\psi)+Q_i\dot{v}_{0z}\beta_i=0,\quad i\geq 4. \qquad (3.79)$$

Here v_{0x} and v_{0z} are projections of the translational velocity onto axes of Oxz, $\omega(t)$ is the angular velocity of the coordinate system $Oxyz$ with respect to $O'x'y'z'$.

The introduced coefficients are calculated by formulae

$$\sigma_i^2=2giE_i;\quad P_{2i-1}=-\frac{8E_{2i-1}l}{\pi^2(2i-1)},\quad P_{2i}=0;\quad Q_i=2iE_i,$$
$$S_i=\frac{2l}{\pi i}\tanh\left(\frac{i\pi}{2l}h\right),\quad i\geq 1, \qquad (3.80)$$

where σ_i is the natural frequency of mode i. Further,

$$\begin{aligned}
d_1=&2\frac{E_0}{E_1}+E_1;\quad d_2=2E_0\left(-1+\frac{4E_0}{E_1E_2}\right);\\
d_3=&-2\frac{E_0}{E_2}+E_1;\quad d_4=-4\frac{E_0}{E_1}+2E_2;\\
d_5=&E_2-2\frac{E_0E_2}{E_1^2}-\frac{4E_0}{E_1};\quad d_6=3E_3-\frac{6E_0}{E_1},\\
d_7=&-3E_0-9\frac{E_0E_3}{E_1}+24\frac{E_0^2}{E_1E_2};\quad d_8=-6\frac{E_0}{E_2}+3E_3,
\end{aligned}$$

$$d_9 = -6E_0 - 24\frac{E_0E_3}{E_1} + 48\frac{E_0^2}{E_2E_2} + 24\frac{E_0^2E_3}{E_1^2E_2},$$
$$d_{10} = 3E_3 - 6\frac{E_2E_0}{E_1E_2} - 6\frac{E_0E_3}{E_1E_2} - 6\frac{E_0}{E_2}$$

(note, that expressions for some coefficients responsible for the highest-order terms differ from the reported by Faltinsen *et al.* (2000) [45], but are consistent with the further investigations by Faltinsen & Timokha (2001) [49]; the numerical difference is negligible and effect less than 0.1% in all the simulations).

The first two nonlinear equations of (3.78) couple β_1 with β_2 and do not depend on β_3. The third mode component is excited by rigid body motions and the first and second modes. The first mode will be finite, if it is excited at the natural frequency for the first mode. This is caused by nonlinear effects and will become more evident in the next subsection on the steady–state resonant regimes.

3.2.2 Steady-state resonant waves

The theory of steady-state solutions of the nonlinear sloshing problem in a rectangular tank was created by Faltinsen (1974) [43] based on Moiseev's [129] method. The constructed asymptotic modal system (3.78) makes it possible to generalise results of this theory.

Let us first consider the surge excitations expressed by $\boldsymbol{v}_0 = (-H\sigma\sin(\sigma t), 0, 0)$ and set up $\omega = \psi \equiv 0$. The steady-state wave are associated with periodic solutions of (3.78) satisfying

$$\beta_i(t + 2\pi/\sigma) = \beta_i(t), \quad \dot{\beta}_i(t + 2\pi/\sigma) = \dot{\beta}_i(t). \tag{3.81}$$

To construct the asymptotic periodic solutions of (3.78), we impose the first approximation of the primary mode in the form

$$\beta_1(t) = A\cos\sigma t + o(A) \tag{3.82}$$

and substitute it into (3.78). Accounting for the periodicity condition (3.81), this yields

$$\beta_2 = A^2(l_0 + h_0\cos(2\sigma t)) + o(A^2), \tag{3.83}$$

where

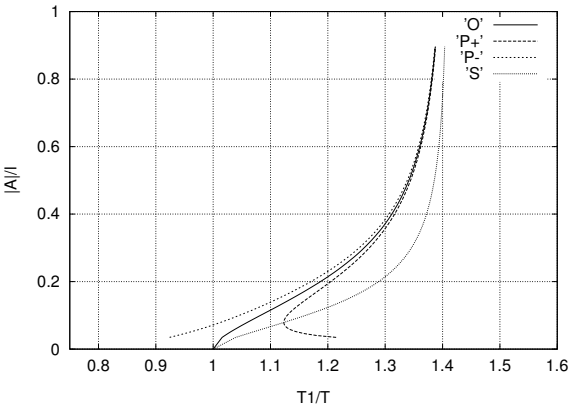

$h/l = 0.173, H/l = 0.0173;\ i(2, \bar{h}) = 0.9$

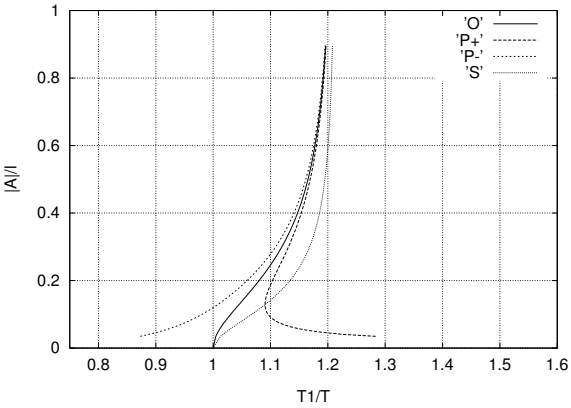

$h/l = 0.23121, H/l = 0.0173;\ i(2, \bar{h}) = 0.85$

Fig. 3.6. Amplitude (A)–frequency (σ) response curves $P_{\pm}$ for nonlinear sloshing due to surge excitation ($\sigma/\sigma_1 = T1/T$). h is the mean water depth, l is the tank breadth, H is the surge amplitude. $i(2, \bar{h})$ is defined by (3.89) and implies the secondary resonance prediction.

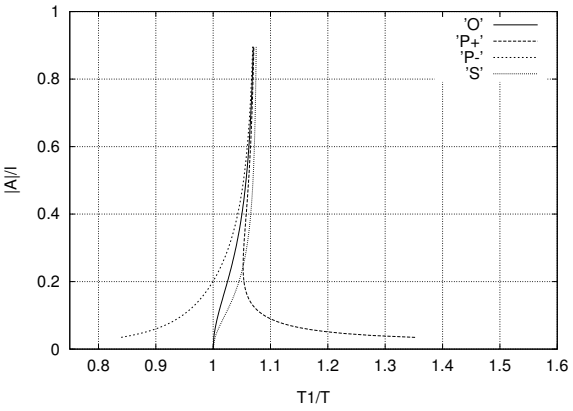

$h/l = 0.289$, $H/l = 0.0173$; $i(2, \bar{h}) = 0.8115$

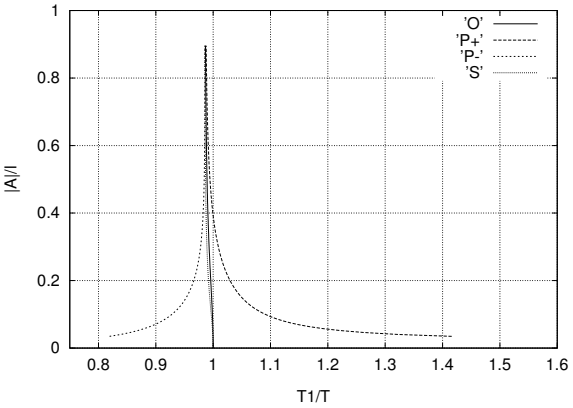

$h/l = 0.34821$, $H/l = 0.0173$; $i(2, \bar{h}) = 0.782$

Fig. 3.6 (continued):

$$l_0 = \frac{d_4 - d_5}{2\bar{\sigma}_2^2}; \quad h_0 = \frac{d_5 + d_4}{2(\bar{\sigma}_2^2 - 4)}, \quad \bar{\sigma}_i = \frac{\sigma_i}{\sigma}, \quad i = 1, 2. \tag{3.84}$$

The amplitude $A \sim \epsilon^{1/3}$ of the primary mode can be found by substituting (3.82) - (3.83) into the first equation of (3.78) and collecting Fourier terms of the lowest order. The non-dimensional secular equation coupling the primary mode amplitude A, the forcing frequency σ, the breadth l and the fluid depth h (normalisation implies dividing of all length variables by l) takes the following form

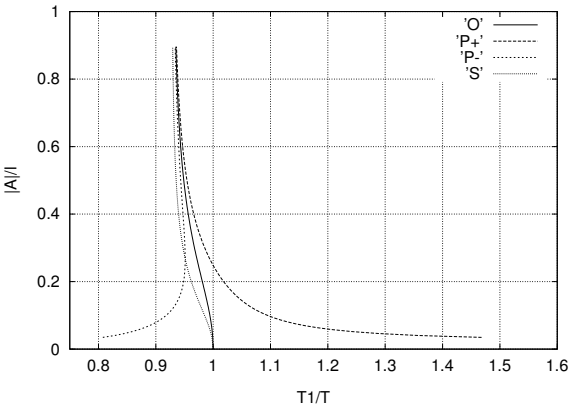

$h/l = 0.40462, H/l = 0.0173;\ i(2,\bar{h}) = 0.7604$

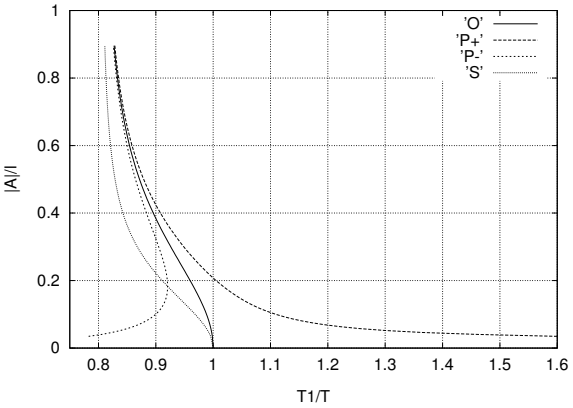

$h/l = 1.0, H/l = 0.0173;\ i(2,\bar{h}) = 0.7085$

Fig. 3.6 (continued):

$$\Pi_h(\bar{\sigma}_1, \bar{\sigma}_2, \bar{A}) = (\bar{\sigma}_1^2 - 1)\bar{A} + m_1(\bar{\sigma}_2, \bar{h})\bar{A}^3 - \bar{P}_1\bar{H} = 0, \tag{3.85}$$

$$m_1(\bar{\sigma}_2, \bar{h}) = \bar{d}_1(-\bar{l}_0(\bar{\sigma}_2) + \tfrac{1}{2}\bar{h}_0(\bar{\sigma}_2)) - \tfrac{1}{2}\bar{d}_2 - 2\bar{d}_3\bar{h}_0(\bar{\sigma}_2), \tag{3.86}$$

where the overbar denotes non–dimensional values.

The coefficient m_1 in Eq. (3.85) depends on the depth/breadth ratio and the excitation frequency ($\bar{\sigma}_i, i = 1, 2$). The latter dependence has not been presented by Faltinsen (1974) [43] for frequency–amplitude secular equations, but only appeared in the paper by Faltinsen *et al.* (2000) [45].

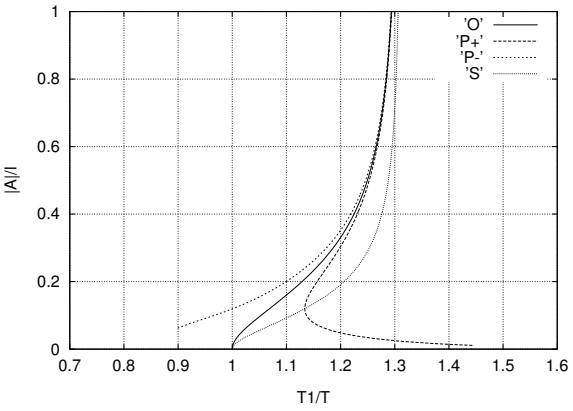

$\frac{z_0}{l} = 0, \frac{h}{l} = 0.2, \psi_0 = 0.1rad, i(2, \bar{h}) = 0.874$

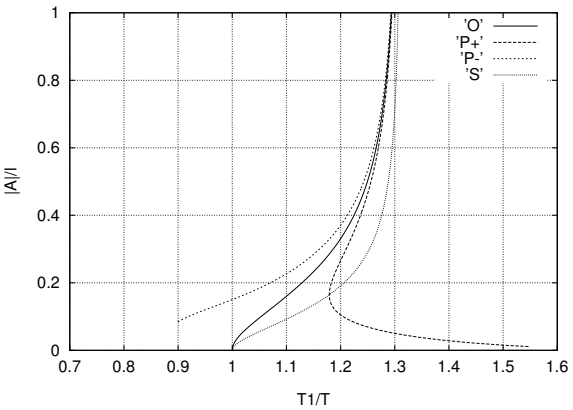

$\frac{z_0}{l} = 0, \frac{h}{l} = 0.2, \psi_0 = 0.2rad, i(2, \bar{h}) = 0.874$

Fig. 3.7. Amplitude (A)–frequency (σ) response curves $P_{\pm}$ for nonlinear sloshing due to pitch excitation ($\sigma/\sigma_1 = T1/T$). h is the mean water depth, l is the tank breadth, ψ_0 is the pitch amplitude, $(0, -z_0)$ is the position of pitch axis. $i(2, \bar{h})$ is defined by (3.89) and implies the secondary resonance prediction.

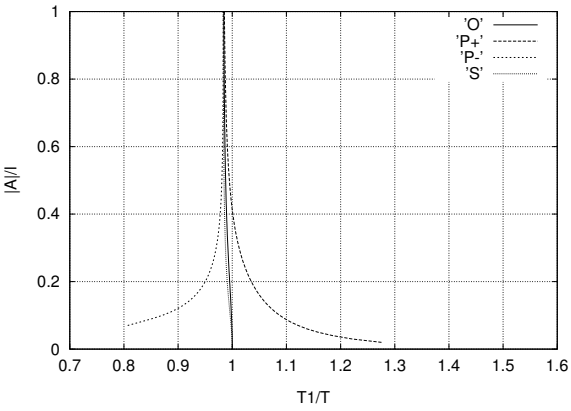

$\frac{z_0}{l} = 0.15, \frac{h}{l} = 0.35, \psi_0 = 0.1rad, i(2, \bar{h}) = 0.78$

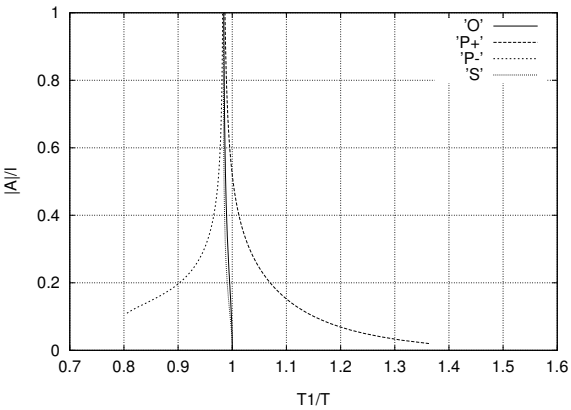

$\frac{z_0}{l} = 0.15, \frac{h}{l} = 0.35, \psi_0 = 0.2rad, i(2, \bar{h}) = 0.78$

Fig.3.7 (continued):

The earlier theory gave m_1 to be only a function of h/l. In order to compare both results we need to give the following remark.

Remark 3.5. For any asymptotic sloshing theory with one dominating mode, the nonlinear secular equation describing the dependence of the amplitude/breadth ratio $\bar{A}$ versus the excitation frequency σ has the same general form

$$\Pi_h(\frac{\sigma_1}{\sigma}, \frac{\sigma_2}{\sigma}, \bar{A}) = 0,$$

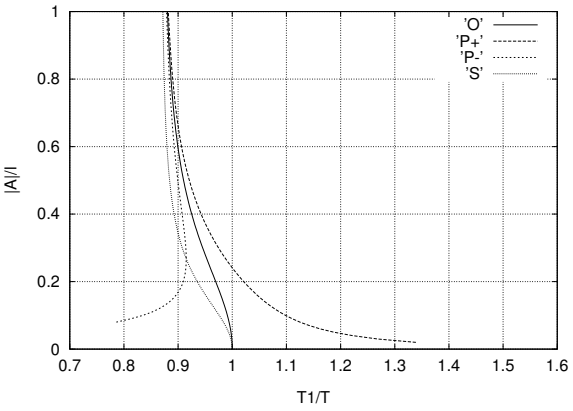

$\frac{z_0}{l} = 0.3, \frac{h}{l} = 0.5, \psi_0 = 0.1 rad, i(2, \bar{h}) = 0.737$

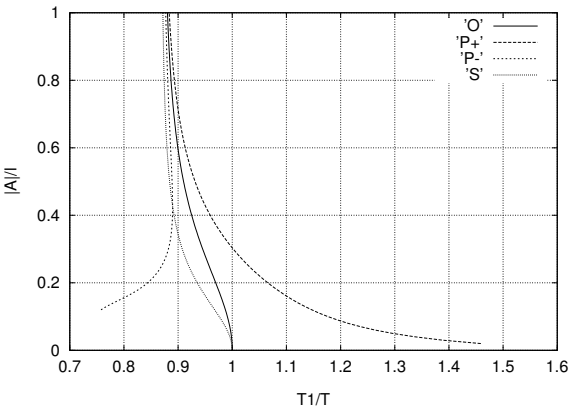

$\frac{z_0}{l} = 0.3, \frac{h}{l} = 0.5, \psi_0 = 0.2 rad, i(2, \bar{h}) = 0.737$

Fig. 3.7 (continued):

where σ_1 is lowest natural frequency and the function Π is expanded in a Taylor series. The approach by Moiseev (1958) [129] and Faltinsen (1974) [43] gives the expansion near the point $(\bar{\sigma}_1, \frac{\sigma_2}{\sigma 1}, 0)$ (for a fixed $\bar{h}$). The present modal approach has no asymptotic restrictions on the value of σ and, therefore, includes only power series in $\bar{A}$, i.e.

$$\Pi_h(\frac{\sigma_1}{\sigma}, \frac{\sigma_2}{\sigma}, \bar{A}) = \Pi(\frac{\sigma_1}{\sigma}, \frac{\sigma_2}{\sigma}, 0) +$$

$$+\frac{\partial \Pi}{\partial \bar{A}}(\frac{\sigma_1}{\sigma},\frac{\sigma_2}{\sigma},0)\bar{A}+\tfrac{1}{2}\frac{\partial^2 \Pi}{\partial \bar{A}^2}(\frac{\sigma_1}{\sigma},\frac{\sigma_2}{\sigma},0)\bar{A}^2+\frac{\partial^3 \Pi}{\partial \bar{A}^3}(\frac{\sigma_1}{\sigma},\frac{\sigma_2}{\sigma},0)\frac{1}{6}\bar{A}^3+o(\bar{A}^3).$$

Simple analysis shows that, if $m_1 = 0$ for certain σ and h/l, Eq. (3.85) leads to infinite A and, therefore, our third-order theory fails. The resonant condition with $\sigma = \sigma_1$ implies the critical depth $\bar{h} = h/l = 0.3368...$, which appears as the single root of

$$m_1(\frac{\sigma_2}{\sigma_1},\bar{h}) = 0.$$

The response curves change from being a 'hard–spring' to a 'soft–spring' behaviour at this critical depth. Detailed asymptotic analysis of the response curves near this critical depth was done by Waterhouse (1994) [169] by a fifth-order theory based on Faltinsen–Moiseev's technique. He showed that the curves coincide with a third order theory only for relatively small $\bar{A}$, but new turning points on the branches occur at a critical value of the amplitude/frequency. Sloshing at the critical depth is also affected by the secondary resonance (Faltinsen & Timokha (2001) [49]).

One should note, that our case suggests $m_1 = m_1(\frac{\sigma_2}{\sigma},\bar{h})$. This implies that if a fixed σ is close to the natural frequency σ_1, but $\sigma \neq \sigma_1$, the equation

$$m_1(\frac{\sigma_2}{\sigma},\bar{h}) = 0 \tag{3.87}$$

gives a different value of the critical depth, namely, the critical depth is a function of σ. If a pair $(\sigma,\bar{h})$ satisfies (3.87), then $\bar{A}$ tends to infinity. This is illustrated in Figs. 3.6 and 3.7 by vertical asymptotes for all the branches.

Fig. 3.6 shows the positive and negative solutions (branches P_+, P_-) of the secular algebraic equation (3.85) for different values of the water depth h and fixed amplitude of excitation H. The choice of H corresponds to the experimental values reported later. Branch O is the set of solutions of (3.85) for $H = 0$ (no excitations of the tank). This can be interpreted as the amplitude–frequency dependence for a subset of the nonlinear free-standing waves. The branches differ from curves following from Faltinsen's theory only for large values of $|A|/l$ and far away from the main resonance $\bar{\sigma}_1 = 1$. The last difference is due to the change of m_1 when varying σ. The results agree with the fifth order theory by Waterhouse (1994) [169] for sufficiently small amplitudes.

Similar results on the resonant steady-state solutions are obtained for the sinusoidal pitch excitation. Let us assume the tank is pitching around

the point $(0, 0, -z_0)$ of the mobile coordinate system. We can correct to $O(\epsilon)$ express that

$$\psi(t) = \psi_0 \cos(\sigma t), \quad \dot{v}_{0x} = z_0 \ddot{\psi}(t), \quad \dot{v}_{0z} = 0.$$

The secular equation for response curves takes the following form

$$(\bar{\sigma}_1^2 - 1)\bar{A} + m_1(\bar{\sigma}_2, \bar{h})\bar{A}^3 - \bar{P}_1\psi_0(\frac{z_0}{l} - \frac{S_1}{l} + \frac{g}{l\sigma^2}) = 0 \tag{3.88}$$

It differs from Eq. (3.85) only by the last inhomogeneous term.

Secondary resonance. All the earlier results of § 3.2.2 are based on the assumption that $O(\beta_1^2) = O(\beta_2)$. However, analysis shows that one can find a critical value of σ/σ_1 (slightly away from 1), for which amplitudes of the second mode tend to infinity. This is called the secondary resonance and may happen as $\bar{\sigma}_2^2 \to 4$ (see, the asymptotic solution (3.83) (3.84)). In terms of σ, the secondary resonance condition takes the form

$$\frac{\sigma}{\sigma_1} \to \sqrt{\frac{\tanh(2\pi h/l)}{2\tanh(\pi h/l)}} = i(2, \bar{h}). \tag{3.89}$$

The value $i(2, \bar{h})$ characterises the applicability of our theory (see, Figs. 3.6 and 3.7). The ratio $T_1/T = \sigma/\sigma_1$ must be close to 1 and not close to $i(2, \bar{h})$.

Similarly, we can introduce for the third mode

$$i(3, \bar{h}) = \sqrt{\frac{\tanh(3\pi h/l)}{3\tanh(\pi h/l)}}. \tag{3.90}$$

However, since $i(3, \bar{h}) < i(2, \bar{h})$, the secondary resonance owing to (3.89) is more dangerous.

The trend of the distribution of $i(2, \bar{h})$ shows for $\bar{h}$ small enough (but large for shallow water theory) that $i(2, \bar{h}) \to 1$ as $\bar{h} \to 0$. This means that the secondary resonance can occur for small depths and the asymptotic theory is not applicable for shallow water.

The stability analysis for surge/pitch excited waves in a rectangular container was done by Faltinsen (1974) [43]. We can give reliable new treatment of the stability by introducing branches O and S in Figs. 3.6 and 3.7. The branch O is defined by the equation

$$\text{branch O}: \quad (\bar{\sigma}_1^2 - 1) + m_1(\bar{\sigma}_2, \bar{h})\bar{A}^2 = 0; \tag{3.91}$$

it is the asymptotic curve for P_- and P_+ as $A \to \infty$.

The branch S is the set of all the turning points on $P_\pm$ for various excitation amplitudes $\bar{H}$ (surge excitation) or ψ_0 (pitch excitation). The turning points correspond to when (3.85) has only two solutions. The condition of the two roots of Eq. (3.85) can be found by differentiating (3.85) by A. It takes the form

$$\text{branch S}: \quad (\bar{\sigma}_1^2 - 1) + 3m_1(\bar{\sigma}_2, \bar{h})\bar{A}^2 = 0. \tag{3.92}$$

The branch S does not depend on the excitation amplitude and is only a function of the depth/breadth ratio.

Owing to bifurcation theory, the turning point divides the branch P_+ or P_- into stable and unstable sub-branches. This was shown by Faltinsen (1974) [43] that the upper sub-branch of P_+/P_- corresponds to unstable solutions and the lower sub-branch to stable solutions. The branch P_-/P_+ without a turning point corresponds to stable solutions. When repeating the stability analysis by Faltinsen for our solutions, we arrive at the same result if $\bar{A} \ll 1$. When varying the excitation amplitude, the sub-branch situated between S and O will always correspond to unstable solutions.

3.2.3 Transient regimes. Comparison with experiments

A series of experiments on nonlinear sloshing in a smooth rectangular tank due to horizontal (surge) excitation were conducted and documented by Faltinsen *et al.* (2000) [45]. The tank had a front plate made of plexiglass which is stiffened by two vertical L-beams. The tank was placed on a wagon that could slide back and forth controlled by a hydraulic cylinder. The hydraulic system was strong enough to ensure that the motion inside the tank had little or no effect on the tank motions.

The tank height, breadth and length were respectively $1.05m$, $1.73m$ and $0.2m$. The observed free surface elevation did not vary in the length direction. The amplitude of surge excitation was between 0.02 and $0.08m$. The water depth was varied between 0.2 and $0.6m$. The tank was equipped with three wave probes, referred to as FS1, FS2 and FS3 (see, Fig. 3.8). Wave probes FS1 and FS2 consist of adhesive copper tape directly placed on the tank wall. FS3 is made of steel wire and is standing $0.05m$ from the left wall. The tank position was measured by a position gauge. The sampling frequency was $50Hz$ and the time series were 50 seconds long. Video recordings and visual observation of longer simulations, up to 5 minutes, showed that steady–state oscillations with the

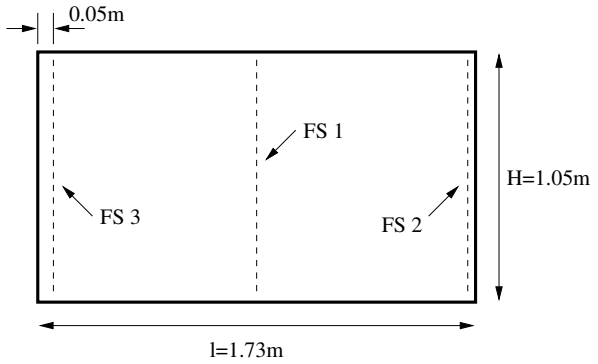

Fig. 3.8. Tank dimensions and wave probe positions used in the experiments.

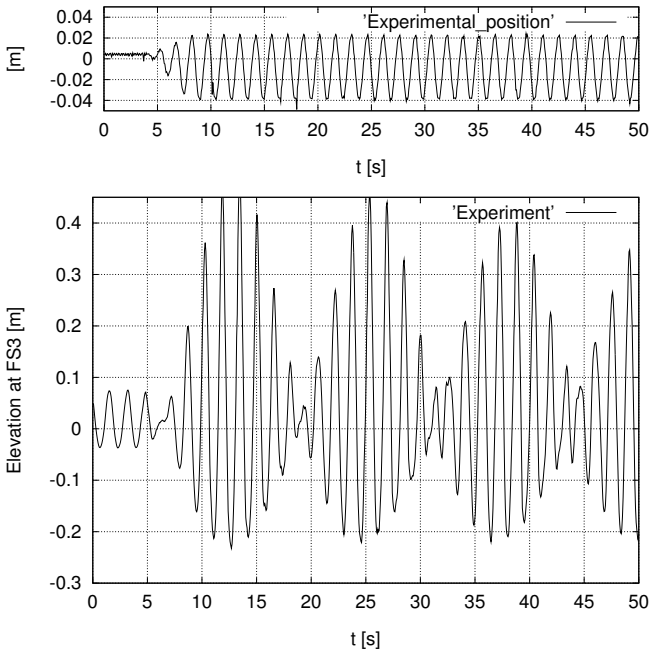

Fig. 3.9. Measured tank position and free surface elevation at wave probe FS3 ($h = 0.6m, T = 1.5s$).

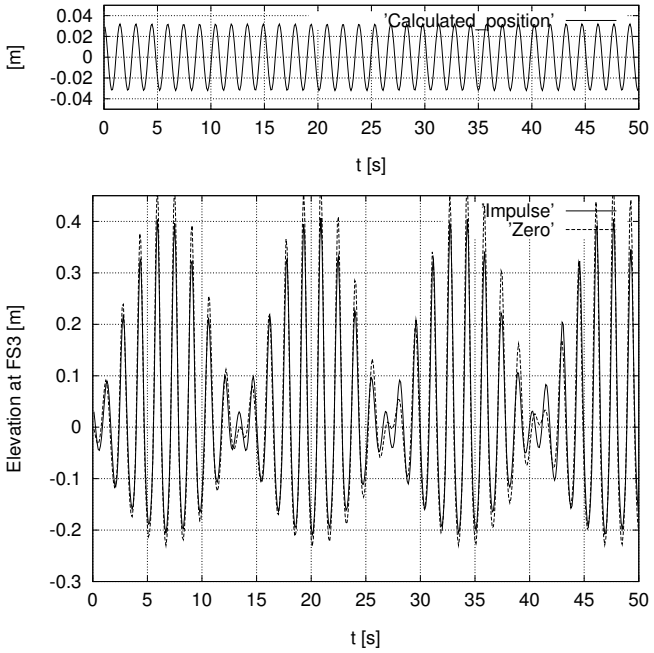

Fig. 3.9 (continued): Calculated tank position and free surface elevation at wave probe FS3 ($h = 0.6m, T = 1.5s$). The curve 'Zero' corresponds to zero-initial conditions, 'Impulse' means initial impulse condition.

forced oscillation period were not achieved. This implies that the dissipation in the smooth tank is very small even relative to the small damping predicted by Keulegan (1959) [91]. A reason may be that the boundary layer flow is laminar in Keulegan's experiments while it is likely to be turbulent in our case. Because transients do not die out, a beating effect occurs. The most interesting stage of transient waves occurs during the first 50 s, when the beating parameters are not stabilised yet. After this time the typical behaviour of the sloshing is repeated. The preliminary analysis has shown that for beating waves of small amplitude the modulated wave is stabilised for even shorter time.

The free surface elevation had small amplitudes in the initial period after the tank was excited. In some of the tests the water was in small-amplitude motion before starting the excitation. Since the proper initial

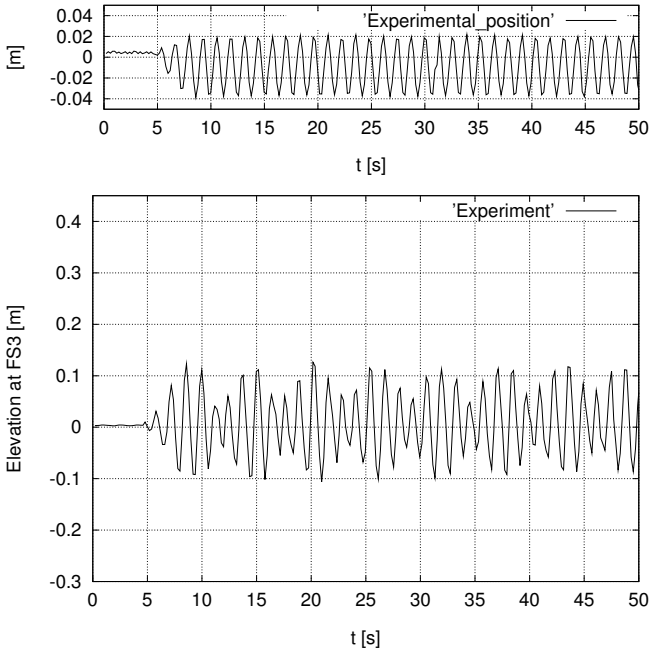

Fig. 3.10. Measured tank position and free surface elevation at wave probe FS3 ($h = 0.6m, T = 1.3s$).

conditions are unknown, two different sets are used to investigate the influence of initial conditions. One set of initial conditions is

$$\beta_i(0) = \dot{\beta}_i(0) = 0, \quad i \geq 1. \tag{3.93}$$

The other is based on the impulse conservation. If $v_{ox} = \sigma H \cos \sigma t$, this gives

$$\beta_i(0) = 0, \quad \dot{\beta}_i(0) = -\sigma P_i H, \quad i \geq 1. \tag{3.94}$$

The numerical time integrations were done by a fourth-order Runge–Kutta method and 11 equations of (3.78) were used. The simulation time on a Pentium II–366 computer was 1/300 of the real time scale.

The examples of Figs. 3.9–3.11 exhibit influence of the initial conditions on the free surface elevation for different forced excitation periods T, water depth h and excitation amplitude H. So, for example, in Fig. 3.9 the effect of initial conditions is not important. However, for the case in

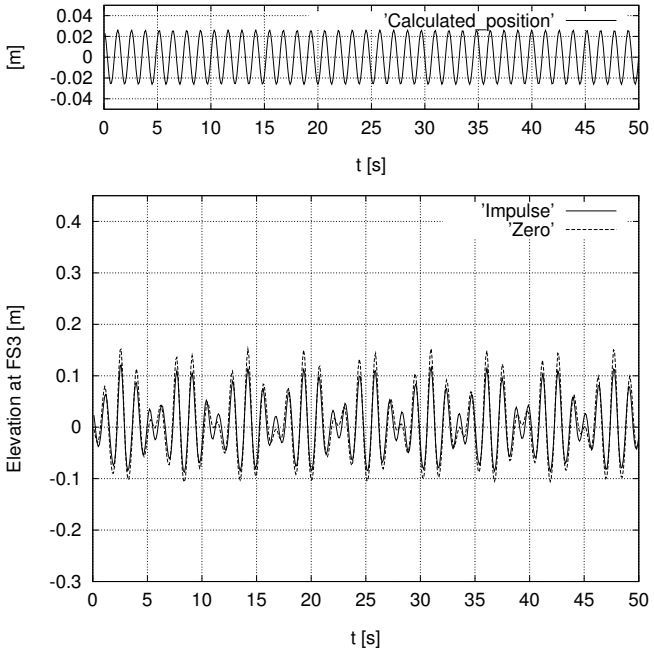

Fig. 3.10 (continued): Calculated tank position and free surface elevation at wave probe FS3 ($h = 0.6m, T = 1.3s$). The curve 'Zero' corresponds to zero-initial conditions, 'Impulse' means initial impulse condition.

Fig. 3.10 the condition of impulse conservation leads to more reasonable description of free surface elevation. Figs. 3.12 and 3.11 also demonstrate good agreement between theory and experiments. The agreement is not perfect in Fig. 3.12, but the difference between experimental and numerical simulation decreases when initial conditions are based on the impulse conservation.

Better agreement between theory and experiment can be achieved by realising that the forced surge oscillation is not harmonic and does not have a constant amplitude during the initial period. This is illustrated in Fig. 3.12 where the excitation period T was not a constant during the first 12 s; it varied from 1.76 s to 1.875 s. This is caused by transient rigid body motions. We assume that these transient motions decay exponentially. This effect was simulated by varying the period and the amplitude of

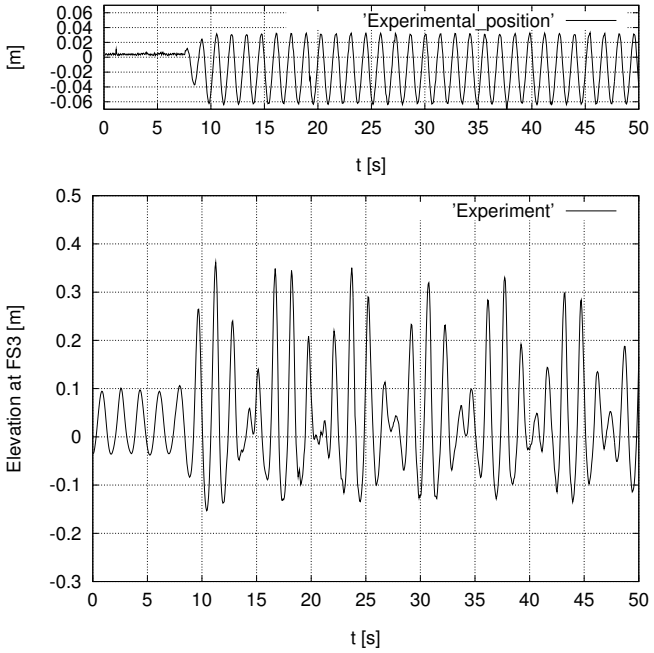

Fig. 3.11. Measured tank position and free surface elevation at wave probe FS3 ($h = 0.5m, T = 1.4s$).

forced excitation in the initial phase. Fig. 3.13 shows the effect of only varying the excitation period. A better agreement with the experiment is then achieved. Separate numerical results showed that the amplitude fluctuations have less effect than variation of the forcing frequency. The latter can be evident by examining the steady–state response in Fig. 3.6.

Our theory assumes that the fluid does not hit the roof. The fluid touches the roof in the case of Fig. 3.12, but this does not have an important effect on the fluid motion. When comparing theoretical and experimental results for a case when heavy impact occurs, it is evident that they do not agree. A possible reason is energy dissipation due to impacts. The impacts cause the ceiling to vibrate which represents energy loss for the fluid motion. Because the tank ceiling is very stiff in the model tests, this is unimportant in the comparative study with experiments. Furthermore, whereas the water hits the ceiling, a jet is formed and eventually

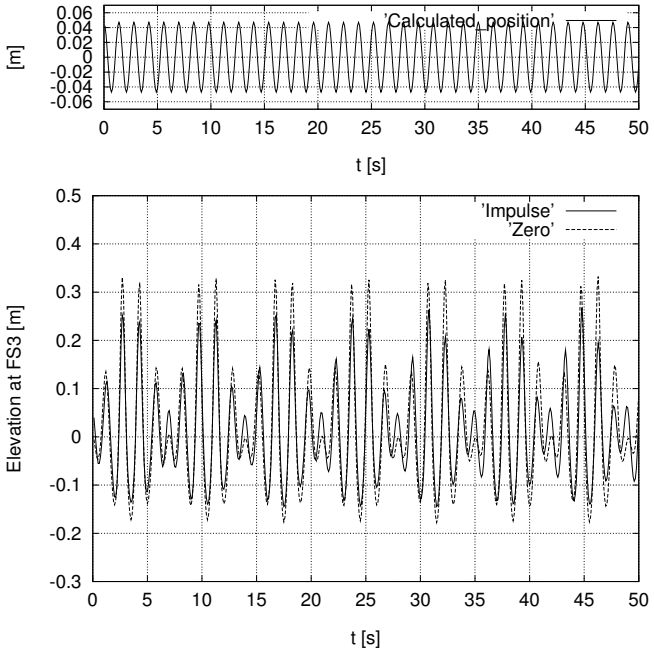

Fig. 3.11 (continued): Calculated tank position and free surface elevation at wave probe FS3 ($h = 0.5m, T = 1.4s$). The curve 'Zero' corresponds to zero-initial conditions, 'Impulse' means initial impulse condition.

the free surface overturns and water hits the free surface. This also causes energy dissipation. An estimate of this energy loss can be calculated by using a generalisation of Wagner' (1932) [166] theory (see, Faltinsen & Rognebakke (1999) [44]) and assuming that the kinetic and potential energy in the jet is dissipated. An equivalent linear damping based on energy conservation can then be included in the differential equations for the generalised coordinates, i.e. the linear damping terms $\alpha_1\dot{\beta}_1$,$\alpha_2\dot{\beta}_2$ and $\alpha_3\dot{\beta}_3$ are incorporated in (3.78). Because the average forced excitation is close to the lowest natural frequency, it is only α_1 that matters. Fig. 3.14 shows satisfactory agreement between theory and experiments by including the damping quantify. The damping will vary from cycle to cycle depending on the severity of the water impact. In the presented case we

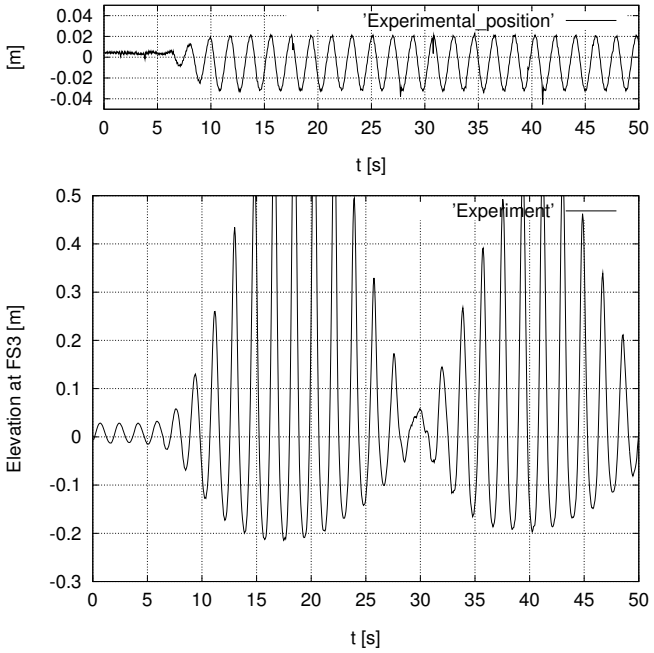

Fig. 3.12. Measured tank position and free surface elevation at wave probe FS3 ($h = 0.5m, T = 1.875s$).

calculated approximately 40% loss of energy in the tank for every cycle due to the two impacts occurring.

The theory will break down for small fluid depths. Fig. 3.15 presents experimental data and numerical simulation for $h/l = 0.173$ and $T_1/T = 0.96$. Because $i_2 = 0.9$, the effect of secondary parametric resonance is important. We note that the wave crest is well predicted, while the theoretical values for the trough is clearly lower then in the experiments. In order to improve the theoretical predictions we have to assume that at least the two lowest modes have the same order of magnitude. This means a complete change of the equation system implying that higher modes have to be introduced in the nonlinear equations. The introduction of the higher modes to be nonlinearly coupled in the nonlinear modal system will effect the difference between trough and crest so that the agreement with experiments may improve. The difference between theory and experiments

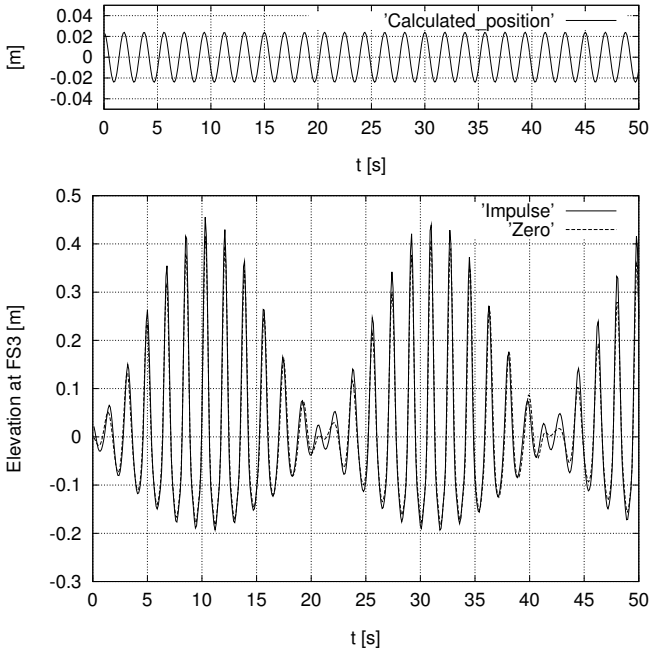

Fig. 3.12 (continued): Measured and calculated tank position and free surface elevation at wave probe FS3 ($h = 0.5m, T = 1.875s$). The curve 'Zero' corresponds to zero-initial conditions, 'Impulse' means initial impulse condition.

are more evident in Fig. 3.16, where $T_1/T = 1.17$ and $h/l = 0.173$. The reason is once more that the primary mode is not dominating and this contradicts to our asymptotic postulation. The interested readers are referred to Faltinsen, Rognebakke & Timokha (2001-2005) [49, 51, 47], in which the secondary resonance, amplification of higher modes and corresponding modifications of asymptotic modal systems are extensively elaborated.

Concluding remarks

Under certain circumstances, the two-dimensional sloshing in a rectangular smooth tank with a finite fluid depth can be theoretically studied by a Moiseev-based modal theory. The tank oscillates with a small magnitude

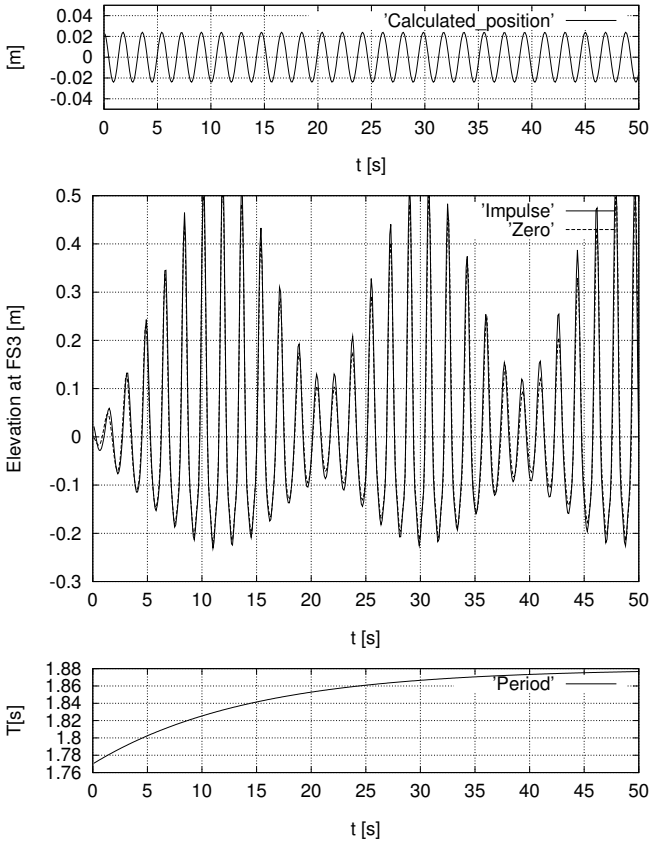

Fig. 3.13. Calculated tank position and free surface elevation at wave probe FS3 for $h = 0.5m$. Effect of varying excitation period exponentially from $1.77s$ to $1.875s$.

and with frequencies, whose average values are close to the lowest natural frequency of the fluid motion. This modal theory is associated with a finite-dimensional system of nonlinear ordinary differential equations (3.78). Its derivations were based on the Miles-Lukovsky modal system under assumption that the lowest mode is a dominant, but higher modes have a higher asymptotic order than the dominant. An important feature of such asymptotic modal modelling is that it makes it possible to

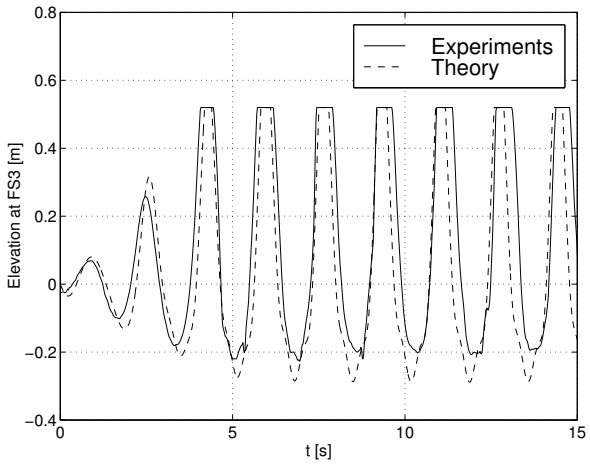

Fig. 3.14. Measured and calculated free surface elevation at wave probe FS3 for $T = 1.71$s, $h = 0.5$m and $H = 0.05$m. Calculations account for wave impact on tank ceiling.

describe both steady-state and transient waves. Because the theory is expressed in terms of a simple system of nonlinear ordinary differential equations, it is considerably simpler than a direct simulations by means of a CFD method.

The asymptotic modal system facilitates studying the steady-state solutions. This can be done by combining variational and asymptotic methods in manner of Faltinsen *et al.* (2000) [45]. The result consists of a secular equation with respect to the primary amplitude, which gives the sloshing amplitude–forcing frequency response. The latter can be drawn as the response curves that are consistent with the fifth order steady–state solution by Waterhouse (1994) [169] and, for small amplitudes, with results by Faltinsen (1974) [43]. Owing to a singularity in the secular equation, one can establish the critical depth $h = 0.3368\ldots$, at which the response curves changes from a 'soft'-spring to a 'hard'-spring behaviour.

In contrast to all the previous theories, the model system captures the secondary resonance phenomena, i.e. amplification of higher modes due to combinatoric internal resonances in the system caused by nonlinearities (Faltinsen & Timokha (2001) [49]). It is from comparative analysis with experimental data that the modal theory is not valid when the water depth (h) becomes small relative to the tank breadth (l). This is due

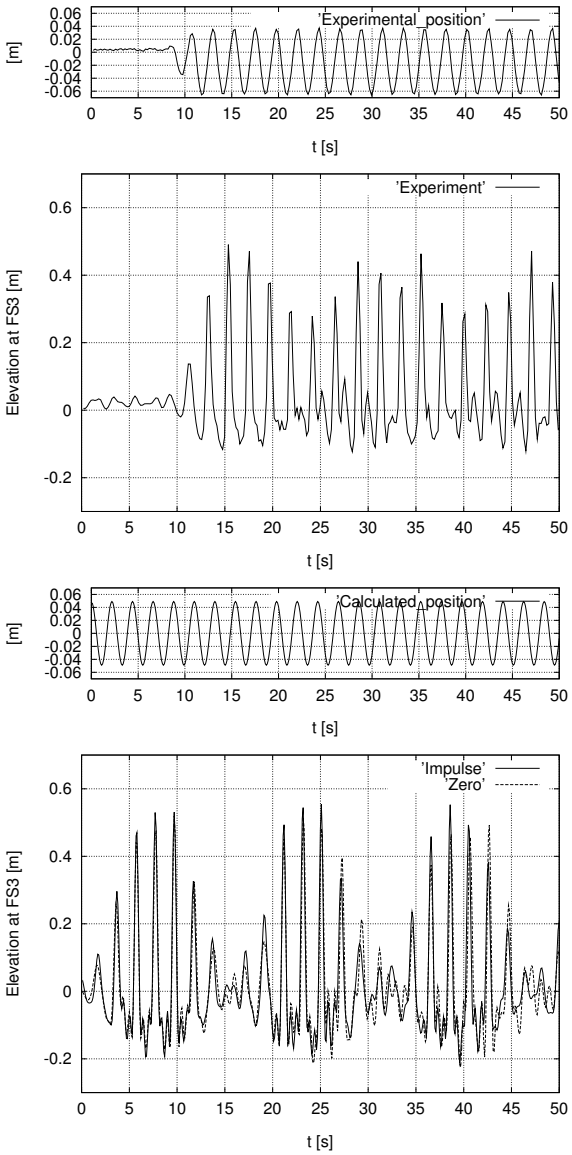

Fig. 3.15. Measured and calculated tank position and free surface elevation at wave probe FS3 ($h = 0.3m, T = 2.2s$).

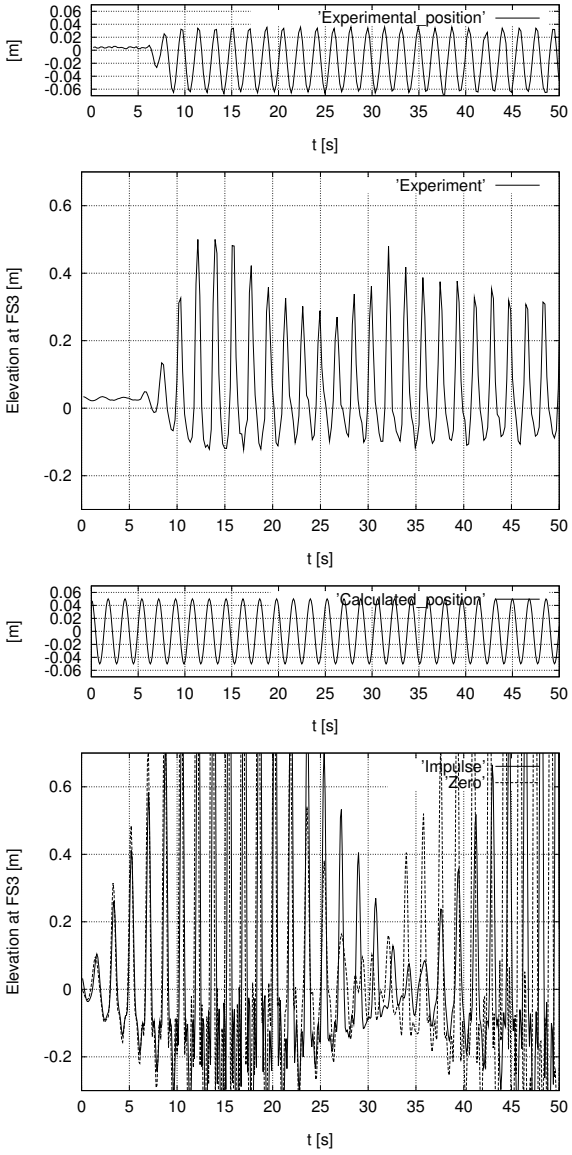

Fig. 3.16. As Fig. 3.15, but $T = 1.8s$.

to the secondary resonance, which activates a tandem of higher modes and forces them to interact nonlinearly with the lowest, primary excited mode. A series of the higher modes should therefore be considered in similar modal analysis to have the same order of magnitude. We demonstrated this point for a tank with $h/l = 0.173$. Faltinsen & Timokha (2002) [51] conducted a series of special studies on what happens when the depth/breadth ratio tends to zero. They placed special emphasis on the so-called intermediate depths, $0.1 \leq h/l \leq 0.28$, and showed that accurate description of the resonant waves needs in that case the forth-order Boussinessq-type asymptotics. Importance of the damping was also pointed out.

Experimental studies by Faltinsen *et al.* (2000) [45] demonstrate that it takes a very long time for transient fluid motion to die out. This does not occur during observation period of 5 minutes, which corresponds to the order of $150 - 200$ oscillations in terms of the excitation period. The consequence is that the steady–state nonlinear analysis in a smooth tank can have limited applicability. Modulated ('beating') waves occur as a consequence of transient and forced oscillations. Since we could not exactly state what the initial conditions were in experiments, a sensitivity study can be performed with different initial conditions in the theoretical model. This fact is especially important for the three-dimensional sloshing (Faltinsen *et al.* (2005) [47]). For the two-dimensional case, the results are not strongly dependent on this, but better agreement between theory and experiments was in general obtained by using initial conditions based on the impulse conservation. For several model tests we observed fluctuations of the exciting frequency in an initial period up to approximately 10 s. This effect was important to be included in the theoretical model. There is good agreement with experimental free surface elevation when $h/l \geq 0.28$. The latter is the limit of applicability of the finite depth theories.

The theory of this section was compared with experiments when heavy water impact on the tank ceiling occurred. The experimental free surface elevations showed a clear influence of the impact. It was speculated that this is due to energy dissipation and phenomenological linear damping terms are introduced in the discrete modal system. Good agreement with the experiments may then be demonstrated. This is an area of future research.

3.3 Sloshing in a circular cylindrical tank

The modal methods can be developed to describe three-dimensional sloshing in a circular cylindrical tank (see, Abramson (1966) [1], Narimanov (1957) [134], Hutton (1963) [80] and Dodge *et al.* (1965) [40]).[2] These are based on an asymptotic procedure, in which the functional sets $\{f_i\}$ and $\{\varphi_n\}$ are associated with the linear sloshing modes

$$\begin{aligned} \bar{f} =& \bar{f}_{nm}(\xi,\eta) = f_{nm}(\xi)\,\sin[\cos]n\eta; \\ f_{nm}(\xi) =& \frac{J_n(\kappa_{nm}\xi)}{J_n(\kappa_{nm})}, \quad J_n'(\kappa_{nm}) = 0. \end{aligned} \tag{3.95}$$

written in the cylindrical coordinate system (z,ξ,η).

Miles (1976) [125], Lukovsky (1976,1990) [113, 114] showed that derivation of asymptotic modal systems may start from the general modal system (3.47) and use Moiseev's asymptotic technique. The latter selects the lowest natural modes $f_{11}(\xi)\sin(\eta)$ and $f_{11}(\xi)\cos(\eta)$ of (3.95) to be dominating and having the lowest asymptotic order $\sim H^{1/3}$, where H is the forcing amplitude (see, Eq. (3.57) and a similarity to the resonant sloshing in a rectangular tank). The primary modes should be coupled nonlinearly and implicitly depend on secondar-order modes. Experimental and theoretical studies by Abramson *et al.* (1962) [4], Abramson *et al.* (1966) [3], Mikishev (1978) [122] and Faltinsen *et al.* (2000) [45] have shown that contribution of the second-order modes cannot be neglected. These nonlinear modal systems are valid when the forcing frequencies are close to the lowest natural frequency.

3.3.1 Asymptotic modal system

By using similar technique as described in § 3.2.1, Lukovsky (1990) [114] have derived a five-dimensional nonlinear modal system for sloshing in a circular cylindrical tank. This modal system accounts for two primary and three secondary modal functions. The system was applied to re-derive several results on steady-state regimes by Dodge *et al.* (1965) [40], Lukovsky (1976) [113], Narimanov *et al.* (1977) [135] and Miles (1984) [126, 127]. Gavrilyuk *et al.* (2000) [65] showed that the model system by Lukovsky (1990) [114] may be a good alternative to the CFD methods for simulating the transient waves and visualising the fluid flows.

[2] Henceforth, we consider the scaled problem, which assumes the radius $R_1 = 1$.

In accordance with Lukovsky (1990) [114], we express the free surface by the following five-modes anzatz:

$$z = f(\xi,\eta,t) = [r_1(t)\sin\eta + p_1(t)\cos\eta]f_{11}(\xi) + p_0(t)f_{01}(\xi) + \\ + [r_2(t)\sin(2\eta) + p_2(t)\cos(2\eta)]f_{21}(\xi). \quad (3.96)$$

Further,we assume harmonic sway excitation, i.e. $\boldsymbol{\omega} = \mathbf{0}$; $v_{0x} = 0$; $v_{0z}(t) = -\sigma H \sin\sigma t$. Lukovsky (1990) [114] showed that the modal equations coupling p_1, r_1, p_2, r_2, p_0 take the following form (we refer interested readers to the original derivations)

$$\ddot{r}_1 + \sigma_1^2 r_1 + d_1^*(r_1^2\ddot{r}_1 + r_1\dot{r}_1^2 + r_1p_1\ddot{p}_1 + r_1\dot{p}_1^2) + d_2^*(p_1^2\ddot{r}_1 + 2p_1\dot{r}_1\dot{p}_1 - \\ - r_1p_1\ddot{p}_1 - 2r_1\dot{p}_1^2) - d_3^*(p_2\ddot{r}_1 - r_2\ddot{p}_1 + \dot{r}_1\dot{p}_2 - \dot{p}_1\dot{r}_2) + d_4^*(r_1\ddot{p}_2 - p_1\ddot{r}_2) + \\ + d_5^*(p_0\ddot{r}_1 + \dot{r}_1\dot{p}_0) + d_6^* r_1\ddot{p}_0 - \sigma^2 P_1^*\cos\sigma t = 0, \quad (3.97a)$$

$$\ddot{p}_1 + \sigma_1^2 p_1 + d_1^*(p_1^2\ddot{p}_1 + p_1\dot{p}_1^2 + r_1p_1\ddot{r}_1 + p_1\dot{r}_1^2) + \\ + d_2^*(r_1^2\ddot{p}_1 + 2r_1\dot{r}_1\dot{p}_1 - r_1p_1\ddot{r}_1 - 2p_1\dot{r}_1^2) + d_3^*(p_2\ddot{p}_1 + r_2\ddot{r}_1 + \dot{r}_1\dot{r}_2 + \\ + \dot{p}_1\dot{p}_2) - d_4^*(p_1\ddot{p}_2 + r_1\ddot{r}_2) + d_5^*(p_0\ddot{p}_1 + \dot{p}_1\dot{p}_0) + d_6^* p_1\ddot{p}_0 = 0, \quad (3.97b)$$

$$\ddot{p}_0 + \sigma_0^2 p_0 + d_{10}^*(r_1\ddot{r}_1 + p_1\ddot{p}_1) + d_8^*(\dot{r}_1^2 + \dot{p}_1^2) = 0, \quad (3.97c)$$

$$\ddot{p}_2 + \sigma_2^2 p_2 + d_9^*(r_1\ddot{r}_1 - p_1\ddot{p}_1) + d_7^*(\dot{r}_1^2 - \dot{p}_1^2) = 0, \quad (3.97d)$$

$$\ddot{r}_2 + \sigma_2^2 r_2 - d_9^*(r_1\ddot{p}_1 + p_1\ddot{r}_1) - 2d_7^*\dot{r}_1\dot{p}_1 = 0, \quad (3.97e)$$

where

$$d_1^* = \frac{d_1}{\mu_1},\ d_2^* = \frac{d_2}{\mu_1},\ d_3^* = \frac{d_3}{\mu_1},\ d_4^* = \frac{d_4}{\mu_1},\ d_5^* = \frac{d_5}{\mu_1},\ d_6^* = \frac{d_6}{\mu_1},$$

$$d_7^* = \frac{d_7}{\mu_2},\ d_8^* = \frac{d_8}{\mu_0}, d_9^* = \frac{d_4}{\mu_2},\ d_{10}^* = \frac{d_6}{\mu_0},\ P_1^* = \frac{H\lambda}{\mu_1}, \quad (3.98)$$

$$\lambda = \rho\int_0^{2\pi}\int_0^1 \xi\sin^2\eta\frac{J_1(k_{11}\xi)}{J_1(k_{11})}d\xi d\eta = 0.9267\ldots$$

and

$$\sigma_i^2 = \frac{g}{R_1}\kappa_i\tanh(\kappa_i h/R_1),$$

where h is the fluid depth and g is the gravity acceleration. The numbers κ_i are the minimal roots of the equations $J_i'(\kappa_i) = 0$. The interested

Table 3.1. Computed coefficients of the modal system (3.97).

h	μ_0	μ_1	μ_2	d_1	d_2	d_3	d_4	d_5	d_6	d_7	d_8
0.20	1.272	1.707	0.539	9.287	4.99	1.821	1.502	4.714	-1.625	2.412	-3.982
0.25	1.103	1.398	0.457	5.024	2.312	1.370	0.903	3.312	-1.023	1.588	-2.679
0.30	1.003	1.197	0.406	3.106	1.157	1.126	0.579	2.551	-0.696	1.42	-1.972
0.40	0.900	0.959	0.350	1.541	0.277	0.885	0.260	1.800	-0.373	0.702	-1.273
0.45	0.874	0.885	0.334	1.189	0.096	0.820	0.175	1.599	-0.287	0.585	-1.086
0.50	0.856	0.828	0.323	0.959	-0.015	0.775	0.115	1.457	-0.225	0.503	-0.954
0.55	0.845	0.784	0.315	0.802	-0.086	0.741	0.072	1.354	-0.181	0.443	-0.857
0.60	0.837	0.750	0.309	0.691	-0.133	0.717	0.040	1.276	-0.147	0.398	-0.785
0.70	0.828	0.700	0.302	0.551	-0.189	0.683	-0.003	1.171	-0.101	0.338	-0.687
0.80	0.824	0.668	0.298	0.471	-0.217	0.662	-0.029	1.107	-0.073	0.302	-0.626
1.00	0.821	0.633	0.295	0.392	-0.242	0.640	-0.056	1.039	-0.043	0.264	-0.563
1.20	0.820	0.616	0.294	0.359	-0.250	0.631	-0.068	1.009	-0.030	0.248	-0.535
1.60	0.820	0.605	0.294	0.337	-0.255	0.624	-0.075	0.989	-0.021	0.237	-0.516
2.00	0.820	0.602	0.294	0.332	-0.256	0.623	-0.077	0.985	-0.019	0.235	-0.511
2.50	0.820	0.602	0.294	0.332	-0.257	0.622	-0.077	0.983	-0.019	0.234	-0.510

readers may find the hydrodynamic coefficients d_i, μ_i in Table 3.1. These were calculated by Lukovsky (1990) [114]. The asterisk '*' will further be omitted.

The system (3.97) is linear in $\ddot{r}_i, \ddot{p}_i$. By inverting the matrix $\mathcal{A} =$

$$\begin{Vmatrix} 1+d_1r_1^2+d_2p_1^2-d_3p_2+d_5p_0 & d_1r_1p_1 - d_2r_1p_1 + d_3r_2 & d_6r_1 & d_4r_1 & -d_4p_1 \\ d_1r_1p_1 - d_2r_1p_1 + d_3r_2 & 1+d_1p_1^2+d_2r_1^2+d_3p_2+d_5p_0 & d_6p_1 & -d_4p_1 & -d_4r_1 \\ d_{10}r_1 & d_{10}p_1 & 1 & 0 & 0 \\ d_9r_1 & -d_9p_1 & 0 & 1 & 0 \\ d_9p_1 & d_9r_1 & 0 & 0 & 1 \end{Vmatrix}$$

it can be formally reduced to the normal form

$$\frac{d^2\boldsymbol{p}}{dt^2} = \boldsymbol{f}(t, \boldsymbol{p}, \dot{\boldsymbol{p}}) = \mathcal{A}^{-1}\boldsymbol{U}(t, \boldsymbol{p}, \dot{\boldsymbol{p}}), \tag{3.99}$$

where $\boldsymbol{p} = (r_1, p_1, p_0, p_2, r_2)^T$.

The initial conditions (3.4) take for (3.99) the following form

$$\begin{aligned} &r_1(0) = r_1^0; \quad p_1(0) = p_1^0; \quad p_0(0) = p_0^0; \quad p_2(0) = p_2^0; \quad r_2(0) = r_2^0, \\ &\dot{r}_1(0) = \dot{r}_1^0; \quad \dot{p}_1(0) = \dot{p}_1^0; \quad \dot{p}_0(0) = \dot{p}_0^0; \quad \dot{p}_2(0) = \dot{p}_2^0; \quad \dot{r}_2(0) = \dot{r}_2^0. \end{aligned} \tag{3.100}$$

3.3.2 Free nonlinear oscillations

Free oscillations of the fluid (the tank is Earth-fixed) are described by solutions of the Cauchy problem (3.97) + (3.100) as $H = 0$. Depending on the initial conditions, these solutions can have periodic or aperiodic structure. The $(2\pi/\sigma)$-periodic solutions with $||\boldsymbol{p}|| \to 0$ as $\sigma \to \sigma_1$ imply nonlinear free-standing waves.

Asymptotic analysis of the free-standing waves. In accordance with Lukovsky (1990) [114] and Faltinsen *et al.* (2003) [46], the primary modal functions are approximated by the periodic terms

$$r_1(t) = A\cos\sigma t + \bar{A}\sin\sigma t,\ p_1(t) = \bar{B}\cos\sigma t + B\sin\sigma t. \tag{3.101}$$

Setting (3.101) in Eqs. (3.97c)-(3.97e) gives

$$p_0(t) = c_0 + c_1\cos 2\sigma t + c_2\sin 2\sigma t,\quad p_2(t) = s_0 + s_1\cos 2\sigma t + s_2\sin 2\sigma t,$$

$$r_2(t) = e_0 + e_1\cos 2\sigma t + e_2\sin 2\sigma t, \tag{3.102}$$

where

$$h_0 = \frac{d_{10}+d_8}{2(\bar{\sigma}_0^2-4)},\ h_2 = \frac{d_9+d_7}{2(\bar{\sigma}_2^2-4)},\ l_0 = \frac{d_{10}-d_8}{2\bar{\sigma}_0^2},\ l_2 = \frac{d_9-d_7}{2\bar{\sigma}_2^2},$$

$$\begin{aligned}
&\bar{\sigma}_m = \frac{\sigma_m}{\sigma},\ m = 0,1,2;\quad c_0 = l_0(A^2+\bar{A}^2+B^2+\bar{B}^2),\\
&c_1 = h_0(A^2-\bar{A}^2-B^2+\bar{B}^2),\quad c_2 = 2h_0(A\bar{A}+B\bar{B}),\\
&s_0 = l_2(A^2+\bar{A}^2-B^2-\bar{B}^2),\quad s_1 = h_2(A^2-\bar{A}^2+B^2-\bar{B}^2),\\
&s_2 = 2h_2(A\bar{A}-B\bar{B}),\quad e_0 = -2l_2(A\bar{B}+B\bar{A}),\\
&e_1 = 2h_2(\bar{A}B-A\bar{B}),\quad e_2 = -2h_2(AB+\bar{A}\bar{B}).
\end{aligned} \tag{3.103}$$

By substituting (3.101) and (3.102) into (3.97a), (3.97b) and using the Fredholm alternative $\int_0^{(2\pi/\sigma)} L_k \cos[\sin]\sigma t dt = 0,\ k = 1,2$, we get the following system of algebraic equations of the unknown variables $A, \bar{A}, B, \bar{B}$

$$\begin{aligned}
&A[\bar{\sigma}_1^2 - 1 - m_1(A^2+\bar{A}^2+\bar{B}^2) - m_2B^2] + m_3\bar{A}B\bar{B} = 0,\\
&\bar{A}[\bar{\sigma}_1^2 - 1 - m_1(A^2+\bar{A}^2+B^2) - m_2\bar{B}^2] + m_3AB\bar{B} = 0,\\
&B[\bar{\sigma}_1^2 - 1 - m_1(B^2+\bar{A}^2+\bar{B}^2) - m_2A^2] + m_3\bar{B}A\bar{A} = 0,\\
&\bar{B}[\bar{\sigma}_1^2 - 1 - m_1(A^2+B^2+\bar{B}^2) - m_2\bar{A}^2] + m_3\bar{A}AB = 0,
\end{aligned} \tag{3.104}$$

where

$$m_1 = -d_5\left(\frac{h_0}{2} - l_0\right) + d_3\left(\frac{h_2}{2} - l_2\right) + 2d_6h_0 + 2d_4h_2 + \frac{d_1}{2};\ \ m_3 = m_1 - m_2,$$

$$m_2 = d_3\left(l_2 + \frac{3}{2}h_2\right) + d_5\left(l_0 + \frac{h_0}{2}\right) - 2d_6h_0 + 6d_4h_2 - \frac{d_1}{2} + 2d_2. \quad (3.105)$$

Remark 3.6. The time-shift substitution $t := t + t_0$ changes the initial time, the meridian-shift substitution $\eta := \eta + \eta_0$ implies a rotation of the cylindrical coordinate system around Ox. One interesting point is that these substitutions can be considered as physically invariants, because they do not give rise to physically different waves. In particular, this means that the time substitution can reduce the primary term (3.101) to have the pure cosine form $r_1(t) = A\cos(\sigma(t+t_0))$, i.e. one can assume $\bar{A} = 0$ in (3.101) and (3.104) as $H = 0$. Further, when analysing (3.104) with $\bar{A} = 0$, $A \neq 0$, $B^2 + \bar{B}^2 \neq 0$ and $m_4 \neq 0$ (see, derivations by Faltinsen *et al.* (2003) [46] for similar systems), we get that $\bar{B}\,B = 0$. However, for the free-standing waves, the case $B = 0$, $\bar{B} \neq 0$ can be omitted because, for this case, the meridian-shift substitution reduces the free surface equation to the following form $f(\eta, \xi, t) = A\cos(\eta)\frac{J_1(k_{11}\xi)}{J_1(k_{11})}\cos(\sigma t) + \ldots$, i.e. $B = \bar{B} = 0$.

Accounting for very detailed algebra by Faltinsen *et al.* (2003) [46] and Remark 3.6, we deduce that when $m_4 \neq 0$ the physically different nonlinear free-standing waves can be associated with solutions of the cubic algebraic system

$$A(\bar{\sigma}_1^2 - 1 - m_1A^2 - m_2B^2) = 0, \quad B(\bar{\sigma}_1^2 - 1 - m_1B^2 - m_2A^2) = 0. \quad (3.106)$$

It has the two solutions:

1. 'Planar' waves ($A \neq 0, B = 0$):

$$\begin{aligned} r_1(t) &= A\cos\sigma t, \quad p_1(t) = 0, \quad r_2(t) \equiv 0, \\ p_k(t) &= A^2(l_k + h_k\cos 2\sigma t), \quad k = 0, 2, \end{aligned} \quad (3.107)$$

where

$$(\bar{\sigma}_1^2 - 1) - m_1A^2 = 0; \quad A^2 = \frac{\bar{\sigma}_1^2 - 1}{m_1}. \quad (3.108)$$

2. 'Swirling', the so-called rotary waves ($A \neq 0, B \neq 0$):

$$
\begin{aligned}
r_1(t) &= A\cos\sigma t, \quad p_1(t) = B\sin\sigma t,\\
p_0(t) &= l_0(A^2+B^2) + h_0(A^2-B^2)\cos 2\sigma t,\\
p_2(t) &= l_2(A^2-B^2) + h_2(A^2+B^2)\cos 2\sigma t,\\
r_2(t) &= -2h_2AB\sin 2\sigma t,
\end{aligned}
\tag{3.109}
$$

where

$$
(\bar\sigma_1^2-1) - m_4A^2 = 0; \quad m_4 = m_1+m_2; \quad A^2 = \frac{\bar\sigma_1^2-1}{m_4}; \quad B^2 = A^2. \tag{3.110}
$$

When $h/R_1 = O(1)$, the secular equations (3.108) and (3.110) make it possible to draw the response curves (backbones) in the $(\sigma/\sigma_1, A/R_1)$-plane. The backbones are drawn for 'planar' and 'swirling' waves in Fig. 3.20 as the branches 'O1' and 'O2', respectively.

The coefficients m_1 and m_4 are functions of h and the asymptotic analysis is invalid as these vanish, i.e. $m_1 = 0$ or $m_4 = 0$. These zeros at a certain h implies the change from a 'soft'-spring to a 'hard'-spring behaviour of the backbones. Either a fifth order theory or a secondary resonance analysis is then required (see, the example, Waterhouse (1994) [169] and Faltinsen & Timokha (2001) [49]) to deal with these critical depths. In the forthcoming simulations, we centres around the case $m_1 > 0, m_4 < 0$, which is true for finite fluid depths, e.g. $h/R_1 \geq 1.0$.

Simulations. For simulations of the free-standing sloshing, suitable initial values may be associated with asymptotic approximations (3.107) and (3.109). This means that

$$
\begin{aligned}
&r_1(0) = A; \quad p_k(0) = A^2(l_k+h_k), \ k = 0,2; \quad p_1(0) = r_2(0) = 0,\\
&\dot r_k(0) = \dot p_k(0) = 0; \ k = 1,2; \quad \dot p_0 = 0
\end{aligned}
\tag{3.111}
$$

for 'planar' waves and

$$
\begin{aligned}
&r_1(0) = A; \ p_1(0) = 0; \quad p_2(0) = A^2(l_2+h_2) + B^2(h_2-l_2),\\
&p_0(0) = A^2(l_0+h_0) + B^2(l_0-h_0), \quad \dot r_1(0) = 0;\\
&\dot p_1(0) = \sigma B; \quad \dot r_2(0) = -4\sigma h_2AB; \quad \dot p_2(0) = 0; \quad \dot p_0(0) = 0
\end{aligned}
\tag{3.112}
$$

for 'swirling'.

'Planar' waves. Abramson *et al.* (1966) [1, 3, 4] and Mikishev (1978) [122] have experimentally shown that the linear sloshing theory in a circular cylindrical tanks with a finite depth is valid only for the wave amplitude/radius ratios that are less than 0.1. In terms of our analysis,

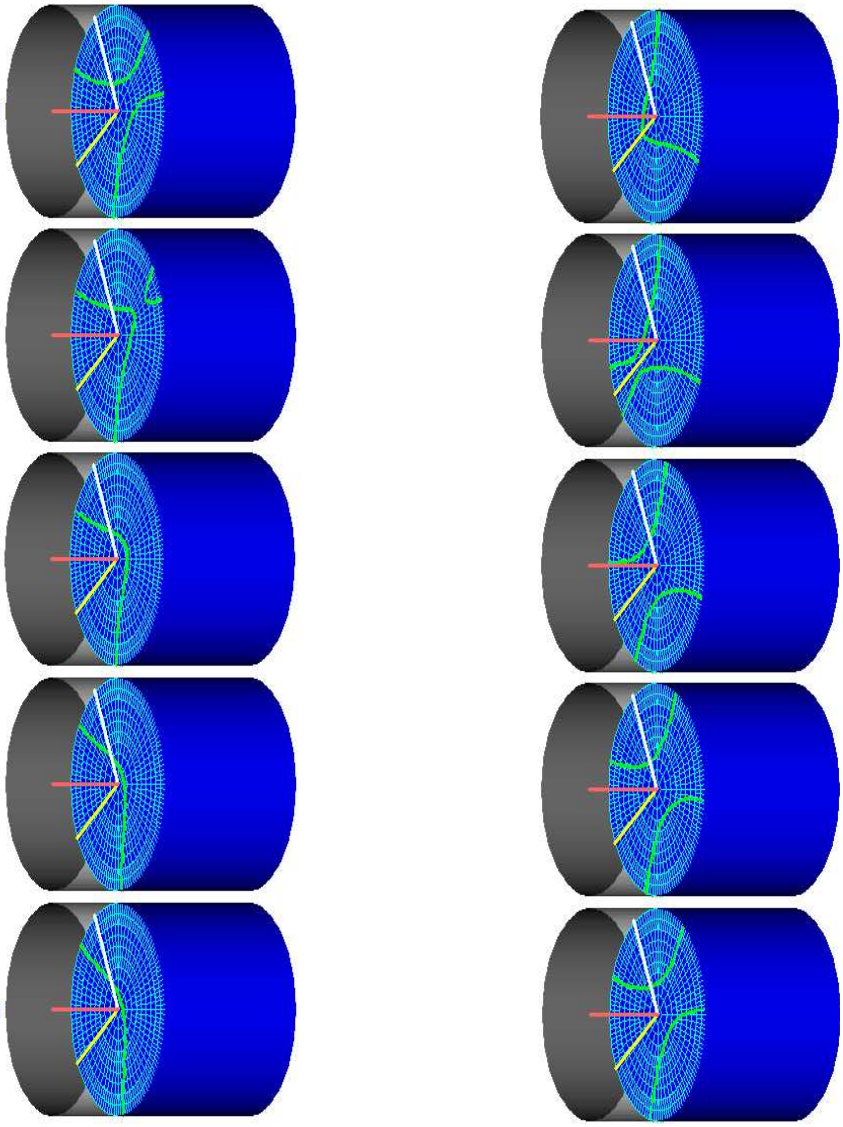

Fig. 3.17. Free-standing waves for $H \equiv 0$, $h/R_1 = 2$. A small–amplitude 'planar' regime. $A/R_1 = 0.0602626$; $\sigma = 4.24$[rad/s]. The non-zero initial conditions are $r_1(0) = 0.0602626$; $p_0(0) = 0.0011363446$; $p_2(0) = -0.00157382$.

this implies $|A|/R_1 < 0.1$. However, the smallness of A does not mean that the nonlinear phenomena disappear (Funakoshi & Inoue (1991) [60], Miles (1984) [126] and Gavrilyuk *et al.* (2000) [65]). We can show this by using the Cauchy problem (3.99) + (3.100).

A series of pictures in Fig. 3.17 is produced by our animation grid program based on the modal system (3.97), (3.111) and Eq. (3.96). A fourth order Runge-Kutta numerical integrator and a Pentium-II 366 computer were used to simulate by (3.99) + (3.100). The simulation time depended on excitation parameters. It varied between 1/50 to 1/200 of the real time scale. Fig. 3.17 visualises nonlinear wave patterns and, thereby, confirms the complicated character of sloshing, even if it is of small amplitude. Nonlinear behaviour is especially evident during a short time ($\Delta t \approx 0.01$ s), at which a winding of the so-called nodal curve (cross-line of the free surface and the mean free surface $x = 0$) becomes quite clear. This is in contrast to the linear sloshing theory, which always attributes the nodal lines as a fixed intersect of a straight line. The curvature of the nodal curve changes when the anti-nodal points (maximum and minimum surface elevations) change their positions and the peak moves between diametrically opposite points of the vertical wall forming a *'travelling'* wave. Importance of the second-order modes increases with A. For larger A, the 'travelling' wave may be clearly visible for the whole period $2\pi/\sigma$. We have also found that the use of asymptotic approximation (3.111) becomes incorrect for $A/R_1 > 0.38$. In that case, simulations based on (3.111) show aperiodic solutions.

'Swirling'. Each column of Fig. 3.18 presents instant views on the free surface shape and the graph $(r_1(t), p_1(t))$. The latter has clearly circular shape and, therefore, confirms the theoretical predictions $|A| = |B|$ following from (3.110). Considering an animation from the columns gives an impression that a 'frozen' surface shape rotates together with the nodal curve. The nodal line has nonzero curvature and does not pass through the cylinder axis. This behaviour was also experimentally observed by Mikishev (1978) [122] and Abramson *et al.* (1966) [3]. Note, that these authors reported that 'swirling' is not stable and breaks down when the wave elevation to the radius ratio is larger than 0.45. In our calculations, this critical ratio has been estimated at 0.43.

Transient waves. The modal functions (r_1, p_2) and (p_1, r_2) imply longitudinal and transversal wave components, respectively. The modal function p_0 corresponds to axial-symmetric derivations. The transient waves in Fig. 3.19 are calculated for $p_1 = r_2 \equiv 0$, which means that the transver-

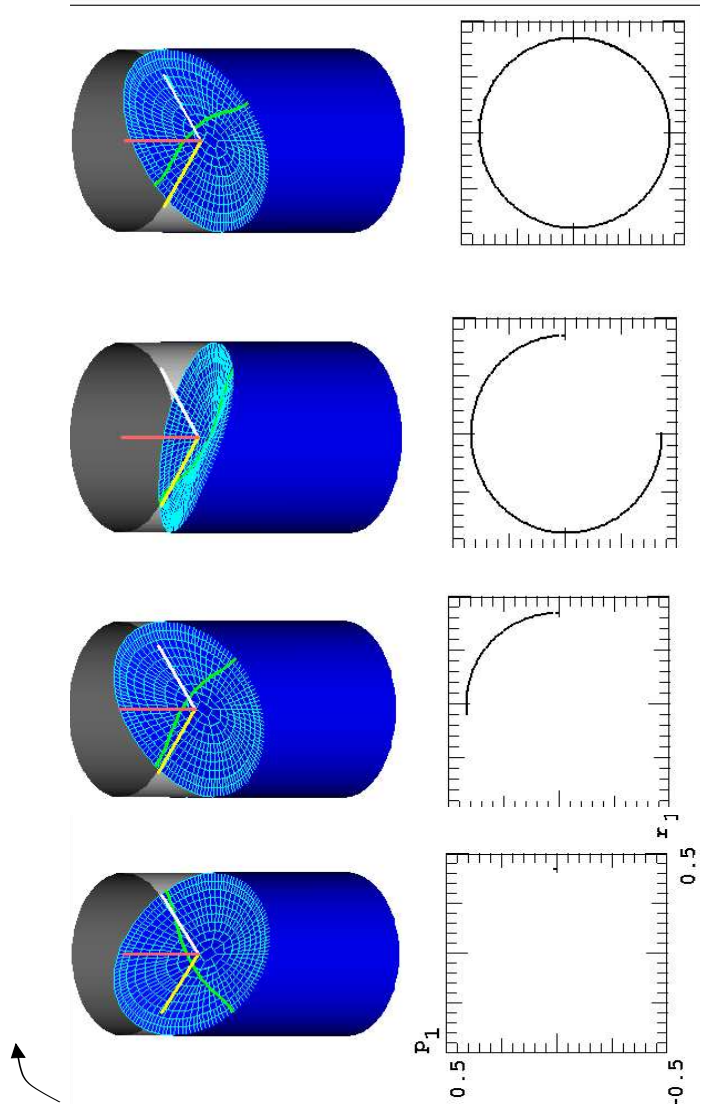

Fig. 3.18. Free-standing waves for $H \equiv 0$, $h/R_1 = 2$. A large-amplitude 'swirling'. $A/R_1 = 0.425$. The non-zero initial conditions are $r_1(0) = 0.425; p_0(0) = 0.056676; p_2(0) = -0.04; \dot{p}_1(0) = 1.8828; \dot{r}_2(0) = 0.347646$.

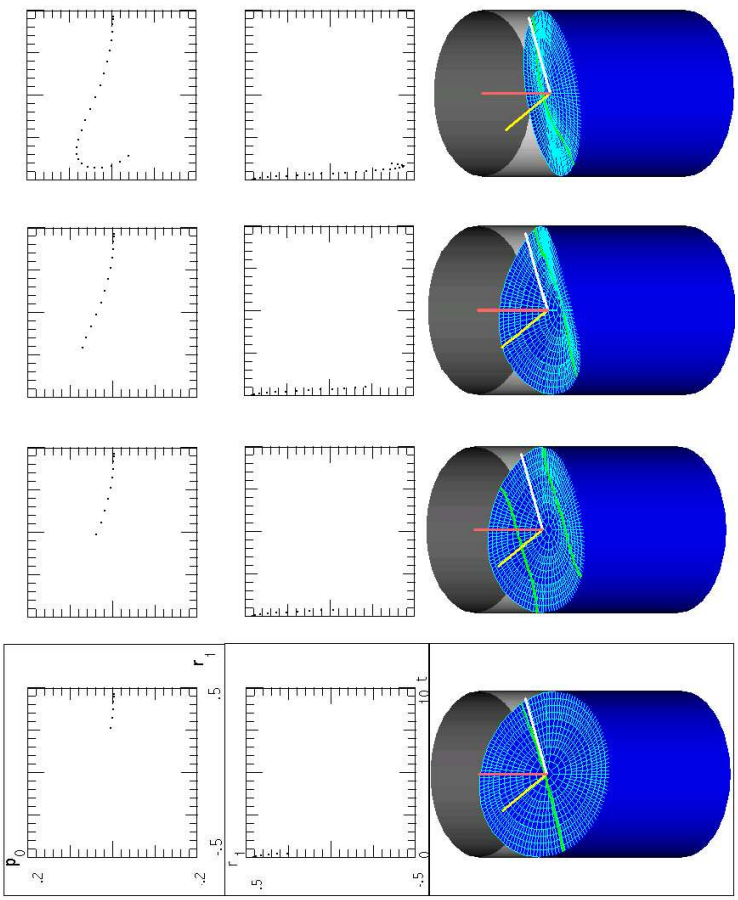

Fig. 3.19. A transient wave for $H \equiv 0$, $h/R_1 = 2$. The non-zero initial condition $r_1(0) = 0.4695$.

sal waves are not excited at $t = 0$. Fig. 3.19 is completed by a series of columns containing three pictures (windows). The first window shows an instant view on the graph $(r_1(t), p_0(t))$. The graph $r_1 = r_1(t)$ and a cam-

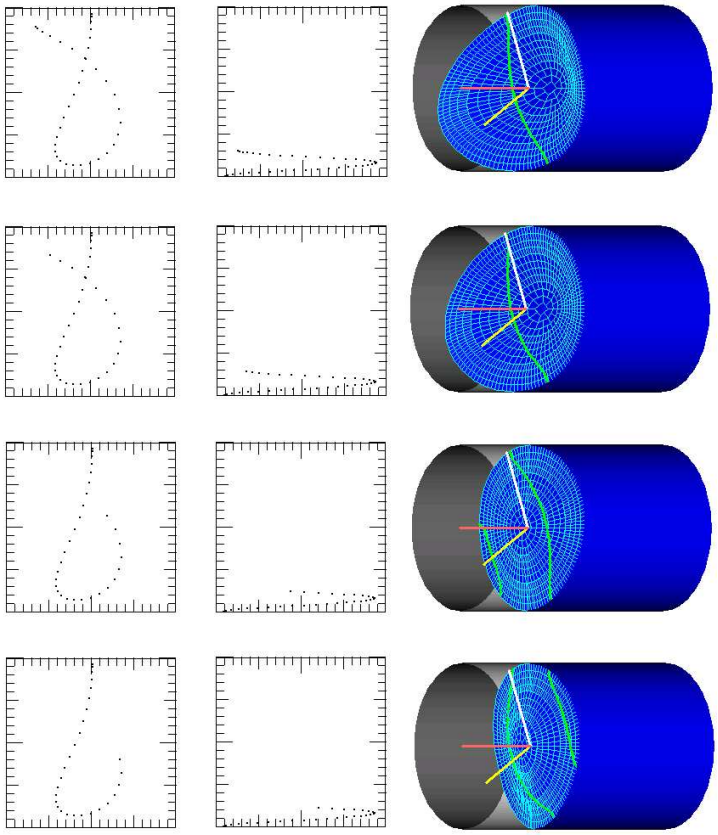

Fig. 3.19 (continued):

era view displaying the corresponding instantaneous free surface shapes are shown in the second and third windows, respectively. The graph of $r_1(t)$ shows that transient motions imply the beating (slow fluctuation of the amplitude).

In addition to the travelling wave, two nonlinear surface waves were discovered in Fig. 3.19. The first is observed as a pair of symmetric crests sliding around the circular wall clockwise in the first instance and coun-

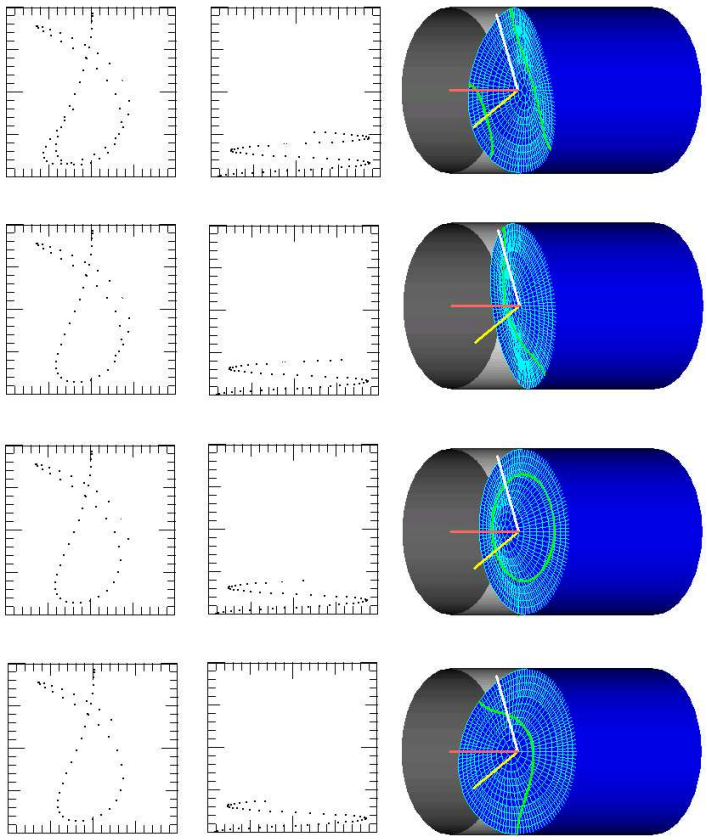

Fig. 3.19 (continued):

terclockwise in the second. Their interferences give rise to a new surface shape with a single peak. Furthermore, we will treat this wave as a 'travelling hollow', because its minimum wave elevation runs along the diameter of the mean free surface. The second wave is similar to the 'planar' regime, but it does not lead to runs of a peak. The minimum wave elevation (hollow) oscillates near the axis of circular cylinder. Nodal curves are non-connected. The two surface peaks coexist in diametrically op-

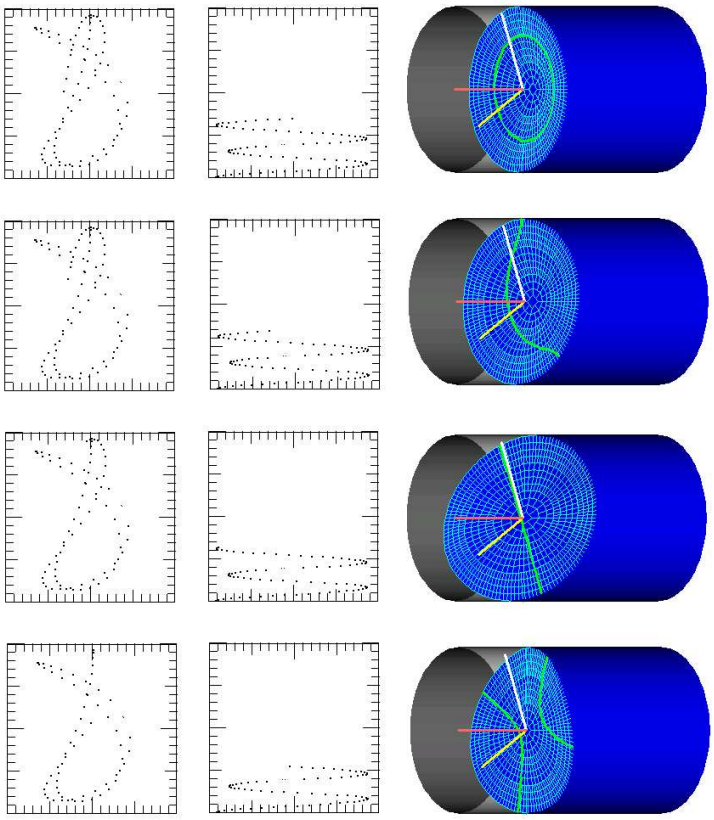

Fig. 3.19 (continued):

posite positions of the free surface. Elevation of the one peak increases, while the other decreases. The physical treatment of this wave may be as an 'underwater stream'. These three wave motions imply the three possible modal energy re-distributions. Denoting the travelling wave as $\mathcal{T}$, the travelling hollow as $\mathcal{H}$ and the 'underwater stream' as $\mathcal{S}$, we observe the following sequence of wave motions $\mathcal{S}\ \mathcal{T}\ \mathcal{T}\ \mathcal{S}\ \mathcal{H}\ \mathcal{T}\ \mathcal{T}\ \mathcal{H}\ \mathcal{H}\ \mathcal{T}\ \mathcal{T}$

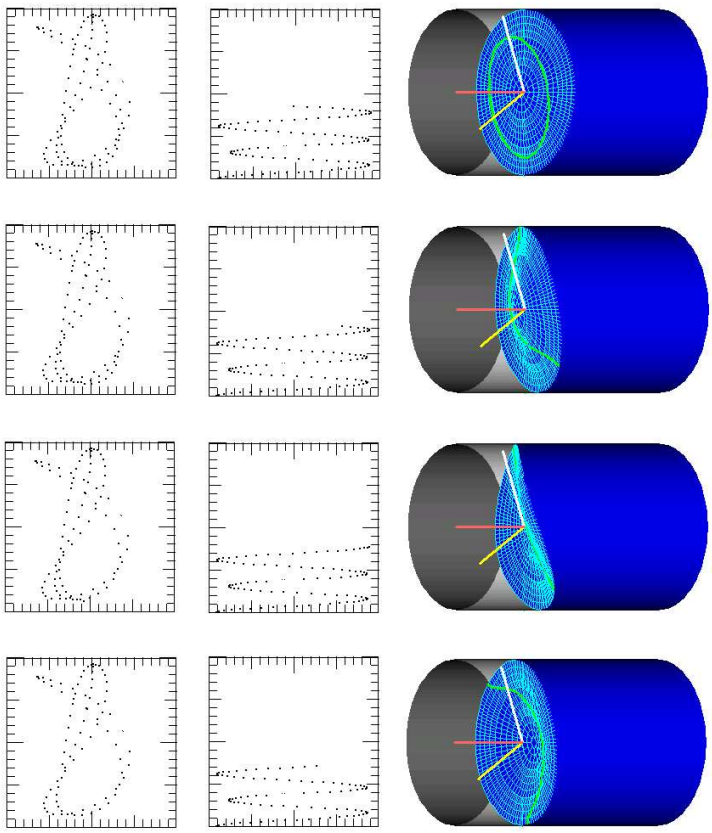

Fig. 3.19 (continued):

$\mathcal{H}\ \mathcal{S}\ \mathcal{S}\ \ \mathcal{T}\ \mathcal{T}\ \mathcal{S}\ \mathcal{H}\ \mathcal{T}\ \mathcal{T}\ \mathcal{S}\ \ldots$ for the case in Fig. 3.19. This sequence can be considered as a visual characteristics of the present transients.

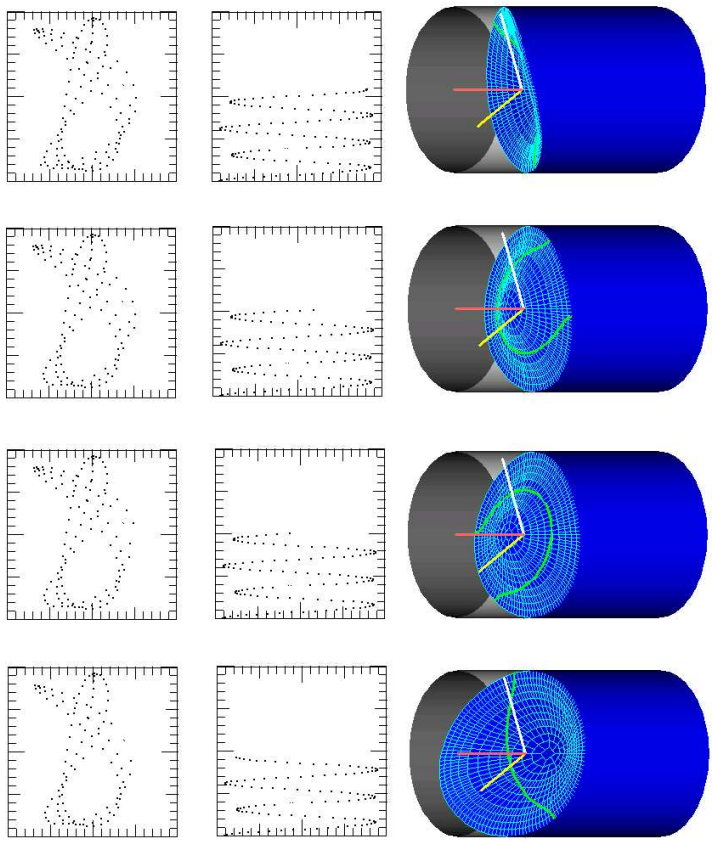

Fig. 3.19 (continued):

3.3.3 Resonant sloshing due to sway excitations

When $H \neq 0$, the modal system (3.97) describes the nonlinear sloshing due to sway (horizontal) excitation, whose $(2\pi)/\sigma$-periodic solutions imply steady-state wave regimes.

Asymptotic analysis of steady-state regimes. When repeating the asymptotic scheme developed in the previous paragraph and account-

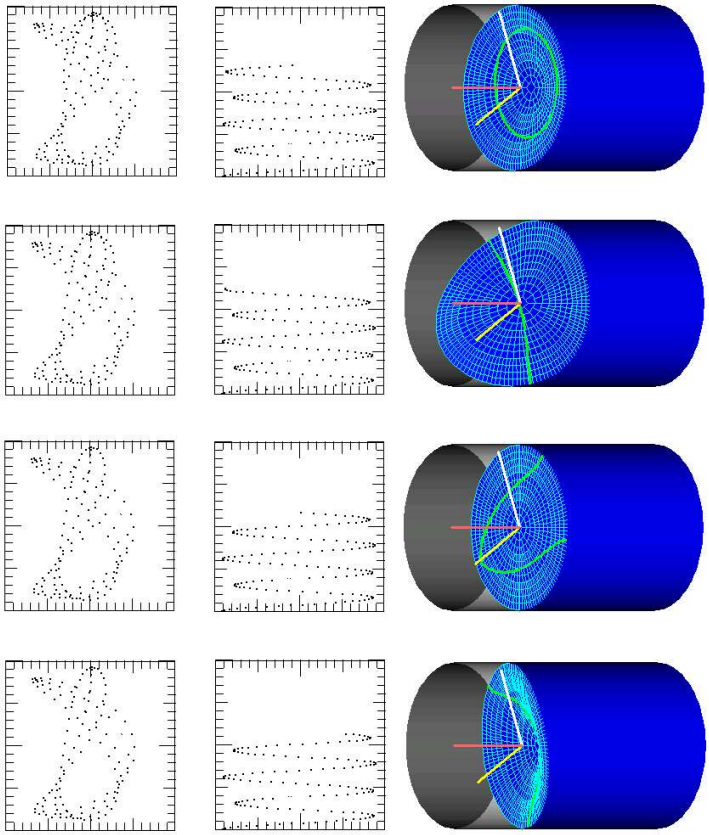

Fig. 3.19 (continued):

ing for the algebra by Faltinsen *et al.* (2003) [46], we get the following simplified secular system

$$\begin{aligned} &A(\bar{\sigma}_1^2 - 1 - m_1 A^2 - m_2 B^2) = P_1^* = H\frac{\lambda}{\mu_1} = H\Lambda, \\ &B(\bar{\sigma}_1^2 - 1 - m_1 B^2 - m_2 A^2) = 0 \end{aligned} \tag{3.113}$$

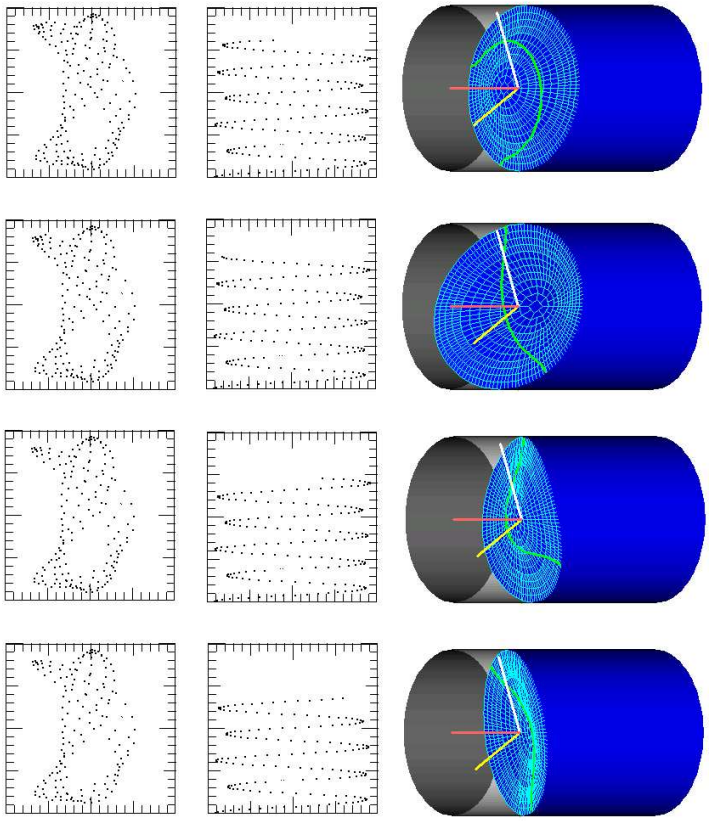

Fig. 3.19 (continued):

for the dominating amplitudes A and B in (3.101). The condition $\bar{A} = \bar{B} = 0$ appears as the resolvability condition (see, Lukovsky (1990) [114] and Faltinsen *et al.* (2003) [46]). Here, P_1^* is the non-dimensional amplitude, which is for brevity assumed to be positive.

In addition, we impose

$$|m_1| \sim |m_2| \sim |m_1 + m_2| \sim |m_1 - m_2| \sim 1, \tag{3.114}$$

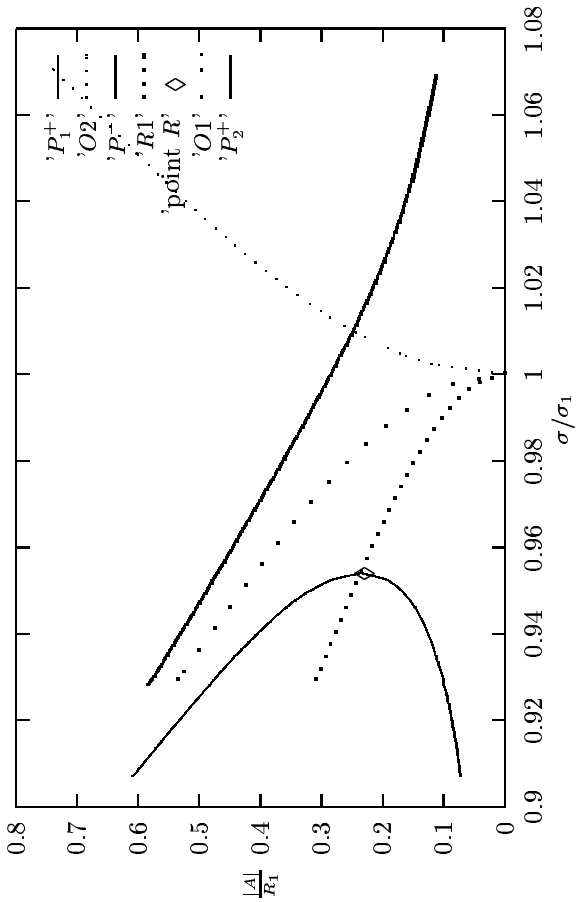

Fig. 3.20. Response curves for 'planar' waves ($B = 0$). Sway excitations with $h/R_1 = 2$, $H/R_1 = 0.01$.

which holds true for the finite fluid depths and focus only on the case

$$m_1 > 0, m_2 < 0, m_4 = m_1 + m_2 < 0, m_5 = \frac{m_1}{m_1 - m_2} > 0 \qquad (3.115)$$

(the inequalities were numerically verified for $h/R_1 \geq 1$). After denoting

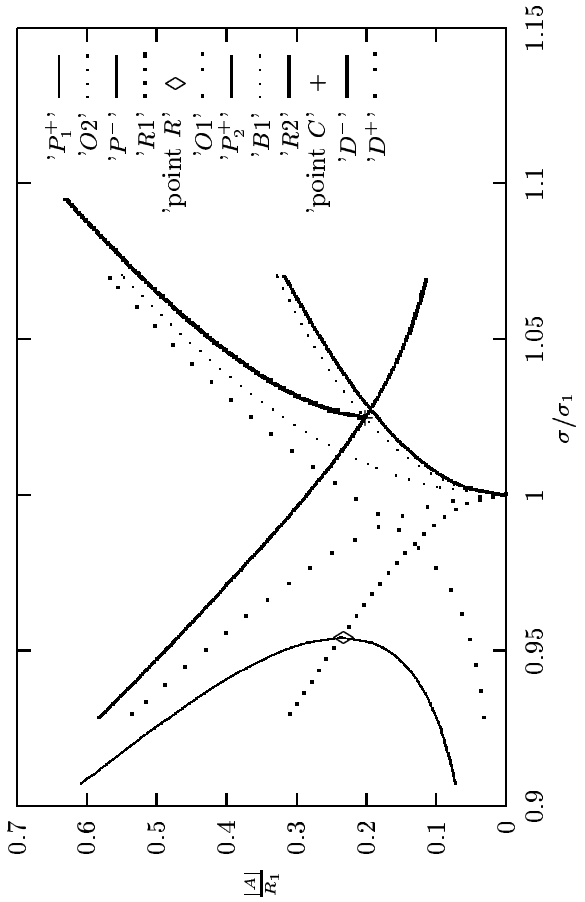

Fig. 3.21. Response curves in the $(\sigma/\sigma_1, |A|/R_1)$-plane for sway excitations. The branches P_1^+, P_1^-, P^- show 'planar' waves, the branches D^+, D^- imply 'swirling'. $h/R_1 = 2, H/R_1 = 0.01$.

$$\Gamma = \bar{\sigma}_1^2 - 1 = \begin{cases} > 0 \; \bar{\sigma}_1^2 > 1 \text{ or } \sigma > \sigma_1, \\ < 0 \; \bar{\sigma}_1^2 < 1 \text{ or } \sigma < \sigma_1, \end{cases}$$

we also introduce the following norm

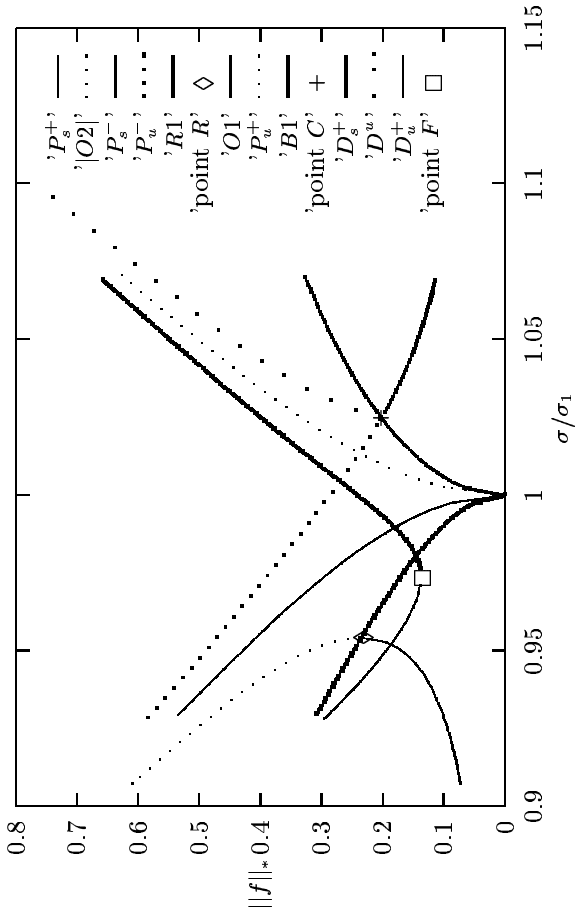

Fig. 3.22. As in Fig. 3.21, but in the $(\sigma/\sigma_1, ||f||)$-plane, where $||f|| = \sqrt{A^2 + B^2}$. $h/R = 2, H/R_1 = 0.01$.

$$||f||_* = \sqrt{A^2 + B^2}/R_1. \tag{3.116}$$

'Planar' waves. When $B = 0$ the system (3.113) is reduced to the algebraic equation

$$A(\Gamma - m_1 A^2) = P_1^*. \tag{3.117}$$

This equation defines A versus $\bar{\sigma}_1 = \sigma_1/\sigma$, or, physically, the maximum wave elevation versus the excitation frequency (correctly to $O(A)$). The branches $P^{\pm}$ yielded by positive and negative roots of (3.117) express the response curves shown in Fig. 3.20. In order to draw these branches we considered the following cases:

- $\Gamma > 0$: Eq. (3.117) can have a single (negative) root, two (one negative and one positive) or three (one negative and two positive) roots. Let Γ_* be a critical value, for which Eq. (3.117) has the two roots. It should belong to

$$\text{branch } R1: \ (A(\Gamma - m_1 A^2) - P_1^*)'_A = \Gamma_* - 3m_1 A^2 = 0. \quad (3.118)$$

  The turning point R can be found from the system (3.117) + (3.118) as dividing P^+ into the two sub-branches P_1^+ and P_2^+. The branch $R1$ collects all the turning points for various P_1^*.
- $\Gamma < 0$: Eq. (3.117) has the single negative root, which belongs to P^-. The branch P^- decreases monotonically with increasing σ/σ_1 and does not intersect P^+.

'Swirling'. If $B \neq 0$, the system (3.113) can be re-written in the following form

$$A(\Gamma - m_4 A^2) = m_5 P_1^*, \quad m_5 = \frac{m_1}{m_1 - m_2}, \ m_4 = m_1 + m_2, \quad (3.119)$$

$$0 \leq B^2 = -\frac{1}{m_1}(m_2 A^2 - \Gamma). \quad (3.120)$$

We demonstrate solutions of (3.119) + (3.120) in the branches D^+ (positive roots) and D^- (negative roots). Here, Eq. (3.119) determines A and Eq. (3.120) defines B^2 through A^2. Because $m_1 > 0$ and $m_2 < 0$, as it is seen from Eq. (3.115), the necessary conditions $B^2 \geq 0$ is fulfilled for $\Gamma > 0$. When $\Gamma < 0$, we should consider

$$\text{branch } B1: \ \Gamma - m_2 A^2 = 0, \quad \Gamma < 0. \quad (3.121)$$

The system (3.119) + (3.120) has no any real solutions as $\Gamma - m_2 A^2 < 0$. This means that there are no real sub-branches of D^+ and D^- under $B1$ in the response plane. We analyse (3.119) for the following cases:

- $\Gamma < 0$: Eq. (3.119) has the single positive root and can have one (turning point) or two negative roots. The set of the turning point (for arbitrary P_1^*) may be presented by

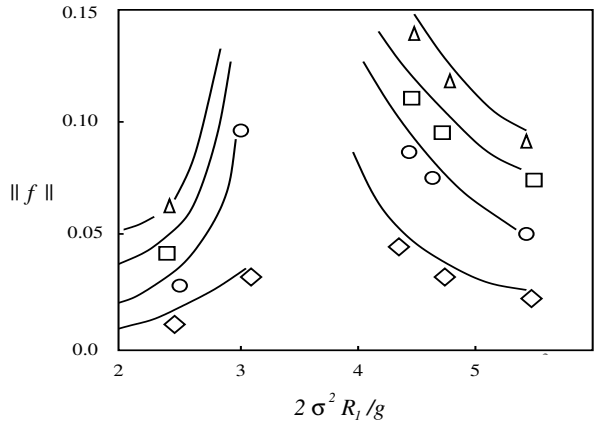

Fig. 3.23. Comparison between theory and experiments by Abramson *et al.* (1966) [3]. 'Planar' steady-state sloshing, $h/R_1 = 2$. Calculated and measured values are present for H/R_1: $\Delta - H/R_1 = 0.0454$; $\square - H/R_1 = 0.0344$; $\bigcirc - H/R_1 = 0.023$; $\Diamond - H/R_1 = 0.0112$.

$$\text{branch } R2: \ (\Gamma A - m_4 A^3 - m_5 P_1^*)' \equiv \Gamma - 3m_4 A^2 = 0. \quad (3.122)$$

Numerical study shows that the branch $R2$ is always situated under the branch $B1$. This means that both D^- and D^+ have no joint points with $R2$ and, therefore, there are no turning points. However, D^- shaves the generic point C with $B1$.

- $\Gamma > 0$: Eq. (3.119) has a single positive solution. The necessary condition $B^2 > 0$ is then satisfied. The branch D^+ (for arbitrary Γ) is shown in Fig. 3.21.

Because $A \not\equiv B$ for the resonantly excited waves, we present in Fig. 3.22 the amplitude response curves, where the norm of periodic solutions is approximated by Eq. (3.116). Another expression for this amplitude norm is

$$||f||_* = \sqrt{\frac{1}{m_4}(2\Gamma - \frac{P_1^*}{A})}/R_1. \quad (3.123)$$

In Fig. 3.22, F and P are the turning points. In accordance with the analysis done by Lukovsky (1990) [114] and Miles (1984) [126, 127], the sub-branches P_s^-, P_s^+ and D_s^+ imply stable steady-state motions.

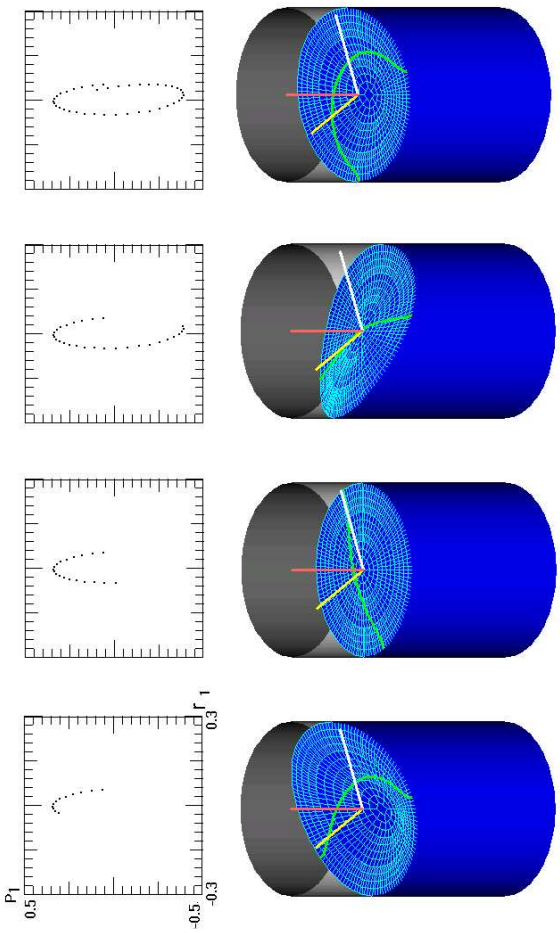

Fig. 3.24. Breakdown of 'rotating' wave. $h/R_1 = 2, H/R_1 = 0.01$.

Validation by experiments. Abramson *et al.* (1966) [3] conducted a series of experimental measurements of the steady-state wave amplitude response due sway excitation. In their experiments, $h = 2m; R_1 = 1m$. The experiments were done for several amplitudes of excitation. Abramson *et al.* (1966) [3] presented the measured data as the half-sum of two

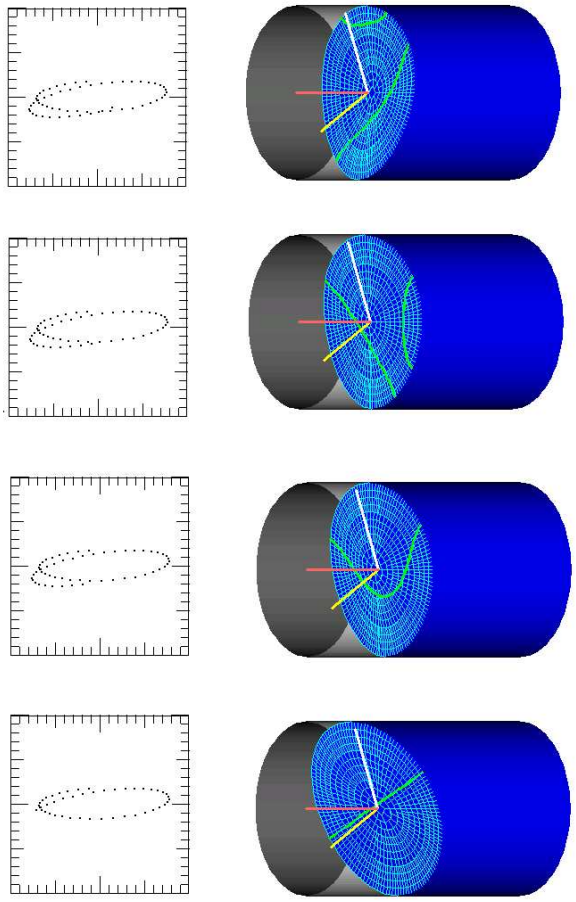

Fig. 3.24 (continued):

diametrically opposite wave elevations near the wall in the plane of excitation Oxz. In our modal treatment, this implies

$$||f|| = \frac{1}{2}(|p_0(t) + r_1(t) - p_2(t)| + |p_0(t) - r_1(t) - p_2(t)|)/R_1.$$

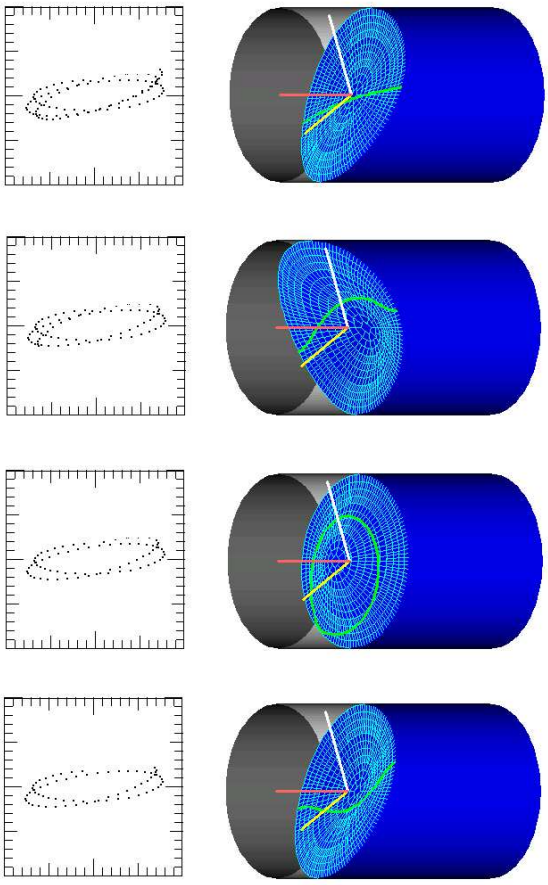

Fig. 3.24 (continued):

We use these experiments to validate our modal approximation. Fig. 3.23 confirms good agreement.

Simulations. Our potential model neglects the viscosity. The damping, however, may be important on the long-time scale, because it causes the free surface oscillations to decay. This means that for a sufficiently

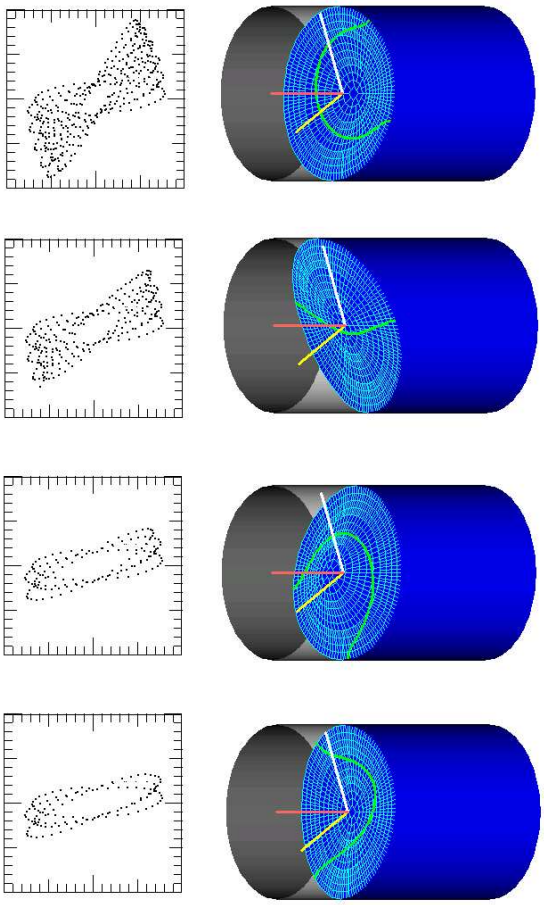

Fig. 3.24 (continued):

long time period the actual surface wave may be close to a stable steady-state wave. When analysing the fluid response in Fig. 3.22, we find a frequency domain, in which no stable steady-state waves occur. This frequency domain is bounded by abscissas of the points P and F. In this domain, beating and chaotic waves never die out. Funakoshi

& Inoue (1991) [60] used the two-dimensional modal system by Miles (1984) [126, 127] to study resonant sloshing in this domain. Influence of second-order modes onto the corresponding wave patterns was nevertheless ignored. Our modal system accounts for that. We conducted a visualisation of sloshing phenomena associated with breakdown of 'planar' waves and 'swirling'. One was established that effect of the second-order modes cannot be neglected because of exotic wave patterns and amazing nodal curves shapes. The simulations demonstrate the breakdown of 'swirling'. It is in good agreement with experimental observations. Since F implies the Hamiltonian Hopf-bifurcation point (henceforth, Hopf-bifurcation), the steady-state 'swirling' corresponding to F can be found from our modal system. At $h/R_1 = 2, H/R_1 = 0.01$, this implies the excitation frequency $\sigma = 4.1332231$ and non-zero initial conditions $r_1(0) = 0.091064535$; $p_1'(0) = 1.3292305$; $r_2'(0) = 0.057897668$. When changing σ to 4.1, we drift the excitation frequency into the mentioned frequency domain between P and F. The result of numerical simulations is present in Fig. 3.24. Here, the parametric graph $(r_1(t), p_1(t))$ shows the longitudinal r_1 and transversal p_1 components, respectively. The camera view shows the grid animated surface shapes.

Initially, the surface waves are physically close to 'swirling', in which the transversal component exceeds the longitudinal component ($B > A$ in context of the introduced approximation). Physically, this means that the fluid mass centre oscillates mainly in the Oyz-plane, i.e. perpendicular to the forcing plane Oxz. Such wave motions cannot be stable and, we believe, this causes the break down. Further simulations confirm that. The transients are shown by the (r_1, p_1)-trajectories. During two periods, the (r_1, p_1)-trajectories have nearly elliptical shapes with a vertical focal axis. Latter on, this axis rotates counterclockwise (see, the graph in the last column of Fig. 3.24). Because the one semi-axis of the ellipse becomes smaller with rotation, the (r_1, p_1)-trajectories in Fig. 3.24 imply waves that are similar to slowly azimuthally-rotated 'planar' waves. A considerable contribution of the three second-order modes to instantaneous waves patterns is confirmed by the grid visualisation, e.g. nodal curves have no a fixed shape and substantially fluctuate. Dynamics of the nodal curves gives also a good treatment of the breakdown: 'swirling' breaks down because a travelling wave emerges. This is demonstrated in the columns 6 and 7 of Fig. 3.24.

Concluding remarks

Asymptotic modal systems may provide time efficient and robust numerical simulations of the tree-dimensional sloshing in mobile tanks. These may combine numerical and analytical methods to approximate the free surface motions and calculate hydrodynamic loads onto the tank. Advantages of the modal modelling are demonstrated in this section for a circular cylindrical tank by using the modal system derived by Lukovsky (1990) [114]. The system couples both the two primary and three second-order modes. Influence of the three second-order modes on wave patterns was investigated for the two test situations: the free oscillations and the resonant sloshing due to sway (horizontal) sinusoidal resonant excitation of the lowest natural frequency. By accounting for the multimodal character of both the steady-state and transient nonlinear waves, various nonlinear phenomena were for the first time described and visualised. Examples are the travelling wave and the hydrodynamic instability implying a passage from 'swirling' to chaotic motions. Simulations by means of the modal system may highlight limitations when the maximum free surface elevation is in the order to the tank radius or the mean fluid depth.

3.4 Sloshing in a conical tank

As it was stressed in § 3.1.3, sloshing in a conical tank will furthermore be considered under assumption that Ox is the vertical axis. Lukovsky (1975) [112] combined the non-conformal mapping technique in manner of § 3.1.3 with Narimanov's asymptotic algorithm and derived, probably at first in the literature, a Duffing-like equation describing the weakly nonlinear behaviour of a single natural mode mode in conical and spherical tanks. Effect of higher, first of all, second-order modes has been neglected. Later on, Lukovsky (1990) [114] generalised the derivations to get a two-dimensional modal system, which couples the pair of primary (longitudinal and transversal) natural modes having the same natural frequency. Once again, the higher modes were not included into analysis. Previous section of this book showed that even in the cases of rectangular and circular cylindrical tanks, accounting for the second-order modes may substantially improve quantitative prediction of steady-state and transient waves. This motivated Lukovsky & Timokha (2000) [120] and Gavrilyuk *et al.* (2005) [67] to generalise earlier Lukovsky's results. These new results are extensively described in the present section.

3.4.1 Natural frequencies and modes

Numerical solutions of the spectral problem (3.34) in a conical domain Q_0 can be found by diverse methods based on spatial discretisation (see, Solaas (1995) [157], Solaas & Faltinsen (1997) [158]). However, because these discrete solutions $\{\varphi_n\}$ are not expandable over the mean free surface Σ_0, their usage in (3.48) is generally impossible. To the authors knowledge, the current scientific literature contains only two numerical approaches to (3.34) which give satisfactory approximations of eigenfunctions $\{\varphi_n\}$ to be used as a basis in the variational scheme of § 3.1.3. The first approach is based on the Treftz method with the harmonic polynomials as a functional basis. Results by Feschenko *et al.* (1969) [53] showed applicability of this approach for computing both eigenvalues and eigenfunctions. The approximate eigenfunctions are harmonic in space and, therefore, expandable over Σ_0. However, because the approximate $\{\varphi_n\}$ do not satisfy zero-Neumann condition on conical walls over Σ_0, inserting them into (3.48) can lead to a numerical error for certain evolutions of $Q(t)$. Physically, the error may be treated as inlet/outlet through the rigid walls over Σ_0.

Another appropriate analytically-oriented approach to (3.34) in a conical domain was reported by Dokuchaev (1964) [41], Bauer (1982) [18] Lukovsky & Bilyk (1985) [116] and Bauer & Eidel (1988) [19]. It consists of replacing the planar surface Σ_0 by an artificial spheric segment. In that case, the problem (3.34) has analytical solutions which coincide with the solid spheric harmonics. Bauer (1982) [18] has shown that an error caused by the replacement is small for relatively small α, his numerical examples agreed well with model tests for $\alpha < \pi/12(rad) = 15^0$.

Combining these two approaches, we will adopt the solid spheric harmonics appearing in the papers by Bauer (1982) [18] and Dokuchaev (1964) [41] as a functional basis in the variational method by Feschenko *et al.* (1969) [53] (instead of the harmonic polynomials). The method will be elaborated in the (x_1, x_2, x_3)-coordinates appeared in section 3.1.3, so that the linear natural modes (eigenfunctions) can be substituted into (3.46), (3.48) and (3.49).

In accordance with definitions in Fig. 3.25, we superpose the origin O with the apex of an inverted cone and direct the Ox-axis up-wards. In that case, the cone is determined by the equation $x = \cot\alpha\sqrt{y^2 + z^2}$ and the mean free surface $\Sigma_0(x = h)$ is a circle of radius $r_0 = h\tan\alpha$, where h is the fluid depth. By substituting $x := x/r_0, y := y/r_0, z := z/r_0$, we

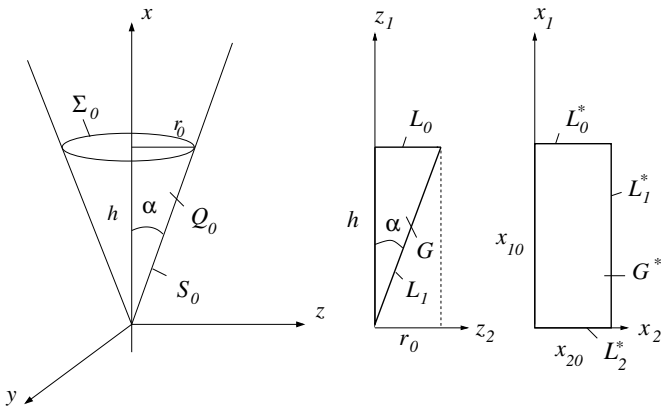

Fig. 3.25. Sketch of a conical tank, its meridional cross-section G and the transformed domain G^*. $x_{10} = h$, $x_{20} = \tan\alpha$.

get a non-dimensional formulation of the spectral problem (3.34). Finally, the resulting transformation (3.39) + (3.42) is proposed,

$$x = x_1; \quad y = x_1 x_2 \cos x_3; \quad z = x_1 x_2 \sin x_3, \tag{3.124a}$$

$$x_1 = \frac{x}{r_0}; \quad x_2 = \sqrt{\frac{y^2+z^2}{x^2}}; \quad x_3 = \arctan\frac{z}{y}, \tag{3.124b}$$

so that (3.43) takes the following form

$$x_1^2 x_2 \frac{\partial^2\psi_m}{\partial x_1^2} - 2x_1 x_2^2 \frac{\partial^2\psi_m}{\partial x_1 \partial x_2} + x_2(1+x_2^2)\frac{\partial^2\psi_m}{\partial x_2^2} + \\ + (1+2x_2^2)\frac{\partial\psi_m}{\partial x_2} - \frac{m^2}{x_2}\psi_m = 0 \ \text{ in } \ G^*, \tag{3.125a}$$

$$x_1^2 x_2 \frac{\partial\psi_m}{\partial x_1} - x_1 x_2^2 \frac{\partial\psi_m}{\partial x_2} = \varkappa_m x_1^2 x_2 \psi_m \ \text{ on } \ L_0^*, \tag{3.125b}$$

$$x_2(x_2^2+1)\frac{\partial\psi_m}{\partial x_2} - x_1 x_2^2 \frac{\partial\psi_m}{\partial x_1} = 0 \ \text{ on } \ L_1^*, \quad m = 0,1,2,\ldots, \tag{3.125c}$$

$$\int_0^{x_{20}} \psi_0 x_2 dx_2 = 0 \ \text{ as } \ m = 0, \tag{3.125d}$$

where $G^* = \{(x_1, x_2) : 0 \le x_1 \le x_{01}, 0 \le x_2 \le x_{20}\}$, $x_{20} = \tan\alpha, x_{10} = h/r_0 = 1/x_{20}$ and

$$a = -\frac{x_2}{x_1}; \quad b = \frac{1}{x_1}; \quad p = x_1^2 x_2; \quad q = -x_1 x_2^2; \quad s = x_2(x_2^2+1); \; c = \frac{1}{x_2}.$$

Each nth eigenvalue of (3.125), $\varkappa_{mn}$, computes the natural circular frequency

$$\sigma_{mn} = \sqrt{\frac{g\varkappa_{mn}}{r_0}} = \sqrt{\frac{g\varkappa_{mn}}{h\tan\alpha}}. \tag{3.126}$$

The surface sloshing modes are defined by ψ_m as follows

$$x_1 = F_{mn}(x_2, x_3) = \varphi_{mn}(x_{10}, x_2, x_3); \quad 0 \le x_2 \le x_{20}, \quad 0 \le x_3 \le 2\pi, \tag{3.127}$$

where

$$\varphi_{mn}(x_1, x_2, x_3) = \psi_{mn}(x_1, x_2)\begin{matrix}\cos\\ \sin\end{matrix} mx_3 \tag{3.128}$$

is the nth eigenfunction of (3.125) corresponding to $\varkappa_{mn}$.

Separation of spatial variables. As proved by Eisenhart (1934) [42], the Laplace equation allows for separation of spatial variables only in 17 inequivalent coordinate systems. The $Ox_1x_2x_3$-coordinate system defined by (3.124a) belongs to the admissible set. The separability of (3.125a) and (3.125c) leads to the following particular solutions $\psi_m[\nu](x_1, x_2) = w_\nu^{(m)}(x_1, x_2) = \left(\frac{x_1}{x_{10}}\right)^\nu v_\nu^{(m)}(x_2)$, where

$$x_2(1+x_2^2)v_\nu^{(m)\prime\prime} + (1+2x_2^2-2\nu x_2^2)v_\nu^{(m)\prime} + [\nu(\nu-1)x_2 - \frac{m^2}{x_2}]v_\nu^{(m)} = 0,$$
$$|v_\nu^{(m)}(0)| < \infty, \tag{3.129a}$$

$$v_\nu^{(m)\prime}(x_{20}) = \nu\frac{x_{20}}{1+x_{20}^2}v_\nu^{(m)}(x_{20}), \quad m = 0, 1, \ldots, \; \nu \ge m. \tag{3.129b}$$

Eqs. (3.129a) + (3.129b) constitute the ν-parametric boundary value problem, which has non-trivial solutions only for certain values of ν. If we input a test ν in the differential equation (3.129a) and output $v_\nu^{(m)\prime}(x_{20})$ and $v_\nu^{(m)}(x_{20})$, the boundary condition (3.129b) plays the role of a transcendental equation with respect to ν. This transcendental equation can be solved by means of an iterative algorithm.

In order to get an approximate $\psi_{mn}(x_1, x_2)$, we should fix m and calculate q lower roots $\{\nu_{m1} < \nu_{m2} < \ldots \nu_{mq}\}$ of this transcendental

Table 3.2. Roots ν_{mn} versus α.

α^0	ν_{11}	ν_{12}	ν_{13}	ν_{14}	ν_{15}	ν_{21}	ν_{22}	ν_{23}	ν_{24}	ν_{25}	ν_{01}	ν_{02}	ν_{03}	ν_{04}	ν_{05}
1	104.99	304.97	488.60	670.205	851.121	174.50	383.74	570.710	754.108	936.145	219.04	401.46	582.397	762.892	943.198
3	34.674	101.33	162.53	223.060	283.375	57.847	127.58	189.907	251.039	311.717	72.682	133.49	193.700	253.964	314.066
5	20.616	60.599	97.322	133.643	169.826	34.525	76.357	113.749	150.427	186.833	43.411	79.894	116.080	152.179	188.240
7	14.594	43.145	69.375	95.3180	121.163	24.536	54.405	81.1110	107.308	133.312	30.867	56.926	82.7725	108.557	134.315
9	11.252	33.450	53.849	74.0267	94.1276	18.991	42.212	62.9802	83.3547	103.579	23.899	44.165	64.2682	84.3227	104.357
11	9.1279	27.281	43.970	60.4780	76.9239	15.466	34.454	51.4435	68.1122	84.6588	19.465	36.046	52.4930	68.9010	85.2922
13	7.6593	23.010	37.131	51.0984	65.0138	13.029	29.084	43.4573	57.5604	71.5606	16.395	30.424	44.3410	58.2245	72.0939
15	6.5842	19.879	32.115	44.2202	56.2799	11.245	25.147	37.6016	49.8230	61.9557	14.145	26.302	38.3630	50.3952	62.4152
17	5.7637	17.485	28.281	38.9607	49.6012	9.8833	22.138	33.1244	43.9067	54.6112	12.424	23.150	33.7917	44.4082	55.0139
19	5.1174	15.596	25.253	34.8086	44.3287	8.8104	19.763	29.5904	39.2363	48.8133	11.066	20.662	30.1829	39.6816	49.1708
21	4.5955	14.078	22.803	31.4476	40.0607	7.9440	17.841	26.7300	35.4560	44.1201	9.9664	18.648	27.2615	35.8554	44.4408
23	4.1656	12.804	20.779	28.6712	36.5350	7.2301	16.255	24.3677	32.3335	40.2434	9.0585	16.984	24.8483	32.6947	40.5334
25	3.8056	11.743	19.079	26.3392	33.5735	6.6322	14.923	22.3837	29.7110	36.9872	8.2960	15.586	22.8213	30.0398	37.2513
27	3.4999	10.840	17.631	24.3529	31.0509	6.1246	13.789	20.6942	27.4773	34.2138	7.6467	14.396	21.0946	27.7782	34.4554
29	3.2374	10.062	16.383	22.6406	28.8764	5.6885	12.812	19.2381	25.5520	31.8231	7.0871	13.370	19.6062	25.8287	32.0452
31	3.0096	9.3846	15.296	21.1494	26.9825	5.3102	11.961	17.9703	23.8755	29.7411	6.5999	12.476	18.3099	24.1307	29.9460
33	2.8104	8.7895	14.341	19.8391	25.3183	4.9791	11.214	16.8565	22.4025	27.9118	6.1719	11.691	17.1708	22.6386	28.1014
35	2.6347	8.2626	13.496	18.6787	23.8444	4.6872	10.554	15.8704	21.0980	26.2917	5.7930	10.996	16.1619	21.3171	26.4675
37	2.4787	7.7930	12.742	17.6438	22.5299	4.4282	9.9647	14.9913	19.9349	24.8470	5.4552	10.376	15.2621	20.1384	25.0104
39	2.3395	7.3717	12.065	16.7151	21.3503	4.1970	9.4368	14.2027	18.8913	23.5507	5.1521	9.8193	14.4547	19.0807	23.7027
41	2.2146	6.9918	11.455	15.8772	20.2858	3.9895	8.9609	13.4913	17.9498	22.3810	4.8788	9.3172	13.7261	18.1263	22.5226
43	2.1020	6.6474	10.901	15.1173	19.3205	3.8025	8.5297	12.8464	17.0961	21.3203	4.6310	8.8619	13.0653	17.2606	21.4524
45	2.0000	6.3339	10.397	14.4251	18.4410	3.6332	8.1373	12.2592	16.3186	20.3541	4.4053	8.4471	12.4633	16.4719	20.4773
47	1.9073	6.0472	9.9359	13.7918	17.6365	3.4795	7.7788	11.7222	15.6074	19.4704	4.1990	8.0677	11.9126	15.7504	19.5852
49	1.8229	5.7842	9.5125	13.2104	16.8977	3.3394	7.4500	11.2294	14.9545	18.6589	4.0097	7.7194	11.4069	15.0879	18.7660
51	1.7456	5.5420	9.1225	12.6746	16.2170	3.2114	7.1474	10.7756	14.3531	17.9113	3.8353	7.3984	10.9409	14.4773	18.0110
53	1.6747	5.3183	8.7620	12.1794	15.5876	3.0940	6.8681	10.3562	13.7972	17.2203	3.6742	7.1017	10.5101	13.9128	17.3131

Table 3.3. Lowest eigenvalues $\varkappa_{mn}$ versus q in (3.130).

$\alpha = \pi/20(rad) = 9^0, x_{10} = 6.31375151$							
q	$\varkappa_{11}$	$\varkappa_{21}$	$\varkappa_{01}$	$\varkappa_{31}$	$\varkappa_{41}$	$\varkappa_{12}$	$\varkappa_{51}$
2	1.69161543	2.84573497	3.74094126	3.94077378	5.00952743	5.25067415	6.06300500
3	1.69160732	2.84570219	3.74076336	3.94070620	5.00941953	5.24048147	6.06285390
4	1.69160621	2.84569706	3.74073562	3.94069466	5.00939994	5.24003415	6.06282517
5	1.69160595	2.84569576	3.74072859	3.94069154	5.00939438	5.23995717	6.06281672
6	1.69160589	2.84569533	3.74072625	3.94069046	5.00939237	5.23993624	6.06281356
$\alpha = \pi/18(rad) = 10^0, x_{10} = 5.67128182$							
q	$\varkappa_{11}$	$\varkappa_{21}$	$\varkappa_{01}$	$\varkappa_{31}$	$\varkappa_{41}$	$\varkappa_{12}$	$\varkappa_{51}$
2	1.67435468	2.82105616	3.72911626	3.90948949	4.97211760	5.24157514	6.01980161
3	1.67434599	2.82102046	3.72891966	3.90941564	4.97199965	5.22929910	6.01963662
4	1.67434484	2.82101505	3.72888985	3.90940338	4.97197880	5.22880337	6.01960605
5	1.67434459	2.82101372	3.72888247	3.90940015	4.97197301	5.22871995	6.01959722
6	1.67434451	2.82101328	3.72888006	3.90939904	4.97197094	5.22869768	6.01959396
$\alpha = \pi/12(rad) = 15^0, x_{10} = 3.73205081$							
q	$\varkappa_{11}$	$\varkappa_{21}$	$\varkappa_{01}$	$\varkappa_{31}$	$\varkappa_{41}$	$\varkappa_{12}$	$\varkappa_{51}$
2	1.58619607	2.69306046	3.66367923	3.74577897	4.77506958	5.19312284	5.79104137
3	1.58618696	2.69301939	3.66343768	3.74569200	4.77493018	5.16902518	5.79084720
4	1.58618598	2.69301414	3.66340610	3.74567963	4.77490880	5.16841246	5.79081567
5	1.58618578	2.69301301	3.66339915	3.74567673	4.77490348	5.16831969	5.79080746
6	1.58618573	2.69301267	3.66339710	3.74567583	4.77490175	5.16829723	5.79080469
$\alpha = 17\pi/180(rad) = 17^0, x_{10} = 3.27085262$							
q	$\varkappa_{11}$	$\varkappa_{21}$	$\varkappa_{01}$	$\varkappa_{31}$	$\varkappa_{41}$	$\varkappa_{12}$	$\varkappa_{51}$
2	1.55008753	2.63970945	3.63425999	3.67685337	4.69150407	5.17167976	5.69346536
3	1.55007920	2.63967004	3.63402305	3.67676884	4.69136817	5.14256261	5.69327620
4	1.55007837	2.63966537	3.63399393	3.67675761	4.69134857	5.14196335	5.69324717
5	1.55007822	2.63966442	3.63398785	3.67675511	4.69134392	5.14187598	5.69323994
6	1.55007819	2.63966415	3.63398613	3.67675437	4.69134247	5.14185572	5.69323759
$\alpha = \pi/6(rad) = 30^0, x_{10} = 1.73205081$							
q	$\varkappa_{11}$	$\varkappa_{21}$	$\varkappa_{31}$	$\varkappa_{01}$	$\varkappa_{41}$	$\varkappa_{12}$	$\varkappa_{51}$
2	1.30439611	2.26316175	3.18028027	3.38567547	4.08059072	4.97694361	4.97189506
3	1.30439483	2.26315048	3.18025142	3.38560609	4.08054108	4.92289813	4.97182421
4	1.30439477	2.26314977	3.18024922	3.38560054	4.08053671	4.92276719	4.97181725
5	1.30439476	2.26314968	3.18024890	3.38559979	4.08053602	4.92274743	4.97181607
6	1.30439476	2.26314966	3.18024884	3.38559965	4.08053587	4.92274426	4.97181580
$\alpha = \pi/4(rad) = 45^0, x_{10} = 1$							
q	$\varkappa_{11}$	$\varkappa_{21}$	$\varkappa_{31}$	$\varkappa_{01}$	$\varkappa_{41}$	$\varkappa_{51}$	$\varkappa_{12}$
2	1.0	1.76737703	2.50492882	2.92657505	3.23112279	3.95154112	4.52585644
3	1.0	1.76737699	2.50492828	2.92657446	3.23112114	3.95153797	4.48306268
4	1.0	1.76737699	2.50492827	2.92657445	3.23112108	3.95153783	4.48301859
5	1.0	1.76737699	2.50492827	2.92657445	3.23112108	3.95153782	4.48301858
6	1.0	1.76737699	2.50492827	2.92657445	3.23112108	3.95153782	4.48301858
$\alpha = \pi/3(rad) = 60^0, x_{10} = 0.577350269$							
q	$\varkappa_{11}$	$\varkappa_{21}$	$\varkappa_{31}$	$\varkappa_{01}$	$\varkappa_{41}$	$\varkappa_{51}$	$\varkappa_{12}$
2	0.67768281	1.21443214	1.73205081	2.20645863	2.24265397	2.74980966	3.25499111
3	0.67767985	1.21443185	1.73205081	2.20645754	2.24265392	2.74980956	3.25499099
4	0.67767981	1.21443185	1.73205081	2.20645754	2.24265392	2.74980956	3.25499099
5	0.67767981	1.21443185	1.73205081	2.20645754	2.24265392	2.74980956	3.25499099
6	0.67767981	1.21443185	1.73205081	2.20645754	2.24265392	2.74980956	3.25499099

equation. The nth $(1 \le n \le q)$ approximate solution of (3.125), which corresponds to $\varkappa_{mn}$, can then be posed as

$$\psi_{mn}(x_1, x_2) = \sum_{k=0}^{q} \bar{a}_{nk}^{(m)} \left(\frac{x_1}{x_{10}}\right)^{\nu_{mk}} v_{\nu_{mk}}^{(m)}(x_2), \tag{3.130}$$

where coefficients $\bar{a}_{nk}^{(m)}$ have to satisfy the supplementary conditions

$$\bar{a}_{n0}^{(m)} = \begin{cases} 0, & m \neq 0, \\ -\sum_{k=1}^{q} \bar{a}_{nk}^{(m)} c_{\nu_{0k}}, & m = 0, \end{cases} \quad c_{\nu_{0k}} = \frac{2}{x_{20}^2} \int_0^{x_{20}} w_{\nu_{0k}}^{(0)}(x_{10}, x_2) x_2 dx_2$$

$(\nu_{m0} = 0,\ v_{\nu_{m0}}^{(m)} = 1)$ to agree with (3.125d).

One should note, that comparing $v_\nu^{(0)}$ with the Legendre function P_ν^0 deduces

$$v_\nu^{(0)}(x_2) = \left(\sqrt{1 + x_2^2}\right)^{\nu} P_\nu^0(1/\sqrt{1 + x_2^2}). \tag{3.131}$$

In view of this point,

$$P_\nu^0(1/\sqrt{1 + x_2^2}) = \sum_{p=1}^{\infty} \frac{(\nu - p + 1)(\nu - p + 1) \dots (\nu + p)}{(p!)^2} \left(\frac{1}{2\sqrt{1 + x_2^2}} - \frac{1}{2}\right)^p \tag{3.132}$$

(Bateman & Erdelyi (1953) [17]) and recurrence formulae for P_ν^m (Lukovsky *et al.* (1984) [115]) re-written in the (x_2, x_3)-coordinates as

$$\begin{aligned} &(\nu + m + 1) v_{\nu+1}^{(m)} = (2\nu + 1) v_\nu^{(m)} - (\nu - m)(1 + x_2^2) v_{\nu-1}^{(m)}, \\ &(\nu + m + 1) x_2 v_\nu^{(m+1)} = 2(m + 1)[(1 + x_2^2) v_{\nu-1}^{(m)} - v_\nu^{(m)}], \\ &\frac{dv_\nu^{(m)}}{dx_2} = \frac{1}{x_2}[\nu v_\nu^{(m)} - (\nu - m) v_{\nu-1}^{(m)}] \end{aligned} \tag{3.133}$$

facilitate computing $v_\nu^{(m)'}(x_2)$ and $v_\nu^{(m)}(x_2)$ for arbitrary x_2, m and $\nu \ge m$. We give some of roots for $m = 0, 1$ and 2 in Table 3.2.

The Treftz method based on (3.130). Representation (3.130) and the Rayleigh-Kelvin minimax principle for the spectral problems (3.125) make it possible to compute approximate eigenvalues $\varkappa_{mn}$. The numerical scheme implies

$$\frac{\partial J_m}{\partial \bar{a}_{ni}^{(m)}} = 0, \quad i = 1, 2, \dots, q; \quad m = 0, 1, 2, \dots, \tag{3.134a}$$

$$J_m = \int_{G^*} \left[p \left(\frac{\partial \psi_m}{\partial x_1} \right)^2 + 2q \frac{\partial \psi_m}{\partial x_1} \frac{\partial \psi_m}{\partial x_2} + s \left(\frac{\partial \psi_m}{\partial x_2} \right)^2 + \right.$$
$$\left. + \frac{m^2}{x_2} \psi_m^2 \right] dx_1 dx_2 - \varkappa \int_{L_0^*} p \psi_m^2 dx_2, \quad m = 0, 1, \ldots \quad (3.134b)$$

and, as a consequence, leads to the spectral matrix problem

$$\det |\{\alpha_{ij}^{(m)}\} - \varkappa \{b_{ij}^{(m)}\}| = 0, \quad i, j = 1, \ldots, q, \quad (3.135)$$

where the symmetric positive matrices $\{\alpha_{ij}^{(m)}\}$ and $\{b_{ij}^{(m)}\}$ are calculated by the following formulae

$$b_{ij}^{(m)} = x_{10}^2 \int_0^{x_{20}} x_2 w_{\nu_{mi}}^{(m)} w_{\nu_{mj}}^{(m)} dx_2, \quad i, j = 1, \ldots, q, \quad (3.136)$$

$$\alpha_{ij}^{(m)} = x_{10} \int_0^{x_{20}} x_2 \left\{ \left[x_{10} \frac{\partial w_{\nu_{mi}}^{(m)}}{\partial x_1} - x_2 \frac{\partial w_{\nu_{mi}}}{\partial x_2} \right] w_{\nu_{mj}}^{(m)} \right\}_{x_1 = x_{10}} dx_2,$$
$$i, j = 1, \ldots, q. \quad (3.137)$$

The spectral problem (3.135) gives not only approximate eigenvalues, but also eigenvectors expressed in terms of coefficients $\{\bar{a}_{nk}^{(m)}, \ k = 1, \ldots, q\}, \ n = 1, \ldots, q$. Being substituted into (3.130), these eigenvectors determine eigenfunctions $\psi_{mn}(x_1, x_2), \ n = 1, \ldots, q$.

Furthermore, positive eigenvalues $\{\varkappa_{mn}, \ n = 1, \ldots, q\}$ of (3.135) are posed in ascending order. Fixing m and evaluating some of the lower approximate $\varkappa_{mn}$ versus q (see, Table 3.3), one displays convergence of the Treftz method. Our numerical experiments with $\varkappa_{m1}, \ m \geq 0$ showed that 5-6 basis functions ($q = 5$ or 6) guarantee 5-6 significant figures, in general, and 10-12 significant figures for $\alpha \geq 45^0$, in particular. Weaker convergence for smaller α can be treated in terms of the mean fluid depth $x_{10} = h$ and geometric proportions of Q_0 versus α. If $\alpha \to 0$ then $x_{10} \to \infty$ and Q_0 becomes geometrically similar to a fairly long circular cylinder. The linear sloshing modes (eigenfunctions of (3.34)) in a circular cylindrical tank are characterised by exponential decaying from Σ_0 to the bottom (see, Lukovsky *et al.* (1984) [115]), but, in contrast, the functions (3.130) have power asymptotics.

Natural frequencies versus α. Fig. 3.26 shows that $\varkappa_{mn}$ and, therefore, σ_{mn}, which are defined by (3.126), decrease monotonically with increasing α. Besides, a general tendency consists of $\varkappa_{mn} \to 0$ as $\alpha \to 90^0$,

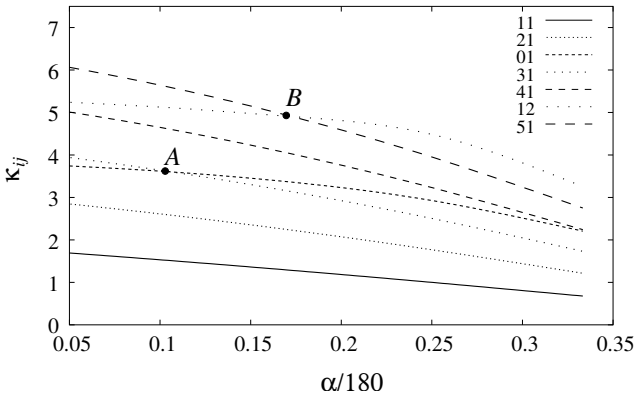

Fig. 3.26. Lowest eigenvalues $\varkappa_{ij}$ versus α(deg).

Table 3.4. Eigenvalues $\varkappa_{01}, \varkappa_{11}$ and $\varkappa_{21}$ versus α.

α^0	$\varkappa_{01}$	$\varkappa_{11}$	$\varkappa_{21}$	α^0	$\varkappa_{01}$	$\varkappa_{11}$	$\varkappa_{21}$
1	3.8228	1.8251	3.0323	29	3.4088	1.3239	2.2939
3	3.8042	1.7925	2.9874	31	3.3616	1.2848	2.2321
5	3.7844	1.7594	2.9414	33	3.3110	1.2452	2.1691
7	3.7633	1.7258	2.8941	35	3.2569	1.2052	2.1049
9	3.7407	1.6916	2.8457	37	3.1991	1.1649	2.0396
11	3.7166	1.6570	2.7960	39	3.1374	1.1242	1.9732
13	3.6909	1.6218	2.7451	41	3.0715	1.0831	1.9056
15	3.6634	1.5862	2.6930	43	3.0013	1.0417	1.8370
17	3.6340	1.5501	2.6397	45	2.9266	1.0000	1.7674
19	3.6025	1.5135	2.5851	47	2.8471	0.9580	1.6967
21	3.5689	1.4765	2.5293	49	2.7628	0.9156	1.6250
23	3.5328	1.4390	2.4723	51	2.6734	0.8730	1.5524
25	3.4943	1.4011	2.4140	53	2.5789	0.8300	1.4788
27	3.4530	1.3627	2.3546				

but each eigenvalue $\varkappa_{mn}$ has a proper decaying gradient. As a result, some of the natural frequencies may become equal at an isolated α. We demonstrate this fact by points A and B in Fig. 3.26. The point A corresponds to $\alpha \approx 19.2^0$, where $\sigma_{31} = \sigma_{01}$, and B occurs at $\alpha \approx 30^0$, where $\sigma_{12} = \sigma_{51}$.

In accordance with theorems by Feschenko *et al.* (1969) [53], the problem (3.34) has a denumerable set of real positive eigenvalues and each $\varkappa_{mn}$

continuously depends on smooth deformations of Q_0. Both appearance and 'split' of multiple eigenvalues are consistent with these theorems. Moreover, the matrices $\{\alpha_{ij}^{(m)}\}$ and $\{b_{ij}^{(m)}\}$ are symmetric and positive and, therefore, the crossings in Fig. 3.26 do not yield a numerical difficulty in solving (3.135) (see, Parlett (1998) [143]). On the other hand, Bauer *et al.* (1975) [20] and Bridges (1987) [31] showed that 'split' of a multiple eigenvalue into simple eigenvalues may lead to secondary bifurcations of nonlinear sloshing regimes.

Shapes of the natural surface modes. Fig. 3.27 shows surface modes defined by (3.127). Normalisation of these modes, which is usually accepted in nonlinear analysis (to interpret each generalised coordinate in (3.46a) as a generalised amplitude of F_{mn}), requires $\psi_{mn}(x_{10}, x_{20}) = 1$. It revises (3.130) to the form

$$\psi_{mn}(x_1, x_2) = \sum_{k=0}^{q} a_{nk}^{(m)} \left(\frac{x_1}{x_{10}}\right)^{\nu_{mk}} v_{\nu_{mk}}^{(m)}(x_2), \tag{3.138}$$

where

$$a_{nk}^{(m)} = \frac{\bar{a}_{nk}^{(m)}}{N_{mn}}; \quad N_{mn} = \psi_{mn}(x_{10}, x_{20}) = \sum_{k=0}^{q} \bar{a}_{nk}^{(m)} v_{\nu_{mk}}^{(m)}(x_{20}) \tag{3.139}$$

and $\{\bar{a}_{nk}^{(m)}\}$ are eigenvectors of (3.135).

Experimental validation. Bauer (1982) [18] has performed experimental measurements of the lowest natural frequency σ_{11} for $\alpha = \pi/6$(rad) $(= 30^0)$ and $\alpha = \pi/12$(rad) $(= 15^0)$ and distinct fluid fillings (depths h). In order to compare our results with his experimental data, we note that $\sigma_{11} = \sqrt{\varkappa_{11} x_{10}}\sqrt{\frac{g}{h}}$ and, therefore, $\sqrt{\varkappa_{11} x_{10}}$, which is an invariant for a fixed α, determines a proportionality coefficient between σ_{11} and $\sqrt{g/h}$. Fig. 3.28 (σ_{11} versus $\sqrt{g/h}$) shows good agreement between our theoretical prediction and experimental results by Bauer (1982) [18]. A statistical experimental estimate of $\sqrt{\varkappa_{11} x_{10}} = 1.63$ for $\alpha = 10^0$ was also published by Mikishev & Dorozhkin (1961) [123]. This value is consistent with our numerical prediction 1.67.

Numerical results in Fig. 3.26 show that the natural frequencies σ_{m1} are approximately in proportion to α (rad) and to $\sqrt{g/r_0}$, namely, $\sqrt{\varkappa_{m1} x_{10}}/\alpha$ is a constant. This deduces the following formula $\sigma_{m1} = C_m \alpha \sqrt{g/r_0}$ (our calculations give, for instance, $C_1 = 0.6158$). Engineering of conical tanks may also be based on the formula (3.126) and numerical results in Table 3.4.

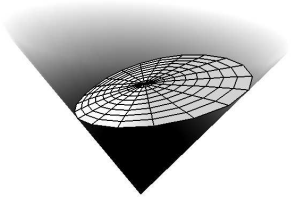

Standing wave with σ_{11}

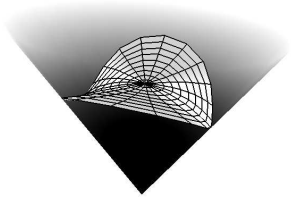

Standing wave with σ_{21}

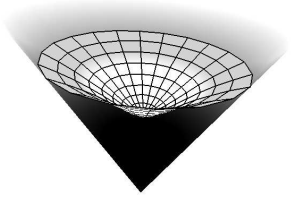

Standing wave with σ_{01}

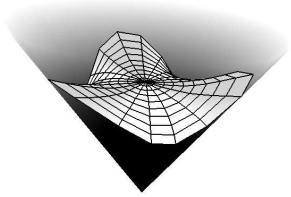

Standing wave with σ_{31}

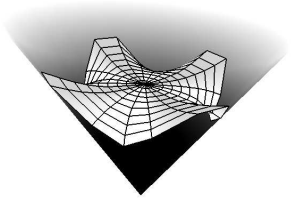

Standing wave with σ_{41}

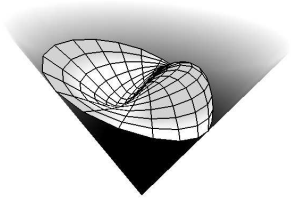

Standing wave with σ_{12}

Fig. 3.27. Natural surface modes for $\pi/4$(rad)=45^0. The asymmetric modes (indexes 11,21,31,41,12) have double multiplicity, their shapes differ from each other by azimuthal rotation of 90^0.

3.4.2 Asymptotic modal system

We normalise the original free boundary problem (3.1) and its modal analogy (3.47) by r_0. This implies

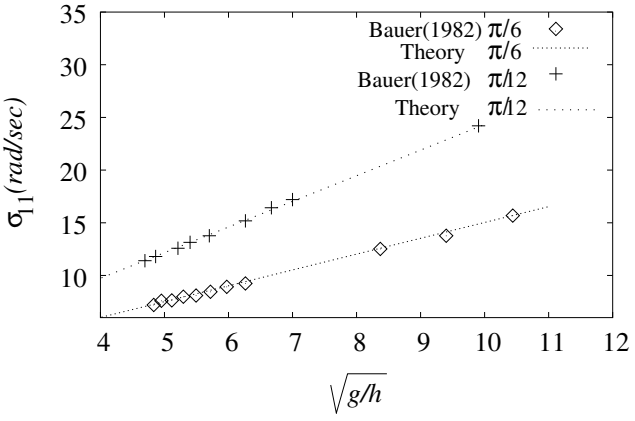

Fig. 3.28. The lowest natural frequency σ_{11} versus $\sqrt{\frac{g}{h}}$. Experimental measurements by Bauer (1982) [18] are compared with our theoretical prediction.

$$\boldsymbol{g} := \frac{\boldsymbol{g}}{r_0}; \quad \dot{\boldsymbol{v}}_0 := \frac{\dot{\boldsymbol{v}}_0}{r_0}; \quad \beta_i(t) := \frac{\beta_i(t)}{r_0}; \quad R_i(t) := \frac{R_i(t)}{r_0^2}, \quad i \geq 1. \quad (3.140)$$

Furthermore, we consider the horizontal harmonic excitations

$$g_1 = -g, \quad g_2 = g_3 = 0; \quad v_{01}(t) = v_{02}(t) \equiv 0, \quad v_{03} = -\epsilon\sigma \sin \sigma t, \quad (3.141)$$

where $\epsilon \ll 1$ is the non-dimensional forcing amplitude and $\sigma \to \sigma_{11}$.

The nonlinear modal system, which is presented in this section, is based on the Moiseyev asymptotics and, therefore, it fails for shallow fluid flows characterised by progressive amplification of higher modes (see, Ockendon & Ockendon (2001) [140] and Faltinsen & Timokha (2002) [51]). The Moiseyev asymptotics (Moiseev (1958) [129]) assumes that the lowest natural modes $F_{11}(x_2, x_3) = \psi_{11}(x_{10}, x_2)\begin{matrix}\sin\\ \cos\end{matrix} x_3$ are of the dominating character. By analysing this asymptotics for tanks of revolution, Lukovsky (1990) [114] proposed and justified the five-dimensional approximate solutions

$$f^*(x_2, x_3, t) = x_{10} + f(x_2, x_3, t) = x_{10} + \beta_0(t) + p_0(t) f_0(x_2) + [r_1(t) \sin x_3 + p_1(t) \cos x_3] f_1(x_2) + [r_2(t) \sin 2x_3 + p_2(t) \cos 2x_3] f_2(x_2), \quad (3.142)$$

$$\varphi(x_1, x_2, x_3) = P_0(t)\psi_{01}(x_1, x_2) + [R_1(t) \sin x_3 + P_1(t) \cos x_3]\psi_{11}(x_1, x_2) +$$

$$+ [R_2(t)\sin 2x_3 + P_2(t)\cos 2x_3]\psi_{21}(x_1, x_2), \quad (3.143)$$

where $f_i(x_2) = \psi_{i1}(x_{10}, x_2),\ i = 0, 1, 2$ (ψ_{i1} are normalised) and

$$r_1 \sim R_1 \sim p_1 \sim P_1 \sim \epsilon^{1/3}; \quad p_0 \sim P_0 \sim r_2 \sim R_2 \sim p_2 \sim P_2 \sim \epsilon^{2/3}. \quad (3.144)$$

When inserting (3.142) and (3.143) into the infinite-dimensional modal system (3.47) and accounting for (3.144), we can get (correctly to $O(\epsilon)$) a nonlinear modal system coupling p_1, r_1, p_0, r_2 and p_2.

Derivation. Solutions (3.142), (3.143) deal with $\{\tilde{f}_i(x_2, x_3)\}$, $\{\varphi_n(x_1, x_2, x_3)\}$ and modal functions $\beta_i(t), R_i(t),\ i \geq 1$ of (3.46) as follows

$$\varphi_1 = \psi_{01};\ \varphi_2 = \psi_{11}\sin x_3;\ \varphi_3 = \psi_{11}\cos x_3;\ \varphi_4 = \psi_{21}\sin 2x_3,$$
$$\varphi_5 = \psi_{21}\cos 2x_3,$$
$$F_1 = f_0(x_2) = \psi_{01}(x_{10}, x_2);\ F_2 = f_1(x_2)\sin x_3 = \psi_{11}(x_{10}, x_2)\sin x_3,$$
$$F_3 = f_1(x_2)\cos x_3 = \psi_{11}(x_{10}, x_2)\cos x_3,$$
$$F_4 = f_2(x_2)\sin 2x_3 = \psi_{21}(x_{10}, x_2)\sin 2x_3,$$
$$F_5 = f_2(x_2)\cos 2x_3 = \psi_{21}(x_{10}, x_2)\cos 2x_3;$$
$$P_0(t) = Z_1(t);\ R_1(t) = Z_2(t);\ P_1(t) = Z_3(t),$$
$$R_2(t) = Z_4(t);\ P_2(t) = Z_5(t),$$
$$\beta_1(t) = p_0(t);\ \beta_2(t) = r_1(t);\ \beta_3(t) = p_1(t);\ \beta_4(t) = r_2(t);\ \beta_5(t) = p_2(t),$$

where

$$f_m(x_2) = a_{10}^{(m)} + \sum_{k=1}^{q} b_k^{(m)}(x_2); \quad b_k^{(m)}(x_2) = a_{1k}^{(m)} v_{\nu mk}^{(m)}(x_2), \quad m = 0, 1, 2.$$

The time-dependent $\beta_0(t) = O(\epsilon^{2/3})$ is a function of p_0, r_1, p_1, r_2 and p_2, i.e.

$$f^* = x_{10} + k_1(r_1^2(t) + p_1^2(t)) + p_0(t)f_0(x_2) + [r_1(t)\sin x_3 + p_1(t)\cos x_3]f_1(x_2) + [r_2(t)\sin 2x_3 + p_2(t)\cos 2x_3]f_2(x_2), \quad (3.145)$$

where the coefficient

$$k_1 = -\frac{1}{x_{10}x_{20}^2}\int_0^{x_{20}} x_2 f_1^2(x_2)dx_2$$

is derived from the volume conservation condition

$$|Q(t)| - |Q_0| = \int_0^{2\pi} \int_0^{x_{20}} (x_{10}^2 f + x_{10} f^2 + \tfrac{1}{3} f^3) x_2 dx_2 dx_3 = 0$$

considered correctly to $O(\epsilon^{2/3})$.

The integrals A_n, A_{nk} and $\partial l_n / \partial \beta_i$ are linearly incorporated in (3.47) and, moreover, these integrals are linear in ρ. The density ρ can therefore be omitted. The integrals can be expanded in series by p_0, r_1, p_1, r_2 and p_2 correctly to $O(\epsilon)$. Accounting for $\frac{dA_n}{dt} = \sum_{i=1}^{5} \frac{\partial A_n}{\partial \beta_i} \dot{\beta}_i$ and pursuing $O(\epsilon)$ in $\frac{\partial A_n}{\partial \beta_i} \dot{\beta}_i$, $\frac{\partial A_n}{\partial \beta_i} Z_n$ and $A_{nk} Z_n$, $Z_n \frac{\partial A_{nk}}{\partial \beta_i} Z_k$ we get

$$\begin{aligned}
A_1 &= a_4(r_1^2 + p_1^2) + a_{17} p_0, \\
A_2 &= a_5 r_1 + a_6 r_1 (r_1^2 + p_1^2) + a_{18}(p_1 r_2 - r_1 p_2) + a_{14} r_1 p_0, \\
A_3 &= a_5 p_1 + a_6 p_1 (p_1^2 + r_1^2) + a_{18}(r_1 r_2 + p_1 p_2) + a_{14} p_1 p_0, \\
A_4 &= a_{13} r_2 - 2 a_7 r_1 p_1; \quad A_5 = a_{13} p_2 + a_7 (r_1^2 - p_1^2)
\end{aligned} \tag{3.146}$$

and

$$\begin{aligned}
&A_{11} = 2a_1; \; A_{21} = A_{12} = a_{15} r_1; \; A_{31} = A_{13} = a_{15} p_1, \\
&A_{22} = 2a_{10} + 2a_{11} r_1^2 + 2a_{12} p_1^2 + 2a_9 p_0 - 2a_{16} p_2, \\
&A_{32} = A_{23} = a_8 r_1 p_1 + 2a_{16} r_2; \quad A_{55} = A_{44} = 2a_2, \\
&A_{33} = 2a_{10} + 2a_{11} p_1^2 + 2a_{12} r_1^2 + 2a_{16} p_2 + 2a_9 p_0, \\
&A_{42} = A_{24} = a_3 p_1; \quad A_{52} = A_{25} = -a_3 r_1; \quad A_{43} = A_{34} = a_3 r_1, \\
&A_{53} = A_{35} = a_3 p_1; \quad A_{41} = A_{14} = A_{51} = A_{15} = A_{54} = A_{45} = 0,
\end{aligned} \tag{3.147}$$

where coefficients $a_1, ..., a_{18}$ are given by the following integrals

$$\begin{aligned}
a_1 &= \pi \int_0^{x_{20}} F_0^{(0,0)}(x_2) x_2 dx_2, \\
a_2 &= \frac{\pi}{2} \int_0^{x_{20}} (F_0^{(2,2)}(x_2) + \frac{4}{x_2^2} B_0^{(2,2)}(x_2)) x_2 dx_2, \\
a_3 &= \frac{\pi}{2} \int_0^{x_{20}} (F_1^{(1,2)}(x_2) + \frac{2}{x_2^2} B_1^{(1,2)}(x_2)) f_1(x_2) x_2 dx_2, \\
a_4 &= \pi \int_0^{x_{20}} (B_0^{(2)}(x_2) f_1^2(x_2) + 2k_1 B_0^{(1)}(x_2)) x_2 dx_2, \\
a_5 &= \pi \int_0^{x_{20}} B_1^{(1)}(x_2) f_1(x_2) x_2 dx_2,
\end{aligned}$$

$$
\begin{aligned}
a_6 =&\pi \int_0^{x_{20}} (\tfrac{3}{4}B_1^{(3)}(x_2)f_1^2(x_2) + 2k_1 B_1^{(2)}(x_2))f_1(x_2)x_2dx_2,\\
a_7 =&-\frac{\pi}{2}\int_0^{x_{20}} B_2^{(2)}(x_2)f_1^2(x_2)x_2dx_2,\\
a_8 =&\frac{\pi}{2}\int_0^{x_{20}} (F_2^{(1,1)}(x_2) - \frac{1}{x_2^2}B_2^{(1,1)}(x_2))f_1^2(x_2)x_2dx_2,\\
a_9 =&\frac{\pi}{2}\int_0^{x_{20}} [F_1^{(1,1)}(x_2) + \frac{1}{x_2^2}B_1^{(1,1)}(x_2)]f_0(x_2)x_2dx_2,\\
a_{10} =&\frac{\pi}{2}\int_0^{x_{20}} (F_0^{(1,1)}(x_2) + \frac{1}{x_2^2}B_0^{(1,1)}(x_2))x_2dx_2,\\
a_{11} =&\frac{\pi}{2}\int_0^{x_{20}} \Big(k_1[F_1^{(1,1)}(x_2) + \frac{1}{x_2^2}B_1^{(1,1)}(x_2)]+\\
&+\tfrac{3}{4}[F_2^{(1,1)}(x_2) + \frac{1}{3x_2^2}B_2^{(1,1)}(x_2)]f_1^2(x_2)\Big)x_2dx_2,\\
a_{12} =&\frac{\pi}{2}\int_0^{x_{20}} \Big(k_1[F_1^{(1,1)}(x_2) + \frac{1}{x_2^2}B_1^{(1,1)}(x_2)] +\\
&+\tfrac{3}{4}[\tfrac{1}{3}F_2^{(1,1)}(x_2) + \frac{1}{x_2^2}B_2^{(1,1)}(x_2)]f_1^2(x_2)\Big)x_2dx_2,\\
a_{13} =&\pi \int_0^{x_{20}} B_2^{(1)}(x_2)f_2(x_2)x_2dx_2,\\
a_{14} =&2\pi \int_0^{x_{20}} B_1^{(2)}(x_2)f_0(x_2)f_1(x_2)x_2dx_2,\\
a_{15} =&\pi \int_0^{x_{20}} F_1^{(0,1)}(x_2)f_1(x_2)x_2dx_2,\\
a_{16} =&\frac{\pi}{4}\int_0^{x_{20}} [F_1^{(1,1)}(x_2) - \frac{1}{x_2^2}B_1^{(1,1)}(x_2)]f_2(x_2)x_2dx_2,\\
a_{17} =&2\pi \int_0^{x_{20}} B_0^{(1)}(x_2)f_0(x_2)x_2dx_2,\\
a_{18} =&\pi \int_0^{x_{20}} B_1^{(2)}f_1(x_2)f_2(x_2)x_2dx_2.
\end{aligned}
$$

Here, we introduce the functions $B_0^{(1)}, B_0^{(2)}, B_1^{(1)}$, $B_1^{(2)}, B_1^{(3)}, B_2^{(1)}, B_2^{(2)}$, $B_0^{(2,2)}$, $B_1^{(1,2)}$, $B_0^{(1,1)}, B_1^{(1,1)}, B_2^{(1,1)}$ and $F_0^{(0,0)}, F_0^{(1,1)}, F_0^{(2,2)}, F_1^{(0,1)}, F_1^{(1,2)}, F_1^{(1,1)}, F_2^{(1,1)}$ depending on $b_k^{(m)}(x_2)$ and

$$c_k^{(m)}(x_2) = a_{1k}^{(m)} \frac{dv_{\nu_{mk}}^{(m)}}{dx_2}, \quad m = 0, 1, 2; \ k = 0, 1, \ldots, q.$$

These functions are expressed as follows

$$B_m^{(1)}(x_2) = x_{10}^2 \sum_{k=0}^{q} b_k^{(m)}(x_2); \quad B_m^{(2)}(x_2) = \frac{x_{10}}{2} \sum_{k=0}^{q} (\nu_{mk} + 2) b_k^{(m)}(x_2),$$

$$B_m^{(3)}(x_2) = \tfrac{1}{6} \sum_{k=0}^{q} (\nu_{mk} + 2)(\nu_{mk} + 1) b_k^{(m)}(x_2), \quad m = 0, 1, 2;$$

$$B_0^{(m,n)}(x_2) = x_{10} \sum_{i,j=1}^{q} \frac{b_i^{(m)}(x_2) b_j^{(n)}(x_2)}{\nu_{mi} + \nu_{nj} + 1},$$

$$B_1^{(m,n)} = \sum_{i,j=1}^{q} b_i^{(m)}(x_2) b_j^{(n)}(x_2);$$

$$B_2^{(m,n)} = \frac{1}{2x_{10}} \sum_{i,j=1}^{q} (\nu_{mi} + \nu_{nj}) b_i^{(m)} b_j^{(n)}, \quad m, n = 1, 2;$$

$$\Pi_{ij}^{(m,n)}(x_2) = \nu_{mi}\nu_{nj} b_i^{(m)} b_j^{(n)} - x_2(\nu_{mi} b_i^{(m)} c_j^{(n)} + \nu_{ni} b_i^{(n)} c_j^{(m)}) + \\ + (1 + x_2^2) c_i^{(m)} c_j^{(n)},$$

$$F_0^{(m,n)}(x_2) = x_{10} \sum_{i,j=1}^{q} \frac{\Pi_{ij}^{(m,n)}(x_2)}{\nu_{mi} + \nu_{nj} + 1}; \quad F_1^{(m,n)}(x_2) = \sum_{i,j=1}^{q} \Pi_{ij}^{(m,n)}(x_2),$$

$$F_2^{(m,n)}(x_2) = \frac{1}{x_{10}} \sum_{i,j=1}^{q} (\nu_{mi} + \nu_{nj}) \Pi_{ij}^{(m,n)}(x_2), \quad m, n = 0, 1, 2.$$

The relationship (3.144) and $g_1 = -g, g_2 = g_3 = 0$ mean that the terms $\frac{\partial l_2}{\partial \beta_i}$ and $\frac{\partial l_3}{\partial \beta_i}$ of (3.47) should be calculated correctly to $O(1)$ as follows

$$\frac{\partial l_2}{\partial \beta_i} = \begin{cases} 0, & \beta_i \not\equiv p_1 \\ \lambda, & \beta_i \equiv p_1 \end{cases}; \quad \frac{\partial l_3}{\partial \beta_i} = \begin{cases} 0, & \beta_i \not\equiv r_1 \\ \lambda, & \beta_i \equiv r_1 \end{cases}; \quad \lambda = x_{10}^3 \pi \int_0^{x_{20}} x_2^2 f_1(x_2) dx_2. \tag{3.148}$$

The scalar function l_1 reads as

$$l_1 = l_1^{(0)} + [l_1^{(1)}(r_1^2 + p_1^2) + l_1^{(2)} p_0^2 + l_1^{(3)}(r_2^2 + p_2^2) + l_1^{(4)}(r_1^2 + p_1^2)^2 +$$

$$+ l_1^{(5)}(\tfrac{1}{2}p_1^2 p_2 - \tfrac{1}{2}r_1^2 p_2 + r_1 p_1 r_2) + l_1^{(6)} p_0 (r_1^2 + p_1^2)], \quad (3.149)$$

where

$$l_1^{(0)} = \tfrac{\pi}{4} x_{10}^4 x_{20}^2; \quad l_1^{(1)} = \tfrac{1}{2} x_{10}^2 G_{11}; \quad l_1^{(2)} = \tfrac{1}{2} x_{10}^2 G_{00}; \quad l_1^{(3)} = \tfrac{1}{2} x_{10}^2 G_{22},$$
$$l_1^{(4)} = \tfrac{3}{16} G_{1111} + \tfrac{3}{2} x_{10} k_1 G_{11}; \quad l_1^{(5)} = 2 x_{10} G_{211}; \quad l_1^{(6)} = 2 x_{10} G_{011}$$

and

$$G_{00} = 2\pi \int_0^{x_{20}} x_2 f_0^2 dx_2; \quad G_{11} = \pi \int_0^{x_{20}} x_2 f_1^2 dx_2,$$
$$G_{22} = \pi \int_0^{x_{20}} x_2 f_2^2 dx_2; \quad G_{011} = \pi \int_0^{x_{20}} f_0 f_1^2 x_2 dx_2,$$
$$G_{211} = \pi \int_0^{x_{20}} x_2 f_2 f_1^2 dx_2; \quad G_{1111} = \pi \int_0^{x_{20}} x_2 f_1^4 dx_2.$$

Consider (3.47a) as a system of linear algebraic equations in $Z_k(t)$. Accounting for (3.146) and (3.147) and solving (3.47a) correctly to $O(\epsilon)$, one obtains

$$\begin{aligned}
R_1(t) =& Q_1 \dot{r}_1 + C_2 r_1^2 \dot{r}_1 + D_3 p_1^2 \dot{r}_1 + C_1 r_1 p_1 \dot{p}_1 + \\
&+ D_2(r_2 \dot{p}_1 - p_2 \dot{r}_1) + C_3(p_1 \dot{r}_2 - r_1 \dot{p}_2) + \\
&+ B_0 p_0 \dot{r}_1 + B_3 r_1 \dot{p}_0, \\
P_1(t) =& Q_1 \dot{p}_1 + C_2 p_1^2 \dot{p}_1 + D_3 r_1^2 \dot{p}_1 + C_1 p_1 r_1 \dot{r}_1 + \\
&+ D_2(r_2 \dot{r}_1 + p_2 \dot{p}_1) + C_3(r_1 \dot{r}_2 + p_1 \dot{p}_2) + \\
&+ B_0 p_0 \dot{p}_1 + B_3 p_1 \dot{p}_0, \\
P_0(t) =& C_0(r_1 \dot{r}_1 + p_1 \dot{p}_1) + D_0 \dot{p}_0, \\
R_2(t) =& Q_2 \dot{r}_2 - D_1(r_1 \dot{p}_1 + p_1 \dot{r}_1), \\
P_2(t) =& Q_2 \dot{p}_2 + D_1(r_1 \dot{r}_1 - p_1 \dot{p}_1),
\end{aligned} \quad (3.150)$$

where

$$C_0 = \frac{a_4}{a_1} - \frac{a_5 a_{15}}{4 a_1 a_{10}}; \quad D_0 = \frac{a_{17}}{2 a_1},$$
$$C_1 = \frac{1}{a_{10}}\left(a_6 - \frac{a_4 a_{15}}{2 a_1} - \frac{a_5 a_8}{4 a_{10}} + \frac{a_5 a_{15}^2}{8 a_1 a_{10}}\right),$$
$$Q_2 = \frac{a_{13}}{2 a_2}; \quad C_3 = \frac{1}{2 a_{10}}\left(a_{18} - \frac{a_3 a_{13}}{2 a_2}\right),$$

$$B_0 = \frac{1}{2a_{10}}(a_{14} - \frac{a_5 a_9}{a_{10}}); \quad Q_1 = \frac{a_5}{2a_{10}},$$
$$B_3 = \frac{1}{2a_{10}}(a_{14} - \frac{a_{15} a_{17}}{2a_1}); \quad D_1 = \frac{a_7}{a_2} + \frac{a_3 a_5}{4a_2 a_{10}},$$
$$D_2 = \frac{1}{2a_{10}}(a_{18} - \frac{a_5 a_{16}}{a_{10}}),$$
$$D_3 = \frac{a_6}{2a_{10}} + Q_1(\frac{a_3^2}{4a_2 a_{10}} - \frac{a_{12}}{a_{10}} + \frac{a_3 a_7}{a_2 a_5}); \quad C_2 = D_3 + C_1.$$

Substituting (3.146), (3.147), (3.148), (3.149) and (3.150) in (3.47b) and gathering the terms up to $O(\epsilon)$ lead to a modal system with the coefficients

$$\begin{aligned}
&\mathcal{D}_1 = \frac{d_1}{\mu_1}; \quad \mathcal{D}_2 = \frac{d_2}{\mu_1}; \quad \mathcal{D}_3 = \frac{d_3}{\mu_1}; \quad \mathcal{D}_4 = \frac{d_4}{\mu_1}; \quad \mathcal{D}_5 = \frac{d_5}{\mu_1},\\
&\mathcal{D}_6 = \frac{d_6}{\mu_1}; \quad \mathcal{D}_7 = \frac{d_7}{\mu_2}; \quad \mathcal{D}_8 = \frac{d_8}{\mu_0}; \quad \mathcal{D}_9 = \frac{d_4}{\mu_2}; \quad \mathcal{D}_{10} = \frac{d_6}{\mu_0},\\
&\mathcal{G}_1 = \frac{d_1^k}{\mu_1 \varkappa_{11}}; \quad \mathcal{G}_2 = \frac{2d_2^k}{\mu_1 \varkappa_{11}}; \quad \mathcal{G}_3 = \frac{2d_3^k}{\mu_1 \varkappa_{11}}; \quad \mathcal{G}_4 = \frac{d_2^k}{\mu_2 \varkappa_{21}},\\
&\mathcal{G}_5 = \frac{d_3^k}{\mu_0 \varkappa_{01}}; \quad \Lambda = \frac{\lambda}{\mu_1},
\end{aligned} \tag{3.151}$$

where

$$\begin{aligned}
&\mu_0 = a_{17} D_0; \quad \mu_1 = a_5 Q_1; \quad \mu_2 = a_{13} Q_2,\\
&d_1 = 2a_4 C_0 + 2a_7 D_1 + a_5 C_2 + 3a_6 Q_1; \quad d_2 = a_5 D_3 + a_6 Q_1 + 2a_7 D_1,\\
&d_3 = a_5 D_2 + a_{18} Q_1; \quad d_4 = 2a_7 Q_2 - a_5 C_3; \quad d_5 = a_5 B_0 + a_{14} Q_1,\\
&d_6 = 2a_4 D_0 + a_5 B_3; \quad d_7 = d_4 + \tfrac{1}{2} d_3; \quad d_8 = d_6 - \tfrac{1}{2} d_5,\\
&d_1^k = 4l_1^{(4)}; \quad d_2^k = \tfrac{1}{2} l_1^{(5)}; \quad d_3^k = l_1^{(6)}.
\end{aligned}$$

The modal system takes the following form:

$$\begin{aligned}
&\ddot{r}_1 + \sigma_1^2 r_1 + \mathcal{D}_1(r_1^2 \ddot{r}_1 + r_1 \dot{r}_1^2 + r_1 p_1 \ddot{p}_1 + r_1 \dot{p}_1^2) +\\
&+ \mathcal{D}_2(p_1^2 \ddot{r}_1 + 2p_1 \dot{r}_1 \dot{p}_1 - r_1 p_1 \ddot{p}_1 - 2r_1 \dot{p}_1^2) - \mathcal{D}_3(p_2 \ddot{r}_1 - r_2 \ddot{p}_1 + \dot{r}_1 \dot{p}_2 - \dot{p}_1 \dot{r}_2) +\\
&+ \mathcal{D}_4(r_1 \ddot{p}_2 - p_1 \ddot{r}_2) + \mathcal{D}_5(p_0 \ddot{r}_1 + \dot{r}_1 \dot{p}_0) + \mathcal{D}_6 r_1 \ddot{p}_0 +\\
&+ \sigma_1^2 \left[\mathcal{G}_1 r_1 (r_1^2 + p_1^2) + \mathcal{G}_2 (p_1 r_2 - r_1 p_2) + \mathcal{G}_3 r_1 p_0\right] + \Lambda \dot{v}_{03} = 0,
\end{aligned} \tag{3.152a}$$

$$\ddot{p}_1 + \sigma_1^2 p_1 + \mathcal{D}_1(p_1^2\ddot{p}_1 + p_1\dot{p}_1^2 + r_1 p_1 \ddot{r}_1 + p_1\dot{r}_1^2) +$$
$$+ \mathcal{D}_2(r_1^2\ddot{p}_1 + 2r_1\dot{r}_1\dot{p}_1 - r_1 p_1\ddot{r}_1 - 2p_1\dot{r}_1^2) + \mathcal{D}_3(p_2\ddot{p}_1 + r_2\ddot{r}_1 + \dot{r}_1\dot{r}_2 + \dot{p}_1\dot{p}_2) -$$
$$- \mathcal{D}_4(p_1\ddot{p}_2 + r_1\ddot{r}_2) + \mathcal{D}_5(p_0\ddot{p}_1 + \dot{p}_1\dot{p}_0) + \mathcal{D}_6 p_1\ddot{p}_0 +$$
$$+ \sigma_1^2\left[\mathcal{G}_1 p_1(r_1^2 + p_1^2) + \mathcal{G}_2(r_1 r_2 + p_1 p_2) + \mathcal{G}_3 p_1 p_0\right] = 0, \quad (3.152b)$$

$$\ddot{r}_2 + \sigma_2^2 r_2 - \mathcal{D}_9(p_1\ddot{r}_1 + r_1\ddot{p}_1) - 2\mathcal{D}_7\dot{r}_1\dot{p}_1 + \sigma_2^2\left[2\mathcal{G}_4 r_1 p_1\right] = 0, \quad (3.152c)$$

$$\ddot{p}_2 + \sigma_2^2 p_2 + \mathcal{D}_9(r_1\ddot{r}_1 - p_1\ddot{p}_1) + \mathcal{D}_7(\dot{r}_1^2 - \dot{p}_1^2) -$$
$$- \sigma_2^2\left[\mathcal{G}_4(r_1^2 - p_1^2)\right] = 0, \quad (3.152d)$$

$$\ddot{p}_0 + \sigma_0^2 p_0 + \mathcal{D}_{10}(r_1\ddot{r}_1 + p_1\ddot{p}_1) + \mathcal{D}_8(\dot{r}_1^2 + \dot{p}_1^2) +$$
$$+ \sigma_0^2\left[\mathcal{G}_5(r_1^2 + p_1^2)\right] = 0. \quad (3.152e)$$

Here $\sigma_1 = \sigma_{11}$, $\sigma_2 = \sigma_{21}$ and $\sigma_0 = \sigma_{01}$ are defined by (3.126). In order to help readers we give approximate values of the hydrodynamic coefficients $\Lambda, \mathcal{D}_i$ and $\mathcal{G}_i$ (versus α) in Table 3.5. The modal system (3.152) differs from (3.97a)-(3.97e) (circular cylindrical tank) and Faltinsen *et al.* (2003) [46] (square-base tank) by terms in the square brackets. These terms appear due to non-vertical walls, the coefficients $\mathcal{G}_i$ vanish as $\alpha \to 0$.

Because to the authors knowledge the nonlinear fluid sloshing in a conical tank has never been studied and, as matter of fact, the modal system (3.152) has no analogies in the scientific literature, we tried our best to quantify its applicability. The quantification can be based on results by Ockendon *et al.* (1996,2001) [141, 140] and Faltinsen & Timokha (2002) [51] that associate failure of the Moiseyev ordering (3.144) with the secondary (internal) resonance. The secondary resonance has also been discussed by Bryant (1989) [32] (circular basin), it was examined for large amplitude forcing by Faltinsen & Timokha (2001) [49] (rectangular tank) and La Rocca *et al.* (1997,2000) [98, 99] and Faltinsen *et al.* (2003,2005) [46, 47] (square base tank). Quantification of critical semi-apex angles α, which yield the secondary resonance phenomena, can be done by analysing the dispersion relationship and higher periodic harmonics of steady-state solutions as $\sigma = \sigma_1$. Because of dramatical growth of the damping for higher harmonics and modes (Faltinsen *et al.* (2005,2006) [47, 48]), our analysis can be limited to the second-order

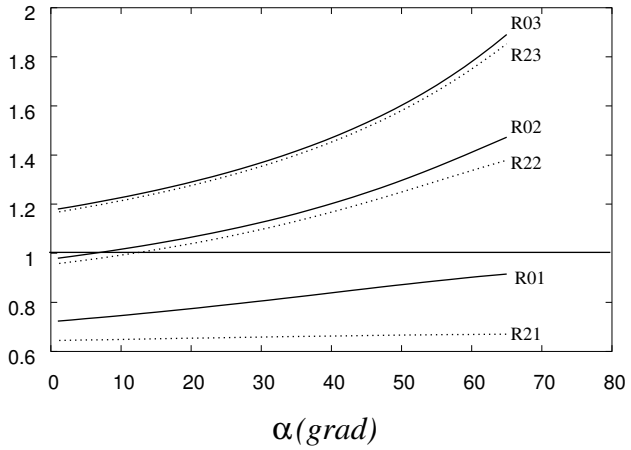

Fig. 3.29. $R0i$ and $R2i$ versus α.

terms. In that case, influence of the secondary resonance is associated with the equalities

$$R0i = \frac{1}{2}\sqrt{\frac{\varkappa_{0i}}{\varkappa_{11}}} = 1, \quad R2i = \frac{1}{2}\sqrt{\frac{\varkappa_{2i}}{\varkappa_{11}}} = 1, \quad i \geq 1. \tag{3.153}$$

Fig. 3.29 shows the graphs of $R1i$ and $R0i$ versus α. Using the resonance conditions (3.153) we predict the secondary resonance about $\alpha = 6^0$ (by mode 02) and $\alpha = 12^0$ (by mode 22). When assuming $R0i$, $R2i$ close, but not equal to 1, for instance, $|R2i, R0i - 1| < 0.1$, we deduce that the Moiseyev-based modal system (3.152) is applicable for $25^0 < \alpha < 60^0$.

3.4.3 Resonant sloshing due to sway excitation

By using (3.144) and accounting for results by Gavrilyuk *et al.* (2000) [65] Faltinsen *et al.* (2003) [46], we pose the dominating modal functions of (3.142) in the form (3.101), where, as earlier, $A, \bar{A}, B$ and $\bar{B}$ are unknown constants (dominating amplitudes) and σ is the excitation frequency. Representation (3.101) defines steady-state sloshing. By substituting (3.101) into (3.152c) - (3.152e) and gathering primary harmonics, the Fredholm alternative deduces (3.102) - (3.103), where

$$h_0 = \frac{\mathcal{D}_{10} + \mathcal{D}_8 - \bar{\sigma}_0^2 \mathcal{G}_5}{2(\bar{\sigma}_0^2 - 4)}, \quad l_0 = \frac{\mathcal{D}_{10} - \mathcal{D}_8 - \bar{\sigma}_0^2 \mathcal{G}_5}{2\bar{\sigma}_0^2},$$

Table 3.5. Coefficients of the nonlinear modal system (3.152) versus α.

α^0	$\mathcal{D}_1$	$\mathcal{D}_2$	$\mathcal{D}_3$	$\mathcal{D}_4$	$\mathcal{D}_5$	$\mathcal{D}_6$	$\mathcal{D}_7$	$\mathcal{D}_8$	$\mathcal{D}_9$	$\mathcal{D}_{10}$
25	-0.1165	-0.4152	1.6116	-0.5428	2.0291	0.6715	0.6055	-0.3634	-1.2498	0.7113
27	-0.1927	-0.4287	1.6707	-0.5790	2.0773	0.7271	0.5954	-0.3428	-1.3445	0.8001
29	-0.2744	-0.4447	1.7330	-0.6163	2.1288	0.7833	0.5860	-0.3217	-1.4432	0.8964
31	-0.3623	-0.4635	1.7990	-0.6550	2.1838	0.8402	0.5773	-0.2999	-1.5465	1.0009
33	-0.4575	-0.4853	1.8691	-0.6953	2.2427	0.8980	0.5694	-0.2772	-1.6548	1.1146
35	-0.5609	-0.5106	1.9438	-0.7375	2.3060	0.9571	0.5623	-0.2536	-1.7689	1.2387
37	-0.6740	-0.5397	2.0236	-0.7818	2.3742	1.0177	0.5560	-0.2287	-1.8893	1.3742
39	-0.7984	-0.5731	2.1093	-0.8285	2.4478	1.0802	0.5506	-0.2026	-2.0170	1.5225
41	-0.9360	-0.6115	2.2015	-0.8780	2.5276	1.1450	0.5461	-0.1748	-2.1527	1.6851
43	-1.0891	-0.6556	2.3011	-0.9308	2.6145	1.2126	0.5426	-0.1454	-2.2978	1.8636
45	-1.2608	-0.7064	2.4092	-0.9872	2.7093	1.2837	0.5402	-0.1139	-2.4532	2.0600
47	-1.4546	-0.7650	2.5270	-1.0480	2.8134	1.3588	0.5390	-0.0802	-2.6207	2.2763
49	-1.6750	-0.8330	2.6559	-1.1136	2.9281	1.4389	0.5392	-0.0440	-2.8019	2.5153
51	-1.9277	-0.9123	2.7976	-1.1851	3.0552	1.5248	0.5408	-0.0050	-2.9990	2.7797
53	-2.2200	-1.0052	2.9543	-1.2633	3.1967	1.6179	0.5442	0.0372	-3.2146	3.0731

α^0	$\mathcal{G}_1$	$\mathcal{G}_2$	$\mathcal{G}_3$	$\mathcal{G}_4$	$\mathcal{G}_5$	Λ	k_1
25	-0.2541	0.6810	0.7638	0.4550	0.1446	1.3135	-0.1324
27	-0.2981	0.7388	0.8314	0.4965	0.1604	1.2872	-0.1425
29	-0.3469	0.7983	0.9007	0.5395	0.1774	1.2597	-0.1529
31	-0.4009	0.8597	0.9717	0.5841	0.1957	1.2311	-0.1634
33	-0.4607	0.9233	1.0448	0.6307	0.2155	1.2013	-0.1743
35	-0.5272	0.9896	1.1202	0.6795	0.2370	1.1704	-0.1855
37	-0.6012	1.0588	1.1984	0.7307	0.2603	1.1384	-0.1972
39	-0.6840	1.1316	1.2797	0.7848	0.2857	1.1054	-0.2094
41	-0.7768	1.2084	1.3647	0.8420	0.3136	1.0713	-0.2221
43	-0.8815	1.2899	1.4539	0.9028	0.3440	1.0361	-0.2356
45	-1.0000	1.3767	1.5482	0.9678	0.3774	1.0000	-0.2500
47	-1.1350	1.4697	1.6483	1.0376	0.4142	0.9629	-0.2653
49	-1.2897	1.5700	1.7552	1.1128	0.4548	0.9249	-0.2818
51	-1.4683	1.6787	1.8703	1.1944	0.4996	0.8859	-0.2997
53	-1.6760	1.7972	1.9951	1.2834	0.5493	0.8461	-0.3192

$$h_2 = \frac{\mathcal{D}_9 + \mathcal{D}_7 + \bar{\sigma}_2^2 \mathcal{G}_4}{2(\bar{\sigma}_2^2 - 4)},\ l_2 = \frac{\mathcal{D}_9 - \mathcal{D}_7 + \bar{\sigma}_2^2 \mathcal{G}_4}{2\bar{\sigma}_2^2};\quad \bar{\sigma}_m = \frac{\sigma_m}{\sigma},\ m = 0, 1, 2.$$

By inserting (3.101), (3.102) into (3.152a), (3.152b) and using the Fredholm alternative, we derive the following system of nonlinear algebraic equations coupling $A, \bar{A}, B$ and $\bar{B}$

$$\begin{aligned}
&A[\bar{\sigma}_1^2 - 1 - m_1(A^2 + \bar{A}^2 + \bar{B}^2) - m_2 B^2] + m_3 \bar{A} B \bar{B} = H\Lambda,\\
&\bar{A}[\bar{\sigma}_1^2 - 1 - m_1(A^2 + \bar{A}^2 + B^2) - m_2 \bar{B}^2] + m_3 A B \bar{B} = 0,\\
&B[\bar{\sigma}_1^2 - 1 - m_1(B^2 + \bar{A}^2 + \bar{B}^2) - m_2 A^2] + m_3 \bar{B} A \bar{A} = 0,\\
&\bar{B}[\bar{\sigma}_1^2 - 1 - m_1(A^2 + B^2 + \bar{B}^2) - m_2 \bar{A}^2] + m_3 \bar{A} A B = 0,
\end{aligned} \tag{3.154}$$

where

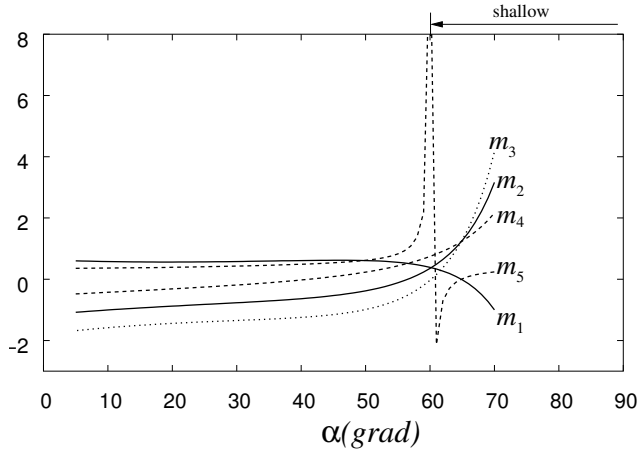

Fig. 3.30. $m_i(\sigma_1, \alpha)$ as functions of α.

$$
\begin{aligned}
m_1 &= -\mathcal{D}_5(\tfrac{1}{2}h_0 - l_0) + \mathcal{D}_3(\tfrac{1}{2}h_2 - l_2) + 2\mathcal{D}_6 h_0 + 2\mathcal{D}_4 h_2 + \tfrac{1}{2}\mathcal{D}_1 - \\
&\quad - \bar{\sigma}_1^2 \left[\tfrac{3}{4}\mathcal{G}_1 - \mathcal{G}_2(l_2 + \tfrac{1}{2}h_2) + \mathcal{G}_3(l_0 + \tfrac{1}{2}h_0)\right], \\
m_2 &= \mathcal{D}_3(l_2 + \tfrac{3}{2}h_2) + \mathcal{D}_5(l_0 + \tfrac{1}{2}h_0) - 2\mathcal{D}_6 h_0 + 6\mathcal{D}_4 h_2 - \tfrac{1}{2}\mathcal{D}_1 + 2\mathcal{D}_2 - \\
&\quad - \bar{\sigma}_1^2 \left[\tfrac{1}{4}\mathcal{G}_1 + \mathcal{G}_2(l_2 - \tfrac{3}{2}h_2) + \mathcal{G}_3(l_0 - \tfrac{1}{2}h_0)\right], \\
m_3 &= m_2 - m_1.
\end{aligned}
\tag{3.155}
$$

The system (3.154) is similar to the original eq. (14) by Gavrilyuk *et al.* (2000) [65] (sloshing in circular cylindrical tanks); its resolvability condition is $m_3 \neq 0$. Solutions of (3.154) depend on the actual values of m_i which are functions of σ and α ($m_i = m_i(\sigma, \alpha)$). Taking into account that $\sigma \approx \sigma_1$, we can consider $m_i(\sigma_1, \alpha)$ (see, the graphs in Fig. 3.30). These graphs establish that $m_3 > 0$ for $\alpha < 60^0$ and $\sigma \to \sigma_1$.

Using derivations of the previous section and Faltinsen *et al.* (2003) [46], the system (3.154) can be re-written in the equivalent form

$$
\begin{aligned}
&A(\bar{\sigma}_1^2 - 1 - m_1 A^2 - m_2 B^2) = H\Lambda, \\
&B(\bar{\sigma}_1^2 - 1 - m_1 B^2 - m_2 A^2) = 0, \quad \bar{A} = \bar{B} = 0.
\end{aligned}
\tag{3.156}
$$

Vanishing $\bar{A}$ and $\bar{B}$ makes it possible to treat A and B as dominating longitudinal (along oscillations of the tank) and transversal (perpendicular to the oscillations) amplitudes of steady-state waves, respectively. The system (3.156) has only two classes of solutions. The first class suggests $B = 0$ and describes 'planar' regime. Eqs. (3.156) take then the following form

$$A(\bar{\sigma}_1^2 - 1 - m_1 A^2) = \Lambda H; \quad B = 0. \tag{3.157}$$

The second class ($B^2 > 0$) describes 'swirling' (wave patterns imitate a rotation of the fluid volume around axis Ox). The algebraic system (3.156) falls then into the single equation with respect to A

$$A(\bar{\sigma}_1^2 - 1 - m_4 A^2) = m_5 \Lambda H, \quad m_5 = -\frac{m_1}{m_3}, \quad m_4 = m_1 + m_2 \tag{3.158}$$

and the auxiliary formula for computing B

$$B^2 = \frac{1}{m_1}(\bar{\sigma}_1^2 - 1 - m_2 A^2) = \frac{1}{m_1}\left(m_5 \frac{\Lambda H}{A} + m_1 A^2\right) > 0. \tag{3.159}$$

Lukovsky (1990) [114] and Faltinsen *et al.* (2003) [46] showed that response curves of 'planar' and 'swirling' depend on m_1 and m_4, respectively. Zeros of m_1 and m_4 at isolated semi-apex angles α imply a passage from a 'hard-spring' to a 'soft-spring' behaviour. If $\alpha < 60^0$, response curves of the 'planar' regime are always characterised by the 'soft-spring' behaviour (similar to the case of circular cylindrical tanks, Lukovsky (1990) [114]). However, the response curves of 'swirling' change their behaviour at $\alpha \approx 41.1^0$ ($x_{10} = h/r_0 = 1.14\ldots$). Fig. 3.31 and Fig. 3.32 show the typical branching for $\alpha = 30^0$ and $\alpha = 45^0$, respectively. The stability analysis used technique by Faltinsen *et al.* (2003) [46].

The system (3.152) is linear in $\ddot{r}_i, \ddot{p}_i$. By inverting the matrix $\mathcal{A} =$

$$\begin{pmatrix}
1+\mathcal{D}_1 r_1^2+\mathcal{D}_2 p_1^2-\mathcal{D}_3 p_2+\mathcal{D}_5 p_0 & (\mathcal{D}_1 - \mathcal{D}_2) r_1 p_1 + \mathcal{D}_3 r_2 & -\mathcal{D}_4 p_1 & \mathcal{D}_4 r_1 & \mathcal{D}_6 r_1 \\
(\mathcal{D}_1 - \mathcal{D}_2) r_1 p_1 + \mathcal{D}_3 r_2 & 1+\mathcal{D}_1 p_1^2+\mathcal{D}_2 r_1^2+\mathcal{D}_3 p_2+\mathcal{D}_5 p_0 & -\mathcal{D}_4 r_1 & -\mathcal{D}_4 p_1 & \mathcal{D}_6 p_1 \\
-\mathcal{D}_9 p_1 & -\mathcal{D}_9 r_1 & 1 & 0 & 0 \\
\mathcal{D}_9 r_1 & -\mathcal{D}_9 p_1 & 0 & 1 & 0 \\
\mathcal{D}_{10} r_1 & \mathcal{D}_{10} p_1 & 0 & 0 & 1
\end{pmatrix}$$

it can be re-written in the normal form (3.99), where $\boldsymbol{p} = (r_1, p_1, r_2, p_2, p_0)^T$ and

$$U_1 = -\sigma_1^2(r_1 + \mathcal{G}_1 r_1(r_1^2 + p_1^2) + \mathcal{G}_2(p_1 r_2 - r_1 p_2) + \mathcal{G}_3 r_1 p_0) -$$

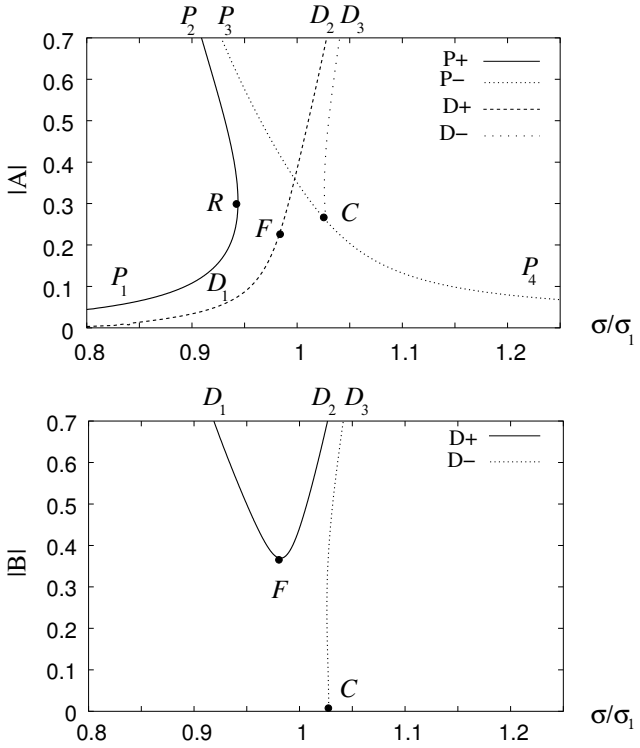

Fig. 3.31. Longitudinal (A) and transversal (B) amplitudes of steady-state resonant motions versus σ/σ_1. The results are given for $\alpha = 30^0$ and $H = 0.02$. Branches P_1P_2 and P_3P_4 imply 'planar', D_1D_2 denotes 'swirling' waves. R is the turning point, which divides the branch $P+$ into stable (P_1R) and unstable RP_2 subbranches. C is the Poincaré-bifurcation point. Here P_4C denotes the stable 'planar' solutions and CP_3 presents unstable ones. 'Swirling' is associated with the branches $D-$ and $D+$. The Hopf-bifurcation point F divides $D+$ into D_1F and FD_2, where D_1F implies unstable solutions, but FD_2 denotes a stable 'swirling'. There are no stable steady-state solutions for σ/σ_1 between abscissas of R and F.

$$
\begin{aligned}
&- \mathcal{D}_1 r_1(\dot{r}_1^2 + \dot{p}_1^2) - 2\mathcal{D}_2\dot{p}_1(p_1\dot{r}_1 - r_1\dot{p}_1) + \mathcal{D}_3(\dot{r}_1\dot{p}_2 - \dot{p}_1\dot{r}_2) - \mathcal{D}_5\dot{r}_1\dot{p}_0 + \\
&+ \Lambda H\sigma^2 \cos\sigma t;\\
U_2 = &-\sigma_1^2(p_1 + \mathcal{G}_1 p_1(r_1^2 + p_1^2) + \mathcal{G}_2(r_1r_2 + p_1p_2) + \mathcal{G}_3 p_1 p_0) - \\
&- \mathcal{D}_1 p_1(\dot{p}_1^2 + \dot{r}_1^2) - 2\mathcal{D}_2\dot{r}_1(r_1\dot{p}_1 - p_1\dot{r}_1) - \mathcal{D}_3(\dot{r}_1\dot{r}_2 + \dot{p}_1\dot{p}_2) - \mathcal{D}_5\dot{p}_1\dot{p}_0;
\end{aligned}
$$

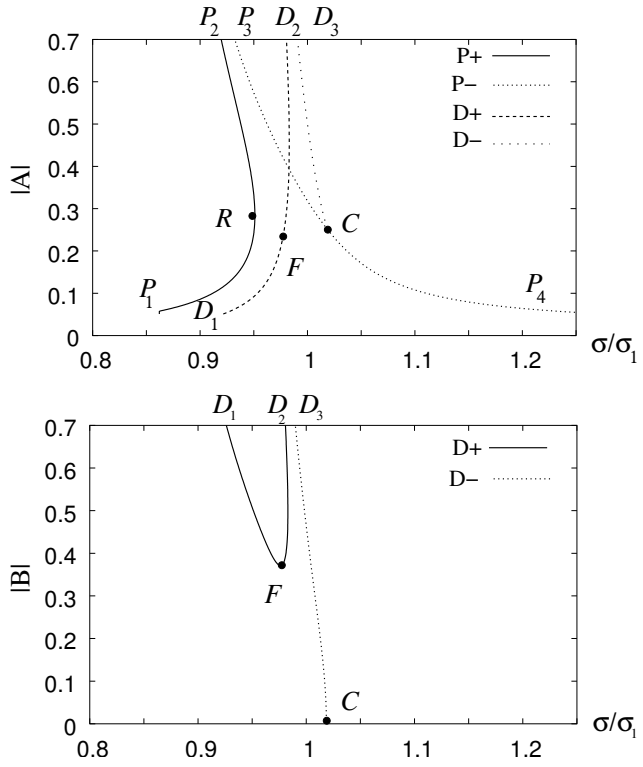

Fig. 3.32. The same as in Fig. 3.31, but for $\alpha = 45^0$.

$$U_3 = -\sigma_2^2(r_2 + 2\mathcal{G}_4 r_1 p_1) + 2\mathcal{D}_7 \dot{r}_1 \dot{p}_1;$$
$$U_4 = -\sigma_2^2(p_2 - \mathcal{G}_4(r_1^2 - p_1^2)) - \mathcal{D}_7(\dot{r}_1^2 - \dot{p}_1^2);$$
$$U_5 = -\sigma_0^2(p_0 + \mathcal{G}_5(r_1^2 + p_1^2)) - \mathcal{D}_8(\dot{r}_1^2 + \dot{p}_1^2).$$

The initial conditions should be defined from (3.100).

We solved the Cauchy problem (3.99), (3.100) by the fourth-order Runge-Kutta method. The simulations were made by a Pentium-II 366 computer. The simulation-time depended on the parameters of excitation. It varied between 1/10 to 1/300 of the real time-scale. Solutions (3.101), (3.102) made it possible to get initial conditions (3.100) to simulate steady-state regimes. These initial conditions were

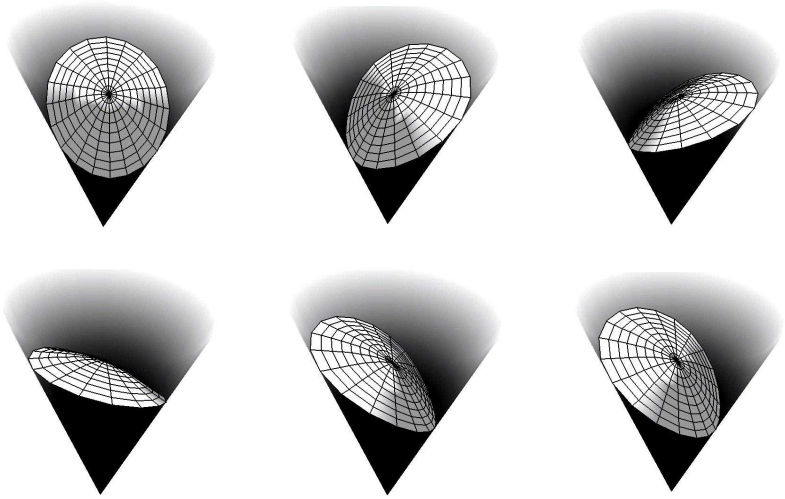

Fig. 3.33. Visualisation of 'swirling' for $\alpha = 30^0$, $H = 0.02$, $\sigma/\sigma_1 = 0.9967, A = 0.35, B = 0.419$ with $r_1(0) = 0.35, p_2(0) = 0.122, p_0(0) = 0.469$, $\dot{p}_1(0) = 0.1494, \dot{r}_2(0) = 0.316$.

$$\begin{aligned} &r_1(0) = A; \quad p_k(0) = A^2(l_k + h_k), \ k = 0, 2; \quad p_1(0) = r_2(0) = 0, \\ &\dot{r}_k(0) = \dot{p}_k(0) = 0; \ k = 1, 2; \quad \dot{p}_0 = 0 \end{aligned} \tag{3.160}$$

for 'planar', and

$$\begin{aligned} &r_1(0) = A; \ p_1(0) = 0; \quad p_2(0) = A^2(l_2 + h_2) + B^2(h_2 - l_2), \\ &p_0(0) = A^2(l_0 + h_0) + B^2(l_0 - h_0), \\ &\dot{r}_1(0) = 0; \quad \dot{p}_1(0) = \sigma B; \quad \dot{r}_2(0) = -4\sigma h_2 AB; \quad \dot{p}_2(0) = 0; \quad \dot{p}_0(0) = 0 \end{aligned} \tag{3.161}$$

for 'swirling' regime, respectively.

Typical three-dimensional wave patterns are presented in Fig. 3.33, 3.34 and 3.35. In particular, Fig. 3.34 and 3.35 illustrate the travelling wave phenomenon (see, movements of the peak C), which is explainable by contributions of the second-order modal functions r_2, p_2 and p_0.

Concluding remarks

Linear and nonlinear sloshing of an incompressible fluid in a conical tank was analysed within the framework of inviscid potential theory. Using a domain transformation technique by Lukovsky (1975) [112] and a functional basis, which satisfies both the Laplace equation and the Neumann boundary condition on the tank walls, we found the approximate linear sloshing modes. The method guarantees 5-6 significant figures of the linear natural frequencies with only 5-6 basis functions. The numerical results were validated by experimental data.

By utilising the approximate linear natural modes and results by Lukovsky (1990) [114] and Faltinsen *et al.* (2000) [45], we derived a nonlinear finite-dimensional asymptotic modal system. The derived modal system is a novelty in the scientific literature. It couples five natural modes and makes it possible to analyse resonant sloshing due to a horizontal harmonic excitation with the forcing frequency close to the lowest natural frequency. Applicability of the modal system is limited by possible progressive activation of higher modes caused by the secondary resonance. This was predicted for the semi-apex angles 6^0 and 12^0. Besides, shallow fluid sloshing (Faltinsen & Timokha (2002) [51] and Ockendon & Ockendon (2001) [140]) was quantified for $\alpha > 60^0$. Our nonlinear modal theory should be applicable in the range $25^0 < \alpha < 60^0$. Passage to $\alpha > 60^0$ needs significant revisions of the present modal technique towards the Boussinesq asymptotics, in the manner of Faltinsen *et al.* (2002) [51].

The analysis finds 'planar' and 'swirling' steady-state regimes as well as a frequency domain, where 'chaotic' waves (there are no stable steady-state regimes) are realised. Advantages and possibilities of the modal system in engineering and for visualising realistic wave patterns were demonstrated. A further perspective can be a detailed study of "chaotic" waves. The papers by Funakoshi & Inoue (1990,1991) [59, 60] are useful in this context.

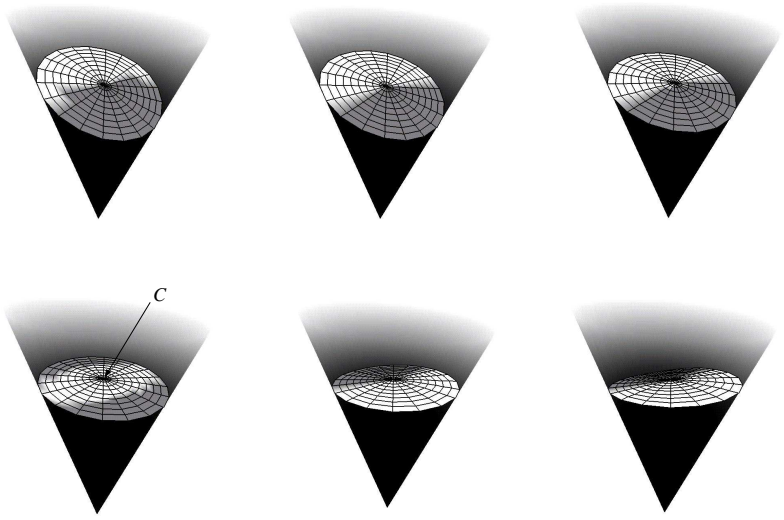

Fig. 3.34. Visualisation of 'planar' regime for $\alpha = 30^0$, $H = 0.02$, $\sigma/\sigma_1 = 0.936$, $A = 0.2$ with $r_1(0) = 0.2, p_2(0) = -0.0117$, $p_0(0) = 0.00314$.

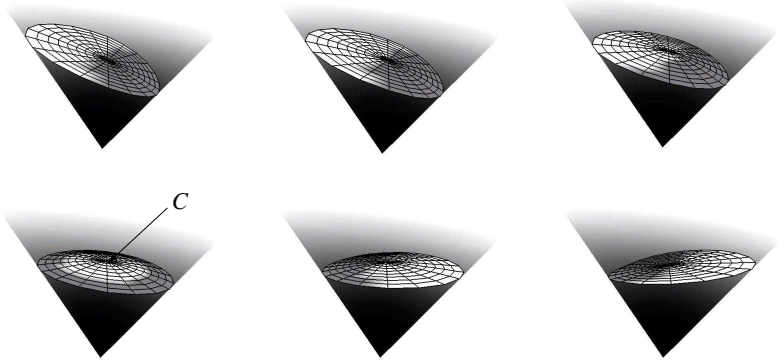

Fig. 3.35. Visualisation of 'planar' regime for $\alpha = 45^0$, $H = 0.02$, $\sigma/\sigma_1 = 0.9463$, $A = 0.2$ with $r_1(0) = 0.2, p_2(0) = -0.011$, $p_0(0) = -0.1137$.

Compressible potential flows with free boundaries

Surveys by Nevolin (1984) [137], Perlin & Schwartz (2000) [144], Faltinsen & Timokha (2001, 2002) [49, 51], Ibrahim *et al.* (2001,2005) [83, 82] and La Rocca *et al.* (2002,2005) [100, 101] as well as previous chapter outline theoretical and experimental results emphasising nonlinear gravity/capillary-gravity waves of the contained fluid due to resonant forcing. Incompressible potential flow is common and the forcing frequency is close to the lowest natural frequency. The interfacial waves occur relative to a static hydrodynamic equilibrium caused by surface tension and gravitation, which plays the role of a zero-order approximation in suitable asymptotic schemes (Faltinsen & Timokha (2002) [50]).

Contactless technology in chemical industry and material science may utilise acoustic loads for positioning the fluid, e.g. droplets, within the container (see, experiments on-board the Second United States Microgravity Lab by Wang (1996) [167], Apfel *et al.* (1998) [9] and Lie *et al.* (1998) [104] as well as model tests obtained within the framework of the NASA KS-135 space program by Wanis *et al.* (1999) [168] and the MICREX experimental program of the European Space Agency, Lierke (1991) [106]). This requires to account for the compressibility. The same is true for the high-frequency vibrations of the container that have been examined by Lubimov & Cherepanov (1981, 1986) [109, 110], Bezhdenezhnikh *et al.* (1991) [27], Khenner *et al.* (1999) [92] and Ivanova *et al.* (1998, 2001) [84, 85, 86]. These vibrations yield a variety of prominent physical phenomena and change the time-averaged fluid shapes, e.g. sawtooth (between two-layer fluids of similar densities) and inclined (fluid-gas system) reliefs were detected by Wolf (1969) [171], Bezdenezhnikh *et al.* (1984) [26] and Ganiyev *et al.* (1977) [61]. Theoretical studies are as a rule based on either equivalent pendulum-like mechanical models, or CFD-methods, or asymptotic schemes (Lubimov & Cherepanov (1986) [110], Beyer *et al.* (2001) [24]).

The time-averaged interfacial shapes owing to high-frequency loads, have been called the *vibroequilibria*. First observations of the vibroequilibria were reported by Faraday (1831) [52]. Experimental series 39-52 of his manuscript describe the flattening of fluid drops hanging beneath a vibrating plate. New era in studying the vibroequilibria have started with experiments by Wolf (1969, 1970) [171, 172] and, later on, by Lyubimov & Cherepanov (1981, 1986) [109], Bezdenezhnikh *et al.* (1991) [27], Khenner *et al.* (1999) [92] and Ivanova *et al.* (1998, 2001) [84, 85, 86]. Many physical phenomena observed in these works may methodologically be explained in terms of 'vibrational forces/energy' concept proposed by Kapitsa (1952) [90] and developed by Blekhman (1999) [29] for simple mechanical systems.

Analysis of the vibroequilibria was mainly conducted for relevant problems, in which convectional flows are of principal concern, e.g. influence of the modulated gravity field on melt crystallisation has been studied by Anilkumar *et al.* (1993) [8] and Lee *et al.* (1996) [104]. However, the fluid behaviour can in some cases be considered within the framework of an inviscid fluid model with irrotational flows. This occurs, for example, when the fluid density significantly larger than of the surrounding gas. Corresponding experiments were presented by Wolf (1969) [171], Ganiyev *et al.* (1977) [61] and Bezdenezhnikh *et al.* (1984) [26]. Assuming a perfect fluid with irrotational flow makes it possible to adopt Lagrangian (Hamiltonian) technique (Lukovsky & Timokha (1995) [117]) and, as a result, to derive a *variational theory of vibroequilibria*.

4.1 Variational principles

Lichtenstein (1929) [105], in his classical textbook, seemingly was the first, who gave a general formulation of Hamilton's principle for the motion of compressible fluids under various boundary conditions. Later on, Friedrichs (1934) [57] recognised the variational characterisation of free boundaries in steady potential flows. Since then, in a large number of contributions by Bateman (1930) [14], Bateman *et al.* (1956) [16], Berdichevskii (1983) [21], Luke (1967) [111], Lukovsky (1990) [114], Miles (1976) [125], Petrov (1964) [146] further types of variational principles were employed to characterise the non-stationary motion of a free boundary flow. Despite of a success in the mathematical treatment of compressible flows with the fixed boundaries (see, Lions (1998) [107]), strong

mathematical results on the fluid motion, e.g. long-time existence, blow-up, remained rare as long as the free boundaries are involved. Even for the local initial value problem, rigorous theories have reached only limited success. For diverse existence results compare e.g. Beyer & Günther (1998) [23], Myshkis *et al.* (1986) [132], Nishida (1986) [138], Ovsyannikov *et al.* (1985) [142] and the literature cited inside. The difficulties originate in the nonlinearity and complicated coupling between the boundary conditions and the governing differential equations. On the other hand, due to their practical relevance, the corresponding free boundary problems continue to challenge numerically-interested mathematicians to test new algorithms and software, see e.g. Cai *et al.* (1998) [33]. Numerical schemes based on variational formulations have proved useful in this contents (Wendlandt & Marsden (1997) [170]).

In this section, we centres around Hamilton's principles applied to non-stationary compressible fluid flows with the free boundary. It is aimed at formulating a variety of the principles governing the compressible potential flows driven by volume forces as well as by the surface tension and acoustic loading along the free and fixed (container-) boundary parts, respectively. A part of these principles (Theorem 4.1) requires the solution of a time-dependent family of the Neumann problems for computing the Hamilton action, the so-called kinematic subproblems. This preliminary step may be avoided at the expense of introducing additional state variables. The latter is performed in detail in Theorems 4.3 and 4.4.

4.1.1 Definitions

Let $x = (x_1, x_2, x_3)$ be Euclidean coordinates in $\mathbb{R}^3$ and let t denote the time. We consider the unsteady motion of a compressible fluid occupying a time-dependent bounded domain $Q(t)$, which contacts the walls of a rigid container $\widetilde{Q} = \{x \in \mathbb{R}^3 \,|\, \eta(x) < 0\}$, where η is a smooth function. Let $\partial Q(t) = S_1(t) \cup S_2 \cup \Sigma(t)$ with $S_1, S_2 \subseteq \partial\widetilde{Q}$, where S_2 denotes the (time-independent) location of an acoustic source and $\Sigma(t) = \{x \in \widetilde{Q} \,|\, \xi(x,t) = 0\}$ is the moving free boundary. Further, $\nabla\xi$ is always assumed to point out to the exterior of $Q(t)$. If $\varphi = \varphi(x,t)$, $p = p(x,t)$ and $\rho = \rho(x,t)$ are velocity potential, pressure and density of the fluid, respectively, then the free boundary problem considered here reads as

$$\rho\nabla\left(\dot{\varphi} + \frac{1}{2}|\nabla\varphi|^2 + U\right) = -\nabla p \quad \text{in} \quad Q(t), \tag{4.1}$$

$$\dot{\rho} + \operatorname{div}(\rho \nabla \varphi) = 0 \quad \text{in} \quad Q(t) \tag{4.2}$$

subject to the boundary conditions

$$\partial_n \varphi = 0 \text{ on } S_1(t);\ \partial_n \varphi = -|\nabla \xi|^{-1} \dot{\xi} \text{ on } \Sigma(t);\ \rho \partial_n \varphi = V \text{ on } S_2, \tag{4.3}$$

where $U = U(x,t)$ is the potential of the volume forces and $V = V(x,t)$ implies the normal velocity on the acoustic vibrator S_2.

Throughout this section, ∂_n is the derivative relative to the outer normal $n = (n_1, n_2, n_3)$ of $\partial Q(t)$ and the dot denotes differentiation with respect to the time. On $\Sigma(t)$ and $\partial\Sigma(t)$, respectively, the free boundary conditions

$$p - 2\sigma H = p_0 \quad \text{on} \quad \Sigma(t), \tag{4.4}$$

$$-\nabla \eta \nabla \xi = \beta |\nabla \eta| |\nabla \xi| \quad \text{on} \quad \partial\Sigma(t) \tag{4.5}$$

have to be fulfilled. H denotes the mean curvature of Σ, p_0 is the outer atmospheric pressure, which we assume to be constant, σ is coefficient of the surface tension and β is the relative adhesion coefficient between the fluid and the bounding walls.

The equations above are completed by a barotropic pressure-density relation

$$\rho = \rho(p). \tag{4.6}$$

Additionally, to guarantee mass conservation we impose

$$\int_{S_2} V \, dS = 0 \tag{4.7}$$

as an constraint to V.

4.1.2 Variational formulations

To establish Hamilton's principle for (4.1)-(4.6), we temporally fix ξ and ρ and let φ be a solution (defined to within a constant) of the Neumann problem

$$\operatorname{div}(\rho \nabla \varphi) = -\dot{\rho} \quad \text{in} \quad Q(t), \tag{4.8}$$

$$\partial_n \varphi = 0 \text{ on } S_1(t);\ \rho \partial_n \varphi = V \text{ on } S_2;\ \partial_n \varphi = -|\nabla \xi|^{-1} \dot{\xi} \text{ on } \Sigma(t). \tag{4.9}$$

As long as ρ is bounded positively against zero, Eq. (4.8) is uniformly elliptic. To guarantee the resolvability of the Neumann problem (4.8),

(4.9), we must impose Eq. (4.7) and restrict ξ and ρ, which we choose as state variables, to satisfy the constraint

$$\int_{Q(t)} \dot{\rho}\, dQ - \int_{\Sigma(t)} \rho |\nabla \xi|^{-1} \dot{\xi}\, d\Sigma = 0.$$

This implies

$$\int_{Q(t)} \rho\, dQ = \text{const}, \tag{4.10}$$

i.e. conservation of the total mass. Letting $W = W(\rho)$ the inner energy density of the fluid, then

$$p = \rho^2 W'(\rho) \tag{4.11}$$

gives the inverse function to (4.6). With this notation

$$\begin{aligned} L(t, \xi, \rho, \dot{\xi}, \dot{\rho}) = \int_{Q(t)} \rho \left(\frac{1}{2} |\nabla \varphi|^2 - W(\rho) - U \right) dQ - \\ - \sigma \Big(|\Sigma(t)| - \beta |S_1(t)| \Big) - p_0 |Q(t)| \end{aligned} \tag{4.12}$$

defines the Lagrangian of (4.1)-(4.6). In (4.12) the term $\sigma|\Sigma(t)|$ corresponds to the free surface energy and $\beta|S_1(t)|$ measures the wetting energy. Due to the compressibility we have to include the work $p_0|Q(t)|$ of external pressure.

Theorem 4.1. *For a fixed time interval* $[t_1, t_2]$ *let*

$$A(\xi, \rho) = \int_{t_1}^{t_2} L\, dt \tag{4.13}$$

denote the action corresponding to (4.12)*, considered under the restriction* (4.10)*, and subject to*

$$\delta\xi|_{t_1,t_2} = 0, \quad \delta\rho|_{t_1,t_2} = 0. \tag{4.14}$$

Then any sufficiently regular solution ξ, ρ *of the variational equations*

$$\delta_\xi A(\xi, \rho)\{\delta\xi\} + \delta_\rho A(\xi, \rho)\{\delta\rho\} = 0 \tag{4.15}$$

– for all variations $\delta\xi, \delta\rho$ *compatible with* (4.10), (4.14) *– satisfies the equations of motion* (4.1)-(4.6) *in* $[t_1, t_2]$ *(with the velocity potential* φ *computed from* (4.8), (4.9) *and the pressure given by* (4.11)*).*

Proof. Our starting point is the weak formulation of the Neumann problem (4.8) defining φ in dependence on ξ, ρ:

$$\int_{Q(t)} \dot{\rho}\psi \, dQ = \int_{Q(t)} \rho\nabla\varphi\nabla\psi \, dQ - \int_{S_2} V\psi \, dS + \int_{\Sigma(t)} \rho\dot{\xi}\psi|\nabla\xi|^{-1} \, d\Sigma$$

for all sufficiently smooth functions $\psi = \psi(\cdot, t)$ on $Q(t)$. Remembering the general differentiation rule for integrals over a time-dependent domain

$$\frac{d}{dt}\int_{Q(t)} f \, dQ = -\int_{\Sigma(t)} f\dot{\xi}|\nabla\xi|^{-1} \, d\Sigma + \int_{Q(t)} \dot{f} \, dQ, \tag{4.16}$$

(note that $\nabla\xi$ is directed toward the exterior of $Q(t)$) deduces

$$\frac{d}{dt}\int_{Q(t)} \rho\psi \, dQ - \int_{Q(t)} \rho\dot{\psi} \, dQ = \int_{Q(t)} \rho\nabla\varphi\nabla\psi \, dQ - \int_{S_2} V\psi \, dS. \tag{4.17}$$

The functional (4.12) is subject to (4.10) and, therefore, computing its derivative requires

$$\int_{Q(t)} \delta\rho \, dQ - \int_{\Sigma(t)} \rho\delta\xi|\nabla\xi|^{-1} \, d\Sigma = 0$$

for the variations $\delta\xi, \delta\rho$. In the following, partial derivatives $\delta_\xi A, \delta_\rho A$ are computed under that assumption. We start with variations of A with respect to ρ. From the definition of L and A we get immediately

$$\delta_\rho A = \int_{t_1}^{t_2}\int_{Q(t)} \delta\rho\left(\frac{1}{2}|\nabla\varphi|^2 - \frac{d}{d\rho}(\rho W) - U\right) + \rho\nabla\varphi\nabla\delta\varphi \, dQdt. \tag{4.18}$$

On the other hand, setting $\psi = \varphi$ in the ρ-variation of equation (4.17) and using (4.14) yields

$$\int_{t_1}^{t_2}\int_{Q(t)} \rho\nabla\varphi\nabla\delta\varphi \, dQdt = -\int_{t_1}^{t_2}\int_{Q(t)} \delta\rho\big(\dot{\varphi} + |\nabla\varphi|^2\big) \, dQ \, dt.$$

Substituting this into (4.18) finally gives

$$\delta_\rho A = -\int_{t_1}^{t_2}\int_{Q(t)} \delta\rho\left(\dot{\varphi} + \frac{1}{2}|\nabla\varphi|^2 + \frac{d}{d\rho}(\rho W) + U\right) dQ.$$

Similarly, by computing variations of A with respect to ξ, we get

$$\delta_\xi A = \int_{t_1}^{t_2} \Big\{ \int_{Q(t)} \rho \nabla\varphi \nabla\delta\varphi \, dQ -$$
$$- \int_{\Sigma(t)} \delta\xi |\nabla\xi|^{-1} \left(\frac{\rho}{2} |\nabla\varphi|^2 - \rho W - \rho U - p_0 - 2\sigma H \right) d\Sigma +$$
$$+ \sigma \int_{\partial\Sigma} \delta\xi \big(|\nabla\xi|^{-1} |\nabla\eta|^{-1} \nabla\eta\nabla\xi + \beta \big) \, dl \Big\} \, dt, \quad (4.19)$$

(concerning the variation of the surface area see, e.g. Giusti (1984) [76]).

Furthermore, variation of (4.17) with respect to ξ implies

$$\int_{t_1}^{t_2} \int_{Q(t)} \rho \nabla\varphi \nabla\delta\varphi \, dQ dt = - \int_{t_1}^{t_2} \int_{\Sigma(t)} \rho \big(\dot\varphi + |\nabla\varphi|^2 \big) \delta\xi |\nabla\xi|^{-1} \, d\Sigma dt,$$

hence

$$\delta_\xi A = \int_{t_1}^{t_2} \Big\{ \int_{\Sigma(t)} \left(\rho \Big(\dot\varphi + \frac{1}{2} |\nabla\varphi|^2 + W + U \Big) + p_0 + 2\sigma H \right) \delta\xi |\nabla\xi|^{-1} \, d\Sigma +$$
$$+ \sigma \int_{\partial\Sigma} \delta\xi \big(|\nabla\eta|^{-1} |\nabla\xi|^{-1} \nabla\eta\nabla\xi + \beta \big) \, dl \Big\} \, dt. \quad (4.20)$$

Obviously, the integrals on the right-hand sides of (4.19), (4.20) can be thought of as linear functionals, in which the variables $\delta\xi$, $\delta\rho$ are not coupled. Adopting this point of view, comparison of (4.19), (4.20) with (4.15) via the Lagrange multiplier rule leads to

$$\delta_\rho A\{\delta\rho\} = - \int_{t_1}^{t_2} \lambda \int_{Q(t)} \delta\rho \, dQ \, dt,$$
$$\delta_\xi A\{\delta\xi\} = \int_{t_1}^{t_2} \lambda \int_{\Sigma(t)} \rho \delta\xi |\nabla\xi|^{-1} \, d\Sigma \, dt$$

for all $\delta\xi$, $\delta\rho$ with a time-dependent Lagrange multiplier $\lambda = \lambda(t)$, i.e.

$$\begin{aligned} &\dot\varphi + \frac{1}{2} |\nabla\varphi|^2 + \frac{d}{d\rho}(\rho W) + U = \lambda \quad \text{in} \quad Q(t), \\ &\rho \left(\dot\varphi + \frac{1}{2} |\nabla\varphi|^2 + U + W \right) + p_0 + 2\sigma H = \lambda\rho \quad \text{on} \quad \Sigma(t), \end{aligned} \quad (4.21)$$

and, as a result of variation along $\partial\Sigma$,

$$|\nabla\eta|^{-1} |\nabla\xi|^{-1} \nabla\eta\nabla\xi + \beta = 0.$$

When computing the pressure p from (4.11), the latter implies (4.1)-(4.6). □

Remark 4.2. From (4.11) and (4.21) it follows

$$\rho\left(\dot\varphi + \frac{1}{2}|\nabla\varphi|^2 + U + W\right) + p = \lambda\rho$$

along any extremal. Without loss of generality, by adding a suitable time-dependent constant to φ we can assume $\lambda = 0$. According to this normalisation of φ, we get

$$\begin{aligned} A = &\int_{t_1}^{t_2}\left\{\int_{Q(t)}(p-p_0)\,dQ - \sigma\big(|\Sigma(t)| - \beta|S_1(t)|\big)\right\}dt \\ &+ \int_{t_1}^{t_2}\int_{S_2} V\varphi\,dS\,dt + \int_{Q(t)}\rho\varphi\,dQ\,\Big|_{t_1}^{t_2} \end{aligned}$$

(along an extremal). Here, the kinetic energy is expressed as an integral over the pressure, cf. also Hargreaves (1908) [79].

In Theorem 4.1, the velocity potential appears as a solution of the Neumann problem (4.8)-(4.9). Generally, for numerical purposes it is desirable to exclude this constrain. Following ideas by Bateman *et al.* (1956) [16] and Luke (1967) [111], we furthermore consider φ as an additional independent variable. In that case, Eq. (4.8) as well as the boundary conditions (4.9) turn into natural optimality conditions, which may be derived from the φ-variations of the functional

$$J(\xi,\rho,\varphi) = \int_{t_1}^{t_2}\left\{\int_{Q(t)} -\rho\Big(\dot\varphi + \frac{1}{2}|\nabla\varphi|^2\Big)\,dQ + \int_{S_2} V\varphi\,dS\right\}dt.$$

Indeed,

$$\delta_\varphi J = \int_{t_1}^{t_2}\left\{\int_{Q(t)} -\rho(\delta\dot\varphi + \nabla\varphi\nabla\delta\varphi)\,dQ + \int_{S_2} V\delta\varphi\,dS\right\}dt$$

and, after integration by parts

$$\delta_\varphi J = \int_{t_1}^{t_2}\left\{\int_{Q(t)}\big(\dot\rho + \operatorname{div}(\rho\nabla\varphi)\big)\delta\varphi\,dQ -\right.$$

$$- \int_{S_1(t)} \rho \partial_n \varphi \delta\varphi \, dS - \int_{S_2} (\rho \partial_n \varphi - V) \delta\varphi \, dS -$$
$$- \int_{\Sigma(t)} \rho(\partial_n \varphi - \dot{\xi} |\nabla \xi|^{-1}) \delta\varphi \, dS \Big\} \, dt - \int_{Q(t)} \rho \delta\varphi \, dQ \Big|_{t_1}^{t_2},$$

$\delta_\varphi J(\xi, \rho, \varphi)\{\delta\varphi\} = 0$ for all $\delta\varphi$ with $\delta\varphi|_{t_1,t_2} = 0$ implies φ to be a solution of (4.8), (4.9). The resolvability condition for (4.8), (4.9) is met automatically. With this independent velocity potential φ, one obtains

$$J = \int_{t_1}^{t_2} \int_{Q(t)} \frac{1}{2} \rho |\nabla \varphi|^2 \, dQ \, dt + \int_{Q(t)} \rho \varphi \, dQ \Big|_{t_1}^{t_2}.$$

The ξ, ρ-variations of the second term on the right-hand side vanishes if $\delta\xi$, $\delta\rho$ satisfies (4.14). Thus, we get after comparison with (4.12) and Theorem 4.1:

Theorem 4.3. *Any sufficiently regular critical point* (ξ, ρ, φ) *of the functional*

$$B(\xi, \rho, \varphi) = \int_{t_1}^{t_2} \Big\{ \int_{Q(t)} -\rho \Big(\dot{\varphi} + \frac{1}{2} |\nabla \varphi|^2 + U + W(\rho) \Big) \, dQ -$$
$$- \sigma \big(|\Sigma(t)| - \beta |S_1(t)| \big) + \int_{S_2} V \varphi \, dS - p_0 |Q(t)| \Big\} \, dt$$

subject to

$$\delta\xi|_{t_1,t_2} = 0, \quad \delta\rho|_{t_1,t_2} = 0, \quad \delta\varphi|_{t_1,t_2} = 0$$

satisfies (4.1)-(4.6). □

The following Theorem 4.4, where ξ and φ have been introduced as independent variables, can be viewed as a counterpart to Theorem 4.3. Let P be a primitive of $1/\rho$:

$$P(\tau) = \int \frac{d\tau}{\rho(\tau)} + \text{const},$$

where the constant is chosen such that

$$\frac{d}{d\rho} \big(\rho W(\rho) \big) = P\big(\rho^2 W'(\rho) \big). \tag{4.22}$$

Because P is strictly monotone, the inverse function P^{-1} exists. With this function we have:

Theorem 4.4. *Under the constraints*

$$\delta\xi|_{t_1,t_2} = 0, \quad \delta\varphi|_{t_1,t_2} = 0$$

any sufficiently regular critical point (ξ, φ) *of the functional* $C = C(\xi, \varphi)$ *with*

$$C(\xi,\varphi) = \int_{t_1}^{t_2} \Big\{ \int_{Q(t)} P^{-1}\Big(-\dot\varphi - \frac{1}{2}|\nabla\varphi|^2 - U\Big)\, dQ - \\ - \sigma\big(|\Sigma(t)| - \beta|S_1(t)|\big) + \int_{S_2} V\varphi\, dS - p_0|Q(t)|\Big\}\, dt$$

satisfies (4.1)-(4.6).

Proof. For given (ξ, φ) we determine $\rho = \rho[\xi, \varphi]$ with

$$\dot\varphi + \frac{1}{2}|\nabla\varphi|^2 + U + W(\rho) + \rho W'(\rho) = 0 \quad \text{in} \quad Q(t).$$

This is equivalent to

$$\delta_\rho B(\xi, \rho, \varphi)\{\delta\rho\} = 0 \quad \text{for all} \quad \delta\rho \tag{4.23}$$

with the functional $B = B(\xi, \rho, \varphi)$ from Theorem 4.3. In view of (4.22), this means

$$-\Big(\dot\varphi + \frac{1}{2}|\nabla\varphi|^2 + U\Big) = \frac{d}{d\rho}\big(\rho W(\rho)\big) = P\big(\rho^2 W'(\rho)\big) \\ = P\Big(-\rho\Big(\dot\varphi + \frac{1}{2}|\nabla\varphi|^2 + U + W\Big)\Big),$$

hence, $C(\xi, \varphi) = B(\xi, \rho, \varphi[\xi, \varphi])$ and Theorem 4.3 gives the assertion. □

4.2 Variational vibroequilibria

When a high-frequency vibrational loading is included, compressible potential flows may behave in an unexpected way, so that the time-averaged shapes of the free surface become far from the capillary meniscus. These time-averaged shapes are called the *vibroequilibria*. By transformation to non-dimensional variables and introduction of a small parameter characterising the high-frequency contributions of the excitation we construct,

via truncating the Hamilton action, a class of oscillatory solutions. Their time-averaged free boundaries turn out to be critical points of a functional, which can be considered as a quasi-potential for the vibroequilibria, a *vibropotential*. This is outlined in Theorems 4.6 and 4.7. To get further information about the principal symbol and the mapping properties of the corresponding Jacobi operator in Theorem 4.10 we compute the second variation of this potential. This makes it possible to prove that local minima of the vibropotential imply vibroequilibria, which are stable relative to small perturbations.

In the following, the free boundary problem (4.1)-(4.6) is considered with a time-dependent potential

$$U(x,t) = -gx_3 - \omega^2 a_i x_i \sin(\omega t)$$

(usual summation convention over repeated indexes is used), in which

$$\omega \to \infty, \qquad \omega|a| = \text{const}, \tag{4.24}$$

i.e. under the influence of a time-periodic volume force with an amplitude increasing proportionally to the forcing frequency. Further, we disregard any additional acoustic source at the boundary, hence, we may set $V = 0$ and $S(t) = S_1(t) + S_2$, and (4.6) is specified to the adiabatic pressure-density relation

$$\rho = \rho_0 (p/p_0)^{1/\gamma} \qquad (\gamma > 1).$$

For our purposes it is advantageous to rewrite the system (4.1)-(4.6) in a non-dimensional form. Letting l be a representative length, we replace the original domains and variables according to

$$Q_{new}(t) = l^{-1} Q(t), \quad \Sigma_{new}(t) = l^{-1}\Sigma(t), \quad x_{new} = l^{-1}x, \quad t_{new} = \omega t,$$

as well as

$$\varphi_{new} = \varphi/l^2\omega, \quad p_{new} = p/\rho_0 l^2\omega^2, \quad \rho_{new} = \rho/\rho_0,$$
$$p_{0,new} = p_0/\rho_0 l^2\omega^2, \quad a_{new} = a/|a|.$$

Then, introducing the non-dimensional parameters

$$\varepsilon = |a_{orig}|/l, \quad \mu = \sigma/\omega^2 |a_{orig}|^2 l\rho_0, \quad b = gl^2\rho_0/\sigma \text{ (“Bond number”)},$$

and retaining the original notation, the system (4.1)-(4.6) takes the form

$$\rho\nabla\Big(\dot\varphi+\frac{1}{2}|\nabla\varphi|^2+\mu\varepsilon^2 bx_3+\varepsilon a_i x_i\sin t\Big)=-\nabla p, \tag{4.25}$$

$$\dot\rho+\operatorname{div}(\rho\nabla\varphi)=0 \quad \text{in} \quad Q(t), \tag{4.26}$$

subject to the boundary conditions

$$\partial_n\varphi=0 \ \text{ on } \ S(t), \quad \partial_n\varphi=-|\nabla\xi|^{-1}\dot\xi \ \text{ on } \ \Sigma(t), \tag{4.27}$$

$$p-2\mu\varepsilon^2 H=p_0 \ \text{ on } \ \Sigma(t), \quad -\nabla\eta\nabla\xi=\beta|\nabla\eta||\nabla\xi| \ \text{ on } \ \partial\Sigma(t). \tag{4.28}$$

With respect to the new variables the pressure-density relation reads as

$$\rho=(p/p_0)^{1/\gamma}. \tag{4.29}$$

According to (4.24), we consider (4.25)-(4.29) under hypothesis that $\varepsilon \ll 1$ and μ, b are fixed. Attention is paid to a cylindrical container $\widetilde{Q}=B\times[0,\infty)$ over a fixed bottom $B\subset\mathbb{R}^2$ and the free surface is assumed to be a graph over B:

$$\Sigma(t)=\{x\in\mathbb{R}^3 \mid x_3=\zeta(x_1,x_2,t),(x_1,x_2)\in B\},$$

i.e. $\xi=x_3-\zeta$.

According to Theorem 4.1, which is referred to in the following exclusively, we obtain (4.25)-(4.29) as the Euler-Lagrange equation of the action-functional

$$A(\zeta,\rho;\varepsilon)=\int_{t_1}^{t_2}\Big\{\int_{Q(t)}\rho\Big(\frac{1}{2}|\nabla\varphi|^2-W-\mu\varepsilon^2 bx_3-\varepsilon a_i x_i\sin t\Big)\,dQ- \\ -\mu\varepsilon^2\big(|\Sigma(t)|-\beta|S(t)|\big)-p_0|Q(t)|\Big\}\,dt \tag{4.30}$$

under the mass conservation condition. As a consequence of the adiabatic pressure-density relation, the inner energy density is given by

$$W(\rho)=\text{const}+p_0\rho^{\gamma-1}/(\gamma-1).$$

In the following we construct the 2π-periodic asymptotic solutions (in the sense explained below) of the variational equation

$$\delta A(\zeta,\rho;\varepsilon)=0 \quad \text{subject to} \quad \delta\int_{Q(t)}\rho\,dx=0. \tag{4.31}$$

Accordingly, the time varies in $S^1 = \mathbb{R}/2\pi$. Choosing $t_1 = 0, t_2 = 2\pi$, we have to replace (4.14) by the periodicity conditions

$$\zeta(\cdot, 0) = \zeta(\cdot, 2\pi), \quad \rho(\cdot, 0) = \rho(\cdot, 2\pi).$$

In the zero-approximation, when $\varepsilon = 0$, any pair $(\zeta_0, 1)$ with a time-independent shape $\zeta_0 = \zeta_0(x_1, x_2)$ of the free surface is a solution of (4.31), which simply reflects the fact that an isolated fluid at rest is in a neutral equilibrium. Let

$$Q_0 = \{x \in \mathbb{R}^3 \mid (x_1, x_2) \in B, 0 < x_3 < \zeta_0(x_1, x_2)\},$$

then

$$A(\zeta_0, 1; 0) = -2\pi\big(p_0 + W(1)\big)|Q_0| = 0, \tag{4.32}$$

if the inner energy density W is suitably normalised: $W(1) + W'(1) = 0$. A closer look at (4.30) shows, that

$$\delta A(\zeta_0, 1; 0) = 0 \quad \text{for arbitrary variations } \delta\zeta, \delta\rho \tag{4.33}$$

under this normalisation. Therefore it is reasonable to choose the solution

$$\zeta_\varepsilon = \zeta_0(x_1, x_2) + \varepsilon\zeta_1(x_1, x_2, t), \quad \rho_\varepsilon = 1 + \varepsilon\rho_1(x, t) \tag{4.34}$$

as the starting point for our construction. Here ζ_1 is normalised by the mean value zero in time, i.e.

$$\int_0^{2\pi} \zeta_1(x_1, x_2, t)\, dt = 0. \tag{4.35}$$

The side condition in (4.31) requires

$$|Q_0| = \int_B \zeta_0(x_1, x_2)\, dB = \text{const}, \tag{4.36}$$

$$\int_{Q_0} \rho_1(x, t)\, dQ + \int_B \zeta_1(x_1, x_2, t)\, dB = 0. \tag{4.37}$$

In view of (4.32), (4.33), inserting (4.34) into (4.30) gives

$$A(\zeta_\varepsilon, \rho_\varepsilon, \varepsilon) = \varepsilon^2 \widetilde{A}(\zeta_0, \zeta_1, \rho_1) + O(\varepsilon^3) \tag{4.38}$$

with

$$\widetilde{A} = \int_0^{2\pi} \Big\{ \int_{Q_0} \frac{1}{2}|\nabla\varphi_1|^2 - \frac{\rho_1^2}{2k^2} - \mu b x_3 - a_i x_i \rho_1 \sin t \, dQ - \\ - \int_{\Sigma_0} a_i x_i \zeta_1 \sin t \, dB \Big\} dt - 2\pi\mu\big(|\Sigma_0| - \beta|S_0|\big). \quad (4.39)$$

Here, the wave number $k = (\gamma p_0)^{-1/2}$ has been introduced, Σ_0, S_0 denote the free and wetting parts of ∂Q_0, respectively, and φ_1 is the first order term in the expansion

$$\varphi(\zeta_\varepsilon, \rho_\varepsilon) = \varepsilon\varphi_1(\zeta_0, \zeta_1, \rho_1) + O(\varepsilon^2).$$

As may be read off (4.26), (4.27), the velocity potential φ_1 is solution of the Neumann problem

$$\begin{aligned} \Delta\varphi_1 &= -\dot{\rho}_1 \ \text{ in } \ Q_0; \quad \partial_n\varphi_1 = 0 \ \text{ on } \ S_0, \\ \partial_n\varphi_1 &= (1 + |\nabla\zeta_0|^2)^{-1/2}\dot{\zeta}_0 \ \text{ on } \ \Sigma_0. \end{aligned} \quad (4.40)$$

The expansion (4.38) makes it possible to define the pair $(\zeta_\varepsilon, \rho_\varepsilon)$ as an *ε-approximate solution* of (4.31) if $(\zeta_0, \zeta_1, \rho_1)$ is a critical point of the truncated action, i.e.

$$\delta\widetilde{A}(\zeta_0, \zeta_1, \rho_1) = 0 \quad (4.41)$$

for all variations $\delta\zeta_0, \delta\zeta_1, \delta\rho_1$ compatible with (4.35)-(4.37). To determine solutions of (4.41), first, we have to compute the ζ_1, ρ_1-variations of $\widetilde{A}$.

Proposition 4.5. *For a fixed ζ_0, solution of the Euler-Lagrange equations*

$$\delta_{\zeta_1}\widetilde{A}(\zeta_0, \zeta_1, \rho_1)\{\delta\zeta_1\} + \delta_{\rho_1}\widetilde{A}(\zeta_0, \zeta_1, \rho_1)\{\delta\rho_1\} = 0$$

– for all variations $\delta\zeta_1, \delta\rho_1$ compatible with (4.35), (4.37) – leads to a time-periodic boundary value problem for an inhomogeneous wave equation:

$$\ddot{\varphi}_1 - k^{-2}\Delta\varphi_1 = -a_i x_i \cos t \quad \textit{in} \quad Q_0 \times S^1, \quad (4.42)$$

$$\partial_n\varphi_1 = 0 \ \textit{ on } \ S_0 \times S^1, \qquad \dot{\varphi}_1 = -a_i x_i \sin t \ \textit{ on } \ \Sigma_0 \times S^1, \quad (4.43)$$

$$\int_0^{2\pi} \partial_n\varphi_1(\cdot, t)\, dt = 0 \quad \textit{on} \quad \Sigma_0. \quad (4.44)$$

After solving (4.42)-(4.44) we get ζ_1, ρ_1 from

$$\dot{\zeta}_1 = (1 + |\nabla\zeta_0|^2)^{1/2}\partial_n\varphi_1 \quad \textit{on} \quad \Sigma_0 \times S^1, \quad (4.45)$$

$$\rho_1 = -k^2(\dot{\varphi}_1 + a_i x_i \sin t) \quad in \quad Q_0 \times S^1. \tag{4.46}$$

In view of (4.35), ζ_1 *is determined uniquely by* (4.45).

Proof. Any stationary point of $\delta\widetilde{A} = 0$ subject to (4.35), (4.37) satisfies

$$\dot{\varphi}_1 + k^{-2}\rho_1 = -a_i x_i \sin t + \lambda(t) \quad \text{in} \quad Q_0 \times S^1, \tag{4.47}$$

$$\dot{\varphi}_1 = -a_i x_i \sin t - \lambda(t) + c(x) \quad \text{on} \quad \Sigma_0 \times S^1 \tag{4.48}$$

with two Lagrangian multipliers λ and c. Since

$$\int_0^{2\pi} \lambda(t)\, dt = 2\pi c(x)$$

by (4.48), it follows $c(x) = c = \text{const}$. After normalising φ_1, we may assume $\lambda = \text{const} = c$. In that case, integration of (4.47) yields

$$2k^2\pi c|Q_0| = \int_0^{2\pi}\int_{Q_0} \rho_1\, dQdt = -\int_0^{2\pi}\int_B \zeta_1\, dBdt = 0$$

because of (4.35), hence $c = 0$. Now, after differentiation with respect to t, (4.47), (4.48) imply (4.42), (4.43).
□

To outline the resolvability of the boundary value problem (4.42)-(4.44), let $\Lambda(\zeta_0)$ denote the spectrum of the Neumann-Dirichlet problem for the Laplace equation:

$$\Delta u + \lambda u = 0 \ \text{ in } \ Q_0; \quad \partial_n u = 0 \ \text{ on } \ S_0, \quad u = 0 \ \text{ on } \ \Sigma_0. \tag{4.49}$$

Under mild regularity assumptions on Σ_0 and ∂B, the embedding of the Sobolev space $H^1(Q_0)$ into $L^2(Q_0)$ is compact and the trace operator $u \mapsto u|_{\Sigma_0}$ maps $H^1(Q_0)$ into $H^{1/2}(\Sigma_0)$ continuously, see e.g. Nečas (1964)[136]. Then the set $\Lambda(\zeta_0)$ consists of a countable number of positive reals with the unique limit point $+\infty$. For $k^2 \notin \Lambda(\zeta_0)$

$$\varphi_1(x,t) = \psi(x)\cos t \tag{4.50}$$

is a solution of (4.42)-(4.43) if ψ is chosen according to

$$\Delta\psi + k^2\psi = k^2 a_i x_i \ \text{ in } \ Q_0; \ \partial_n\psi = 0 \ \text{ on } \ S_0; \ \psi = a_i x_i \ \text{ on } \ \Sigma_0. \tag{4.51}$$

Then, in view of (4.50), we get via (4.45), (4.46)

$$\zeta_1(x_1,x_2,t)=\zeta_1^\star(x_1,x_2)\sin t,\qquad \rho_1(x,t)=\rho_1^\star(x)\sin t, \tag{4.52}$$

with

$$\zeta_1^\star=(1+|\nabla\zeta_0|^2)^{1/2}\partial_n\psi,\qquad \rho_1^\star=k^2(\psi-a_ix_i). \tag{4.53}$$

Moreover, if $n^2k^2\notin\Lambda(\zeta_0)$ for all $n\in\mathbb{Z}$, then (4.50) is the unique solution to within a constant. This is easily seen from the Fourier separation method.

Concerning the remaining derivative of $\widetilde{A}$ by ζ_0 we get, after calculation along the lines followed from the proof of Theorem 4.1,

$$\begin{aligned}\delta_{\zeta_0}\widetilde{A}=\int_0^{2\pi}\int_{\Sigma_0}\Big\{&-\frac{1}{2}|\nabla\varphi_1|^2+\dot\zeta_1\partial_3\varphi_1-\dot\rho_1\varphi_1-\frac{\rho_1^2}{2k^2}-\\&-\mu\varepsilon^2bx_3-(a_ix_i\rho_1+a_3\zeta_1)\sin t\Big\}\,\delta\zeta_0\,dB\,dt+\\&+2\pi\mu\int_B\operatorname{div}\mathsf{T}\zeta_0\delta\zeta_0\,dB-2\pi\mu\int_{\partial B}(\nu\cdot\mathsf{T}\,\zeta_0-\beta)\delta\zeta_0\,dl,\end{aligned}$$

where the variation $\delta\zeta_0$ is compatible with the side conditions (4.36), (4.37). To shorten the notation, the nonlinear operator

$$\mathsf{T}\zeta_0=(1+|\nabla\zeta_0|^2)^{-1/2}\nabla\zeta_0$$

and the outer normal ν to ∂B have been introduced. Evaluating $\delta_{\zeta_0}\widetilde{A}$ at the extremal ζ_1,ρ_1 of Proposition 4.5 leads to

Theorem 4.6. *If $k^2\notin\Lambda(\zeta_0)$ and ψ, $\zeta_1^\star$, $\rho_1^\star$ are taken from* (4.51), (4.53) *then the pair*

$$(\zeta_\varepsilon,\rho_\varepsilon)=(\zeta_0+\varepsilon\zeta_1^\star\sin t,1+\varepsilon\rho_1^\star\sin t)$$

defines an ε-approximate solution of $\delta A=0$, if and only if,

$$4\mu H+\frac{1}{2}|\nabla(\psi-a_ix_i)|^2-2\mu bx_3=\lambda\quad on\quad\Sigma_0, \tag{4.54}$$

$$\nu\cdot\mathsf{T}\zeta_0=\beta\quad on\quad\partial B \tag{4.55}$$

with a Lagrange multiplier $\lambda=const.$ □

The principal part $H = \frac{1}{2}\mathrm{div}\mathsf{T}\zeta_0$ of (4.54) is the mean curvature of Σ_0; hence, the problem (4.54) generalises the equilibrium condition for a fluid-air interface in a vertical gravity field known from the capillarity theory. In our setting, due to vibration, an additional nonlinear first-order pseudo-differential operator appears in the equilibrium condition. Alternatively, (4.54) can be viewed as a counterpart to Bernoulli's equation for incompressible fluid flows. We call any surface Σ_0 given by a solution ζ_0 of (4.54), (4.55) the *vibrocapillary equilibrium.*

An integration of (4.54) by parts yields

$$2\mu\big(\beta\,|\partial B| - b\,|Q_0|\big) \le |B|\lambda,$$

which means that the Lagrange multiplier λ in (4.54) is bounded from below in terms of the given data. In the pure capillary case there holds equality.

As is clear from the above reasoning equations (4.54), Eq. (4.55) must appear as a variational equation.

Theorem 4.7. *Under the assumptions of Theorem 4.6 any solution* ζ_0 *of the equilibrium equations* (4.54), (4.55) *is a critical point of the time-independent functional*

$$\Pi(\zeta_0) = -\frac{1}{\pi}\widetilde{A}(\zeta_0, \zeta_1^\star \sin t, \rho_1^\star \sin t)$$

under the volume conserving variations. The explicit expression of Π *reads as*

$$\Pi(\zeta_0) = 2\mu\big(|\Sigma_0| - \beta|S_0|\big) + \frac{1}{2}\int_{Q_0}\big(|\nabla\psi|^2 - k^2(\psi - a_i x_i)^2 + 4\mu b x_3\big)\,dQ.\square$$

Henceforth, Π is called the *quasi-potential of vibroequilibria* or *vibropotential.* In order to gain an insight into diverse mapping properties of the quasi-potential Π, we study its second variation $\delta^2\Pi$. This may be of particular interest in the stability analysis as well as in various numerical approaches. We identify functions originally defined on Σ_0 by constant continuation along x_3-direction with functions on B. Obviously, the second variation of the capillary term $\Pi_0(\zeta_0) = |\Sigma_0| - \beta|S_0|$ in Π reads as

$$\delta^2\Pi_0(\zeta_0)\{h,h\} = \int_B \big(|\nabla h|^2 - (\mathsf{T}\zeta_0\cdot\nabla h)^2\big)n_3\,dB.$$

Since admissible variations h must have mean value zero, this implies

$$\delta^2 \Pi_0(\zeta_0)\{h,h\} \geq pos.C^{te}\|h\|_1^2$$

in view of Friedrich's inequality and $|\mathsf{T}\zeta_0| < 1$. Here and in the following $\|\cdot\|_s$ denote the norm in the Sobolev space H^s. Introducing the tangential gradient $\nabla_{\Sigma_0} = (D_1, D_2, D_3)$ and the Laplace-Beltrami operator Δ_{Σ_0}:

$$\nabla_{\Sigma_0} = \nabla - n\partial_n, \qquad \Delta_{\Sigma_0} = D_i D_i$$

there holds $|\nabla h|^2 - (\mathsf{T}\zeta_0 \cdot \nabla h)^2 = |\nabla_{\Sigma_0} h|^2$ and an integration by parts implies

$$\delta^2 \Pi_0(\zeta_0)\{h,h\} = -\int_{\Sigma_0} h \mathrm{div}_{\Sigma_0}\left(n_3^2 \nabla_{\Sigma_0} h\right) d\Sigma$$

if $h = 0$ on ∂B. Remembering the relation

$$\Delta_{\Sigma_0} n_j = -c^2 n_j - 2D_j H,$$

where c^2 is the sum of the squares of the principal curvatures of Σ_0, see e.g. Giusti (1984) [76], we infer

$$\begin{aligned}\mathrm{div}_{\Sigma_0}\left(n_3^2 \nabla_{\Sigma_0}\right) &= \mathrm{div}_{\Sigma_0}\left(n_3 \nabla_{\Sigma_0}(n_3 h)\right) - \mathrm{div}_{\Sigma_0}\left(n_3 h \nabla_{\Sigma_0}(n_3)\right) = \\ &= n_3\left(\Delta_{\Sigma_0}(n_3 h) + (2D_3 H + c^2 n_3)h\right).\end{aligned}$$

Hence

$$Lh = -n_3 \Delta_{\Sigma_0}(n_3 h) - n_3(2D_3 H + c^2 n_3)h$$

gives the Euler-Lagrange operator to $\delta^2 \Pi_0$.

According to Theorem 4.6 the first variation of the nonlocal part

$$\Pi_1(\zeta_0) = \frac{1}{2}\int_{Q_0} \left(|\nabla\psi|^2 - k^2(\psi - a_i x_i)^2\right) dQ.$$

of Π reads as

$$\delta\Pi_1(\zeta_0)\{h\} = -\frac{1}{2}\int_{\Sigma_0} |\nabla(\psi - a_i x_i)|^2 h \, dB.$$

This implies

$$\begin{aligned}&\delta^2 \Pi_1(\zeta_0)\{h,h\} = \\ &\quad = -\int_{\Sigma_0} \Big(\nabla(\psi - a_i x_i)\nabla\delta\psi + h\nabla(\psi - a_i x_i)\nabla(\psi_{x_3} - a_3)\Big) h \, dB.\end{aligned}$$

Here, $\delta\psi$ has to satisfy the Dirichlet-Neumann problem

$$\Delta\delta\psi + k^2\delta\psi = 0 \text{ in } Q_0; \quad \partial_n\delta\psi = 0 \text{ on } S, \quad \delta\psi = (a_3 - \psi_{x_3})h \text{ on } \Sigma_0.$$

Considering the expression for the Laplacian relative to normal and tangential derivatives along Σ_0

$$\Delta = \partial_n^2 - 2H\partial_n + \Delta_{\Sigma_0}, \qquad \partial_n^2 = n_i n_j \partial_i \partial_j$$

and $\psi - a_i x_i|_{\Sigma_0} = 0$, $\Delta\psi|_{\Sigma_0} = 0$, we get

$$\partial_n^2(\psi - a_i x_i) = 2H\partial_n(\psi - a_i x_i).$$

In view of $\partial_3 = n_3\partial_n + D_3$, there holds

$$\partial_n\partial_3 = n_3\partial_n^2 + n_i D_3 \partial_i = n_3\partial_n^2 + D_3\partial_n - (D_3 n_i)\partial_i$$

and consequently

$$\partial_n(\psi_{x_3} - a_3) = (2n_3 H + D_3)\partial_n(\psi - a_i x_i).$$

Thus, we have proved:

Proposition 4.8. *Under the assumption $k^2 \notin \Lambda(\zeta_0)$ let*

$$C_{\Sigma_0} : H^{1/2}(\Sigma_0) \to H^{-1/2}(\Sigma_0), \quad C_{\Sigma_0}(u) = \partial_n\widetilde{u}|_{\Sigma_0},$$

be the "capacity operator" where $\widetilde{u}$ denotes the solution of

$$\Delta\widetilde{u} + k^2\widetilde{u} = 0 \text{ in } Q_0; \quad \partial_n\widetilde{u} = 0 \text{ on } S, \quad \widetilde{u} = u \text{ on } \Sigma_0.$$

Then there holds

$$\delta^2\Pi_1(\zeta_0)\{h,h\} = \int_{\Sigma_0} (\psi_{x_3} - a_3)hC_{\Sigma_0}\big((\psi_{x_3} - a_3)h\big)\,d\Sigma - \\ - \frac{1}{2}\int_{\Sigma_0} h^2(4n_3H + D_3)|\nabla(\psi - a_i x_i)|^2\,dB$$

for variations h with mean value zero. □

In view of

$$\int_{\Sigma_0} uC_{\Sigma_0}u\,d\Sigma_0 = \int_{Q_0} |\nabla\widetilde{u}|^2 - k^2\widetilde{u}^2\,dQ,$$

the principal part of the capacity operator is positive, hence Proposition 4.8 implies:

Corollary 4.9. *If the data are sufficiently regular, then $\delta^2\Pi_1(\zeta_0)$ is bounded on the Sobolev-space $H^{1/2}(B)$:*

$$-C^{te}\|h\|_0^2 \le \Pi_1(\zeta_0)\{h,h\} \le C^{te}\|h\|_{\frac{1}{2}}^2.$$

If additionally

$$|\psi_{x_3} - a_3| \ge c > 0 \quad on \quad \Sigma_0,$$

then $\delta^2\Pi_1(\zeta_0)$ satisfies the Garding-type inequality

$$\Pi_1(\zeta_0)\{h,h\} \ge pos.C^{te}\|h\|_{\frac{1}{2}}^2 - C^{te}\|h\|_0^2.$$

□

To collect the results of this section in a general statement, we introduce the Jacobi operator $J(\zeta_0)$ of Π via

$$\delta^2\Pi(\zeta_0)\{g,h\} = \int_{\Sigma_0} gJ(\zeta_0)\{h\}\,d\Sigma_0 \quad \text{if} \quad g|_{\partial B} = h|_{\partial B} = 0.$$

Theorem 4.10. *Assuming the data to be sufficiently regular gives:*
(i) The bilinear form $\delta^2\Pi(\zeta_0)$ satisfies the Garding-type inequality

$$\Pi(\zeta_0)\{h,h\} \ge pos.C^{te}\|h\|_1^2 - C^{te}\|h\|_0^2.$$

(ii) $J(\zeta_0)$ reads as

$$J(\zeta_0)h = -2\mu n_3 \Delta_{\Sigma_0}(n_3 h) + (\psi_{x_3} - a_3)C_{\Sigma_0}\big((\psi_{x_3} - a_3)h\big) + mn_3 h$$

with

$$m = -2\mu c^2 n_3 - 2n_3 H|\nabla(\psi - a_i x_i)|^2 + 2b\mu n_3^2 - \\ - D_3\Big(4\mu H + \frac{1}{2}|\nabla(\psi - a_i x_i)|^2 - 2b\mu x_3\Big).$$

In particular

$$m = -2\mu c^2 n_3 - 2n_3 H|\nabla(\psi - a_i x_i)|^2 + 2b\mu n_3^2, \tag{4.56}$$

if ζ_0 is a critical point of Π.
□

Note, that the nonlocal term in (4.56) may be replaced by

$$2n_3H|\nabla(\psi - a_ix_i)|^2 = 2n_3H(2\lambda + 4\mu bx_3 - 8\mu H).$$

Finally, we place emphasis on a simple stability criterion. Obviously, for sufficiently small wave numbers k the capacity operator is nonnegative. Therefore, if $H \leq 0$ and $bn_3 \geq c^2$, then a vibrocapillary equilibrium is stable in the sense that

$$\delta^2\Pi(\zeta_0)\{h,h\} \geq pos.C^{te}\|h\|_1^2.$$

for all "interior" variations h with mean value zero. This indicates that for convex equilibrium shapes a "vibro-force" may cause a stabilising effect.

4.3 Two-dimensional vibroequilibria

The present section gives examples of numerical vibroequilibria for small wave numbers k and two-dimensional fluid flows in basins of rectangular shape. The quasi-potential $\Pi(Q_0) = \Pi(\zeta_0)$ from Theorem 4.7, whose local minima coincide with the stable vibroequilibria, will be used. Main advantage of numerical schemes resting the computations upon minimisation of the functional is that these are easily combinable with the stability analysis. However, these are characterised by some difficulties. The first one is associated with analytical description of the admissible vibroequilibria, on which the functional should be minimised, and their discretisation. The second consists in matching the minimisation with solving the Dirichlet-Neumann boundary value problem for the wave function. Some approaches, which make it possible to overcome these difficulties, were proposed by Gavrilyuk *et al.* (2004) [66] and Timokha (2005) [164].

4.3.1 Statement of the problem

Earlier, we have mathematically studied the free boundary problem on forced motions of a perfect compressible fluid $Q_f(t)$ (irrotational flows) in a rigid tank Q, which performs translatory harmonic high-frequency vibrations with the velocity $\boldsymbol{v} = -\nu A\sin(\nu t)\boldsymbol{a}, ||\boldsymbol{a}|| = 1$. Following the original assumptions we considered small amplitudes (amplitude/tank size ratio $\epsilon = A/l \ll 1$) and the forcing frequency ν, which exceeds significantly the primary natural frequency of the linear sloshing ν_0 (the

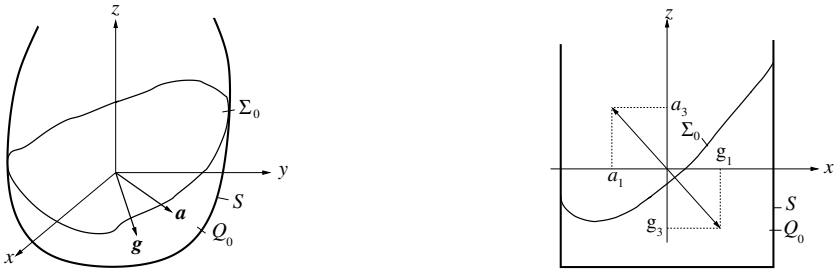

Fig. 4.1. Sketch of a vibroequilibrium in the three-dimensional case (a) and within the framework of two-dimensional flows (b). The unit guiding vector $\boldsymbol{a} = (a_1, a_2, a_3)^T$, the frequency ν and the amplitude A are time independent constants. The fluid domain $Q_f(t)$ is confined to the wetted surface $S_f(t) = \partial Q \cap \partial Q_f(t)$ and the free surface $\Sigma_f(t)$, so that $Q_0 = \langle Q_f \rangle$, $\Sigma_0 = \langle \Sigma_f \rangle$ and $S = \langle S_f \rangle$.

latter is caused by the gravitation and the surface tension), i.e. $\nu_0/\nu = O(\epsilon)$. In that case, the mean (time-averaged) free boundary $\Sigma_0 = \langle \Sigma_f \rangle$ is governed by the free boundary problem (4.54) + (4.55). The mean (time-averaged) domain $Q_0 = \langle Q_f \rangle$ bounded by $\Sigma_0 = \langle \Sigma_f \rangle$ and $S = \langle S_f \rangle$ is the vibroequilibrium (see, Fig. 4.1 (a)).

Along with the differential statement, Theorem 4.7 and the consequent Jacoby operator analysis employ the variational formulation: *the vibroequilibrium Q_0 is dynamically stable, if and only if, it delivers a local minimum of the following functional (vibropotential):*

$$\Pi_0(Q_0) = \eta_1(|\Sigma_0| - \cos\alpha|S|) - \eta_2 \int_{Q_0} (g_1 x + g_2 y + g_3 z) dQ + \\ + \int_{Q_0} (|\nabla\psi|^2 - k^2(\psi - a_1 x - a_2 y - a_3 z)^2) dQ \underset{Q_0}{\to} \min, \quad (4.57)$$

subjected to

$$Q_0 \subset Q; \quad \int_{Q_0} dQ = V = const \quad (4.58)$$

and

$$\Delta\psi + k^2\psi = k^2(a_1 x + a_2 y + a_3 z) \ in \ \ Q_0, \\ \partial_n\psi = 0 \ on \ \ S; \ \ \psi = a_1 x + a_2 y + a_3 z \ on \ \Sigma_0. \quad (4.59)$$

Here,[1] $|\cdot|$ is the area, ∂_n is the outer normal derivative to ∂Q_0, $\boldsymbol{g} = (g_1, g_2, g_3)$, $|\boldsymbol{g}| = 1$ is the unit guiding vector of gravitation, α is the contact angle, k is the wave number of acoustic field modulated in the fluid, V is the fluid volume.

The integral equation (4.58) defines the volume (mass) conservation condition. The Dirichlet-Neumann boundary value problem (4.59) expresses dependence of the [wave] function $\psi(x, y, z)$ on Q_0. The function ψ appears in the first-order approximation of the steady-state fluid motions, namely, the velocity potential of the original evolutional problem is posed in the form $\epsilon\psi(x, y, z)\cos(\nu t) + o(\epsilon)$ (mathematical details can be found in the previous section). Physically, these high-frequency steady-state fluid motions are induced by vibrations of the tanks (rigid structure) and can only be possible due to mobility of $\Sigma_f(t)$ and compressible (acoustic) fluid flows (incompressible flows imply $k = 0$).

We introduced also two dimensionless numbers η_1 and η_2 calculated by the formulae $\eta_1 = 4\mu$, $\eta_2 = -4\mu\mathrm{Bo}$, where $\mu = \sigma/(\nu^2 A^2 l\rho) > 0$, $\mathrm{Bo}{=}gl^2\rho/\sigma$ ($\pm$Bo is the Bond number; the sign depends on direction of gravitation vector, see Myshkis *et al.* (1987) [132]), g is the gravity acceleration, ρ is the fluid density and σ is the coefficient of the surface tension. The solution of (4.57)-(4.58) (shapes Q_0) depends on the five dimensionless parameters V, α, k, η_1 and η_2. Further, the functional (4.57) can be considered as the sum of three physically different terms. The first and second terms (at η_1 and η_2) express contributions of the surface tension and the gravitation, respectively. The ratio $|\eta_2/\eta_1| = |\mathrm{Bo}|$ is the gravitation/surface tension energy relationship (see, Myshkis *et al.* (1987, 1992) [132, 133]). The third [integral] term of Π_0 implies the so-called vibrational energy (Blekhman (1999) [29]). The vibrational energy implies both the averaged (per forcing period) kinetic energy of steady-state fluid motions caused the surface/interface waves and the averaged (acoustic) energy associated with the compressibility.

After assuming $k = 0$ (incompressible flows have early been postulated by Lyubimov *et al.* (1981) [109], Bezdenezhnikh *et al.* (1991) [27], in some exercises by Timokha (1997) [162], Khenner *et al.* (1999) [92] and Ivanova *et al.* (2001) [85]), we focus on vibroequilibria in a parallelepipedal tank Q with the vectors $\boldsymbol{g}$ and $\boldsymbol{a}$ to be coplanar to the Oxz-plane. When $k = 0$, the vibrational energy (the last summand of Π_0) coincides with the averaged kinetic energy of steady-state motions.

[1] For physical clarity, we denote $(x_1, x_2, x_3) = (x, y, z)$ and redefine the Bond number as $\mathrm{Bo}{=}b$.

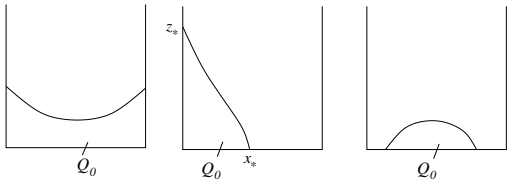

Fig. 4.2. Three admissible vibroequilibria in a rectangular tank: (a) curvilinear trapezoid, (b) curvilinear triangle and (c) drop upon a plate (bottom).

Further, admissible domains Q_0 are single-connected with a piece-smooth boundary shaped as shown in Fig. 4.2. Let $2l$ be the tank breadth (distance between walls parallel to the Oyz-plane) and $2L$ be the tank width (distance between walls parallel to the Oxz-plane). Assumption $l/L \ll 1$ makes it possible to neglect the meniscus along the Oy-axis and reduces the original problem (4.57)–(4.59) to the following formulation in the Oxz-plane

$$\Pi(Q_0) = \eta_1(|\Sigma_0| - \cos\alpha|S|) - \\ - \eta_2 \int_{Q_0} (g_1 x + g_3 z) dQ + \int_{Q_0} |\nabla\psi|^2 dQ \underset{Q_0}{\to} \min, \quad (4.60)$$

subjected to the following two-dimensional boundary value problem

$$\Delta\psi = 0 \text{ in } Q_0; \ \partial_n\psi = 0 \text{ on } S; \ \psi = a_1 x + a_3 z = w(x,z) \text{ on } \Sigma_0 \quad (4.61)$$

and the volume conservation condition (4.58). Here, in accordance with notations in Fig. 4.1 (b), Q_0, S and Σ_0 deal with their traces on the Oxz-plane, such that $|\cdot|$ is the length of corresponding curves.

4.3.2 Numerical method

Faraday (1831) [52], Wolf (1969, 1970) [171, 172] and Bezdenezhnikh *et al.* (1984) [26] have experimentally shown that high-frequency vertical vibrations ($\boldsymbol{a}||\boldsymbol{g}$) of the tank can dynamically stabilise the Rayleigh–Taylor interfacial instability of the planar potential equilibrium. Review by Nevolin (1984) [137] treats this point as the vibration-induced stability by parametric excitation of a multidimensional nonlinear system. One way to obtain corresponding theoretical conclusions is to involve

the Mathieu analysis of small free surface perturbations. The use of the variational formulation (4.60), (4.61), (4.58) is an alternative approach.

When the capillary meniscus has a planar shape and is perpendicular to $\boldsymbol{g} = (0, 0, g_3)^T$, $g_3 = 1$ (gravity acceleration is directed upward) and $\alpha = \pi/2$, it becomes unstable due to the Rayleigh-Taylor instability for (Myshkis *et al.* (1987, 1992) [132, 133])

$$-\mathrm{Bo} = \frac{\eta_2}{\eta_1} > \varkappa_1^2, \quad \varkappa_1 = \frac{\pi}{2}. \tag{4.62}$$

Assuming $\boldsymbol{a} || \boldsymbol{g}$ makes it possible to find the analytical solution of (4.60), (4.61), (4.58). It is $z = 0$ (horizontal planar vibroequilibrium) and ψ =const By employing the positiveness of Jacobi's operator of (4.60) or, alternatively, the positiveness of its spectrum (explicit form of the Jacobi operator was derived by Beyer *et al.* (2001) [24], but spectral methods were developed by Lukovsky & Timokha (1996) [118]) we arrive at the stability criterion of the planar vibroequilibrium as follows

$$\eta_2 < \eta_1 \varkappa_1^2 + \varkappa_1 \tanh(\varkappa_1 h). \tag{4.63}$$

Comparing (4.62) and (4.63) deduces that even if (4.62) holds true (unstable capillary surface), conditions (4.63) can be fulfilled (vibroequilibrium is stable) for sufficiently small $\eta_1 = O(1/\nu^2)$ and $\eta_2 = O(1/\nu^2)$ owing to the passage $\nu \to \infty$.

Another analytical solution

$$\psi = C_1 = \mathrm{const}; \quad a_1 x + a_3 z = C_1 \tag{4.64}$$

of (4.60), (4.61), (4.58) exists for $\eta_1 = \eta_2 = 0$ ($\nu = \infty$). Here, $\mathit{\Pi}$ possesses its absolute minimum ($\mathit{\Pi} = 0$) and Σ_0 is as shown in Fig. 4.3.

Experiments by Wolf (1969, 1970) [171, 172] and Bezdenezhnikh *et al.* (1984) [26] described also vibrational phenomena, which cannot easily be related to the vibration-induced parametric stabilisation. This is for instance an 'inclined' stationary interfacial relief occurring in a horizontally-vibrated tank ($\boldsymbol{a} \perp \boldsymbol{g}$) along the Ox-axis. Wolf (1969) [171] and Timokha (1997) [162] have intuitively explained this inclination by using a pendulum phenomenological model. Details on the pendulum modelling are presented in the book by Ibrahim (2005) [82]); analysis of the pendulum dynamics due to a high-frequency external forcing is for instance given by Kapitsa (1952) [90], Landau & Lifschitz (1962) [102] and Blekhman (1999) [29].

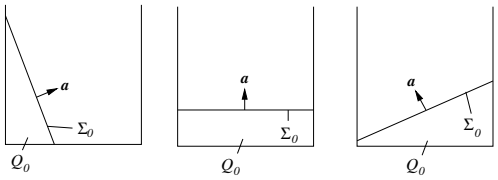

Fig. 4.3. The sketch of possible stable vibroequilibria in the limit $\nu \to \infty$ ($\eta_1 \sim \eta_2 \to 0$). The planar free boundary Σ_0 is perpendicular to the guiding vector $\boldsymbol{a}$.

In the most general case, the vibroequilibria should be found from numerical minimisation of (4.60) subjected to (4.61) and (4.58). An algorithm must consist in selecting an admissible class of Q_0 with its appropriate parametrisation/discretisation $Q_0 = Q_0(d_1, \ldots, d_{M1})$, $d_i \in \mathbb{R}$ and in matching a robust numerical scheme for the Dirichlet-Neumann boundary value problem (4.61). The solver of (4.61) must keep uniform accuracy for any admissible $Q_0(d_1, \ldots, d_{M_1})$.

For domains in Fig. 4.2, we assume that Σ_0 allows either $z = f(x)$ or $x = f(z)$ normal form presentation. The functions $f(\cdot)$ will in numerical schemes be associated with the cubic splines by Forsyth *et al.* (1977) [54]

$$f(\cdot) \cong A_i(f_k) + B_i(f_k)(\cdot - \cdot_i) + C_i(f_k)(\cdot - \cdot_i)^2 + D_i(f_k)(\cdot - \cdot_i)^3, \quad (4.65)$$

where A_i, B_i, C_i, D_i are functions of $f_k = f(\cdot_k)$ defined in the mesh points $\cdot_k$, $k = 0, \ldots, M$, $M \geq 4$. Since this spline technique does not need any additional conditions at the endpoints of $[\cdot_0, \cdot_M]$, Q_0 becomes a function of $\{f_k, k = 0, \ldots, M\}$. The variables $\{f_k\}$ are subjected to the volume conservation condition (4.58). To avoid the latter restriction we will use a re-parametrisation $f_k = f_k(d_i), k = 0, \ldots, M$ aiming to satisfy (4.58) for the independent variables $\{d_k \in \mathbb{R},\ k = 0, \ldots, M1\}$. Proceeding this way, the functional Π becomes a function of $\{d_k, k = 1, \ldots, M1\}$.

The minimisation needs both a solution $\psi \in W_2^1(Q_0)$ of (4.61) and computation of the last integral term in (4.60). Using Green's identity for the integral term

$$\int_{Q_0} (\nabla\psi)^2 dQ = \int_{\Sigma_0} \partial_n\psi \; w \; d\Gamma$$

implies that its calculation needs only the Neumann trace $\partial_n\psi$ on Σ_0. Hence, the boundary element methods for (4.61) seem to be the most

efficient approach to match solution of the Dirichlet-Neumann problem with minimising the vibropotential.

Let $P(\xi,\eta) \in \partial Q_0$ and $P^*(x.z) \in Q_0$ be two arbitrary points on the boundary and in an open part of Q_0, respectively. When using representation of a harmonic function via single and double layer potentials, we get (Mikhlin (1977) [121] p. 207)

$$\psi(x,z) = \frac{1}{2\pi} \oint\limits_{\partial Q_0} \left[\ln \frac{1}{R} \partial_{n_P} \psi - \psi \partial_{n_P} \ln \frac{1}{R} \right] d\Gamma_P, \tag{4.66}$$

where $R = R(\xi,\eta;x,z) = \sqrt{(\xi-x)^2+(\eta-z)^2}$. Here, $\ln \frac{1}{R}$ is the two-dimensional free space Green function and $\mathbf{n}_P$ means a unit vector normal from ∂Q_0 in the point P pointing out of the domain Q_0. In accordance with the rules for the single and double layer potentials, the integral representation (4.66) can be traced on the boundary and re-written as follows

$$\omega_{(x,z)}\psi(x,z) = \oint\limits_{\partial Q_0} \left[\ln \frac{1}{R} \partial_{n_P} \psi - \psi \partial_{n_P} \ln \frac{1}{R} \right] d\Gamma_{(\xi,\eta)}, \tag{4.67}$$

where $P^*(x,z) \in \partial Q_0$ and $\omega_{(x,z)}$ is the solid angle at $P^*(x,z)$ ($\omega_{(x,z)} = \pi$ for smooth pieces of the boundary).

The Dirichlet trace $\psi = w(x,z)$ is known on Σ_0, while the Neumann trace $\partial_n \psi = 0$ is given on the remaining part S. Then for $P^* \in \partial Q_0$ the integral representation (4.67) yields the integral equation on ∂Q_0

$$\int_{\Sigma_0} \left[\Phi \ln \frac{1}{R} - w \partial_{n_{(\xi,\eta)}} \ln \frac{1}{R} \right] d\Gamma_{(\xi,\eta)} - \int_S \Psi \partial_{n_{(\xi,\eta)}} \ln \frac{1}{R} d\Gamma_{(\xi,\eta)} = \\ = \omega_{(x,z)} \begin{cases} w(x,z), & (x,z) \in \Sigma_0; \\ \Psi(x,z), & (x,z) \in S, \end{cases} \tag{4.68}$$

where $\partial_{n_P} = \partial_{n_{(\xi,\eta)}}$. This integral equation couples two unknown functions

$$\Phi = \partial_n \psi \quad \text{on} \quad \Sigma_0; \quad \Psi = \psi \quad \text{on} \quad S \tag{4.69}$$

and falls, in fact, into a system of integral equations defined on smooth pieces of ∂Q_0.

∂Q_0 in Fig. 4.2 consists at most of four smooth portions. The most complex case (curvilinear trapezoid) is presented in Fig. 4.2 (a). The integral equation (4.68) takes in this case the following form

$$\int_{-1}^{1} \Phi(\xi)\sqrt{1+f'^2(\xi)}\left[\ln\frac{1}{R}\right]_{\eta=f(\xi)} d\xi + \int_{0}^{f(-1)} \Psi_-(\eta)\left[\partial_\xi \ln\frac{1}{R}\right]_{\xi=-1} d\eta -$$
$$- \int_{-1}^{1} w(\xi)\left[\partial_\eta \ln\frac{1}{R} - f'(\xi)\partial_\xi \ln\frac{1}{R}\right]_{\eta=f(\xi)} d\xi -$$
$$- \int_{0}^{f(1)} \Psi_+(\eta)\left[\partial_\xi \ln\frac{1}{R}\right]_{\xi=1} d\eta + \int_{-1}^{1} \Psi_0(\xi)\left[\partial_\eta \ln\frac{1}{R}\right]_{\eta=0} d\xi =$$
$$= \pi \begin{cases} w(x,f(x)), & z=f(x), \quad -1<x<1; \\ \Psi_0(x), & z=0, \quad -1<x<1; \\ \Psi_-(z), & x=-1, \quad 0<z<f(-1); \\ \Psi_+(z), & x=1, \quad 0<z<f(1), \end{cases} \tag{4.70}$$

where the Neumann trace $\Phi = \Phi(x) \in W^{-1/2}[-1,1]$ was previously defined in (4.69) and the Dirichlet trace Ψ is a continuous function on the flat portions S_- (wetted left wall), S_+ (wetted right wall) and S_0 (bottom). When taking into account the regularity results by Grisvard (1985) [78], Ψ falls into three functions (densities)

$$\Psi = \begin{cases} \Psi_0(x), \ -1<x<1; \\ \Psi_-(z), \ 0<z<f(-1); \quad \Psi_0(-1)=\Psi_-(0); \quad \Psi_0(1)=\Psi_+(0). \\ \Psi_+(z), \ 0<z<f(1); \end{cases} \tag{4.71}$$

The system of integral equations (4.70) couples the unknowns Φ, Ψ_0, Ψ_- and Ψ_+. The integral kernels of (4.70) can be explicitly calculated for admissible domains in Figs. 4.2 (a,b). Several kernels are of regular character (or have removable singularities) in their closed domains of definition. Other kernels have either the logarithmic singularity (associated with the single layer potential) or power singularity (associated with the double layer potential) at the corner points (endpoints). Solution ψ and, therefore, the unknown densities Φ, Ψ_0, Ψ_+ and Ψ_- almost always have singularities at the corner points (Lukovsky *et al.* (1984) [115] and Grisvard (1985) [78]). Singular character of the double layer potential kernels and densities depends on both the contact angle and the curvature of Σ_0. This means that boundary element schemes may lead to a considerable error and, therefore, a refining mesh procedure is needed for varying Q_0. Generally speaking, this causes time-inefficient computations.

We survived the appropriate boundary element algorithms based on integral systems similar to (4.70). Typical ones are exemplified by Misuno & Kodama (1990) [128] and Landrini *et al.* (1999) [103] imple-

menting the boundary element scheme for the time-stepping in an evolutional fluid sloshing problem. As matter of fact, Misuno & Kodama (1990) [128] ignored the mentioned corner singularities, while Landrini *et al.* (1999) [103] have only discussed them. Since these papers considered nearly-rectangular domains Q_0 with a nearly-right contact angle between Σ_0 and S (in terms of our definitions), the corresponding solutions are only singular in the sense of higher derivatives. In the contrast, shapes of Q_0 are more complicated and, therefore, ψ may have corner singularities in the first derivatives. Their capturing becomes of primary concern. An example of an appropriate boundary element scheme is given by Kress (1990) [96]. He developed a numerical scheme for the Dirichlet boundary value problem and showed that following this scheme makes it possible to produce a special mesh grading, which captures the singularities automatically depending on Q_0, so that refining mesh procedure is not required. Gavrilyuk & Timokha (2003) [74] have modified this scheme for the Dirichlet-Neumann problems.

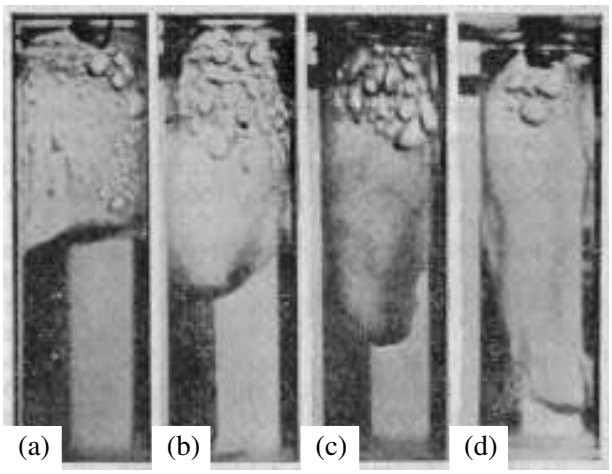

Fig. 4.4. The photos from the model tests by Ganiev *et al.* (1977) [61] posed from left to right with increasing excitation frequency. Part (c) indicates symmetric vibroequilibria, (d) shows asymmetric vibroequilibrium.

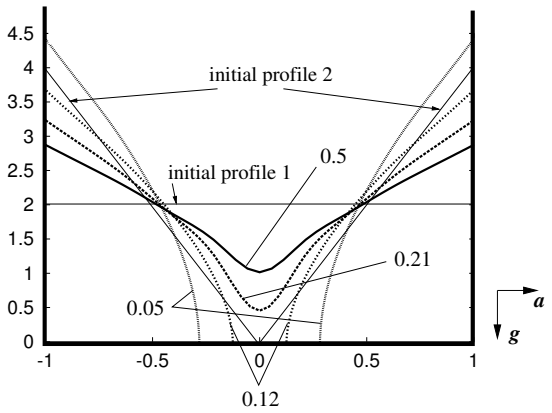

Fig. 4.5. The Oz-symmetric two-dimensional vibroequilibria for $\eta_1 = 0$ (earth-based conditions) and $V = 4$ ($h = 2$). The vibroequilibria are labelled by values of η_2. 'Initial profile 1' is used to calculate single-connected solutions ($\eta_2 = 0.5$ and 0.21). Disconnected domains are calculated with 'initial profile 2' ($\eta_2 = 0.12$ and 0.05). The critical value of η_2, at which vibration separates the fluid into two equal subdomains, is predicted about 0.205.

4.3.3 Numerical results and discussion

Numerical results below have been obtained with the maximum dimensions $M = 20$ (number of the mesh points for spline approximations of Σ_0) and $N_1 = ... = N_4 = 50$ (number of the mesh points on the smooth portions of ∂Q_0). Numerical procedure required typically $N_1 \approx ... \approx N_4 \approx 30$ and $M = 10$ to get 4-5 significant figures of the solution in an uniform metrics. The maximum dimensions were used to calculate 'critical' vibroequilibria, at which Q_0 splits into two sub-volumes. Procedure of numerical minimisation adopted a quasi-Newton method by Kahaner *et al.* (1988) [88]. The iteration number depended on the number of the mesh points and was typically between 5 and 50. The calculations have been done on a Pentium-II-366 computer. Calculation time has been affected by η_1, $\eta_2, M, N_1, \ldots, N_4$ and initial shape of Σ_0. It was typically (for our non-optimised FORTRAN-code) between 15-600 s.

Wolf (1969) [171], Ganiyev *et al.* (1977) [61] and Bezdenezhnikh *et al.* (1984) [26] established experimentally two typical vibroequilibria occurring in a horizontally vibrating tank filled by a fluid-gas system ('gas density'/'fluid density'$\ll$ 1). The first one consists in an 'inclination'

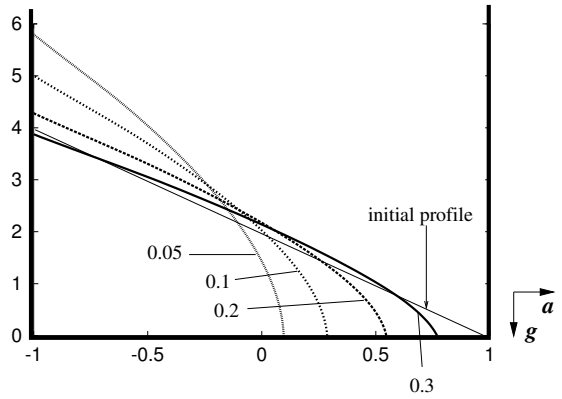

Fig. 4.6. Asymmetric vibroequilibria under the terrestrial conditions ($\eta_1 = 0$) for $V = 4$. These are obtained with triangular 'initial profile' as an initial approximation of Σ_0. The vibroequilibria are labelled by values of η_2. Stable asymmetric vibroequilibria do not realise for $\eta_2 > 0.302$.

(re-orientation) of the fluid, i.e. Σ_0 becomes geometrically close to an inclined plane (Fig. 4.2 b,d). The second type of vibroequilibria deals with the Oz-symmetric solutions, such that Σ_0 forms a 'cavity'-like profile (Fig. 4.4, c). The latter may also split into two equal sub-volumes localised at the opposite walls.

Vibroequilibria under terrestrial conditions ($\eta_1 = 0$). A macroscopic fluid volume under terrestrial conditions is characterised by large Bond numbers (Myshkis *et al.* (1987, 1992) [132, 133]). This implies $|1/\mathrm{Bo}|=|\eta_1/\eta_2| \ll 1$. Assuming $|\eta_2| = O(1)$ gives $|\eta_1| \ll 1$. This means that the surface tension gives negligible small contribution relative to the gravitation and the vibrational energy. We will therefore adopt $\eta_1 = 0$. In turn, terms containing α disappear from the functional Π. Solutions of the variational problem (4.60), (4.61), (4.58) become then depending on two parameters η_2 and V (dimensionless mean fluid depth $h = V/2$). We centre our numerical examples around the case $h = O(1)$. Shallow and intermediate fluid depth (Faltinsen & Timokha (2002) [51] estimated them for $h \lesssim 0.24$) as well as fairly deep fluid depths are not analysed. Depending on the initial shape of Σ_0, η_2 and h, the computations give either symmetric or asymmetric profiles Σ_0. There are also pairs (η_2, h), for which these solutions co-exist. This means that the problem (4.60),

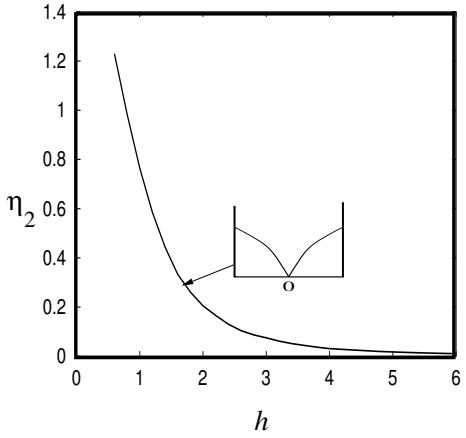

Fig. 4.7. The pairs (h, η_2) at which the symmetric single-connected vibroequilibria become disconnected. The surface tension is ignored ($\eta_1 = 0$).

(4.58), (4.61) may be not uniquely solvable (it has, at least, two local minima).

A typical strategy to distinguish the co-existing solutions consists in performing the numerical minimisations with different initial boundary shapes. Either initial shape can physically be treated as an instantaneous wave pattern occurring during initial transients. We used the two transient scenarios. The first scenario suggested that there are no transients at all (transient waves of negligible small amplitude). The second one suggests asymmetric, triangular profile (see, Fig. 4.6) associated with instantaneous wave profiles (bores, run-up etc.) mentioned and illustrated by Faltinsen & Timokha (2002) [51]. Some numerical results presented in Fig. 4.5 and 4.6 exemplify how these two scenarios lead to different vibroequilibria.

The vibroequilibria with $\eta_2 = 0.5$ and 0.21 in Figs 4.5 were obtained by assuming the first transient scenario. The computations used 'initial profile 1'. Whenever $\eta_2 > 0.205$, this initial position of Σ_0 in our iterative minimisation procedure has led to an axial-symmetric Q_0s. For $\eta_2 \leq 0.205$, the numerical scheme can diverge due to intersection between Σ_0 and the bottom. The second transient scenario assumed triangular initial approximations of Q_0 ('initial profile' in Fig. 4.6). Whenever $\eta_2 < 0.302$,

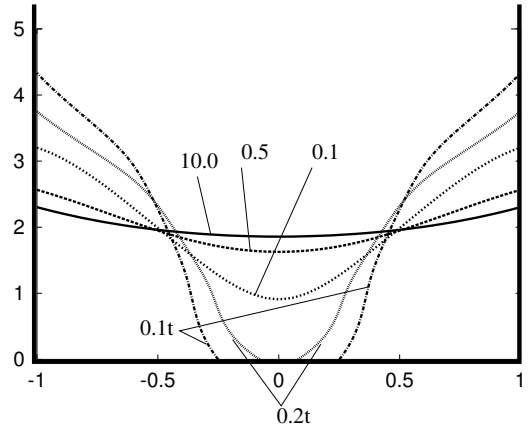

Fig. 4.8. The Oz-symmetric two-dimensional vibroequilibria for $\eta_2 = 0$ (zero-gravitation conditions), $\alpha = \pi/4$ and $V = 4$. The vibroequilibria are labelled by values of η_1. 'Initial profile 1' (see Fig. 4.5) was used to calculate single-connected solutions ($\eta_1 = 10.0, 0.5$ and 0.1) 'Initial profile 2' was adopted to get the non-connected vibroequilibria labelled by $0.2t$ and $0.1t$ (for $\eta_1 = 0.2$ and 0.1 respectively).

this initial approximation in the iterative procedure has led to asymmetric Σ_0. Examples are presented in Fig. 4.6. These asymmetric solutions are absent for $\eta_2 > 0.302$ (due to their instability).

Hence, for $\eta_1 = 0, V = 4$ and $\eta_2 > 0.302$, the two initial transient scenarios give exclusively symmetric stable vibroequilibria, but when $0.205 < \eta_2 < 0.302$ both symmetric and asymmetric vibroequilibria may be established. Asymmetric vibroequilibria exist also for $\eta_2 < 0.205$ (see examples in Fig. 4.6). For $\eta_2 < 0.205$, the fluid can also fall into the two equal Oz-symmetric portions. The developed algorithm makes it possible to find these vibroequilibria when starting iterations with 'initial profile 2' shown in Fig. 4.5 (see examples with $\eta_2 = 0.12$ and 0.05 in Fig. 4.5).

This is of especial interest to find critical pairs (η_2, h), at which the fluid splits in the Oz-symmetric way. This splitting occurs when $x_* = 0$ as depicted in Fig. 4.2 (b). By using the last condition for each sub-volume, we established η_2 versus h and presented it in Fig. 4.7. The graph demonstrates, that the critical η_2 increases with decreasing h and, therefore, the smaller fluid volumes are separated by vibrations with lower

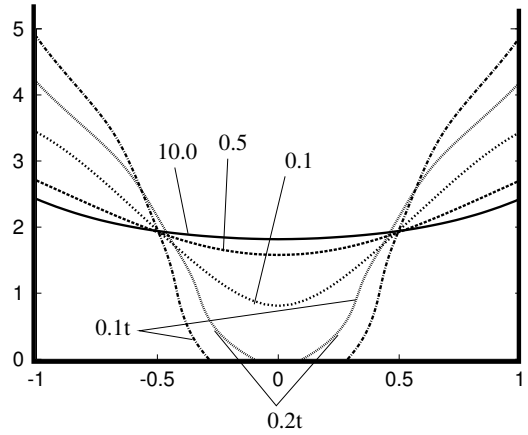

Fig. 4.9. The same as in Fig. 4.8, but $\alpha = \pi/6$.

excitation frequency (because $\eta_2 = O(1/\nu^2)$). The splitting would hard occur for fairly deep fluid, because the critical $\eta_2 \to 0$ as $h \to \infty$, and, therefore, critical $\nu \to \infty$.

Vibroequilibria under zero-gravity conditions ($\eta_2 = 0$). Zero-gravity (microgravity) condition implies $|\mathrm{Bo}| = |\eta_2/\eta_1| \ll 1$ (Myshkis *et al.* (1987, 1992) [132, 133]). In this case, the solution of (4.60), (4.61), (4.58) depends on three dimensionless numbers V, η_1 (we assume $\eta_1 = O(1)$ and, in turn, $\eta_2 = 0$) and α. When following the two transient scenarios introduced above (starting minimisation from either planar or triangular initial profiles), the computations demonstrate both symmetric and asymmetric solutions. These appear in the same way as it has been identified in the previous paragraph. There are only minor local geometric differences at the contact points influenced by different contact angles. The corresponding numerical examples are given in Figs. 4.8 and 4.9. We should note that our previous strategy consisting of estimating the critical pairs (h, η_1), at which the fluid may split into two symmetric portions, fails. This is owing to a hysteresis in the dependence of η_1 on h. Significant region of η_1 has been found, where both single-connected and disconnected symmetric solutions co-exist. The corresponding profiles in Figs. 4.8 and 4.9 are exemplified by 0.1 and 0.1t. These profiles were obtained with the same $\eta_2 = 0, V = 4, \alpha = \pi/4$ $(\pi/6)$ and $\eta_1 = 0.1$, but for different initial approximations (transient scenarios). The hysteresis can

be explained by a jump of the surface energy (due to the surface tension) established in different capillary problems (Myshkis *et al.* (1987) [132]).

4.3.4 Faraday's drops

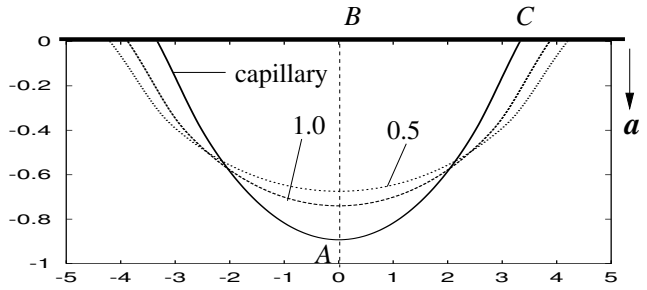

Fig. 4.10. The flattening capillary drop with decreasing $\eta_1 = O(1/\nu^2)$ (increasing the forcing frequency ν) on a vibrating plate. Zero-gravity conditions ($\eta_2 = 0$), $V = 2$ and $\alpha = \pi/6$. The curves are labelled by η_1.

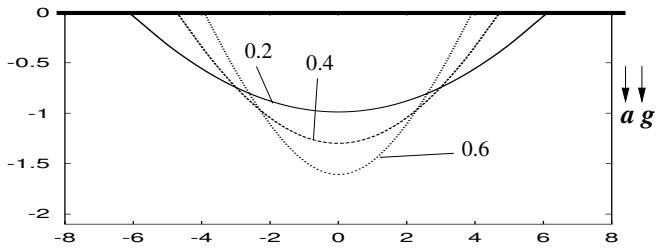

Fig. 4.11. Stabilisation and the flattering of a drop hanging beneath a vibrating plate. The surface tension is ignored ($\eta_1 = 0$), $V = 4$. The curves are labelled by values of η_2. The critical value of η_2, when the drop becomes unstable is estimated near $\eta_2 = 0.73$.

The capillary drops on a rigid plate were in details investigated by Myshkis *et al.* (1987, 1992) [132, 133]. When these drops are modified by

vertical vibrations (Faraday (1831) [52]) both the variational vibroequilibria and the proposed numerical technique can be used. The flattening with decreasing η_1 (increasing ν) is exemplified in Fig. 4.10. The calculations are consistent with Faraday's experimental observations.

Vibrations of the plate may significantly influence the drop extent occurring with increasing Bond number (η_2) and prevent its fall from the plate (the drop becomes unstable for non-small Bond numbers due to the Rayleigh-Taylor instability). Our test computations emphasise the limit case $\eta_1 = 0$ and $\eta_2 = O(1)$ (this means an infinite Bond number, i.e. $|\eta_2/\eta_1| = |\mathrm{Bo}| \gg \infty$). When there are no vibrations, the conditions $\mathrm{Bo} \gg 1$ and $g_3 = -1$ (gravity acceleration is directed downward) lead immediately to fall of the drop from the plate (Myshkis *et al.* (1987) [132]). In contrast, the numerical vibroequilibria in Fig. 4.11 are stable. The critical η_2, at which the drop becomes unstable and falls from the vibrating plate, is found near 0.73.

Concluding remarks

The two-dimensional vibroequilibria may occur in a parallelepipedal tank forced harmonically with a high frequency. In our numerical examples, the gravity acceleration and the guiding vibration vector are coplanar and belonging to the Oxz-plane. The analysis is based on a variational concept of the vibroequilibria. The vibropotential contains two quantities associated with the surface tension and the gravitation, respectively, as well as the third quantity implying Kapitsa's vibrational energy. When the first two quantities are negligible relative to the vibrational energy ($\eta_1 = \eta_2 = 0$), there exists an analytical solution of the variational problem delivering its absolute minimum. The time-averaged free surfaces are then perpendicular to the vibration. For vertical vibrations of the container, the variational concept can explain the vibration-induced stability (stabilisation of the Rayleigh-Taylor instability), which has been experimentally observed by Wolf (1970) [172].

The vibropotential is subjected to the Dirichlet-Neumann boundary problem. We approximate its solution by a modified boundary element method, which captures the singular character at the corner points. The method provides an automatic mesh grading.

Vibroequilibria under terrestrial (large Bond number) and microgravity conditions (small Bond number) in a horizontally vibrating rectangular container were numerically studied. It was shown that vibration may

either split the fluid domain into two equal sub-domains or ensure the fluid volume near a vertical walls (inclination, re-orientation). The vibroequilibria depend on the dimensionless numbers η_1 and η_2, the mean fluid volume and initial approximations of the free surface. The initial approximations can be treated as instant wave patterns occurring when the vibroforcing starts. Experimental observations by Wolf (1969) [171], Bezdenezhnikh *et al.* (1984) [26] and Ganiyev *et al.* (1977) [61] were qualitatively described. The vibrostabilisation and the flattening of a drop hanging beneath a vibrating plate were described (Faraday's (1831) [52] drops).

Even if $k = 0$ (incompressible fluid) and the problem is considered in the two-dimensional statement, there are serious numerical difficulties to classify the vibroequilibria. The first one gives rise from analytical description of the admissible vibroequilibria, on which the functional should be minimised, and their discretisation. In particular, the fluid domain can split into two and more subdomains (homogenisation). The second difficulty consists of matching the minimisation with solving the Dirichlet-Neumann boundary value problem constraining a test vibroequilibrium and the wave function. Some additional efforts are required to overcome these difficulties for the three-dimensional case (see, Beyer *et al.* (2004) [25]) and $k \neq 0$ (compressible flows).

References

1. *Abramson, H.N.* The dynamic behavior of liquids in moving containers.— Washington DC: NASA, SP-106, 1966.— 456pp.
2. *Abramson, H.N., Bass, R.L., Faltinsen, O.M., Olsen, H.A.* Liquid slosh in LNG Carriers // *Proceedings of the Tenth Symposium on Naval Hydrodynamics, June 24-28, 1974. Cambridge, Massachusetts. ACR-204.*— 1974.— P. 371–388.
3. *Abramson, H., Chu, W., Kana, D.* Some studies of nonlinear lateral sloshing in rigid container // *J. of Appl. Mech., Trans. ASME.*— 1966.— **33**, №4.— P. 66–74.
4. *Abramson, H.N., Ganza, L.R., Kana, D.D.* Liquid sloshing in compartmented cylindrical tank // *ARS J.*— 1962.— **32**, №6.— P. 978–980
5. *Agmon, S.* On the eigenfunctions and on the eigenvalues of general elliptic boundary value problems // *Commun. Pure & Appl. Math.*— 1962.— **15**.— P. 119–147.
6. *Aliabadi, S., Johnson, A., Abedi, J.* Comparison of finite element and pendulum models for simulation of sloshing // *Computers & Fluids.*— 2003.— **23**.— P. 535–545.
7. *Amosov, B.A.* On the approximate solution of elliptic pseudodifferential equations on a smooth closed curve // *ZAA.*— 1990.— **9**, №6.— P. 545–563.
8. *Anilkumar, A.V., Grugel, R.N., Shen, X.F, Wang, T.G.* Control of thermocapillary convection in a liquid bridge by vibration // *J. Appl. Phys.*— 1993.— **73**, №9.— P. 4165–4170.
9. *Apfel R.E., Tian Y., Jankovsky J., Shi T., Chen X., Holt R.G., Trinh E., Croonguist A., Thornton K.C., Sacco A.Jr., Colemen C., Leslie F.W., Matthiesen D.H.* Free oscillations and surfactant studies of superdeformed drops in microgravity // *Phys. Rev. Lett.*— 1998.— **78**, №10.— P. 1912–1915.

10. *Arov, D.Z., Gavrilyuk, I.P., Makarov, V.L.* Representation and approximation of solutions of initial value problems for differential equations in Hilbert space based on the Cayley transform // Progress in partial differential equations.— Vol. 1, Pitman Research Notes in Mathematics Series.— Pont-á-Mousson 1994: Longman, 1995.— P. 40–50.
11. *Arov, D.Z., Gavrilyuk, I.* A method for solving of initial value problems for linear differential equations in Hilbert spaces based on the Cayley transform // *Numer. Funct. Anal. and Optimiz.*— 1993.— **14**, №4-5.— P. 456–473.
12. *Ashyralyev, A., Sobolevskii, P.E.* Well-posedness of parabolic difference equations.— Birkhäuser: Verlag, 1994.— 349pp.
13. *Aubin, J.-P.* Approximation of elliptic boundary-value problems.— New York-London-Sidney-Toronto: Wiley-Interscience, a Division of John Wiley & Sons, Inc., 1972.— 356pp.
14. *Bateman, H.* Irrotational motion of a compressible inviscid fluid // *Proc. Nat. Acad. Sci.*— 1930.— **16**.— P. 816–825.
15. *Bateman, H.* Partial differential equations of mathematical physics.— N.–Y.: Dover Publ., 1944.— 522pp.
16. *Bateman, H., Dryden, H.L., Murnaghan, F.D.* Hydrodynamics.— New York: Dover Publ., 1956.— 634pp.
17. *Bateman, H., Erdelyi, A.* Higher transcendental functions.— New York, Toronto, London: McGraw – Hill Book Company, Inc., 1953.— 396pp.
18. *Bauer, H.F.* Sloshing in conical tanks // *Acta Mechanica.*— 1982.— **43**, №3–4.— P. 185–200.
19. *Bauer, H.F., Eidel, W.* Non–linear liquid motion in conical container // *Acta Mechanica.*— 1988.— **73**, №1–4.— P. 11–31.
20. *Bauer, L., Keller, H.B., Reiss, E.L.* Multiple eigenvalues lead to secondary bifurcation // *SIAM Reviews.*— **17**.— P. 101-122.
21. *Berdichevskii, V.L.* Variational principles of continuum mechanics.— Moscow: Nauka, 1983.— 660pp. (in Russian)
22. *Bernardi, C., Maday, Y.* Approximations spectrales de problémes aux limites elliptiques.— Paris: Springer-Verlag, 1992.— 242pp.
23. *Beyer, K., Günther, M.* On the Cauchy problem for a capillary drop. Part I: Irrotational motion // *Math. Meth. Appl. Sci.*— 1998.— **21**.— P. 1149–1183.
24. *Beyer, K., Gawrilyuk, I., Günther, M., Lukovsky, I., Timokha, A.* Compressible potential flows with free boundary. Part I: Vibricapillary equilibria // *ZAMM.*— 2001.— **81**, №4.— P. 261–271.
25. *Beyer, K., Günther, M., Timokha, A.* Variational and finite element analysis of vibroequilibria // *Comput. Methods in Appl. Math.*— 2004.— **4**, №3.— 290–323.
26. *Bezdenezhnikh, N.K., Briskman, B.A., Lubimov, D.V., Cherepanov, A.A., Sharov, M.T.* Control of stability of two-fluid

interface by means of vibrations, electric and magnetic fields // *All-Union Seminar on Hydromechanics and Heat- and Mass Transfer: Abstracts, Chernogolovka, 1984.*— 1984.– P. 18–20.

27. *Bezdenezhnykh, N.A., Briskman, V.A., Lapin, A.Yu., Lyubimov, D.V., Lyubimova, T.P., Tscherepanov, A.A., Zakharov, I.V.* The influence of high-frequency tangential vibrations on stability of the fluid interface in microgravity // *"Microgravity Fluid Mechanics", Proceedings of IUTAM Symp., Bremen, 1991.*– 1992.— Berlin, etc.: Springer.— 137–144.
28. *Billingham, J.* Nonlinear sloshing in zero gravity // *J. Fluid Mech.*— 2002.— **464**.— P. 365–391.
29. *Blekhman, I.I.* Vibrational mechanics.— Singapore: World Scientific, 1999.— 398pp.
30. *Bramble, J. H., Schatz, A.H., Thomée, V., Wahlbin, L.* Some convergence estimates for semi-discrete galerkin type approximations for parabolic equations // *SIAM J. Numer. Anal.*— 1977.— **14**.— P. 218–241.
31. *Bridges, T.J.* Secondary bifurcation and change of type for three dimensional standing waves in finite depth // *J. Fluid Mech.*— **179**.— P. 137–153.
32. *Bryant, P.J.* Nonlinear progressive waves in a circular basin // *J. Fluid Mech.*— 1989.— **205**.— P. 453–467.
33. *Cai, X., Langtangen, H.P., Nielsen, B.F., Tveito, A.* A finite element method for fully nonlinear water waves // *J. Comput. Physics.*— 1998.— **143**.— P. 544–568.
34. *Cariou, A., Casella, G.* Liquid sloshing in ship tanks: a comparative study of numerical simulation // *Marine Structure.*— 1999.— **12**.— P. 183–198.
35. *Celebi, S.M., Akyildiz, H.* Nonlinear modelling of liquid sloshing in a moving rectangular tank // *Ocean Engineering.*— 2002.— **29**.— P. 1527–1553.
36. *Chester, W.* Resonant oscillation of water waves. I. Theory // *Proceedings of Royal Society of London.*— 1969.— **306**.— P. 5–22.
37. *Chester, W., Bones, J.A.* Resonant oscillation of water waves. II. Experiment // *Proceedings of Royal Society of London.*— 1968.— **306**.— P. 23–30.
38. *Cocciano, B., Faetti, S., Nobili, M.* Capillary effects on surface gravity waves in a cylindrical container: wetting boundary conditions // *J. Fluid Mech.*— 1991.— **231**.— P. 325–343.
39. *Dautray, R., Lions, J.L.* Mathematical analysis and numerical methods for science and technology. Vol. 5: Evolutions problems I.— Springer-Verlag, 1992.— 709pp.
40. *Dodge, F.T., Kana, D.D., Abramson, H.N.* Liquid surface oscillations in longitudinally excited rigid cylindrical containers // *AIAA J.*— 1965.— **3**, №4. — P. 685–695.

41. *Dokuchaev, L.V.* On the solution of a boundary value problem on the sloshing of a liquid in conical cavities // *J. Applied Math. Mech.*— 1964.— **28**.— P. 176–180.
42. *Eisenhart, L.P.* Separable systems of staeckel // *Ann. Math.*— 1934.— **35**, №2.— P. 284–305.
43. *Faltinsen, O.M.* A nonlinear theory of sloshing in rectangular tanks // *J. Ship. Res.*— 1974.— **18**.— P. 224–241.
44. *Faltinsen, O.M., Rognebakke, O.F.* Sloshing and slamming in tanks // *Proceedings of Hydronav'99.– Manoeuvering'99.*— Gdansk – Ostroda, Poland, 1999.
45. *Faltinsen, O.M., Rognebakke, O.F., Lukovsky, I.A., Timokha, A.N.* Multidimensional modal analysis of nonlinear sloshing in a rectangular tank with finite water depth // *J. Fluid Mech.*— 2000.— **407**.— P. 201–234.
46. *Faltinsen, O.M., Rognebakke, O.F., Timokha, A.N.* Resonant three-dimensional nonlinear sloshing in a square base basin // *J. Fluid Mech.*— 2003.— **487**.— P. 1–42.
47. *Faltinsen, O.M., Rognebakke, O.F., Timokha, A.N.* Resonant three-dimensional nonlinear sloshing in a square base basin. Part 2. Effect of higher modes // *J. Fluid Mech.*— 2005.— **523**.— P. 199–218.
48. *Faltinsen, O.M., Rognebakke, O.F., Timokha, A.N.* Transient and steady-state amplitudes of resonant three-dimensional sloshing in a square base tank with a finite fluid depth // *Physics of Fluids.*— 2006.— **18**.— P. 012103-1—012103-14.
49. *Faltinsen, O.M., Timokha, A.N.* Adaptive multimodal approach to nonlinear sloshing in a rectangular tank // *J. Fluid Mech.*— 2001.— **432**.— P. 167–200.
50. *Faltinsen, O.M., Timokha, A.N.* Analytically-oriented approaches to two-dimensional fluid sloshing in a rectangular tank (survey) // *Proceedings of the Institute of Mathematics of NASU.*— 2002.— **44**.— P. 321–345.
51. *Faltinsen, O.M, Timokha, A.N.* Asymptotic modal approximation of nonlinear resonant sloshing in a rectangular tank with small fluid depth // *J. Fluid Mech.*— 2002.— **470**.— P. 319–357.
52. *Faraday, M.* On a peculiar class of acoustic figures and on certain forms assumed by groups of particles upon vibrating elastic surfaces // *Phil. Trans. Roy. Soc. London.*— 1831.— **121**.— P. 299–430.
53. *Feschenko, S.F., Lukovsky, I.A., Rabinovich, B.I., Dokuchaev, L.V.* The methods for determining the added fluid masses in mobile cavities.— Kiev: Naukova dumka, 1969.— 250pp. (in Russian)
54. *Forsythe, GE.., Malcolm, M.A., Moler, C.B.* Computer methods for mathematical computations. Prentice-Hall Series in Automatic Computation.— New York: Prentice-Hall Inc., 1977.— 259pp.
55. *Frandsen, J.B.* Sloshing motions in excited tanks // *J. Comput. Phys.*— 2004.— **196**.— P. 54–87.

56. *Friedmann, A., Shinbrot, M.* The initial value problem for the linearized equations of water-waves // *J. Math. Mech.*— 1967.— **17**.— P. 107–180.
57. *Friedrichs, K.O.* Über ein Minimumproblem für Potentialströmungen mit freiem Rande // *Math. Ann.*— 1934.— **109**.— P. 60–82.
58. *Fujita, H., Suzuki, T.* Evolution problems // In: "Handbook of Numerical Analysis" /Ed. by P. Ciarlet, J. L. Lions/.— North Holland: Elsevier Science Publishers B. V., 1991.— Vol. II.— P. 789–928.
59. *Funakoshi, M., Inoue, S.* Bifurcations of limit cycles in surface waves due to resonant forcing // *Fluid Dyn. Res.*— 1990.— **5**, №4.— P. 255–271.
60. *Funakoshi, M., Inoue, S.* Bifurcations in resonantly forced water waves // *Eur. J. Mech., B/Fluids.*— 1991.— **10**.— P. 31–36.
61. *Ganiev, R.F., Lakiza, V.D., Tsapenko, A.S.* On dynamic behavior of liquid free surface in microgravity conditions under vibration loading // *Sov. Appl. Mech.*— 1977.— **13**, №5.— P. 102–107.
62. *Garipov, R.M.* On the linear theory of gravity waves: the theorem of existence and uniqueness // *Archive Rat. Mech. Anal.*— 1967.— **24**.— P. 352–362.
63. *Gavrilyuk, I.P.* Strongly P-positive operators and explicit representations of the solutions of initial value problems for second order differential equations in Banach space // *J. Math. Anal. and Appl.*— 1999.— **236**.— P. 327-349.
64. *Gavrilyuk, I.P., Kulyk, A.B., Makarov, V.L.* Integral equations of the linear sloshing in an infinite chute and their discretization // *Comp. Methods Appl. Math.*— 2001.— **1**, №1.— P. 39–61.
65. *Gavrilyuk, I., Lukovsky, I., Timokha, A.* A multimodal approach to nonlinear sloshing in circular cylindrical tank // *Hybrid Methods in Engineering.*— 2000.— **2**, №4.— P. 463–483.
66. *Gavrilyuk, I., Lukovsky, I., Timokha, A.* Two-dimensional variational vibroequilibria and Faraday's drops // *ZAMP.*— 2004.— **55**.— P. 1015-1033.
67. *Gavrilyuk, I., Lukovsky, I., Timokha, A.* Linear and nonlinear sloshing in a circular conical tank // *Fluid Dyn. Res.*— 2005.— **37**.— P. 399–429.
68. *Gavrilyuk, I.P., Makarov, V.L.* Representation and approximation of the solution of an initial value problem for a first order differential equation in Banach space // *ZAA.*— 1996.— **15**, №2.— P. 495–527.
69. *Gavrilyuk, I.P., Makarov, V.L.* Representation and approximation of the solutions of second order differential equations with unbounded operator coefficients in Hilbert space // *ZAMM.*— 1996.— **76**, suppl. 2.— P. 527–528.
70. *Gavrilyuk, I.P., Makarov, V.L.* Explicit and approximate solutions of second order evolution differential equations in Hilbert space // *Numer. Meth. Partial Diff. Equations.*— 1999.— **15**.— P. 111–131.

71. *Gavrilyuk, I., Makarov, V., Chapko, R.* On the numerical solution of linear evolution problems with an integral operator coefficient // *J. Integral Eq. Appl.*— 1998.— **10**, №4.— P. 1–20.
72. *Gavrilyuk, I.P., Makarov, V.L.* Strongly positive operators and numerical algorithms without accuracy saturation.— Kiev: Insitute of Mathematics of NASU, 2005.— 499pp.
73. *Gavrilyuk, I.P., Makarov, V.L.* Algorithms without accuracy saturation for evolution equations in Hilbert and Banach spaces // *Math. Comp.*— 2005.— **74**.— P. 555-583.
74. *Gavrilyuk, I., Timokha, A.* A Nysröm-Kress scheme for a Dirichlet-Neumann boundary value problem associated with fluid sloshing in a rectangular tank // *Proceedings of the Institute of Mathematics of the NASU.*— 2003.— **47**.— 284-301.
75. *Gerrits, J.* Dynamics of liquid-filled spacecraft. Numerical simulation of coupled solid-liquid dynamics: Ph.d. Thesis.— Rijksaniversiteit Groningen, 2001.
76. *Giusti, E.* Minimal surfaces and functions of bounded variation.— Boston Basel Stuttgart: Birkhäuser Verlag, 1984.— 240pp.
77. *Goldstein, J.A.* Semigroups of linear operators and applications.— Oxford, New York: Oxford University Press, Clarendon Press, 1985.— 245pp.
78. *Grisvard, P.* Elliptic problems in nonsmooth domains.— Boston, MA: Pitman (Advanced Publishing Program), 1985.— 410pp.
79. *Hargneaves, R.* A pressure–integral as kinetic potential // *Phil. Magazine.*— 1908.— **16**.— P. 436–444.
80. *Hutton, R.E.* An investigation of nonlinear, non-planar oscillations of liquid in cylindrical containers // *In "Technical Notes, NASA, D-1870", Washington, 1963.*– P. 145–153.
81. *Hermann, M., Timokha, A.* Modal modelling of the nonlinear resonant sloshing in a rectangular tank I: A single-dominant model // *Math. Models Methods in Appl.Sciences.*— 2005.— **15**, №9.– P. 1431–1458.
82. *Ibrahim, R.A.* Liquid sloshing dynamics.— Cambridge: Cambridge Universtity Press, 2005.— 948pp.
83. *Ibrahim, R.A., Pilipchuk, V.N., Ikeda, T.* Recent advances in liquid sloshing dynamics // *Appl. Mech. Rev.*— 2001.— **54**, №2.— P. 133–199.
84. *Ivanova, A.A., Kozlov, V.G., Liubomov, D.V., Liubimova, T.P., Merady, S., Roux, B.* Structure of averaged flow driven by a vibrating body with a large-curvature edge // *Fluid Dyn.*— 1998.— **33**, №5.— P. 656–665.
85. *Ivanova, A.A., Kozlov, V.G., Evesque, P.* Interface dynamics of immiscible fluids under horizontal vibration // *Fluid Dyn.*— 2001.— **36**, №3.— P. 362–366.
86. *Ivanova, A.A., Kozlov, V.G., Tasjkinov, S.I.* Interface dynamics of immiscible fluids under circularly polarized vibration (experiment) // *Fluid Dyn.*— 2001.— **36**, №6. — P. 871–879.

87. *John, F.* Two-dimensional potential flows with a free boundary // *Communic. Appl. Math.*.— 1953.— **6**.— P. 497–503.
88. *Kahaner, D., Moler, C., Nash, S.* Numerical methods and software.— New York: Prentice-Hall, 1988.— 456pp.
89. *Kanwal, R.P.* Linear integral equations. — Boston, MA: Birkhäuser Boston, Inc., 1997.— 318pp.
90. *Kapitsa, P.L.* The pendulum with a vibrating point of suspension // *Adv. Phy. Sc.*— 1952.— **44**, №1.— P. 34–42.
91. *Keulegan, G.H.* Energy dissipation in standing waves in rectangular basin // *J. Fluid Mech.*— 1959.— **6**.— P. 33–50.
92. *Khenner, M.V., Lyubimov, D.V., Belozerova, T.S., Roux, B.* Stability of plane-parallel vibrational flow in a two-layer system // *Eur. J. Mech. B/Fluids.*— 1999.— **18**.— P. 1085–1101.
93. *Kochin, N.E., Kibel, I.A., Roze, N.V.* Theoretical hydromechanics.— New-York-London-Sydney: Interscience Publishers John Wiley & Sons, 1964.— 577pp.
94. *Krein, S.G.* Linear differential operators in Banach spaces.— Boston, Birkhäuser Boston, 1982.— 102pp.
95. *Kress, R.* Linear integral equations.— Berlin: Springer-Verlag, 1989.— 299pp.
96. *Kress, R.* A Nyström methods for boundary integral equations in domains with corners // *Numer. Math.*— 1990.— **58**.— P. 145–161.
97. *Kress, R., Sloan, I.* On the numerical solution of a logarithmic integral equation of the first kind for the Helmholtz equation // *Numer. Math.*— 1993.— **66**.— P. 199–214.
98. *La Rocca, M., Mele, P., Armenio, V.* Variational approach to the problem of sloshing in a moving container // *J. Theo. and Appl. Fluid Mech.*— **1**, №4.— P. 280–310.
99. *La Rocca, M., Sciortino, G., Boniforti, M.* A fully nonlinear model for sloshing in a rotating container // *Fluid Dyn. Res.*— 2000.— **27**.— P. 23–52.
100. *La Rocca, M., Sciortino, G., Boniforti, M.* Interfacial gravity waves in a two-fluid system // *Fluid Dyn. Res.*— 2002.— **30**, №1.— P. 31–66.
101. *La Rocca, M., Sciortino, G., Adduce, C., Boniforti, M.* Experimental and theoretical investigation on the sloshing of a two-liquid system with free surface // *Physics of Fluids.*— 2005.— **17**, №6.— P. 062101-1–062101-17.
102. *Landau, L.D., Lifschitz, E.M.* Mechanics. Course of Theoretical Physics, Vol. 1.— Oxford-London-New York-Paris: Pergamon Press, Addison-Wesley Publishing Co., Inc., Reading, Mass, 1960.— 165pp.
103. *Landrini, M., Grytøyr, G., Faltinsen, O.M.* A B-spline based BEM for unsteady free-surface flows // *J. Ship Res.*— 1999.— **43**, №1.— P. 13–24.

104. *Lee, C.P., Anilkumar, A.V., Hmelo, A.B., Wang, T.G.* Equilibrium of liquid drops under effects of rotation and acoustic flattening: Results from usml-2 experiments in space // *J. Fluid Mech.*— 1998.— **354**.— P. 43–67.
105. *Lichtenstein, L.* Grundlagen der Hydromechanik.— Berlin: Springer-Verlag, 1968.— 506pp.
106. *Lierke, E.G.* Acoustic positioning. in summary review of sounding rocket experiments in fluid science and material sciences (post-flight) // *In: "TEXUS 1 to 20, MASTER 1 and 2", ESA SP-1132, February 1991.*— 1991.— P. 362–365.
107. *Lions, P.-L.* Mathematical topics in fluid machanics. Vol. 2: Compressible models.— New York: The Clarendon Press, Oxford University Press, 1998.— 348pp.
108. *Löfström, J.* Interpolation of boundary value problems of Neumann type on smooth domains // *J. London Math. Soc.*— 1992.— **46**, №2.— P. 499–516.
109. *Lubimov, D.V., Cherepanov, A.A., Briskman, V.A.* Control of the fluid free surface by fluctating fields // *In: "Abstracts of II All-Union Seminal on Hydromechanics and Heat- and Mass Transfer", Perm, 1981.*— P. 112–114.
110. *Lubimov, D.V., Cherepanov, A.A.* Development of a steady relief at the interface of fluids in a vibrational field // *Fluid Dyn.*— 1986.— **21**. — P. 849–854.
111. *Luke, J.C.* A variational principle for a fluid with a free surface // *J. Fluid Mech.*— 1967.— **27**.— P. 395–397.
112. *Lukovsky, I.A.* Nonlinear oscillations of a fluid in tanks of complex shape.— Kiev: Naukova dumka, 1975.– 180pp. (in Russian)
113. *Lukovsky, I.A.* Variational method in the nonlinear problems of the dynamics of a limited liquid volume with free surface // *In book: "Oscillations of elastic constructions with a liquid".*— Moscow: Volna, 1976.— P. 260–264. (in Russian)
114. *Lukovsky, I.A.* Introduction to nonlinear dynamics of a solid body with a cavity including a liquid.— Kiev: Naukova dumka, 1990.— 296pp. (in Russian)
115. *Lukovsky, I.A., Barnyak, M.Ya., Komarenko, A.N.* Approximate methods of solving the problems of dynamics of a limited liquid volume.— Kiev: Naukova dumka, 1984.— 228pp. (in Russian)
116. *Lukovsky, I.A., Bilyk, A.N.* Forced nonlinear oscillations of a liquid in a moving axial-symmetric conical tanks // *In book: "Numerical-analytical methods of studying the dynamics and stability of multidimensional systems".*— Kiev: Institute of Mathematics, 1985.— P. 12–26. (in Russian)
117. *Lukovsky, I.A., Timokha, A.N.* Variational methods in nonlinear dynamics of a limited liquid volume.— Kiev: Institute of Mathematics, 1995.– 400pp. (in Russian)

118. *Lukovsky, I.A., Timokha, A.N.* One version of the linearized theory of nonstationary boundary-value problems with free boundary // *Ukrainian Math. J.*— 1996.— **48**, №6.— P. 890-904.
119. *Lukovsky, I.A., Timokha, A.N.* Nonlinear theory of fluid sloshing in mobile tanks: classical and non-classical problems (survey) // *In book: "Problems of Analytical Mechanics and its Applications".*— Kiev: Institute of Mathematics, 1999.— P. 169–200. (in Russian)
120. *Lukovsky, I.A., Timokha, A.N.* Modal modeling of nonlinear fluid sloshing in tanks with non-vertical walls. non-conformal mapping technique // *Int. J. Fluid Mech. Res.*— 2002.— **29**, №2.— P. 216–242.
121. *Mikhlin, S.G.* Partielle Differentialgleichungen in der mathematischen Physik. Mathematische Lehrbücher und Monographien, I. Abteilung: Mathematische Lehrbücher.— Berlin: Akademie-Verlag, 1978.— 519pp.
122. *Mikishev, G.I.* Experimental methods in the dynamics of spacecraft.— Moscow: Mashinostroenie, 1978.– 196pp. (in Russian)
123. *Mikishev, G.I., Dorozhkin, N.Y.* An experimental investigation of free oscillations of a liquid in containers // *Izvestiya Akademii Nauk SSSR, Otdelenie Tekhnicheskikh Nauk Mekhanika Mashinostroenie.*— 1961.— №4.— P. 48–53. (in Russian)
124. *Mikishev, G.I., Rabinovich, B.I.* Dynamics of a rigid body with cavities filled partially by a liquid.— Moscow: Mashinostroenie, 1968.— 346pp. (in Russian)
125. *Miles, J.W.* Nonlinear surface waves in closed basins // *J. Fluid Mech.*— 1976.— **75**.— P. 419–448.
126. *Miles, J.W.* Internally resonant surface waves in a circular cylinder // *J. Fluid Mech.*— 1984.— **149**.— P. 1–14.
127. *Miles, J.W.* Resonantly forced surface waves in a circular cylinder // *J. Fluid Mech.*— 1984.— **149**.— P. 15–31.
128. Mizuno Akisato, Kodama Yoshihiro. Analysis of nonlinear wave–making phenomena by means of boundary element method // *Research Reports of Kogakuin University.*— 1990.— №69.— P. 15–20.
129. *Moiseev, N.N.* On the theory of nonlinear vibrations of a liquid of finite volume // *J. Appl. Math. and Mech.*— 1958.— **22**.— P. 860–872.
130. *Moiseev N.N., Rumyantsev V.V.* Dynamic stability of bodies containing fluid.— New York: Springer, 1968.— 326pp.
131. *Morand, H. J.-P., Ohayon, R.* Fluid structure interaction. Applied numerical methods.— Chichester, New York, Brisbane, Toronto, Singapore, Jouhn Wiley & Sons, 1995.— 212pp.
132. *Myshkis, A.D., Babsky, V.G., Kopachevskii, N.D., Slobozhanin, L.D., Typsov, A.D.* Low-gravity fluid mechanics. Mathematical theory of capillary phenomena.— Berlin, Heidelberg: Springer-Verlag, 1987.— 583pp.
133. *Myshkis, A.D., Babsky, V.G., Zhukov, M.Yu., Kopachevskii, N.D., Slobozhanin, L.D., Typsov, A.D.* Methods for solving hydromaechanic

problems in zero-gravity.— Kiev: Naukova dumka, 1992.— 620pp. (in Russian)

134. *Narimanov, G.S.* Movement of a tank partly filled by a fluid: the taking into account of non–smallness of amplitude // *J. Appl. Math. and Mech. (PMM).*— 1957.— **21**.— P. 513–524. (in Russian)
135. *Narimanov, G.S., Dokuchaev, L.V., Lukovsky, I.A.* Nonlinear dynamics of a flying apparatus with a liquid.— Moscow: Mashinostroenie, 1977.– 208pp. (in Russian)
136. *Nečas, J.* Les méthodes directes en théorie des équations elliptiques.— Prague: Academia, 1964.– 340pp.
137. *Nevolin, V.G.* Parametric excitation of surface waves // *J. Engineering Physics and Thermophysics.*— 1984.— **47**, №6.— P. 1482–1494.
138. *Nishida, T.* Equations of fluid dynamics – free surface problems // *Comm. Pure Appl. Math.*— 1986.— **39**, Suppl.— P. 221–237.
139. *Ockendon, J.R., Ockendon, H.* Resonant surface waves // *J. Fluid Mech.*— 1973.— **59**.— P. 397–413.
140. *Ockendon, H., Ockendon, J.R.* Nonlinearity in fluid resonances // *Meccanica.*— 2001.— **36**.— P. 297–321.
141. *Ockendon, H., Ockendon, J.R., Waterhouse, D.D.* Multi-mode resonance in fluids // *J. Fluid Mech.*— 1996.— **315**.— P. 317–344.
142. *Ovsyannikov, L.V., Makarenko, N.I., Nalimov, V.I., etc.* Nonlinear problems of the theory of surface and interior waves.— Novosibirsk: Nauka, 1985.– 540pp. (in Russian)
143. *Parlett, B.N.* The symmetric eigenvalue problem.— Philadelphia, PA: SIAM, 1998.— 398pp.
144. *Perlin, M., Schultz, W.W.* Capillary effects on surface waves //*Annu. Rev. Fluid Mech.*— 2000.— **32**.— P. 241–274.
145. *Perko, L.M.* Large-amplitude motions of liquid-vapour interface in an accelerating container // *J. Fluid Mech..*— 1969.— **35**, part 1.— P. 77–96.
146. *Petrov, A.A.* Variational statement of the problem of liquid motion in a container of finite dimensions // *J. Appl. Math. and Mech.*— 1964.— **28**, №4.— P. 917–922.
147. *Quarteroni, A., Valli, A.* Numerical approximation of partial differential equations.— Berlin et al.: Springer-Verlag, 1994.– 543pp.
148. *Reeder, J., Shinbrot, M.* The initial value problem for surface waves under gravity. II. The simplest 3-dimensional case // *Indiana University Math. J.*— 1976.— **25**, №11.— P. 1049–1071.
149. *Reeder, J., Shinbrot, M.* The initial value problem for surface waves under gravity. III. Uniformly analytic initial domains // *J. Math. Anal. and Appl.*— 1979.— **67**.— P. 340–391.
150. *Ryshik, I.M., Gradstein, I.S.* Tables of series, products and integrals.— Moscow: Nauka, 1963.— 936pp. (in Russian)

151. *Samarskii, A.A.* Theorie der Differenzenverfahren.— Leipzig: Akademische Verlagsgesellschaft Geest & Portig K.-G., 1984.— 356pp.
152. *Samarskii, A.A., Makarov, V.L* Stability and regularization of three-level difference schemes with unbounded operator coefficients in Banach spaces // *SIAM J. Num. Anal.*.— 2001.— **39**, №2.— P. 708–723.
153. *Sames, P.C., Marcouly, D., Schellin, T.* Sloshing in rectangular and cylindrical tank // *J. Ship Res.*— 2002. — **46**, №3.— P. 186–200.
154. *Schatz, A.H., Thomee, V., Wendland, W.L.* Mathematical theory of finite and boundary element methods.— Basel: Birkhäuser Verlag, 1990.— 276pp.
155. *Shankar, P.N., Kidambi, R.* A modal method for finite amplitude, nonlinear sloshing // *Pramana – J. of Physics.*— 2002.— **59**, №4.— P. 631–651.
156. *Shinbrot, M.* The initial value problem for surface waves under gravity. I. The simplest case // *Indiana University Math. J.*— 1976.— **25**, №3.— P. 281–300.
157. *Solaas, F.* Analytical and numerical studies of sloshing in tanks. Ph.D. Thesis / Norwegian Institute of Technology.— Trondheim, 1995.
158. *Solaas, F., Faltinsen, O.M.* Combined numerical and analytical solution for sloshing in two-dimensional tanks of general shape // *J. Ship Res.*— 1997.— **41**.— P. 118–129.
159. *Suetin, P.* Classical orthogonal polynomials.— Moscow: Nauka, 1979.— 415pp. (in Russian)
160. *Szegö, G.* Orthogonal polynomials.— New York: American Mathematical Society, 1939.— 401pp.
161. *Tal-Ezer, H.* Spectral methods in time for hyperbolic equations // *SIAM J. Numer. Anal.*— 1989.— **23**.— P. 11–26.
162. *Timokha, A.N.* Effect of lateral vibration of a tank on free surface of the fluid // *Technical Mechanics.*— 1997.— **5**.— P. 33–41. (in Russian)
163. *Timokha, A.N.* Note on ad hoc computing based upon a modal basis // *Proceedings of the Institute of Mathematics of NASU.*— 2002.— **44**.— P. 269–274.
164. *Timokha, A.N.* Planimetry of vibrocapillary equilibria at small wave numbers // *Int. J. Fluid Mech. Res.*— 2005.— **32**, №4.— 454-487
165. *Tsai, W.-T., Yue, D.K.-P., Yip, K.M.K.* Resonantly excited regular and chaotic motions in a rectangular wave tank // *J. Fluid Mech.*— 1990.— **216**.— P. 343–380.
166. *Wagner, H.* Über Stoss- und Gleitvorgange an der Oberfläche von Flüssigkeiten // *ZAMM.*— 1932.— **12**.— P. 193–235.
167. *Wang, T.* Drop physics module / drop dynamics experiment: 90-day science report // *The second United States Microgravity Laboratory (USML-2).*— 1996.— P. 69–71.
168. *Wanis, S., Sercovich, A., Komerath, N.* Acoustic shaping in microgravity: higher order surface shapes // AIAA Paper, N 99-0954.

169. *Waterhouse, D.D.* Resonant sloshing near a critical depth // *J. Fluid Mech.*— 1994.— **281**.— P. 313–318.
170. *Wendlandt, J.M., Marsden, J.E.* Mechanical integrators derived from a discrete variational principle // *Physica D.*— 1997.— **106**.— P. 223–246.
171. *Wolf, G.H.* The dynamic stabilisation of the rayleigh-taylor instability and the corresponding dynamic equilibrium // *Z. Physik.*— 1969.— **227**, №3.— P. 291–300.
172. *Wolf, G.H.* Dynamic stabilisation of the interchange instability of a liquid-gas interface // *Phys. Rev. Let.*— 1970.— **24**, №9.— P. 444–446.

Наукове видання

I. P. Gavrilyuk, I. A. Lukovsky,
V. L. Makarov, A. N. Timokha

Evolutional Problems of the Contained Fluid

Редактор О. М. Тимоха
Комп'ютерний оригінал-макет Д. О. Ситник

Підписано до друку 01.03.2006. Формат 60×84/16. Папір офс. Офс. друк.
Фіз.-вид. арк. 15,0. Умов. друк. арк. 14,0. Зам. № 77. Наклад 300 пр.

Інститут математики НАН України.
01601 Київ 4, МСП, вул. Терещенківська, 3.